ASSESSMENT OF URBAN HEAT: APPROACHING WALKABILITY FROM A MULTI-SCALAR PERSPECTIVE

A THESIS SUBMITTED TO
THE GRADUATE SCHOOL OF NATURAL AND APPLIED SCIENCES
OF
MIDDLE EAST TECHNICAL UNIVERSITY

BY

SHIZA MUSHTAQ

IN PARTIAL FULFILLMENT OF THE REQUIREMENTS
FOR
THE DEGREE OF MASTER OF SCIENCE
IN
URBAN DESIGN IN CITY AND REGIONAL PLANNING

JANUARY 2023

Approval of the thesis:

ASSESSMENT OF URBAN HEAT: APPROACHING WALKABILITY FROM A MULTI-SCALAR PERSPECTIVE

submitted by **SHIZA MUSHTAQ** in partial fulfillment of the requirements for the degree of **Master of Science** i**n Urban Design in City in Regional Planning, Middle East Technical University** by,

Prof. Dr. Halil Kalıpçılar
Dean, Graduate School of **Natural and Applied Sciences** _____

Prof. Dr. Serap Kayasü
Head of the Department, **City and Regional Planning** _____

Prof. Dr. Müge Akkar Ercan
Supervisor, **City and Regional Planning, METU** _____

Examining Committee Members:

Assoc. Prof. Ender Peker
City and Regional Planning, METU _____

Prof. Dr. Müge Akkar Ercan
City and Regional Planning, METU _____

Assoc. Prof. Dr. Ezgi Orhan
City and Regional Planning, Çankaya University _____

Date: 27.01.2023

I hereby declare that all information in this document has been obtained and presented in accordance with academic rules and ethical conduct. I also declare that, as required by these rules and conduct, I have fully cited and referenced all material and results that are not original to this work.

Name Last name: Shiza Mushtaq

Signature:

ABSTRACT

ASSESSMENT OF URBAN HEAT: APPROACHING WALKABILITY FROM A MULTI-SCALAR PERSPECTIVE

Mushtaq, Shiza
Master of Science, City and Regional Planning
Supervisor: Prof. Dr. Muge Akkar Ercan

January 2023, 215 pages

Under the impacts of climate change, the growing intensity of heat waves pose a significant public health risk and affect daily life both in living spaces and public places. However, it is possible to mitigate urban heat, increase urban mobility and promote walkability with data-informed urban design policies. The literature on urban mobility examines the walkability capacity of public spaces concerning environmental, social, and human physiological factors. In contrast, fewer studies address the impact of urban heat on walkability by mapping urban and metropolitan systems in detail and at multiscale.

This thesis examines urban heat indicators and their effect on thermal comfort associated walkability in the city by interpreting the empirical findings from this research. It aims to develop an assessment methodology to monitor changes in land use, land surface temperature, and vegetation health in Ankara at multiple scales (provincial, metropolitan, district and neighborhood), using only open-source data. LANDSAT images are utilized to quantify the spatio-temporal LST and Normalized Difference Vegetation Index (NDVI) for selected years between 1990 and 2021. CORINE Land Use/Land Cover (LULC) maps are extracted for the same dates and geographical boundaries.

To further investigate the impacts of urban design interventions at the micro-scale, this thesis analyzes urban design scenarios for four different building blocks with distinct street features through microclimate simulations prepared by using ENVI-met software. These analyses mainly seek to examine and reveal the cooling potential of ground surface permeability, soil type, and shade provided by trees, canopies, or buildings. The findings of this thesis are valuable contributions to the practice of climate-responsive urban design and reinforce the significance of studying walkability in relation to urban heat.

Keywords: Urban Heat, LST, Walkability, Thermal Comfort

ÖZ

KENTSEL ISI DEĞERLENDİRMESİ: YÜRÜNEBİLİRLİĞE ÇOK ÖLÇEKLİ BİR YAKLAŞIM

Mushtaq, Shiza
Yüksek Lisans, Kensel Tasarım, Şehir Bölge Planlama
Tez Yöneticisi: Prof. Dr. Müge Akkar Ercan

Ocak 2023, 215 sayfa

İklim değişikliği etkisinde artan sıcak dalgaları halk sağlığı açısından önemli riskler oluşturmaktadır; hem yaşam alanlarında hem de kamusal alanlarda günlük hayatı etkilemektedir. Veriye dayalı kentsel tasarım politikalarıyla kentsel ısıyı azaltmak, kentsel hareketliliği artırmak ve yürünebilirliği teşvik etmek mümkündür. Kentsel hareketlilik yazınında, kamusal alanların yürünebilirlik kapasitesi çevresel, sosyal ve insanî fizyolojik faktörlerle incelenmektedir. Buna karşılık, daha az sayıda çalışma, kentsel sıcaklığın yürünebilirlik üzerindeki etkisini kentsel ve metropoliten sistemleri ayrıntılı ve çok ölçekli haritalayarak ele almaktadır.

Bu tez, kentsel ısı göstergelerini ve bunların kentte yürünebilirlikle ilişkili termal konfor üzerindeki etkisini incelemektedir. Ampirik araştırma bulgularını kullanarak ve yorumlayarak, Ankara'da arazi kullanımı, arazi yüzey sıcaklığı (AYS) ve bitki örtüsü sağlığındaki değişiklikleri yalnızca açık kaynak verileri kullanarak il, metropoliten, ilçe ve mahalle olmak üzere birden çok ölçekte izleme-değerlendirme yöntemi geliştirmeyi amaçlamaktadır. LANDSAT görüntüleri, 1990 ve 2021 yılları arasında seçilen yıllar için mekân-zaman sürekliliği içerisinde AYS ve Normalleştirilmiş Bitki Örtüsü İndeksi'ni (NBÖİ) ölçmek için kullanmaktadır.

CORINE Arazi Kullanımı/Arazi Örtüsü (LULC) haritaları üretilerek, aynı tarihler ve coğrafi sınırlar için ölçümlenmiştir.

Kentsel tasarım müdahalelerinin mikro ölçekteki etkilerini daha ileri düzeyde incelemek için bu araştırma, ENVI-met yazılımı kullanılarak hazırlanan mikro iklim simülasyonları aracılığıyla farklı sokak özelliklerine sahip dört yapı adası parçası için kentsel tasarım senaryolarını analiz etmektedir. Bu analizler, ağaçların, saçakların ve binaların sağladığı gölgelerin, zemin yüzey geçirgenliğinin, ve toprak tipinin soğutma potansiyellerini ortaya çıkarmayı amaçlamaktadır. Bu tezdeki bulgular, iklime duyarlı kentsel tasarım uygulamalarına değerli katkılar sağlamaktadır; ve yürünebilirliği kentsel ısıyla ilişkili olarak incelemenin önemini pekiştirmektedir.

Anahtar kelimeler: Kentsel Isı, LST, Yürünebilirlik, Termal Konfor

To my Nani

ACKNOWLEDGMENTS

I am extremely grateful to my supervisor for her consistent support and unwavering belief in my abilities. She patiently listened to all my ideas throughout my master's education and provided constructive and timely feedback. She inspires me every day and I could not have imagined a better advisor and mentor for my study and research.

I would like to thank my husband, Hammad, for his continued and unfailing patience, support, and love during my pursuit of this degree. I am also extremely grateful to my parents, Mushtaq and Shaheena, for being the picture of resilience and helping me navigate through every stage of my life. I am thankful to my sister, Maha for her gentle support and ever-calming presence.

I would like to dedicate this thesis to my Nani and Dadi. Their strength and perseverance in the face of life's challenges inspires me every day.

TABLE OF CONTENTS

LIST OF TABLES

TABLES

LIST OF FIGURES

FIGURES

LIST OF ABBREVIATIONS

ASTER	Advanced Spaceborne Thermal Emission and Reflection
AVHRR	Advanced Very High Resolution Radiometer
BLUHI	Boundary Layer Heat Island
BSAA	Bare Soil and Agricultural Areas
BT	Brightness Temperature
CFD	Computational Fluid Dynamics
CLC	CORINE Land Cover
CLUHI	Canopy Layer Heat Island
DEM	Digital Elevation Model
DSM	Digital Surface Model
EMR	Electromagnetic Radiation
EO	Earth Observation
ETM	Enhanced Thematic Mapper
GIS	Geographic Information System
ISL	Inertial Sublayer
LAD	Leaf Area Density
LIDAR	Light Detection and Ranging
LST	Land Surface Temperature
LULC	Land Use Land Cover
MMU	Minimum Mapping Unit

MODIS	Moderate Resolution Imaging Spectroradiometer
MWA	Mono-Window Algorithm
NDVI	Normalized Difference Vegetation Index
OLI	Operational Land Imager
PV	Proportion of Vegetation
RADAR	Radio Detection and Ranging
RSL	Roughness Sublayer
RTE	Radiative Transfer Equation
SAR	Synthetic Aperture Radar
SCA	Single Channel Algorithm
SDG	Sustainable Development Goal
SUHI	Surface Urban Heat Island
SVF	Sky View Factor
SWA	Split Window Algorithm
TIRS	Thermal Infrared Sensor
TM	Thematic Mapper
TOA	Top of Atmospheric Radiance
TSV	Thermal Sensation Vote
UCL	Urban Canopy Layer
USGS	United States Geographical Survey

CHAPTER 1

INTRODUCTION

1.1 Problem Statement

For the past decade, there has been a growing realization that serious efforts must be directed towards mitigating irreversible changes brought on by climate change. Cities are tackling urban challenges whose effects are transboundary in nature and remain unprecedented in scale, complexity, and scope.

The world has already warmed by 1.0℃ above pre-industrial levels due to human activities and maintaining global temperature just below or at 1.5℃ throughout the rest of the century is the recommended pathway to limit climate-associated disasters. In the transport sector, an approximately 30% reduction in final energy use by 2050 is consistent with limiting the 1.5℃ overshoot (IPCC, 2019).

While a shift to cleaner, zero emission transport modes is imperative, solutions to the climate crisis must also address the increased vulnerabilities created by extreme weather events such as high temperatures and flash floods that encourage automobile dependency and discourage active travel modes. When exposed to these events, residential neighborhoods, streets, roads, and public spaces significantly impact daily life. Reducing the exposure of people, buildings and vegetation to these events can have a profound impact on overall mobility. As a result, walkability, being the most sustainable solution, has been a fundamental design and research objective for urban designers.

Past investigations have revealed that extensive use of asphalt, impervious cover, lack of appropriate vegetation, improper maintenance of natural drainage in cities

increase susceptibility to climate extremities (Erkaya, 2022; Yuksel & Yilmaz, 2008; Cicek & Dogan, 2006). The thermal and morphological characteristics of urban surfaces, loss and fragmentation of natural areas, seriously affect urban climate, which may cause cities to be warmer than surrounding areas. This phenomenon is known as the Urban Heat Island (UHI) effect and its intensity varies based on land cover configuration, construction materials, and urban form.

In the face of extreme heat events, which are further catalyzed by anthropogenic climate change, rising urban temperatures can have a direct and important impact on UHI intensities, local climate and can further intensify inner-city urban microclimates. Moreover, longer and hotter summers are a deterrent for citizens to living outdoors. Thermal comfort is one of the main factors affecting pedestrians' positive association with walking in the city, and improving thermal comfort enhances walkability (Nasrollahi et al., 2020). As a result, designing thermally comfortable microclimates in urban areas is extremely important as well.

In recent years, Ankara has experienced a rise in flash floods which have caused destruction of social and economic infrastructures, loss of human lives and degradation of the natural and physical environment. In addition, heat exchange between hard surfaces also contributes to increase in Land Surface Temperature (LST). Since Ankara has unique geomorphological characteristics and relatively more organized urbanization patterns, it presents an interesting case for exploration and analysis.

The case of Ankara is representative of many other cities which need to effectively address three inter-related urban challenges: 1) an intensely densifying city that needs to urgently integrate climate information for sustainable and resilient urban planning; 2) Rising summertime temperatures and the consequent impact on pedestrian thermal comfort; and 3) the projected amplification of such events in the face of climate change.

To address these challenges, sustainable smart cities use communication and information technology. The increased use of real-time monitoring, crowd-sourcing initiatives and sensors have facilitated the availability of large spatial data sets. Advances in urban level geoscience and spatial data analytics have facilitated new means to analyze and visualize spatial data (Goodchild and Haining, 2004).

What is required, therefore, is to push for, and adopt digital innovation, and to re-think the way city planning and mobility is guided. Leveraging the advances in spatial data analytics and geoscience is one of the key contributors in achieving the Sustainable Development Goals (SDGs) (Sachs et al.,2019). The practice of urban planning can benefit greatly from urban analysis tools, such as Geographic Information System (GIS) software, and remote sensing techniques to perform necessary risk assessments and high-level geographical analysis for increased accuracy in data interpretation.

On the other hand, the availability of large-scale spatial data is not equally distributed across different regions. Despite the availability of GIS and Earth Observation (EO) tools, access to consistent and high-quality environmental and geospatial data remains a significant challenge for supporting decision-making processes (Guigoz et al., 2017). Statistical data is extremely varied between municipalities, based on different organizations and time periods. Spatial analyses require an integration of data from different sources and of multiple scales or granularities to achieve consistent and dependable results. Lack of standardization and unclear data collection procedures in spatial analysis and urban computing processes pose a potential risk on the reliability of achieved results (Casali et al., 2022).

Exploring the interdependencies between urban heat dynamics and its impact on humans' associations with walking outdoors requires data-informed urban design strategies to effectively mitigate heat at macro-, meso- and micro-scale.

This thesis focuses on investigating the relationship between urbanization, vegetation, and land surface temperatures in Ankara by monitoring their spatial and

temporal patterns at multiple granularities, using only open-source data. Temporal mapping method enables an examination of the above-mentioned features over time. This initiates an in-depth understanding of the relationship between urban heat parameters as contributors to thermal comfort associated walkability in the city. In this way, this thesis highlights the importance of macro-, meso- and micro-level assessments to propose appropriate urban design strategies specific to the intrinsic nature of cities (spatial configuration and distribution), urban microclimates, and external influences (e.g., seasons, overall climate, landscape typology).

For this study, time series Landsat (TM, ETM+ and OLI and TIRS) satellite data products were employed to quantify the spatio-temporal LST and NDVI for the years 1990, 2000, 2006, 2012, 2018 and 2021. For the same years and geographical boundaries, CORINE Land Use/Land Cover maps were extracted.

A cross-comparison of these maps and quantification of land-use changes creates a GIS-based screening method to reveal the composition and configuration of critical land types and urban design features (e.g., green infrastructure elements, urban surfaces, construction materials, tree morphology) that contribute to extreme heat conditions and thermal discomfort. It also facilitates the identification of key areas where design strategies for improved walkability conditions and climate resilience must be implemented. Additionally, combining GIS analysis and climate simulation tools for a spatio-temporal analysis across multiple scales further improves the validity and reliability of the research outcomes.

1.2 Research Objectives

With the aim to present novel lessons for other cities, the city of Ankara is addressed through a ‘human-centered’ approach to build upon the existing literature in making contemporary cities more thermally resilient and sustainable in an era of climate change.

Through support from a detailed literature review of systematic walkability assessments, this research highlights key methods of analysis and walkability associations. Among the many parameters of a walkable environment, this study particularly seeks to layer key information specific to thermal comfort and how it is related to urban heat dynamics which are further aggrandized by the emergence of extreme climate events.

One of the research objectives is to evaluate factors of peak summer-time Land Surface Temperature in Ankara from 1990 to 2021, through an analysis of land use configuration and composition at multiple scales. At the macro-level, this research examines Ankara within its provincial administrative boundaries and the macroform limits of Ankara city. At the meso-scale, this research studies the largest district of Ankara, i.e., the Çankaya district, while at the micro-scale, it examines Çayyolu sub-district, which is also one of the largest sub-districts of the city with a fast-growing urbanization trend over the last two decades.

This study also aims to quantify the change in built-up and natural areas to initiate a deeper understanding of urban heat parameters. As a focal point, key street segments in Çayyolu are analyzed with respect to different urban blocks, vegetation distribution and urban design characteristics to better understand their impact on LST.

Another significant objective of this thesis is to propose a generic method of geo-spatial analysis using public, open-source data that can be applicable to any spatial context.

1.3 Research Questions

To pursue the objectives of this research, three research questions were derived:

1) How can urban heat assessments inform urban design strategies for thermally comfortable walkable environments?

2) How can climate resilience be incorporated in pedestrian-oriented urban design?
3) How can we accurately produce thermal maps in urban design?

Based on these questions, this study focuses on five objectives:

- The first one is exploring the factors of walkability, explaining how walkability can be assessed and the significance of thermal comfort as a factor of walkability perceptions and pedestrian behavior.
- Explaining how urban heat parameters relate to urban microclimates by re-contextualizing thermal comfort and how it can be influenced by macro-, meso- and micro level urban design strategies.
- The third is exploring remote sensing techniques and existing research, which employ open-source data to produce high-level, geospatial mapping of urban heat, land use/land type and vegetation health.
- The fourth is developing a multi-scalar analysis method to produce temporal maps of Ankara for the years 1990, 2000, 2006, 2012, 2018 and 2021 to reveal urban heat island hotspots through LST, Normalized Difference Vegetation Index (NDVI) and Land Use/Land Cover (LULC) maps. The first level will analyze Ankara province. The second will analyze metropolitan Ankara. The third scale will be analyzing the Çankaya region. Within Çankaya, a finer analysis of the district of Çayyolu will focus on revealing the impact of land use and land-type on urban heat phenomenon within new and emerging neighborhoods.
- Finally, microclimate conditions of selected main arteries of Çayyolu will be analyzed in terms of street features, building blocks along main arterial roads, urban design characteristics and tree configurations to reveal their impact on pedestrian thermal comfort.

1.4 Structure of the Thesis

This thesis is composed of seven sections. The following chapter provides a literature review of existing studies relating to walkability parameters and their impact on pedestrian behavior. It also highlights the significance of thermal conditions of walkable public areas and an overview of heat associated climate extremities in cities. It concludes with a description and summary of geospatial data analysis methods and remote sensing techniques to derive urban heat variables. It defines key concepts including walkability, thermal comfort, urban heat, climate hazards, remote sensing, and urban heat indicators.

The next chapter focuses specifically on the dynamics of climate and comfort by explaining thermal comfort in relation to urban microclimates and summarizes the most relevant climate-responsive, urban design strategies in order to generate scale by scale associations with walkability.

The fourth chapter focuses on the data acquisition process and methodology, i.e., the author's choice of study area, the selected time periods, and scales. It further describes the GIS workflow, environmental modelling tools, remote sensing techniques and the algorithm used to calculate the maps.

The fifth chapter describes the results and derived statistical data. The results are presented in the form of maps and quantifications of the findings to increase comparability and readability of the results.

The sixth chapter presents an in-depth interpretation of the results by lending support from the proposed multi-scalar urban design strategies summarized in the literature review. Finally, the seventh chapter discusses the implications of the findings for future research and urban planning. It also proposes improvements to the proposed methodology in the thesis and how future research can build on the learnings from this exercise.

CHAPTER 2

ASSESSING WALKABILITY AND URBAN HEAT

Walkability is one of the crucial contributing factors of urban environments. Assessing walkability has been widely studied and a thorough body of literature has laid the foundations for future research. This chapter aims to establish a theoretical background through a review of scientific research studies that provide a cross-section of walkability and climate related risks facing cities today.

Walkability cannot be treated as a singular concept. It is, in fact, a multi-level concept which has been the subject of several studies in public health and urban design. A review of walkability literature reveals that 'walkability' has several definitions, some holistic and some very specific. What is most walkable is determined by the purpose behind it (Forsyth, 2015).

A diverse set of methodologies to study walkability have been applied over the last decade. Several metrics to measure walkability have been developed in different geographical locations around the world and in varying scales. Since the concept is multi-scalar and multi-factorial, a diverse body of literature already contains several reviews of walkability research to guide future studies. Existing systematic reviews of walkability provide a strong base for this chapter.

The chapter begins with an overview of walkability associated studies which are categorized according to walkability factors. Each section describes relevant research methodologies that shape the theoretical knowledge and scientific contribution of this thesis. It also discusses the main findings of the studies and the relationship between variables. Finally, a table systematically summarizes the methodology, main findings, and variables of each study.

The second section of this chapter includes an overview of climate effects on walkability, and a summary of prominent climate-related threats namely, urban flooding and rising urban temperatures. It describes the UHI phenomenon in detail, and then explains how remote sensing technologies can be utilized for the assessment and visualization of urban heat.

2.1 Factors Affecting Walkability

Walking behavior includes the choice of walking as a transport mode over other modes, walking frequency and walking time. The decision to walk as a preference over other transportation modes represents the results of an interaction between the person and the walking environment (Liu et al., 2016). In urban design, pedestrian behavior is influenced by subtle qualities of the environment (Belge, 2020).

Environmental interventions aiming to improve activity-friendliness in neighborhoods may not result in desired pedestrian behavior if individuals' perceptions of their environment discourage activity (Boehmer et al., 2006). As summarized in Figure 2.1:, Liu et al. (2016), assumes that overall perceived walkability and walking environmental perceptions mediate between objective measures of walking behavior and the walking environment.

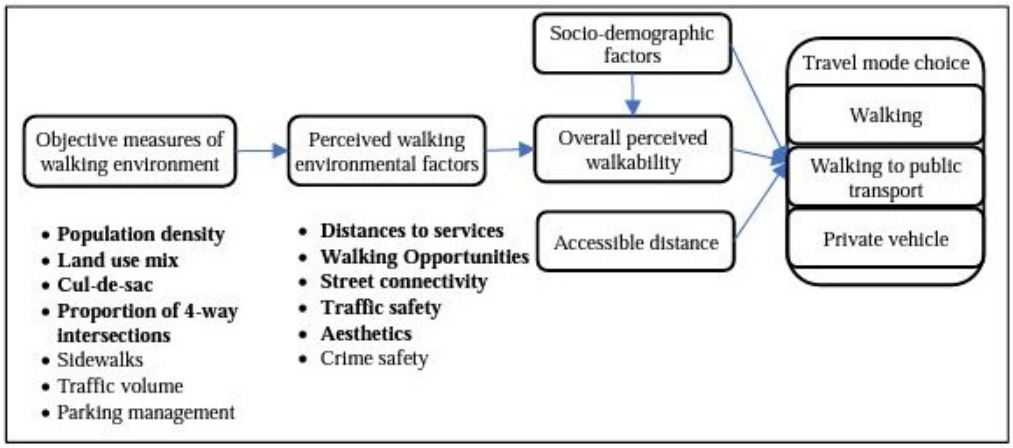

Figure 2.1: Conceptual Model of Walkability factors (Liu et al., 2016)

Subjective measures of the walking environment are self-reported perceptions of the pedestrian environment (Liu et al., 2016). For example, the provision of pedestrian crossing facilities is important in mediating the perceived threat of traffic in walking routes. Objective measures of the pedestrian environment are associated with measuring urban form and urban design characteristics using either field data or existing spatial and land use databases (Liu et al., 2016).

As Figure 2.1: illustrates, objective measures of the walking environment can include land use mix, sidewalks, traffic volume, population density, and parking management. For example, good sidewalk conditions are one of the top priorities of a pedestrian. Sidewalk conditions can be operationalized as presence or continuity of sidewalk, quality of sidewalk (absence/presence of sidewalk), and sidewalk width (Shatu et al., 2019).

Moreover, an individual's socio-demographic characteristics such as age, income, gender, household car ownership have also been found to affect their walking behavior. As a result, socio-demographic factors may influence both the ways an individual perceives within the environment and how they combine into perceived overall walkability. However, they may also influence walking behavior through

other mechanisms, such as, walking motivation and intention, and the availability of alternative modes of transport (Liu et al., 2016).

Increasing the diversity of destinations can contribute to adults engaging in more transport-related walking and achieving recommended levels of physical activity (McCormack et al. 2007). However, current land development patterns and urban sprawl have resulted in increased distances between homes and destinations, lower density suburbs, and disconnected street patterns. These environmental features result in fewer transport-related walking trips, fewer recreational walking trips and less recreational physical activity (Frank and Engelke, 2001, Frank et al., 2003).

Walking is a complex behavior and pedestrians' walking experience, and route choice is affected by various factors. Lee and Shepley (2020) couple student surveys with sketch maps to discover walking route components relating to user perception and evaluation, which influenced route choice. Safety is considered the most important factor. Other factors include sidewalk quality and attractiveness of the built environment.

The following sub-sections are categorized according to the most significant walkability factors and the methods of analysis utilized by the cited researchers.

2.1.1 Safety

Safety is one of the most significant and recurring factors found in walkability literature since pedestrians are among the most vulnerable road users. For areas to be considered 'walkable', improving pedestrian safety can have a positive impact on walking for both transport, and leisure (Chong et al., 2022).

Fyhri et al. (2011) write that feelings of unsafety in pedestrians can be related to fear of accidents as well as fear of violence, crime, or interaction with strangers. Perceptions of insecurity and overall built environment characteristics are key determinants in pedestrians' assessment of walking in the city. The lack of safety culture among the population, and the design of built environment characteristics

favoring motorized transport over pedestrians and bicyclists are some of the prominent explanations for negative associations of safety perception (Villaveces et al., 2012).

According to Villaveces et al. (2012), modifications in the pedestrian environment, such as improved access for pedestrians, widened sidewalks and increased protocols like traffic calming measures for motor vehicles for modified bus rapid transit areas may encourage walkability. Table 2.1 illustrates the perceptions of safety and traffic, safety and crime and acceptable urban characteristics among pedestrians who frequently engage in walking activities. For example, in areas where participants felt their personal safety threatened, traffic-calming measures were reportedly inadequate.

Table 2.1: Perceptions of traffic safety, personal safety, and urban structure by neighborhood residence status among pedestrians who frequently walk. (Villaveces et al., 2012)

	Residents		Non-residents		Pearson χ^2
	Disagree* No. (%)†	Agree No. (%)	Disagree No. (%)	Agree No. (%)	p Value‡
Perceptions of safety and traffic					
Too much traffic	12 (7.9)	140 (92.1)	12 (7.8)	142 (92.2)	0.973
I like walking in this street	60 (39.5)	92 (60.5)	52 (34.2)	100 (65.8)	0.342
I'm forced to walk here due to traffic	123 (82.5)	26 (17.5)	130 (84.4)	24 (15.6)	0.662
Traffic here is slow. Too much traffic	81 (53.6)	70 (46.4)	79 (51.3)	75 (48.7)	0.682
Most drivers exceed speed limits	43 (28.7)	107 (71.3)	51 (34.0)	99 (66.0)	0.319
Pedestrian signals are adequate here	110 (72.9)	41 (27.1)	81 (52.3)	74 (47.7)	<0.001
Signals here make me feel safer	106 (70.2)	45 (29.8)	80 (51.6)	75 (48.4)	0.001
There is too much pollution here	49 (32.7)	101 (67.3)	74 (48.1)	80 (51.9)	0.006
This street is easy to cross	95 (62.9)	56 (37.1)	89 (57.4)	66 (42.6)	0.326
Perceptions of safety and crime					
Streets are well lit at night in this neighbourhood	62 (42.2)	85 (57.8)	39 (39.8)	59 (60.2)	0.711
There is a lot of crime in this neighbourhood	51 (34.7)	96 (65.3)	65 (48.9)	68 (51.1)	0.016
It is unsafe to walk here during the day	97 (63.8)	55 (36.2)	103 (69.1)	46 (30.9)	0.329
It is unsafe to walk here at night	29 (20.4)	113 (79.6)	32 (27.1)	86 (72.8)	0.205
Perceptions of urban characteristics that respondents considered acceptable in neighbourhood					
No of pedestrian crossings of any type	90 (61.4)	56 (44.1)	72 (50.0)	72 (50.0)	0.046
Vehicular access to this street	26 (17.5)	123 (82.5)	41 (27.3)	109 (72.7)	0.040
Access to public transportation in this street	18 (11.9)	133 (88.1)	33 (21.6)	120 (78.4)	0.024
Time to travel in vehicle through this street	28 (18.5)	123 (81.5)	37 (24.5)	114 (75.5)	0.208
Time to walk through this street	40 (26.5)	111 (73.5)	37 (24.2)	116 (75.8)	0.644
Street cleanliness	72 (47.7)	79 (52.3)	48 (31.0)	107 (69.0)	0.003
Noise in this street	112 (74.7)	38 (25.3)	103 (66.5)	52 (33.5)	0.116
No of restaurants	36 (24.6)	110 (75.4)	67 (47.2)	75 (52.8)	<0.000
No of supermarkets and markets	26 (17.5)	123 (82.5)	51 (35.7)	92 (64.3)	<0.000
No of shops	44 (29.7)	104 (70.3)	63 (43.2)	83 (56.8)	0.017
No of schools	39 (27.1)	105 (72.9)	59 (49.2)	61 (50.8)	<0.000
No of bars, discos and clubs	66 (48.2)	71 (51.8)	53 (43.1)	70 (56.9)	0.411
Overall safety	93 (61.6)	58 (38.4)	78 (51.7)	73 (48.3)	0.082
Police and security services	99 (66.9)	49 (33.1)	96 (64.4)	53 (35.6)	0.655

*Disagree includes strongly disagree and disagree; agree includes strongly agree and agree.
†Percentages may not add due to rounding.
‡Statistical significance at values less than 0.05.

On the other hand, ‘perceived safety’ vs ‘actual crime risk’ or ‘fear of crime’ should be treated separately (Jansson, 2019). According to Hinkle (2014), treating all kinds of fear and perception of safety by the same principles endangers the research outcomes and affects the potential for more efficient policies in planning.

While an individual pedestrian’s perceptive experience is difficult to measure, there are certain environmental factors that can enhance the overall experience. A common method to measure perceived safety is to ask travelers or pedestrians if they would “feel comfortable” in a certain situation (Bigazzi et al., 2021).

Chiang et al. (2017) demonstrate a quantitative approach by defining safety through two attributes: ‘Social Safety’ and ‘Traffic Safety’. Social safety is indicated through the presence of graffiti, abandoned houses or cars, pedestrian flow volume, and security of the surroundings. Meanwhile, vehicle flow volume, road safety and traffic signs are attributed as indicators of ‘Traffic Safety’.

Safety features are commonly assessed using surveys, demographic data, or observer audits. Each of these methods has benefits and limitations. For example, attributes associated with perceived safety rely heavily on self-reported values which may result in personal biases. Performing surveys in areas with a high crime rate may even endanger the survey personnel. To perform a large-scale survey, the researcher is met with many practical challenges, which is mainly why walkability surveys are confined to small neighborhoods (Chiang et al., 2017).

As Table 2.1 demonstrates, perceptions regarding safety and crime, are indicated through users’ perception of crime in their neighborhood, adequate nighttime lighting and how unsafe it is to walk during the day vs. in the night (Villaveces et al., 2012). These are all sufficient in assessing ‘sense of perceived safety’ within a systematic assessment of overall perceived walkability. In this sense, the concept of safety is subjective to the scope of the research and intended research outcomes.

2.1.2 Proximity and Mix of Destinations

A walkable environment must provide several intersections between connectivity and different utilities and amenities. Walking trips must not be too long and paths to desired destinations must be relatively direct. Unbalanced growth and planning can create barriers for walkability, where car-oriented spaces take priority, while sidewalk quality is neglected. This often leads to the creation of vibrant pockets where walking is beneficial while the rest of the city is barred from urban vibrancy and liveliness (Zook et al., 2012).

Multiple facilities in a developed urban area encourage active travel for its residents and visitors. Walking becomes an accessible, utilitarian tool to travel between homes, recreational spaces, and retail services, as well as institutions such as schools, offices, community centers and places of worship. Having such services close to one another in compact communities leads to individuals walking up to 2.5 times more than those residing in sparse communities (Baobeid et al, 2021).

King et al. (2015) investigate the effect of proximity to and mix of destinations on walking frequency in Melbourne, Australia. The sample is comprised of 2349 respondents who reside in 50 urban areas. For each survey respondent, a network buffer of 400m, 800m and 1200m was calculated from their place of residence. The locations frequented by the respondents were used to create destination variables, classified into seven different categories. Their analysis reveals the destination counts within the network buffers from each of the respondents' homes. Exposure variables generated for each type of destination include education, café/takeaway stores, transport stops, supermarkets, sports facilities, community resources and small food stores (Table 2.2).

The results conclude that a greater number of destinations and greater destination mix has positive associations with walking frequency. The incentive to walk strengthens when a higher range of tasks and other activities can be performed in a single trip. The study also highlights the effect of walking distance on walking

frequency. By measuring the distribution of destinations within three distinct walking buffers, this exercise further strengthens the possibility of measuring destination mix – a crucial factor for assessing walkability. The study found that increasing the intensity of destinations in areas where they are more dispersed, and or planning neighborhoods with greater destination intensity may increase residents' likelihood of being sufficiently active.

However, the type of destination can alter this relationship. Destinations which support or enable social interaction are the most positive markers of high walking frequency. Also, local destinations within a 10-minute walking radius have greater associations with walking frequency (King et al., 2015).

Table 2.2: Summary of Exposure Variables highlighting the destination types most positively associated with walking (King et al., 2015)

Exposure variable	Buffer (m)	Mean (SD)	Range	Median (IQR)	Variable type (modelled as):	Category cut points		
Education	400	0.59 (0.97)	0–7	0 (0, 1)	Binary	0	1+	
Education	800	2.31 (2.31)	0–14	2 (1, 3)	Tertile	0–1	2–3	4+
Education	1200	5.05 (3.77)	0–20	4 (2, 7)	Tertile	0–3	4–6	7+
Café/takeaway stores	400	0.71 (1.59)	0–16	0 (0, 1)	Binary	0	1+	
Café/takeaway stores	800	4.69 (8.55)	0–56	1 (0, 5)	Tertile	0	1–3	4+
Café/takeaway stores	1200	12.14 (15.66)	0–73	7 (1, 16)	Tertile	0–3	4–11	12+
Transport stops	400	3.5 (3.13)	0–18	3 (1, 6)	Tertile	0	1–3	4+
Transport stops	800	13.42 (8.09)	0–45	13 (8, 18)	Tertile	0–10	11–16	17+
Transport stops	1200	29.75 (15.78)	0–81	27 (19, 39)	Tertile	0–23	24–35	36+
Supermarkets	400	0.05 (0.29)	0–2	0 (0, 0)	Binary	0	1+	
Supermarkets	800	0.31 (0.67)	0–4	0 (0, 0)	Binary	0	1+	
Supermarkets	1200	0.80 (1.02)	0–4	0 (0, 1)	Binary	0	1+	
Sports facilities	400	0.20 (0.52)	0–4	0 (0, 0)	Binary	0	1+	
Sports facilities	800	0.78 (1.05)	0–5	0 (0, 1)	Binary	0	1+	
Sports facilities	1200	1.72 (1.56)	0–8	2 (0, 3)	Tertile	0	1–2	3+
Community resources	400	0.51 (1.01)	0–5	0 (0, 1)	Binary	0	1+	
Community resources	800	2.54 (2.97)	0–15	2 (0, 4)	Tertile	0–1	2–3	4+
Community resources	1200	5.99 (5.56)	0–31	5 (1, 9)	Tertile	0–2	3–7	8+
Small food stores	400	0.71 (1.70)	0–17	0 (0, 1)	Binary	0	1+	
Small food stores	800	4.23 (6.13)	0–55	2 (0, 5)	Tertile	0	1–2	3+
Small food stores	1200	10.48 (11.28)	0–58	7 (2, 15)	Tertile	0–3	4–11	12+

Although King et al., (2015) provide a thorough assessment of type, frequency and proximity of destinations as key parameters affecting walkability, the study lacks visual data. While the results provide significant guidance to urban planners like prioritizing planning of shops, supermarkets, services, and community resources a map of the GIS based network analysis and supplemental diagrams would have enhanced the quality of the research.

On another note, there may be additional co-relations with the density of street network on walking frequency which could have been included in the GIS analysis phase. For example, a sidewalk assessment (is sidewalk on both sides, on only one side or neither?), shade and shadow analysis, level of traffic at peak times, and possibly a study of measurable visual features which may directly affect motivation to walk. Perhaps this could further elucidate on factors affecting the frequency and type of destinations visited.

2.1.3 Visual Features and Physical Atmosphere

Environments that are perceived to be 'more walkable' and environments that combine walkable design features are considered more walkable (Brown et al., 2007). Relatively fewer studies address whether 'microfeatures' of the perceivable physical environment or immediate environmental cues can contribute positively to the pedestrian experience.

Lynch (1980) writes about the significance of small-scale features in walking environments. In 1959, he had participants of a study walk the distance of five blocks and describe what they noticed. Environmental features during the walking experiment were not left unnoticed – specifically features at the small-scale. Some of the features reported by the participants include focal points such as sidewalk quality, aesthetic quality of buildings in the immediate context and navigational signage (Lynch, 1980).

Brown et al. (2007) compare the experience of two routes (demonstrated as two separate studies; Study 1 and Study 2), each with a mix of low-, mixed- and high walkability segments. For each route, participants met with a guide to be briefed properly, sign a consent form, and fill a demographic questionnaire before travelling to the starting point of the specified route in Salt Lake City, Utah.

Figure 2.2 shows different sections of the route. The first image shows an aesthetically pleasing and highly walkable environment, with retail spaces, attractive storefronts, wide sidewalk with trees and soft buffers between the road and sidewalk. Other sidewalk users are also seen sitting on benches and walking by.

The second image shows a segment with mixed features. While there is a clear, unobstructed sidewalk and grass strip separating it from the road, there is an overall lack of street vegetation and places to sit or relax. The wired fence certainly lowers the attractiveness of the environment and lacks urban design elements necessary for pedestrian comfort. The third image shows the least walkable segment. There is no dedicated space for pedestrians, which indicates that the road is also used by cars. This significantly impacts perceptions of safety among pedestrians and may discourage them from walking.

For the outbound trip, participants were asked to describe their experience in terms of what they like or dislike. The same route was retraced during the return trip after which each participant was asked to fill an 18-item questionnaire. Trained raters performed an environmental audit. In the environmental audit, to determine and characterize the difference between walkability of segments (as shown in Figure 2.2), the trained raters used the Irvine-Minnesota Inventory as a rating system. In this system, environmental walkability features are assessed through four classes; 1) Traffic safety, 2) Crime safety, 3) Pedestrian accessibility and 4) Pleasurability (Brown et al., 2007).

Figure 2.2: Examples of High-, Mixed-, and Low-Walkability Segments (Brown et al., 2007)

The open-ended comments which were recorded by the participants were sorted by applying thematic coding. A trained coder categorized the comments according to three categories – positive, neutral, and negative, based on an analysis of the participants' tones. As a result, seven categories were finalized with an additional eighth which was used to classify ambiguous comments.

According to the audit, high level of traffic and environmental safety, pleasant social conditions, greater mix of destinations, more natural features, pleasant aesthetics, and more frequent pedestrian amenities were observed in the most walkable segment. Table 2.4 shows the subscale scores for the environmental audit.

Table 2.3: Questionnaire Results (Brown et al., 2007)

Questionnaire Closed-Ended Judgments of Pleasant Atmosphere and Traffic Safety by Guided Walk Participants: Coefficient Alpha Reliability Tests and Means by Route Segment

		Route Walkability		
		Low	Mixed	High
Pleasant Atmosphere				
Alpha	Study 1	.80	.91	.93
	Study 2	.85	.90	.92
Mean	Study 1	2.26_a	3.48_b	4.53_c
	Study 2	3.17_a	3.02_a	4.12_b
Traffic Safety				
Alpha	Study 1	.80	.84	.74
	Study 2	.78	.75	.77
Mean	Study 1	3.50_a	4.03_b	3.98_b
	Study 2	3.45_a	3.84_b	3.95_b

Note: Ratings use 5-point scales, where 5 is *most positive*. Within rows, means with different subscripts differ at $p < .05$ by a priori t tests.

Table 2.4: Environmental and/or Social Audit Results (Brown et al., 2007)

Means for the Environmental and/or Social Audit by Four Trained Raters

	Low	Mixed	High	F (2,9)	Partial η^2
Traffic safety	$.61_a$	$.68_b$	$.74_c$	19.02**	.81
Environmental safety	$.89_a$	$.82_a$	1.23_b	119.57**	.96
Social milieu	1.08_a	2.46_b	5.10_c	192.61**	.98
Aesthetics	$.45_a$	$.40_a$	$.75_b$	27.38**	.86
Natural features	$.37_a$	$.49_b$	$.50_b$	11.92**	.73
Pedestrian amenities	.00	$.29_a$	1.29_b	—	
Pedestrian access	1.00	1.06	1.00	—	
Diverse land use	$.43_a$	$.38_b$	$.53_c$	54.92**	.92
Density-building height	2.50	1.75	2.00	.33	.07

Note: Higher scores indicate more walkability. Zero variance cells for Access and Amenities preclude F tests. Amenities mixed vs. high $t(6) = 16.97$, $p < .01$. Within rows different subscripts indicate where means differ, with Tukey's post hoc tests at $p < .01$ level, except "Traffic Safety" where $p < .05$. $N = 4$.
*$p < .05$. **$p < .01$.

Table 2.5: Open-Ended Remarks Summarized (Brown et al., 2007)

Open-Ended Remarks: Net Positivity About Each Segment of the Walk

	Study 1					Study 2				
	Walkability of Segment					Walkability of Segment				
	Low	Mixed	High	F(2,38)	Partial η^2	Low	Mixed	High	F(2,74)	Partial η^2
Traffic safety	−.19	.05	−.10	0.57	.03	−.31	.26	−.05	4.39	.11
Environmental safety	-1.24_a	$-.48_a$	$.62_b$	8.26*	.30	$-.59_a$	-3.10_b	1.13_c	40.57*	.52
Attractiveness	$-.10_a$	$.38_a$	2.86_b	17.16*	.48	1.28_a	$.92_a$	4.72_b	19.34*	.34
Social environment	-1.19_a	−.19	$.29_b$	8.15*	.30	$-.36_a$	$-.31_a$	1.41_b	13.52*	.29
Pedestrian amenities	.05	.38	.57	1.86	.09	$.44_a$	$.31_a$	2.54_b	34.67*	.48
Pedestrian access	−.24	.33	.38	2.93	.13	.00	.13	.15	0.85	.02
Land use	.05	.00	.00	0.12	.01	.67	−.03	.87	6.84	.16

Note: Scores are number of positive comments minus number of negative comments. All F values represent the main effect for segment except for Study 1, social milieu, which shows the linear trend, $F(1, 19) = 8.15$. With alpha set at .05, Bonferroni adjustments for the seven variables yield a critical value for Study 1 of $F_{crit} = 8.09$, and for Study 2, $F_{crit} = 7.68$ (Maxwell & Delaney, 2004). Within each row and separately for each study, means with different subscripts differ at $p < .05$ by two-tailed a priori t tests. Hunyh-Feldt adjusted degrees of freedom: Study 1, environmental safety (1.51, 28.73); amenities (1.67, 33.30); access (1.70, 32.21): Study 2, environmental safety (1.86, 68.77), amenities (1.39, 51.23); land use (1.82, 67.38). In Study 1, for pedestrian amenities and land use, segment is the only factor, and error degrees of freedom are 40; sex could not be included as a factor because males did not use the category in at least one segment.
*$p < .05$ with Bonferroni adjustment.

This study reveals that pedestrians are acutely aware and sensitive to different levels of walkability within different segments of an intended route. The differences emerged due to the type of facilities, the aesthetic quality of those spaces and the social scene they attracted. Thus, more walkable segments are perceived to be more attractive, well-maintained, vibrant, and overall, more pleasant.

Furthermore, the objective ratings confirmed that more walkable segments had less traffic, fewer environmental incivilities, and a more pleasant social scene, all pointing to more safety indicators (Brown et al., 2007).

It can also be observed, largely owing to the analysis of open-ended comments in this study that, while it is extremely useful to use macro-level GIS analysis, the study of pedestrian experience is also needed so as not to exclude micro-level features which are crucial to the analysis of walkability.

2.1.4 Thermal Comfort

Thermal comfort is one of the most important factors affecting the quality of outdoor environments for pedestrians (Chen et al., 2015). Thermal comfort significantly influences pedestrians' decision to walk. Unpleasant weather conditions and extreme thermal discomfort may discourage outdoor physical activity. The decline in walking and cycling due to thermal discomfort is met with an increased use of private automobiles (Baobeid et al, 2021).

In most walkability frameworks, thermal conditions of the walking environment have been under-investigated, despite the importance of the outdoor thermal environment for pedestrians. This could be due to the complexity of outdoor environments. The advent of simulation tools has led to a significant increase in simulation-based studies of outdoor environments. In the past few decades, studies were based on mainly questionnaires, field observations and measurements. The aim was to examine the causal links affecting human thermal comfort in outdoor environments (Nasrollahi et al., 2020).

From another perspective, an increasing number of studies focus on improving thermal comfort in outdoor urban spaces to enhance citizens' health, wellbeing and to promote outdoor activities (e.g., walking and cycling).

Nasrollahi et al. (2020) identify key parameters affecting pedestrian thermal comfort in outdoor environments, by reviewing approximately 150 studies and subsequently

categorizing heat-mitigation strategies in four categories; 1) Climatic parameters, 2) Shading effects, 3) Green, blue and white surfaces and 4) Psychological parameters.

Thermal comfort parameters are comprised of several climatic factors. Mean Radiant Temperature (T_{mrt}) has the greatest effect on outdoor thermal comfort, followed by wind speed and direction. Therefore, strategies that aim to reduce T_{mrt} are the most effective, such as the use of shading devices and/or shading strategies (Nasrollahi et al., 2020).

Localized, micro-climatic conditions of an urban space, such as wind speed, solar radiation and air temperature greatly affect pedestrians' comfort and behavior. Moreover, green areas play an important role in the city because they provide shade and help to lower surface temperatures (Leuzinger et al., 2010). The presence of trees and vegetation help to reduce air temperatures through the evapo-transpiration process, provide shade and thermal attenuation by dissipating ambient heat. On the other hand, impervious built surfaces, such as asphalt and concrete, absorb, store and re-radiate more thermal energy per unit area than plants or other pervious surfaces (Samira, et al. 2017).

Samira et al. (2017) compare the performance of an area shaded by trees and the effect of the position and characteristics of the tree canopy on thermal conditions and thermal perception of users in Constantine, Algeria.

For this evaluation, five stations were set up with a Multifunction instrument (LM800) and Pho-radiometer HD2302.0 at a height of 1.5 m. Measurements were recorded every two hours from 06:00 to 20:00 hours. Thermal comfort was evaluated using two methods; PMV calculated and T_{mrt} with software RayMan.

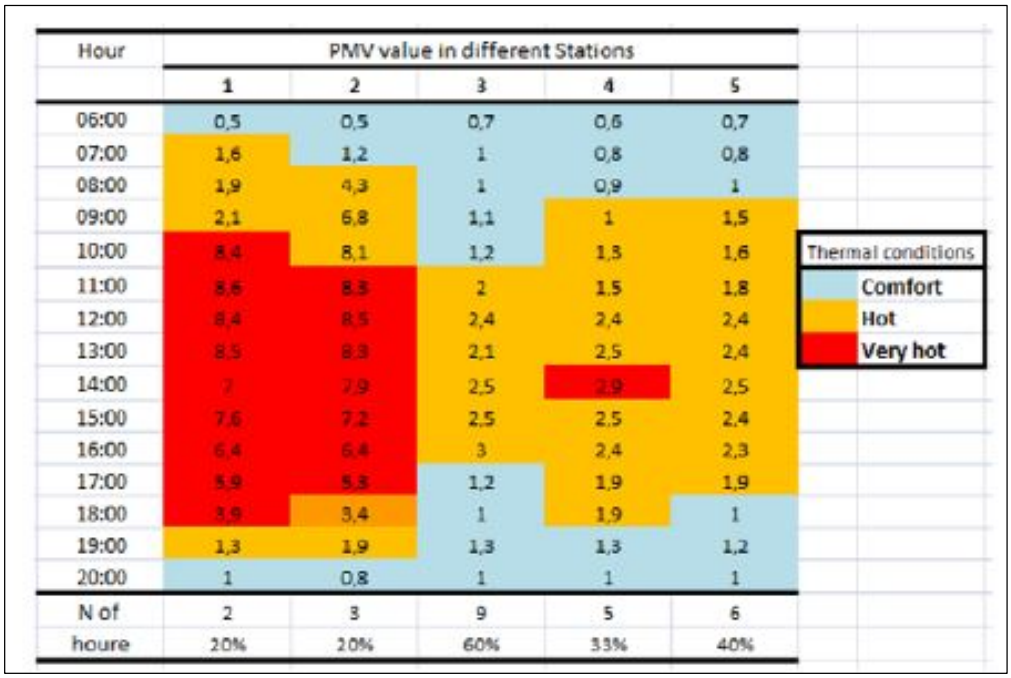

Hour	PMV value in different Stations				
	1	2	3	4	5
06:00	0,5	0,5	0,7	0,6	0,7
07:00	1,6	1,2	1	0,8	0,8
08:00	1,9	4,3	1	0,9	1
09:00	2,1	6,8	1,1	1	1,5
10:00	8,4	8,1	1,2	1,3	1,6
11:00	8,6	8,8	2	1,5	1,8
12:00	8,4	8,5	2,4	2,4	2,4
13:00	8,5	8,8	2,1	2,5	2,4
14:00	7	7,9	2,5	2,9	2,5
15:00	7,6	7,2	2,5	2,5	2,4
16:00	6,4	6,4	3	2,4	2,3
17:00	5,9	5,8	1,2	1,9	1,9
18:00	3,9	3,4	1	1,9	1
19:00	1,3	1,9	1,3	1,3	1,2
20:00	1	0,8	1	1	1
N of houre	2	3	9	5	6
	20%	20%	60%	33%	40%

Figure 2.3: PMV values for 5 stations (Samira et al., 2017)

As Figure 2.3 demonstrates, station 1 (P1) and station 2 (P2) revealed only two hours of comfort in the recorded timeframe. This is mainly due to the incident solar radiation in these locations with negligible shade. P3, P4 and P5 depicted more comfort since solar radiation in these locations is significantly reduced, due to the shade provided by existing tree canopy.

Samira et al. (2017) also used Townscope 3.2 to simulate and assess external thermal comfort by: 1) Changing the position of trees, and 2) Varying the tree canopy sizes.

Urban trees offer a variety of benefits including shade, thermal attenuation, and comfort (Samira, et al. 2017). As Figure 2.4 and 2.5 demonstrate, an introduction of a row of trees reduces global radiation by approximately half an hour, and produces shade, which increases comfort. Moreover, a row of trees also reduces the temperature of surrounding air by 2°C. The results reveal that vegetation has a significant influence on human sensation and PMV. Therefore, tree coverage, canopy size, configuration of space – in terms of degree of enclosure, DoE, and sky

view factor (SVF), are some of the most important indicators when assessing thermal comfort (Samira et al., 2017).

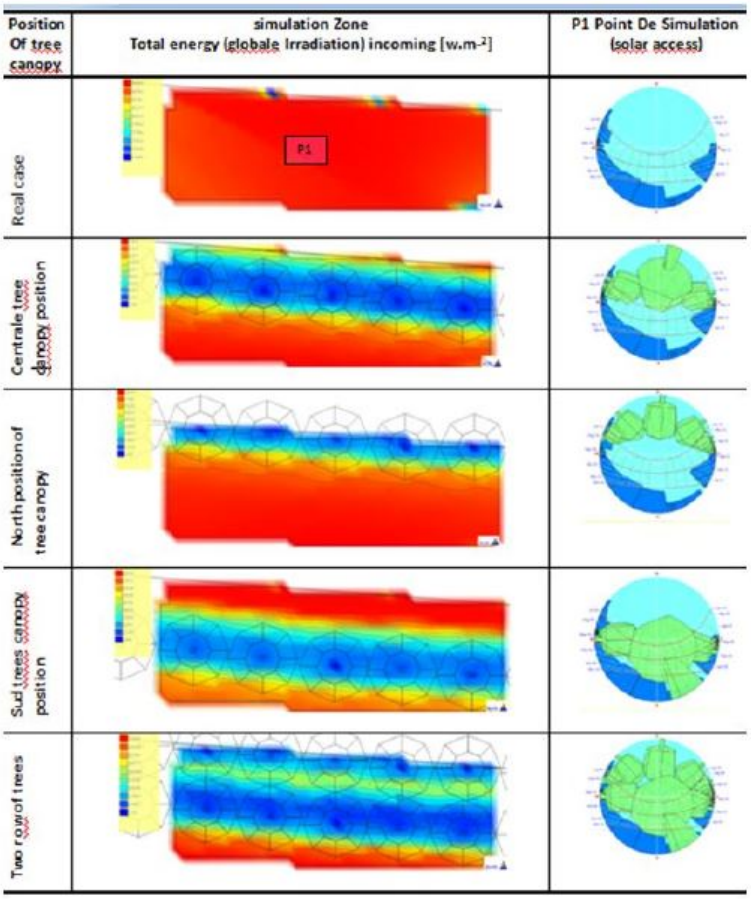

Figure 2.4: Simulation results for various positions of tree canopy (Samira et al., 2017)

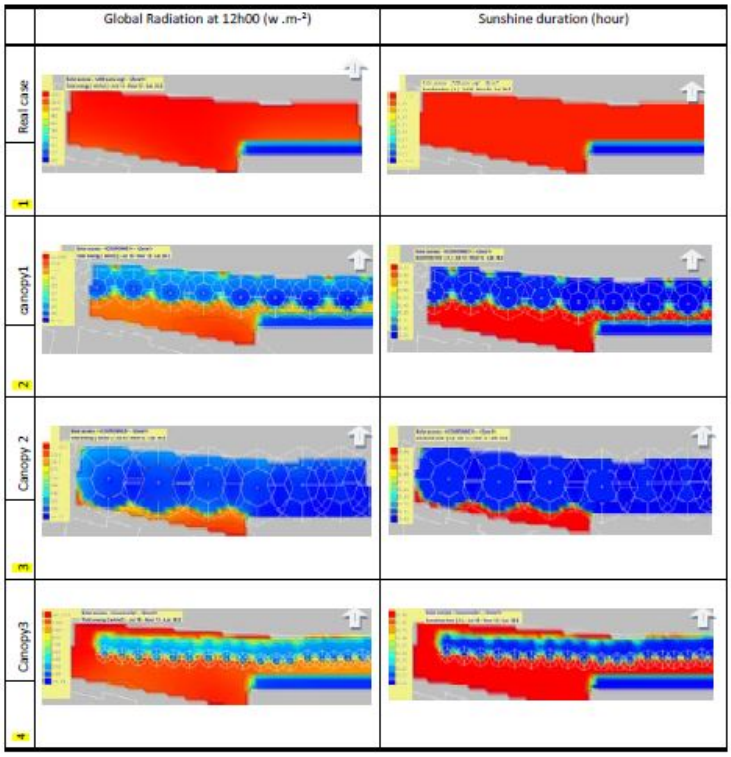

Figure 2.5: Simulation results of various tree canopy sizes (Samira et al., 2017)

Figure 2.6: A Street Covered by Dense Tree Canopy Providing Ample Shade (Mouzon, 2020)

Conclusions derived from this study indicate that tree canopy and its effects depend on tree cover, geometry, incident sunlight and meteorological conditions. Figure 2.6: exemplifies ideal walking conditions with respect to tree canopy and the shade they provide. A dense tree canopy not only provides shade but also creates microclimatic conditions such as indirect, filtered sunlight which reduces direct exposure to harmful UV rays and overheating. In general, there is a positive correlation between shade trees and thermal comfort.

Understanding the effect of the built environment on pedestrian thermal comfort is still limited. Weather challenges are extremely varied across the globe, in terms of temperature, wind speed and relative humidity. Thermal measurements recorded by weather stations but do not accurately represent the thermal sensation of a pedestrian environment and how it is affected by microclimate features such as shade, sunlight, vegetation, and thermal mass of the built environment. As a result, heat mitigation strategies are globally diverse, and their implementation is highly specific to the type of climate. For example, in hot climates, shading, white surfaces and broad leaf vegetation are some strategies that positively impact thermal comfort (Baobeid et al, 2021).

2.1.5 Topographical Features

Urban terrain and sloped streets are one of the key features of physical environment which may affect walking activity. This applies to not just older age groups, but also to the younger population. While city streets may not have an elevation steep enough to discourage active travel, it may still demotivate people to walk a certain distance (Sun et al., 2015).

A sloped urban environment can affect spatial awareness of pedestrians by possibly limiting their line of vision. Similarly, the extra effort required to walk on a sloped path may influence route selection (Greenber et al., 2019). While sloped paths may not increase the distance travelled, they may be perceived as barriers. According to

a study conducted on a hilly campus in Hong Kong, pedestrians tend to overestimate the time it takes to travel uphill, which may be a result of distorted spatial awareness and insufficient knowledge of the built environment (Sun et al., 2015).

To quantify the influence of slope on walking attractiveness, Meeder et al. (2017) used pedestrian counts and data from public transport ridership counts in the city center of Zurich, Switzerland to create a logit model and report its findings. The results suggest that a slope increase of merely 1% results in making the walk approximately 10% less attractive (Meeder et al., 2017).

For older adults, there is a positive relationship between physical activity levels and environmental characteristics. According to a study conducted in 2016, Tanaka et al. found that elderly women living in sloped areas had lower levels of physical activity than those living in flatter locations.

2.2 Review of Walkability Literature

A review of the walkability associated literature in this thesis is summarized in Table 2.6.

Table 2.6 Systematic review of walkability literature

Walkability Parameter + *Location/Scale*	**Research Objective**	**Variables**	**Data Gathering Methods/Tools**	**Data Analysis Methods/Techniques**	**Main Findings**	**Paper Reference**
Presence and Mix of Destinations *Western Australia*	To analyze the relationship between physical activity and proximity and mix of destinations in neighbourhood	Physical activity, destinations present, destination mix, sex, age, education, number of dependents, area level social disadvantage, body mass index (BMI)	Face-to face interviews and follow-up telephone surveys (n=1394)	Physical activity data (n=1394) analyzed, presence and the mix of destinations (within 400 and 1500 m distance from respondents' residences).	1) Proximity and mix of destinations heavily influence walking as a utility, but not walking for recreation or walking for vigorous activity. 2) A greater destination mix may contribute to an increase in physical activity	McCormack et al., (2008)
Built environment characteristics and perceived walkability *Taiwan*	Investigate the relationships between objective and subjective measures of walking environments, walkability and walking associated behaviour.	1) Overall perceived walkability 2) Travel mode choice	Online survey, GIS data, Taiwanese Socio-economic Database, the Taiwanese National Land Surveying Database, and the Taiwanese Traffic Network Digital Map.	Factor analysis (to extract walking environment factors from the 21 indicators) and creation of a generalized structural equation model (GSEM) to verify the hypotheses	1) Objective measures of land-use mix, the number of 4-way intersections and cul-de-sacs, population density, influence perceptions of on-street barriers, distances to services, street connectivity, aesthetics. 2) An individual's perceptions of the walking environment shape overall walkability. Overall walkability increases chances of walkability as preferred travel mode.	Liu et al., (2016)
Subjective street environment data *Brisbane, Australia*	Investigate the relevance of subjective data as a less-expensive proxy for objective data + identifying factors affecting the degree of discordance between them	Subjective street environment data 13 seemingly related street environment variables	Pedestrian-intercept interviews (n=178) , virtual audit and spatial analyses.	1) '% agreement' and 'Kappa coefficent' used to test the agreement between 13 variables of the street environment. 2) Multinomial logistic regression models estimated for each variable in order to test level of agreeability between different factors.	1) Low level of agreeability between objective and subjective attributes. 2) All groups are at-risk of being mismatched, and require implementation of population-based policy interventions to improve perceptions. 3) Subjective measures assess different aspects of the built environment than those measured objectively.	Shatu et al., (2019).

Walking route characteristics *A university campus in Daejoen, South Korea*	To find sustainable design solutions for a walkable environment through an analysis of pedestrian perception and behavior	Walking environment features, smartphone walkers, walkers without smartphone	Student sketch maps, survey questionnaires, and observations and measurements of route features	Multiple statistical tests and models (ANOVA, Wilcoxon test, Friedman's test)	1) "Smartphone walkers" focus more on safety and quality of walking routes, while walkers without phones are more concerned with shortest distance and positive walking experience as significant factors in their route selection. 2) Campus-built environments need improvement by providing solutions that adapt changes in pedestrian behavior and perception.	Lee & Shepley (2020).
Perceptions of safety (and security)	To examine two risk types influence pedestrian behaviour: the risk of being victim of violence, criminal offences, or threats and the risk of being involved in an accident through empirical research	Pedestrians' risk perception, pedestrian decisions before and during walking activities	(not specified)	An overview of theoretical approaches to the psychometric paradigm, risk perception, and the affective approaches to decision-making	1) Feelings of unsafety can be associated with fear of crime, strangers and violence and fear of meeting with accidents. 2) The relationship between the perception of the physical and walking and social environment seemingly depend on the attributes under consideration. 3) Women, the elderly, ethnic minorities and the underprivileged are the most discouraged by fear as a deterrant for walking.	Fyhri et al., (2011).
Perceptions of safety *Cali, Columbia*	To study pedestrians' perceptions of safety and walkability of the urban environment	Common deterrants for pedestrians, built environment factors of walkability	Standardised intercept interviews (n=400) of pedestrians in 20 urban zones (random selection), focus groups	Quantitative data analysis	1) Public transport access is the most positive feature of built environment. 2) Personal safety, lack of respect for norms, and built environment characteristics are the main pedestrian concerns. 3) Frequent obtruction by motor vehicles and narrow sidewalks are a major cause for pedestrian dissatisfaction. 4) A perception of overall insecurity further determines how pedestrians assess or modulate their walking in this city.	Villaveces et al., (2012).

Perceived safety *Odengatan, Stockholm*	To investigate perceived safety factors, and to analyse the contribution of active frontage on street-level perceived safety	Influence of perceived safety aspects on pedestrians feeling of safety. Active frontage and its relation to street users' experiences	Questionnaires, interviews and place observations	Ethnographic Study of Space (TESS)	1) "Mix of people", followed by (informal) "social control" and "urban form", have the highest impact on street users' perception of safety. 2) Active frontage is directly impacts street users' experience and contributes positively to perceived safety	Jansson, C. (2019).
Perceived safety and pedestrian comfort *Vancouver, Canada*	1) To examine perceptions of yielding, comfort, and safety for pedestrian interactions	Travel habits, socio-demographics, and risk aversion, and objective features of the location and interactions.	Video clips of pedestrian interactions and interview questions about yielding, comfort, and risk of injury.	Multiple statistical analyses methods applied by using the "survey" and "clmm" package in R.	1) Similar perceptions of yielding, comfort, and safety between participants who were members of the public and members of an advisory committee. 2) The traffic safety experts had similar views of yielding and comfort to the other participants, but a consistently lower assessment of risk while viewing pedestrians interactions with motor vehicles and bicycles. 3) Participant socio-demographics do not particularly relate to perceptions of yielding, comfort, or risk. However, travel habits do.	Bigazzi et al., (2021).
Walkable environment attributes *Kaohsiung City and Chiayi City, Taiwan*	1) To compare Google Street View assessments of the walkable environment with field assessments by local residents 2) To identify attributes of walkable environments	Assessment of Google Street view as a viable tool for walkability surveys	Hand drawn maps and questionnare, field visit questionnaire, Google Street View assessment questionnaire	IBM SPSS Version 22.0 is used for all data analyses.	1) Alternative paths, road safety, benches, roadside trees, attractive scenery, sidewalk width, pavement smoothness, scooters on sidewalks, and street signs have high corelatability with walkability. 2) The three approaches to assessing neighborhood walkability were highly correlated for traffic safety, aesthetics, sidewalk quality, and physical barriers. 3) Google Street View assessments for neighbourhood walkability are more convenient, safe, low-cost, and efficient.	Chiang et al., (2017)

Presence and Mix of Destinations *Melbourne, Australia*	To examine associations between destination types destination mix walking frequency and physical activity	Types and mix of destinations, walking frequency and physical activity	GIS used to examine three network buffers (400 m, 800 m and 1200 m) of respondents' homes (n=2349).	Multilevel logistic regression to estimate effects of each destination type and destination variety physical activity sufficiency.	1) At 1200 m buffer, all destination types were positively associated with physical activity sufficiency and walking frequency. At 800 m buffer, all destinations (excluding transport stops and sports facilities) were associated with physical activity. At 400 m, food stores and transport stops were associated with walking frequency and sufficient physical activity. 2) Greater destination mix was associated with greater walking frequency.	King et al., (2015).
Walkable route perceptions and physical features *Salt Lake City, USA*	To examine the correlation of Irvine-Minnesota physical environmental audit with real-life experiences.	Physical attributes of walkable street segmants	Trained raters analysis, Tape recorded open-ended descriptions and 18 point scale assessments of guided walk by university students.	Multivariate tests to explore the relationship between participant responses and evaluations of the walkable route segments using the Irvine-Minnesota Inventory (IMI).	1) highly "walkable" sidewalk segments were described as walkable by study participants and perceived as more attractive, pleasant, vibrant, well-maintained and interesting. 2) Measures of walkability association in the IMI are useful, but subjective measures should also be taken into account.	Brown et al., (2007).
Small-scale details or 'microfeatures' *Five blocks*	To identify significant walking environment features	Physical attributes of walkable street segmants	Walkability audits	Descriptive analysis	1) Environmental features including small-scale features are highly noticeable. 2) Sidewalk quality, navigational signage and aesthetic quality of buildings are important environmental features. 2) Striking and pleasing buildings, the micro-scale focal points, and commercial or street signs were also notable features of good walks.	Lynch, K. (1980).

Thermal Comfort	To assess the impact of various strategies on thermal-comfort improvement for pedestrians	peer-reviewed papers published in English within the ScienceDirect, Scopus, Wiley, and Springer databases	Classification of papers according to each heat-mitigation strategy were analyzed, and the findings of each study recorded	Descriptive analysis	1) Mean radiant temperature, wind direction and wind speed are the most impactful microclimate factors affecting outdoor thermal comfort. 2) Increasing vegetation, specifically trees is the most effective heat-mitigation strategies. 3) thermal-comfort level significantly increases by increasing the H/W ratio. 4) Using highly reflective materials in urban canyons is not advisable. 5) Physiological and psychological factors should be considered together to achieve thermal comfort.	Nasrollahi et al., (2020)
Thermal Comfort U*rban park square in Shanghai*	To investigate the role of thermal comfort in evaluation of the outdoor activity	Air temperature (Ta), globe temperature (Tg), relative humidity (RH), wind speed (V), global radiation (G), Physiological Equivalent Temperature (PET) and subjective Thermal Sensation Vote (TSV)	Questionnaire surveys (n=596), in-situ meteorological measurements and unobtrusive observations and computer simulations	1) Pearson correlation analyses between TSV, PET and the micro-meteorological factors. 2) Calculation of Mean Thermals Sensation Votes (MTSVs). 3) Linear regression conducted between MTSV and PET to calculate the neutral PET 4) Behaviour related factors are surveyed to analyse respondents' thermal sensation 5) Simulation of the spatial variation of existing micro-meteorological conditions.	1) Peoples' overall comfort was significantly impacted by their subjective thermal sensation vote (TSV). 2). TSV showed the strongest positive relationship with air temperature and solar radiation in winter. 3) In Shanghai the neutral PET in winter is around 15 to 29 C. 4) People's thermal adaptation was impacted by their stay duration and length of residence in Shanghai.	Chen et al., (2015)
Thermal Comfort *Parts of the city of Basel, Switzerland*	To assess tree crown temperatures of 10 tree species common to Central European cities	Ambient temperature, foliage temperature, air temperature, crown temperature	Aerial scans using a high-resolution thermal camera taken from a helicopter	Histograms of composite thermal images, readings of leaf energy balance, air temperatures, leaf size, wind speed and species-specific leaf boundary layer resistance.	1) Readings show peaks at 18 °C (water), 26 °C (vegetation), 37 °C (streets) and a less obvious one at 45 °C (roofs). 2) Tree crown temperatures ranged from 24-29 °C located in a street at an ambient temperature of 25 °C. 3) Trees in parks were significantly cooler (26 °C) than trees surrounded by sealed ground (27 °C). 4) Small-leaved trees remain cooler than large-leaved trees.	Leuzinger et al., (2010).

Thermal Comfort *five different areas of a square in the city center of Constantine in Algeria*	To examine the performance of shaded areas with five different types of tree coverage, including an open area located in a hot and dry climate without vegetation	Thermal and visual comfort	Summer time readings of air temperature, wind speed, air humidity, solar global radiation, luminance, sky view factors (SVF), comfort surveys	1) Outdoor thermal comfort evaluation for the five stations is done using the two methods: PMV calculated and Tmrt with software RayMan. 2) TownScope 3.2 is used to simulate and assess the external thermal comfort 3) Statistical analysis of survey responses	1) Physiological response is significantly influenced by blocking solar radiation (the effect of shade on thermal comfort under tree canopies). 2) Urban trees influence air temperature and human thermal comfort dependign on local conditions including tree cover, geometry, and prevailing meteorological conditions.	Samira et al., (2017).
Topographical Features *hilly university campus in Hong Kong*	To propose a walking accessibility measure to identify barriers in the walking environment and facilitate comparison of perceptive and real life conditions	Walking behaviors and people's perceptions	A walking-oriented travel dairy, to collect information on travel times and a questionnaire to assess walking time and identify potential barriers	Geographic Information Systems (GIS) software used to map: 1) Daily walking trips 2) 3D pedestrian network 3) Evaluate accessibility	1) Walking in a hilly environment is perceived as a barrier. 2) The increase in pedestrian facilities such as installation of express lifts may increase people's willingness to walk in a hilly environment. 3) Informal walking network has a significant influence on connectivity because of frequency of usage	Sun et al., (2015).
Topographical Features *Haifa and Jerusalem, Israel*	To analyze and accurately predict pedestrian movement in urban scenarios	Physical effort and mutual visibility	Open Street Map (OSM), axial segment map, topographic model	1) A new model to develop 2D axial map into a 3D segment map that represents the topographic aspect of the environment. 2) The Physical Effort Model (PEM), to analyze visual constraints stemming from topographic form	1) Topography can limit the spatial awareness of pedestrians by blocking lines of sight. 2) Walking on steep slopes can impact pedestrians travel mode choice	Greenberg et al., (2019).

Topographical Features *City center of Zurich, Switzerland*	To examine the relation between the slope of the terrain and walking activity	Pedestrian counts, walking frequency	pedestrian counts and public transport ridership counts from 2 tram stops (uphill and downhill) from infrared sensors	1) Calculation of pedestrian counts, tram ridership numbers, (on a typical weekday), modal shares (walking and public transport), and the time difference between walking and alternative modes. 2) The known steepness of the walk and this representation of the cost function, is determined by maximum likelihood estimation.	Steep slopes have a negative impact on walkability associated decisions. A 1% increase in slope makes walking approximately 10% less attractive.	Meeder et al., (2017).
Weather conditions	To provide a systematic overview of weather conditions' influence on daily travel activities	Weather conditions, daily travel	1) A systematic Scopus and Google scholar search with the following search terms: 'weather', 'activities', 'thermal comfort', 'walking', 'travel', 'behaviour', 'transport', 'cycling', or 'recreation', or 'commute', etc.	Systematic review of contextual, methodological, and behavioural backgrounds of the studies	1) Rain, snow, windy, cold and hot weather (above 25–30 C) often discourage open-air transport modes to sheltered modes, decrease visits to outdoor destinations and impact departure times and travel duration. 2) The majority of meteorological data in reviewed studies is retrieved from weather stations located in rural areas, which do not account for variations in microclimatological conditions. 3) Most of the study locations are characterized by temperate or continental climate regimes.	Böcker et al., (2013).

2.3 Effects of Climate Events on Walkability

In 1995, a heat wave in Chicago claimed the lives of over 700 people, primarily affecting poor and disadvantaged communities. In 2018, American filmmaker, Judith Helfand, produced a documentary, "Cooked: Survival by Zipcode" challenging the city administration's description of the heat associated deaths as 'non-violent'. As a result of the fatal heat wave, hundreds of people expired due to poorly ventilated homes and the systemic failures to predict, or adequately adapt to the disaster. The documentary also highlights that present disaster preparation programs do not adequately address the challenges faced by vulnerable communities where poorly designed homes, scare resources, and lack of access to government services all contribute to such disasters.

A recurring theme in systematic reviews of walkability is the lack of association with climatic factors. While research domains from the field of urban design, architecture, transportation planning and public health fields focus heavily on walkability, they often do not mention climatic factors as contributors to walkability.

This could be because most literature and studies relating to walkability are geographically limited. They are mostly focused in dense or excessively urban areas and in temperate zones of the Western world. Such studies may be challenging to apply to other global locations (O'Hare, 2006). However, despite the limitations in literature, there is still considerable mention of the impact of climate on walkability. This is more common in literature published by the public health field, where physiology and human energy is a parameter to consider.

However, only a handful of studies have explored the effect of weather conditions on pedestrian behaviors. With regards to this relationship, studies use automation to record data such as sensory counters and windometers. Usually, such measurements are recorded in micro-scale pedestrian routes and would require a variety of field observations at multiple locations to acquire proper and reliable statistical data.

Using multivariate statistics and climate projections, Bocker et al. (2012) explored the effects of climate change on travel choice behavior in the Netherlands by using travel survey data from 2004 to 2009, and Dutch meteorological data for 2050 climate projections. Positive effects of climate change were observed on walking, cycling and public transport. Moreover, the 2050 projections of increased summer precipitation levels were expected to have a negative effect on total distance travelled and number of walking trips (Bocker et al., 2012).

Figure 2.7: Ideal microclimatic conditions to enhance pedestrian comfort (Katzschner & Thorsson, 2009)

Walking inherently requires interaction with the natural environment. Pedestrians are prone to multiple hazards, such as road accidents, exposure to physical distress and intense weather conditions. In many countries, especially in Europe, pedestrians

and cyclists have become the top priority for road safety and have paved the way for considerable progress in pedestrian safety (Nicole, 2007). Specific interest in pedestrian safety grew considerably since they are the most vulnerable group of travelers. Moreover, increased walkability is critical to sustainability, public health, and quality of life.

It is critical to mention that recent intensification of weather events resulting in warmer summer months and climate related hazards are expected to have a considerable impact on the quality of human life. Even more critical is for planners to be able to foresee future scenarios of micro and macroclimatic conditions, their spatial distribution, and the resulting impact on human life. Only then, climate resilient design strategies can be effectively prioritized.

2.3.1 Urban Flooding

Urban development changes hydrological and hydrometeorological conditions in cities and invariably increases the flood risk brought on by land use and microclimatic changes (Huong and Pathirana, 2013). The increase in the frequency of flood events is partially attributed to extreme precipitation driven by climate change (IPCC, 2007). Rain events are more uncertain, weather events less predictable and thunderstorms more likely.

Since the early 1970s, there has been an alarming increase in the number of flood disasters worldwide, mainly because of economic activities and population growth in flood-prone areas (Konrad, 2003). In cities, flooding events impact urban road networks, mainly due to the high percentage of impermeable surfaces which reduces flow resistance and slows infiltration (Konrad, 2003). Roads naturally become pathways for stormwater runoff, exposing road users, including pedestrians, to a multiplicity of hazards (Konrad, 2003).

Floods occur when large volumes of runoff from rainfall and snowmelt move quickly to feed into streams. The peak discharge is influenced by several factors, including

land use, built environment patterns, vegetation, topography, and geology of stream basins. Absorption properties of urban materials and lack of permeable soil causes excess water to accelerate and produce overland flow. Reduced storage capacity in urban basins results in urban streams rising more quickly during storm events than rural streams. Furthermore, development along stream channels and floodplains or construction that encroaches on floodplains increases the flow resistance and causes backwater to inundate a larger area upstream (Konrad, 2003).

In recent years, due to the rising global flood risks under a changing climate, a significant amount of scientific literature has focused on developing global flood models to examine current and future flood risks (He et al. 2022).

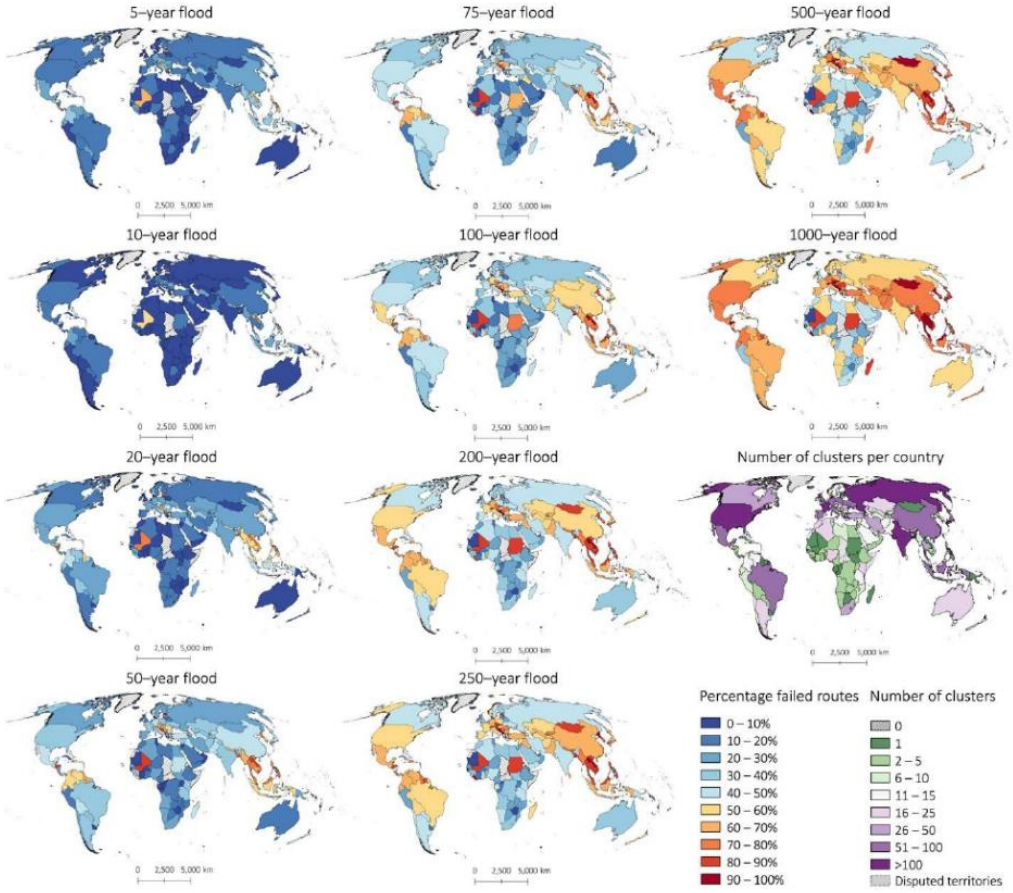

Figure 2.8: Country level percentage average of failed routes over 10 flood return periods (He et al., 2022)

To understand the impact of pluvial and fluvial floods on road networks worldwide under multiple climate scenarios, He et al. (2022) performed a flood risk analysis by layering drivable road networks with spatial clusters and flood maps under 10-year return periods. Among the many useful conclusions drawn from their study, perhaps the most relevant for this research is that indirect impacts of floods on mobility far exceed direct infrastructure exposure.

Failed routes, defined as unviable paths between origin and destination (O-D) under multiple floodwater inundation thresholds and flood return periods are visualized in

Figure 2.8. It can be observed that road networks in East Asia, Southeast Asia, Africa, South Asia, Central America, and South America are comparatively less resilient to flooding events. The indirect impact of floods on mobility is more prominent than direct flood exposure (He et al. 2022).

More and more, cities are becoming hotspots for climate disasters, and countermeasures to urban flooding must prioritize long-term planning since the impacts of climate change are complex and unpredictable (Park & Lee, 2019).

2.3.2 Rising Urban Temperatures

Urban areas alter the original physical characteristics of the landscape by replacing the natural environment with buildings, roads, paved surfaces, and parking lots. This results in an increase in impervious surfaces and introduces anthropogenic heat exchange owing to increased heat storage capacities (Xian and Crane, 2005).

Anthropogenic heat refers to heat produced by human activities. It can vary by the level and type of urban activity and infrastructure, transportation levels and buildings' energy use. Additional factors include weather and geographic location. As a result, there is a marked temperature difference between urban and surrounding rural areas. This difference is referred to as the Urban Heat Island (UHI). The warming that is caused by UHIs over small areas, like cities, can be termed as an example of local climate change.

According to Coffel et al. (2018), there are five key physical drivers of UHI:

1) Increased demand for frictional surfaces in urban areas resulting in an increase of flat and cemented surfaces. This leads to reduced efficiency of convective heat transfer between the lower atmosphere and the surface.
2) Enhanced energy storage capacity due to the use of artificial materials
3) Loss of vegetation cover resulting in reduced evaporative cooling effects.
4) Anthropogenic waste heat released from residential buildings, industrial facilities and transportation means.

5) Increased energy absorption capacities because of low-albedo materials.

While anthropogenic heat emissions can be significantly lowered by employing energy efficient solutions in the building technology and transport sectors, increasing overall vegetative cover, decreasing impervious surfaces, and modifying surface properties of urban materials can reduce waste heat (Figure 2.9:). Waste heat is unnecessary and can be avoided completely if urban planning and policy focuses on its role in UHI formation (EPA, 2009)

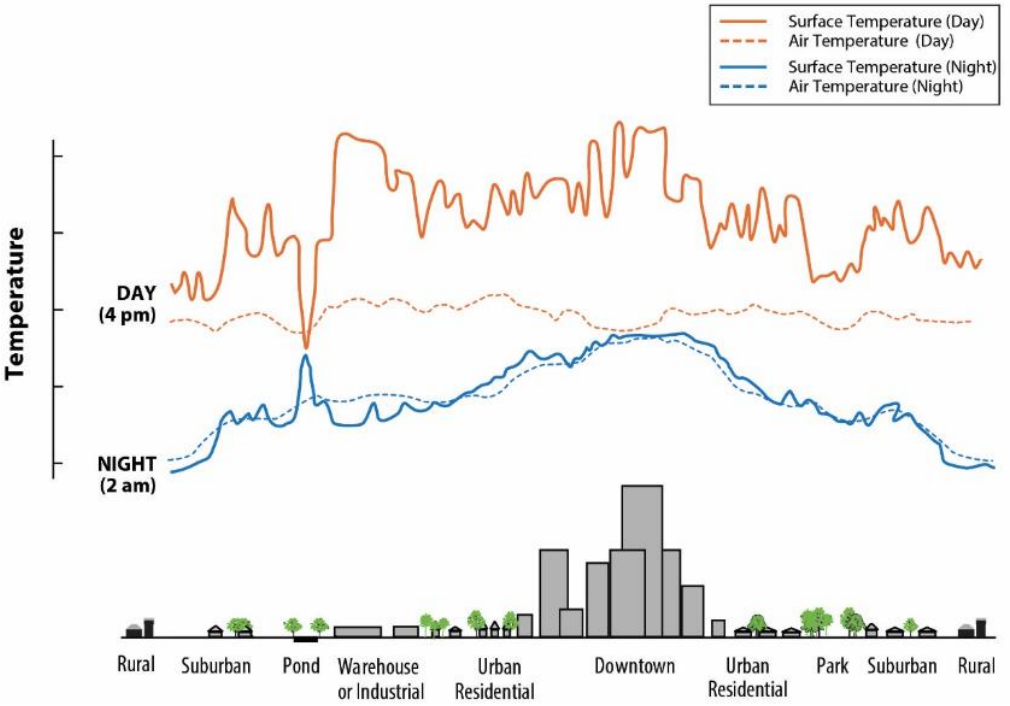

Figure 2.9: Surface Temperature Difference between Day and Night (EPA, 2009).

However, it is important to distinguish between the 'types' of UHI since the observations and responsible processes may differ. As described in Table 2.7, there are three main types of Heat Island, based on scale of impact and their method of measurements.

Table 2.7: Summary of conventional UHI classifications (Kim and Brown, 2021)

UHI Type		Horizontal range	Vertical layer	Impacts
Non-atmospheric UHI	**Surface heat island** (UHI_{Surf})	Micro-scale (1–100 s m), Local-scale (1–10 km), Meso-scale (10 s km)	land surface layer (LSL) (10 s m)	Human thermal comfort
Atmospheric UHI	**Canopy layer heat island** (UHI_{UCL})	Local-scale (1–10 km), Micro-scale (1–100 s m)	building canopy layer (BCL) (10s–100 s m), urban canopy layer (UCL) (25–250 m)	Human thermal comfort, building energy consumption
	Boundary layer heat island (UHI_{UBL})	Meso-scale (10 s km)	urban boundary layer (UBL) (250s - 2500 m)	Air quality, air pollution

1. Surface Heat Island (SUHI) forms due to the heat absorbed and emitted by urban surfaces such as rooftops, roads, and pavements, which is much greater than the extent to which heat is absorbed and emitted by most natural surfaces. SUHI's are more intense during the day.
2. Atmospheric Heat Islands are less intense than surface heat islands. These islands are formed because of warmer air in urban areas compared to cooler air in surrounding, outlying areas (EPA, 2021)

Figures 2.10 to 2.12 illustrate the differences between UHI types.

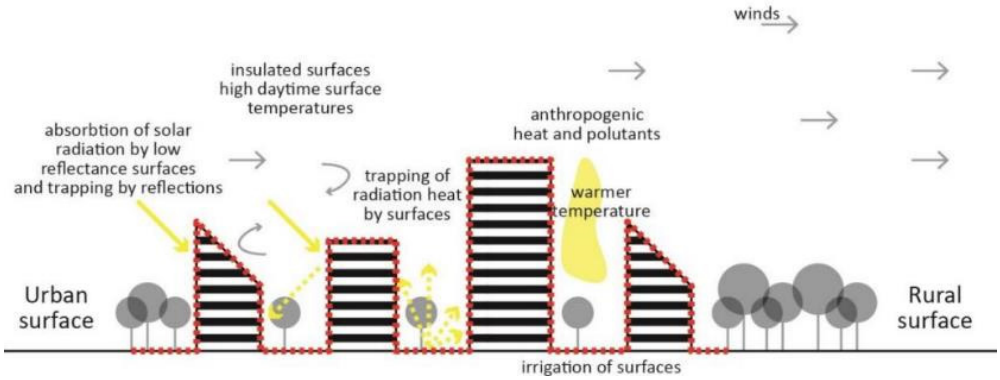

Figure 2.10: Schematic Depiction of SUHI (Branea et al., 2016)

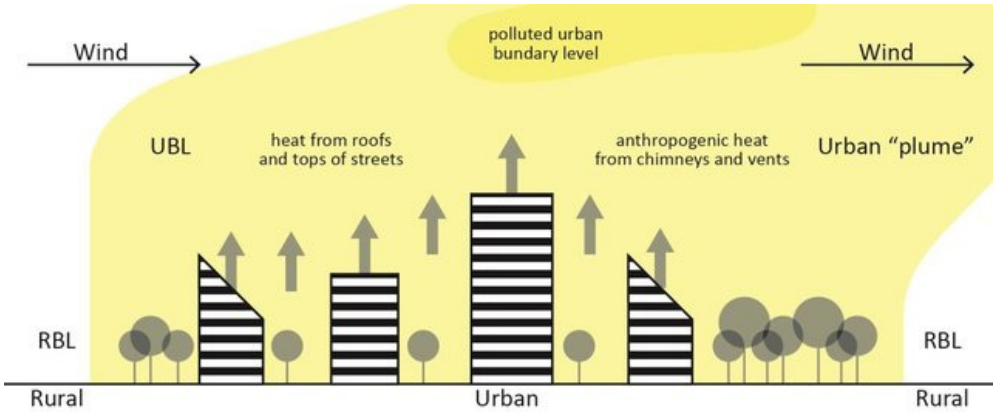

Figure 2.11: Schematic Depiction of BLUHI (Branea et al., 2016)

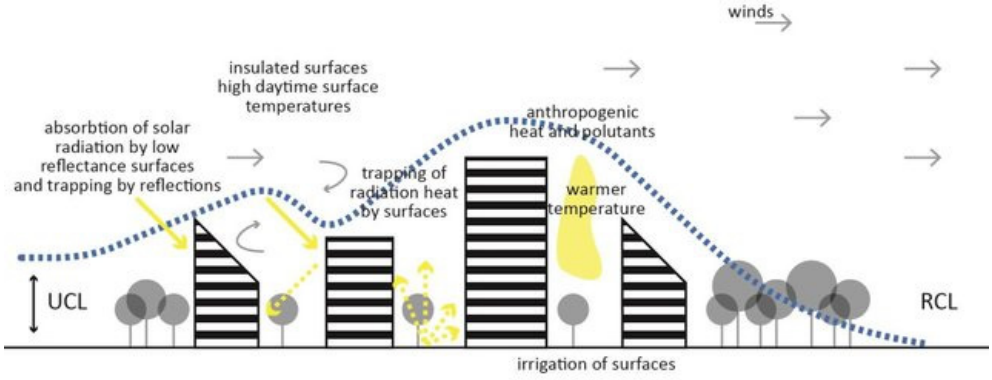

Figure 2.12: Schematic Depiction of CLUHI (Branea et al., 2016)

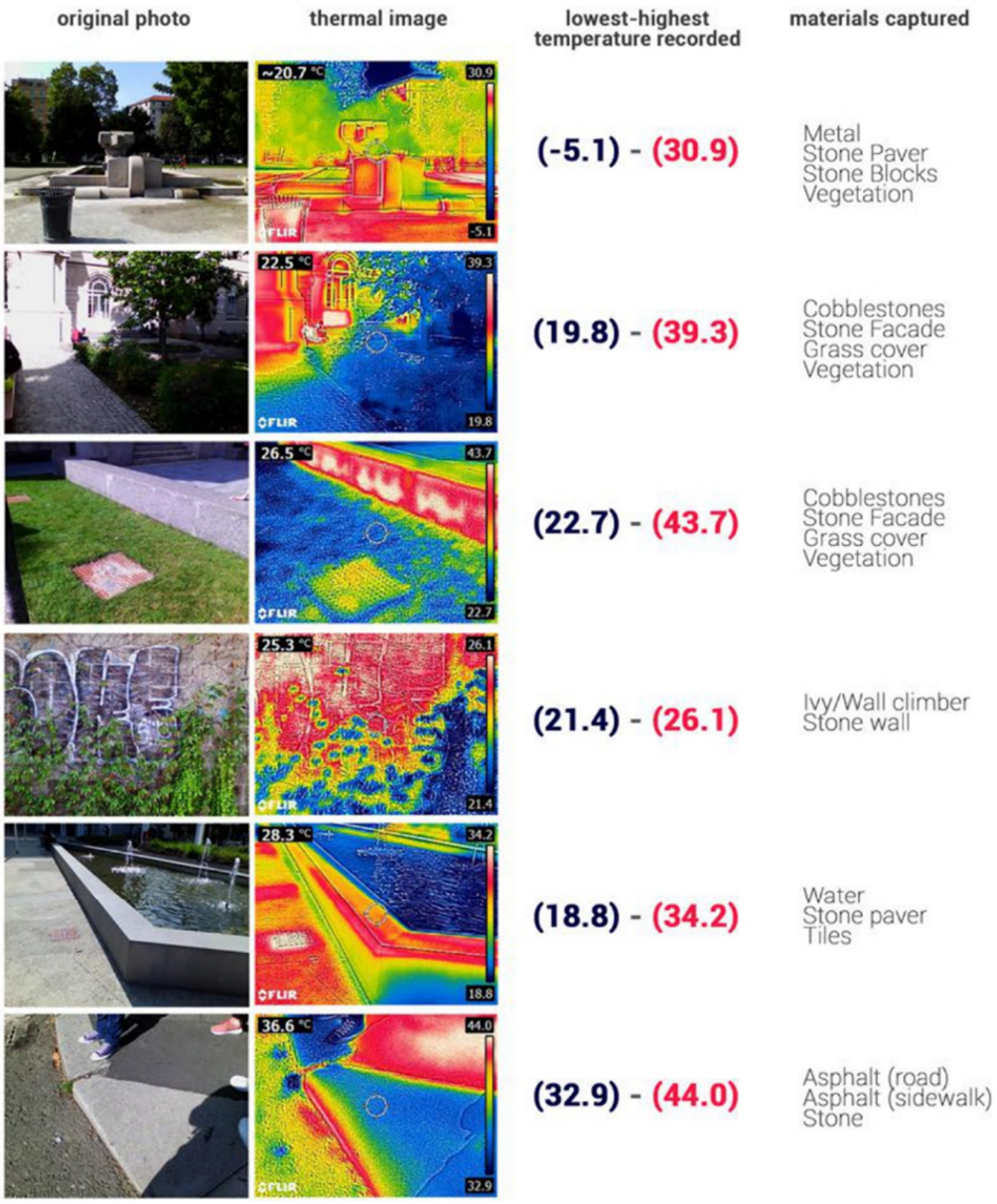

Figure 2.13: Thermal Camera Images Capturing Surface Temperature of Various Urban Surfaces at the Street Scale in Milan, Italy (from the author)

Data collection methods for mapping urban heat depends largely on the type of UHI being measured and the scope of the intended outcome. Another contributing factor

is the spatial and temporal variations that occur based on the type of UHI being measured (as visualized in Figure 2.10 to 2.12).

The scope of the study should also determine the nature of UHI that the researchers intend to analyze. Similarly, the research criteria should also reflect what kind of UHI variation is being studied (Kim & Brown, 2021).

For example, UHI_{Surf} (or SUHI) directly affects pedestrian environments and behavior. Thermal imaging is the main data collection to measure UHI_{Surf}. This includes remote sensing techniques using satellite imagery, thermal images obtained by thermal cameras mounted on UAVs and field measurements from sensors (Wilson, 2018).

Much of the geospatial data used to measure UHIs reflect land surface or air temperatures (Wilson, 2018). Estimating UHI using imagery from satellites (Landsat and Sentinal) is less time consuming and more cost-effective as opposed to data from on-field measurements, which may not be feasible for a large area. The merits of remote sensing technologies are explained in the next section of this chapter.

2.4 Remote Sensing Technologies

Remote sensing technologies gather data about objects and infrastructure on the Earth's surface without maintaining direct contact. Several studies in scientific literature have used remote sensing as a method to analyze spatial data. This technique makes the process of data collection faster and provides a comprehensive view of the target objects. Satellite images and aerial photography obtained with remote sensing can help visualize terrain and surface properties which enables a wide variety of relief operations and analysis. Such features have enabled recent research in the field to make accurate predictions of upcoming disasters, their locations, and associated risks (Munawar et al., 2022).

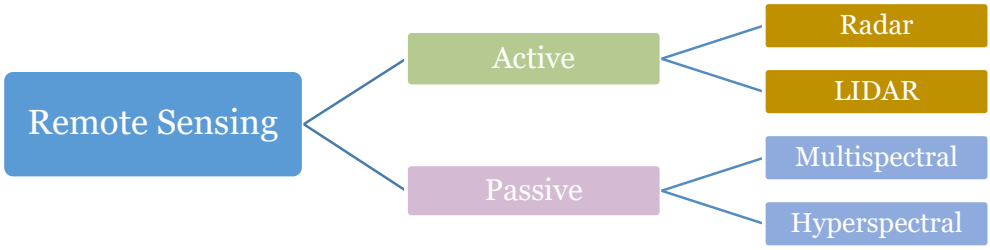

Figure 2.14: Remote Sensing Types

Figure 2.14: shows the types of remote sensors. Active remote sensors use their light to retrieve data from a target location on the Earth's surface, while passive remote sensors use natural light to gain data. Passive modes can be distinguished by the number of bands across which they measure radiance, whereas the active modes are distinguished by the wavelength of the radiation which they emit (Pettorelli et al., 2018).

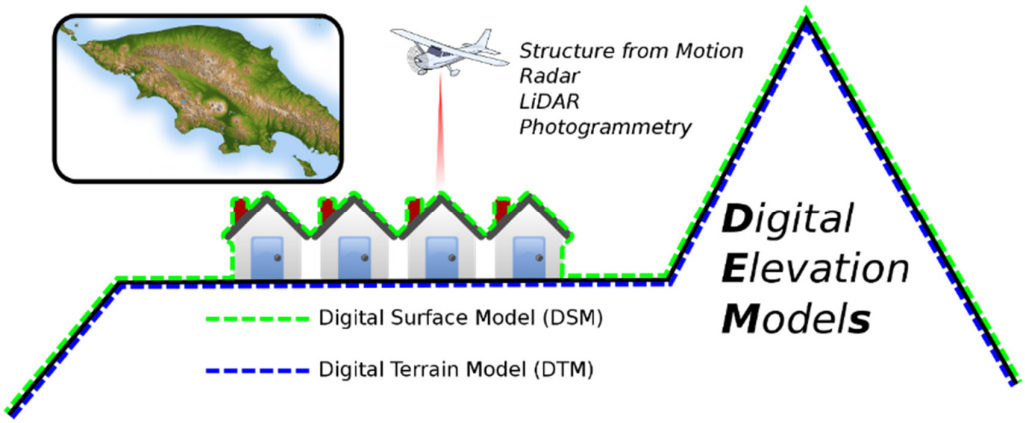

Figure 2.15: Difference between DSM and DTM in Digital Elevation Models (DEM) (Arbeck, 2015)

LIDAR (Light Detection and Ranging) is an active remote sensing technology which uses laser pulses to measure object distances on Earth's surface relative to the sensor. The data obtained is used to produce a 3D model to represent the Earth's shape and surface (Figure 2.16).

LIDAR data is also used to construct a DSM (Digital Surface Model) and DEM (Digital Elevation Model) to depict the ground and non-ground regions (Munawar et al., 2022).

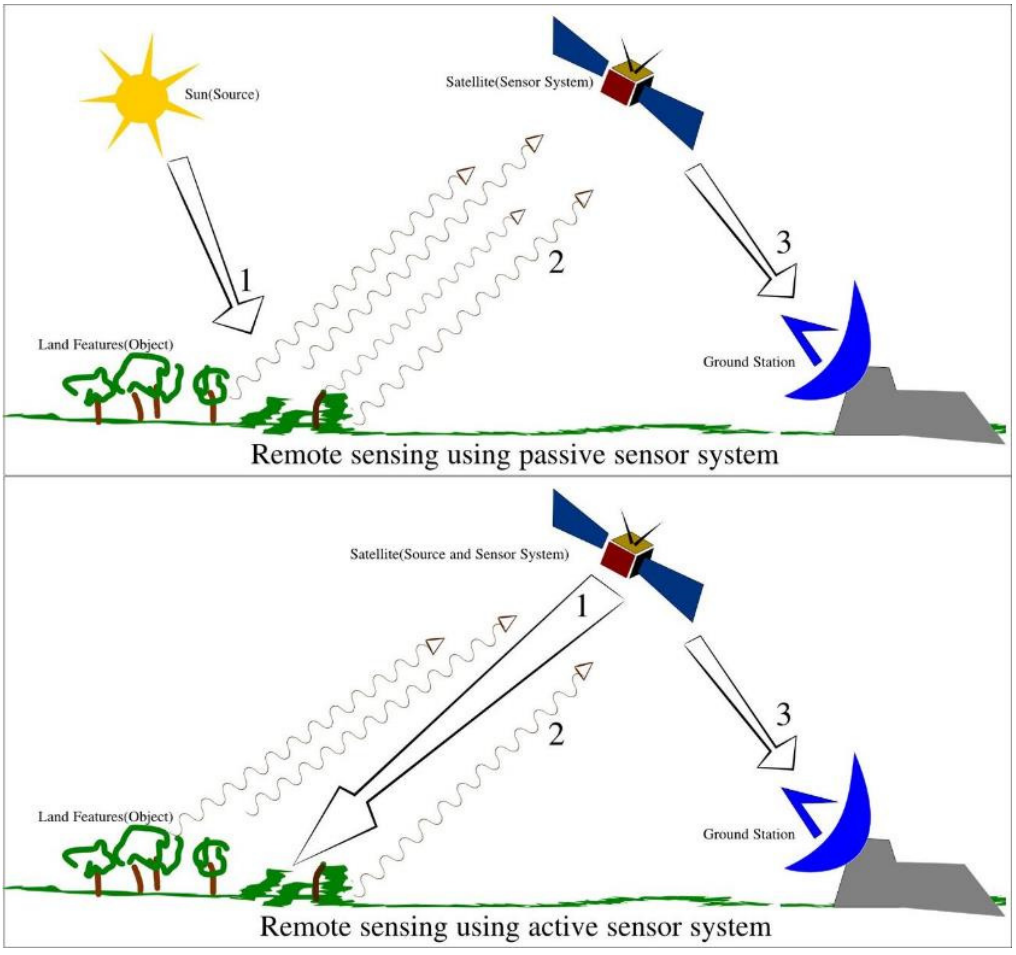

Figure 2.16: Remote Sensing Types (Arkarjun, 2013)

Radar (Radio Detection and Ranging) is another type of active remote sensing technology which uses radio waves to find a variety of object characteristics such as their speed, range, location, and direction. As shown in Figure 2.16:, once the radio waves are returned to the receiver, the processor analyses this data to determine object properties.

When detection through optical remotely sensed data reaches failure, synthetic aperture radar (SAR) comes into play. The prime advantage of this technology is its penetration capacity to bad or extreme weather and light conditions. It can also distinguish between water and light. Combining this data with GIS and data assimilation techniques can work well for risk analyses such as flood mapping and flash flood forecasting (Munawar et al., 2022).

Figure 2.17: Example of High-, Medium- and Low-Resolution Aerial Images

Every satellite image contains several bands each consisting of different wavelength intervals. Hyperspectral images consist of over one hundred contiguous spectral bands. The high resolution of hyperspectral imaging allows for detection, quantification and identification of surface materials and can identify molecular absorption. It also draws inferences related to biological and chemical processes (Munawar et al., 2022).

Therefore, hyperspectral sensors provide an advantage over multispectral sensors. This level of resolution is useful when a fine distinction between minerals or

vegetation species is needed. However, multispectral images are more commonly used for distinguishing between land surface features and patterns (Munawar et al., 2022).

Remote Sensing for LST, NDVI and LULC

UHI and urban hot spots are common indicators to assess thermal properties of urban environments and are indicated by very high LST zones.

LST is the surface radiation level affected by natural vegetation, urban extension, land use configuration and landscaping materials. To measure LST, the most common technique is to use open-source remote sensing methods by measuring the heat energy radiated from the earth's surface.

However, high resolution is critical in such evaluations. High resolution thermal satellite images have a resolution between 3 and 100 meters. The smaller the resolution, the more accurate the analysis (Kızılca, 2022).

For the estimation of LST, Thermal Infrared (TIR) wavelengths between 8 to 15 micrometers (μm) are commonly used (Figure 2.18:).

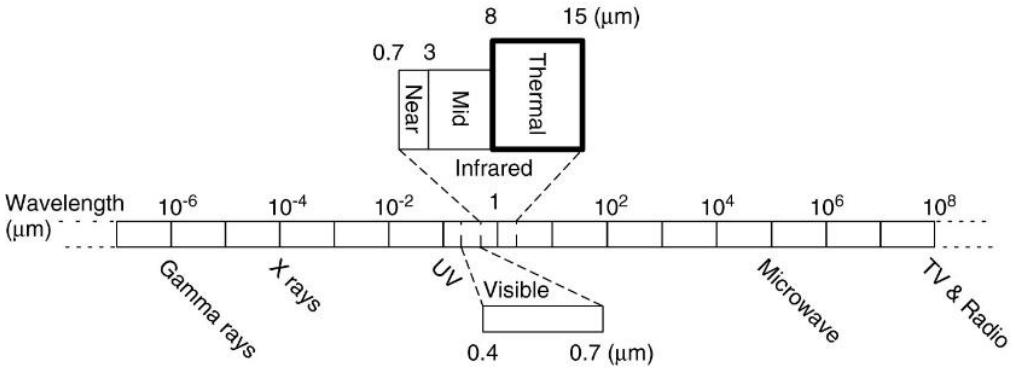

Figure 2.18: Electromagnetic Spectrum arranged by wavelength. Thermal infrared highlighted in bold. (Tomlinson et al., 2011)

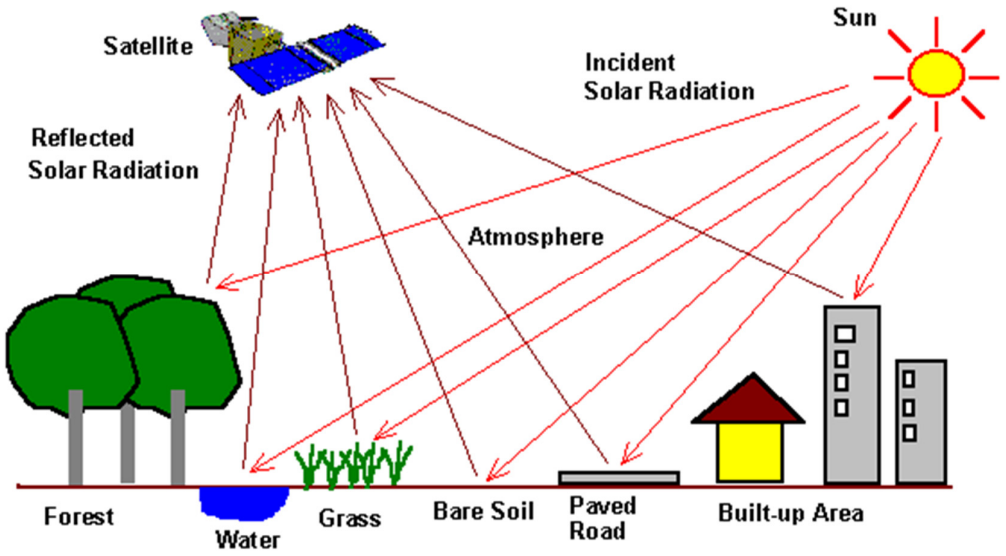

Figure 2.19: Overview of Remote Sensing (Alkhatib, 2012)

A satellite receives radiation as TIR sensors measure the top of atmosphere (TOA) radiance emitted by the Earth's surface. Since different objects emit electromagnetic radiation (EMR) in different ways, the spectral response can be analyzed according to different land types (Figure 2.19).

TIR sensors receive EMR which are then quantified to TOA radiances. This includes upwelling radiances from the ground and atmosphere, and the downwelling radiance emitted by the atmosphere and reflected from the ground (Alkhatib, 2012).

The inverse of Planck's law states:

"The energy emitted by a surface is directly related to its temperature."

This law is used to derive blackbody/brightness temperatures from TOA radiances. There are some factors which can affect TOA radiances:

1) Surface emissivity (vegetation, built-up areas, bare soil, etc.)
2) Atmospheric attenuation (absorption, refraction, reflection or scattering due to water vapor and aerosols)

3) The angle at which a satellite sensor receives radiation (Grover & Singh, 2015).

As listed in Figure 2.20:, there are several geostationary and polar orbiting satellites with sensors, observing in one or multiple bands in the InfraRed (IR) spectral range, such as Landsat 4 and 5 (TM), 7 (ETM+), 8 (TIRS 1 and 2), Moderate Resolution Imaging Spectroradiometer (MODIS), Advanced Very High Resolution Radiometer (AVHRR), Advanced Spaceborne Thermal Emission and Reflection (ASTER) and others (Grover & Singh, 2015).

Satellite	Sensor	Temporal Coverage
*Landsat 4 Landsat 5 Landsat 7 Landsat 8	Thematic Mapper (TM) Enhanced Thematic Mapper (ETM+) [1]Operational Land Imager (OLI) Thermal Infrared Sensor (TIRS)	7/1982 -12/1993 3/1984 - 01/2013 4/1999 - Present 02/2013 - Present
Terra Aqua	Advanced Spaceborne Thermal Emission and Reflection Radiometer(ASTER) & MODIS MODerate-resolution Imaging Spectroradiometer (MODIS)	12/1999 - Present 04/2002 - Present
International Space Station/ ECOsystem Spaceborne Thermal Radiometer Experiment on Space Station (ECOSTRESS)	Prototype HyspIRI Thermal Infrared Radiometer (PHyTIR)	06/2018 - Present
*Suomi National Polar Partnership (NSPP) Joint Polar Satellite System-1 (NOAA 20)	Visible Infrared Imaging Radiometer Suite (VIIRS)	10/2011 - Present 11/2018 - Present
NOAA Operational Series Current: NOAA 15,18,19 ESA- Metop-A & B	Advance Very High-Resolution Radiometer (AVHRR)	1979 - Present
NOAA Geostationary Operational Environmental Satellites (GOES) Current: GOES-16 & GOES-17	Imager & Sounder Advance Baseline Imager (ABI)	1975 - Present
ESA - Sentinel 3A & 3B	Sea and Land Surface Temperature Radiometer (SLSTR)	O2/2016 - Present 04/2018 - Present
ESA - Sentinel 2A & 2B	[1]MultiSpectral Instrument (MSI)	07/2015 - Present 03/2017 - Present

Figure 2.20: Satellites and Sensors for LST estimation (McCartney et al., 2020)

Sensor	Spectral Bands (µm)	Spatial Resolution	Temporal Resolution	Sensor	Spectral Bands (µm)	Spatial Resolution	Temporal Resolution
TM **ETM+** **TIRS**	10.40 - 12.50 10.40 - 12.50 10.6 - 11.19 11.50 - 12.51	120 m (30 m resampled) 60 m (30 m) 100 m 100 m	16 days	**VIIRS**	10.26 - 11.26 11.54 - 12.49	750 m	12 hours
MODIS	10.78 - 11.28 11.77 - 12.27	1 km	12 hours	**AVHRR**	10.30 - 11.30 11.5 - 12.50	1 km & 4 km	
ASTER	10.25 - 10.95 10.95 - 11.65	90 m	12 hours	**VISSR** **ABI**	10.10 - 10.60 **10.80 - 11.60** **11.80 -12.80** 13.0 - 13.6	2 km CONUS and Full Disk	minutes, hours, day/night
PHyTIR	8.28, 8.79, 9.06, 10.5, 12.05	60 m CONUS only	varies/every few days	**SLSTR**	10.45 - 11.24 11.57 - 12.48	1 km	12 hours

Figure 2.21: Spectral Bands for LST (McCartney et al., 2020)

However, LST is largely impacted by Land Use/Land Cover (LULC). Alterations in LULC contribute to biodiversity loss and alter the macro and microclimate. This relationship has been extensively examined and it has been observed that the rising trend of LST is due to the constant replacement of vegetated areas with built-up regions. This results in the formation of UHIs and is reflected in LULC patterns (Rehman, et al. 2022).

Figure 2.22 shows an example of LULC maps obtained for major Turkish cities. The land types are classified in four categories: impervious surface, vegetation, bare soil and agricultural areas, and water. In this study, Dihkan et al. (2018) cross-examined the LST results with LULC types of each city. By doing so, they found that Bare Soil and Agricultural Areas (BSAA) are characterized by very high LST zones which can be attributed to low humidity, high heat absorption capacity and highly sensible heat transfer conditions.

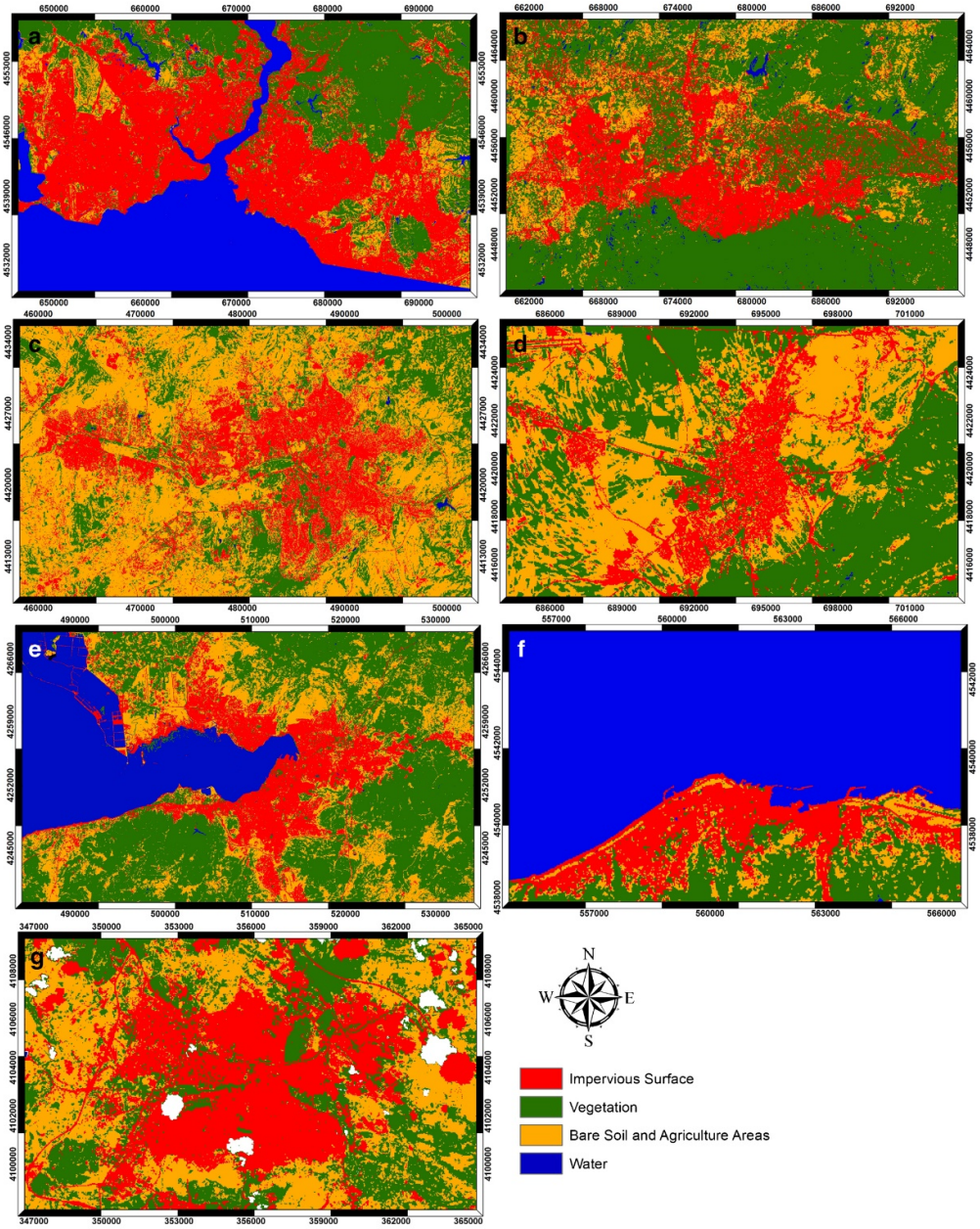

Figure 2.22 LULC Maps of Major Turkish Cities: **a)** Istanbul **b.** Bursa **c.** Ankara **d.** Gaziantep **e.** Izmir **f.** Trabzon and **g.** Erzurum (Dihkan et al., 2018)

To analyze the extent of change in LULC, alterations in the vegetation index are examined side by side (Shi & Chen, 2018). NDVI values are utilized as an indicator of the degree of vegetation greenness (Grover & Singh, 2015). In a Landsat satellite image, the NDVI is generated from the Red and Near-Infrared (NIR) bands. The formula to derive NDVI is written as:

$$NDVI = (BandNIR - BandRed)/ (BandNIR + BandRed)$$

The NDVI ranges from +1 to -1 and appropriately depicts the health and coverage of vegetation in a chosen or specific area. Positive values indicate healthy, green vegetation while negative values indicate non-vegetative cover (Grover & Singh, 2015). Figure 2.23 describes how NDVI reflects the quality of vegetation.

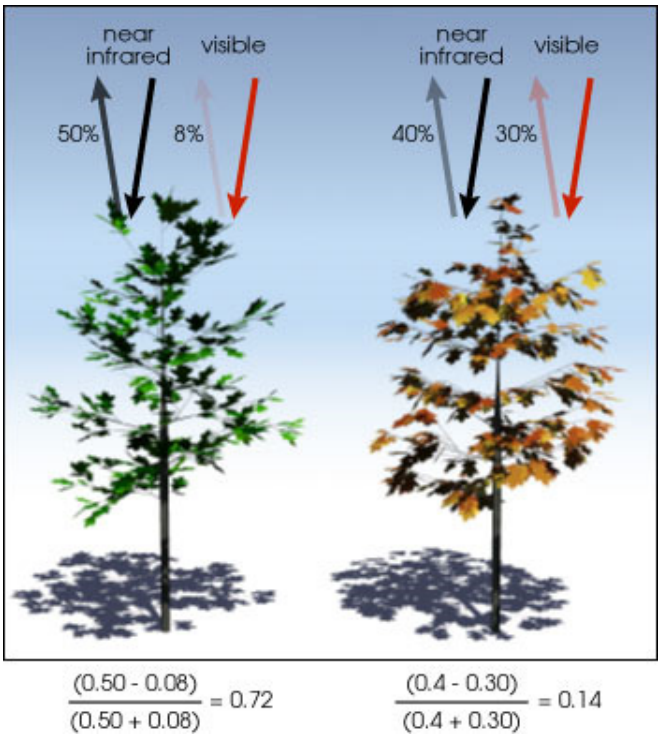

Figure 2.23: How NDVI values provide a reflection of vegetation greenness and health (NASA, 2000)

Wang et al. (2020) employed Landsat time-series data of Nanjing city from 2000, 2014 and 2018 to derive LST distribution and LULC composition maps (Figure 2.24) with the objective to create a simulation for future LULC development and to assess the risk of high LST distribution with the goal of supporting sustainable development.

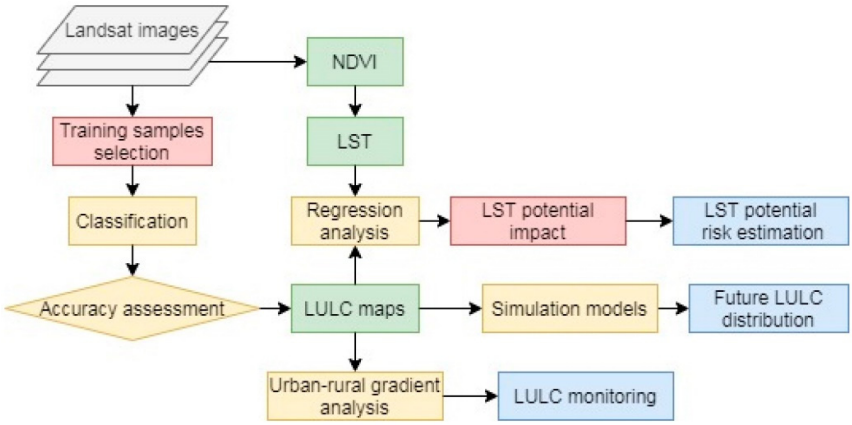

Figure 2.24 Workflow of deriving NDVI, LST and LULC maps (Wang et al., 2020)

Based on the co-relational analysis between landscape composition and LST, forest and cropland have the highest potential in lowering (or cooling) the LST in Nanjing. As shown in Figures 2.25 to 2.27. The expansion of impervious surfaces due to intense urbanization processes within an 18-year period led to an increase in LST, indicating towards the severity of UHI effects (Wang et al., 2020).

Many factors influence LST, resulting in the UHI phenomenon, such as intensity of illumination, temperature, and psychrometrics. LULC is one such factor which remains constant and predominantly causes UHIs. Wang et al. (2020) suggest that analyzing LULC patterns and their relationship with LST helps us to identify the

existing UHI effects in urban or rural lands and consider the possible precautions to be taken for the future.

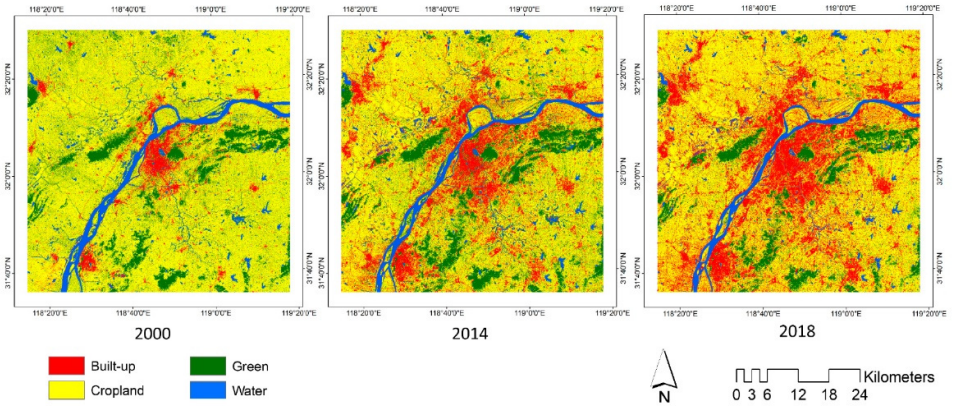

Figure 2.25: LULC Maps of Nanjing: 2000, 2014 and, 2018 (Wang et al., 2020)

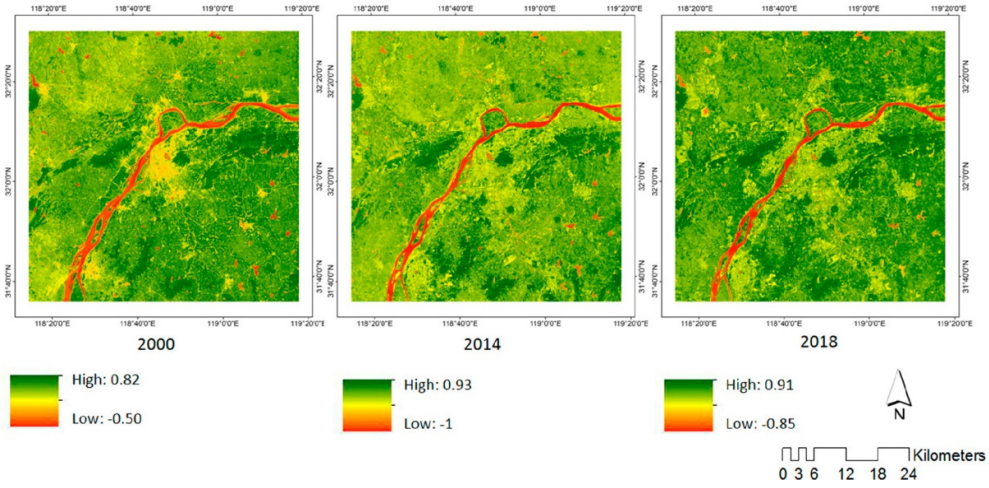

Figure 2.26: NDVI Maps of Nanjing: 2000, 2014 and, 2018 (Wang et al., 2020)

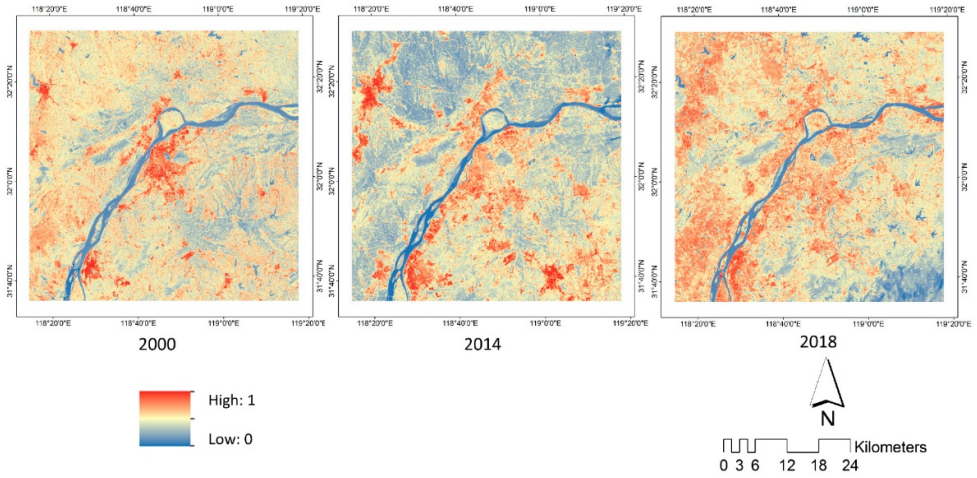

Figure 2.27: LST Maps of Nanjing: 2000, 2014 and, 2018 (Wang et al., 2020)

Positive trends of UHI may be observed in regions where rural areas or areas surrounding urban cities are characterized by forestland. However, this may not be the case everywhere. The contribution of vegetation and green areas in lowering LST is more complex than it appears. The geographical location and configuration of land-types is a significant determinant of UHI (Dihkan et al., 2018).

For example, in Ankara, the highest surface temperatures are observed in meadow areas and dry agricultural lands (Yilmaz, 2013; Dihkan et al., 2018). Depending on the land typology of the region, some land types such as soil and bare land may be warmer than urban surfaces.

Soils have an unstable relationship with temperature. Edmondson et al. study (2016) on the effects of vegetation cover and land use on soil temperature reveal that trees and shrubs may help moderate soil surface temperatures to reduce negative effects of urbanization on microclimatic conditions. In this research, they also compare the effects of vegetation in domestic and non-domestic spaces.

For example, a tree is considered as a ‘carbon sink’ if it absorbs more carbon from the atmosphere than it releases. When the net balance of carbon emissions by forests is negative, forests contribute to mitigating carbon emissions by acting as both a tool

to sequester additional carbon and as carbon reservoirs (Michalak, 2014). Edmondson et al. (2016) measured the environmental impact of trees by quantifying their carbon storage capacity. They found that non-domestic greenspaces have an above-ground carbon storage of 98 kg compared to only 53 kg in domestic green spaces. This stresses the high variability in tree performance. Evolutions in rainfall, temperature and soil moisture can have either damage or positively impacts forest health and productivity (Michalak, 2014). Therefore, it is necessary to examine the health of vegetation to accurately assess its impact on the environment.

In Bursa, Yamak et al.'s study (2021) reveals that high-temperature values are observed in industrial areas, re-enforced concrete structures and bare soil. In some areas, temperature values vary from 5-6 ℃ between the city center and plant-covered areas (Figure 2.28). In the same research, they observe temperature differences up to 10 ℃ within urban areas, while the lowest temperatures are observed in wetlands, forest areas and plant areas.

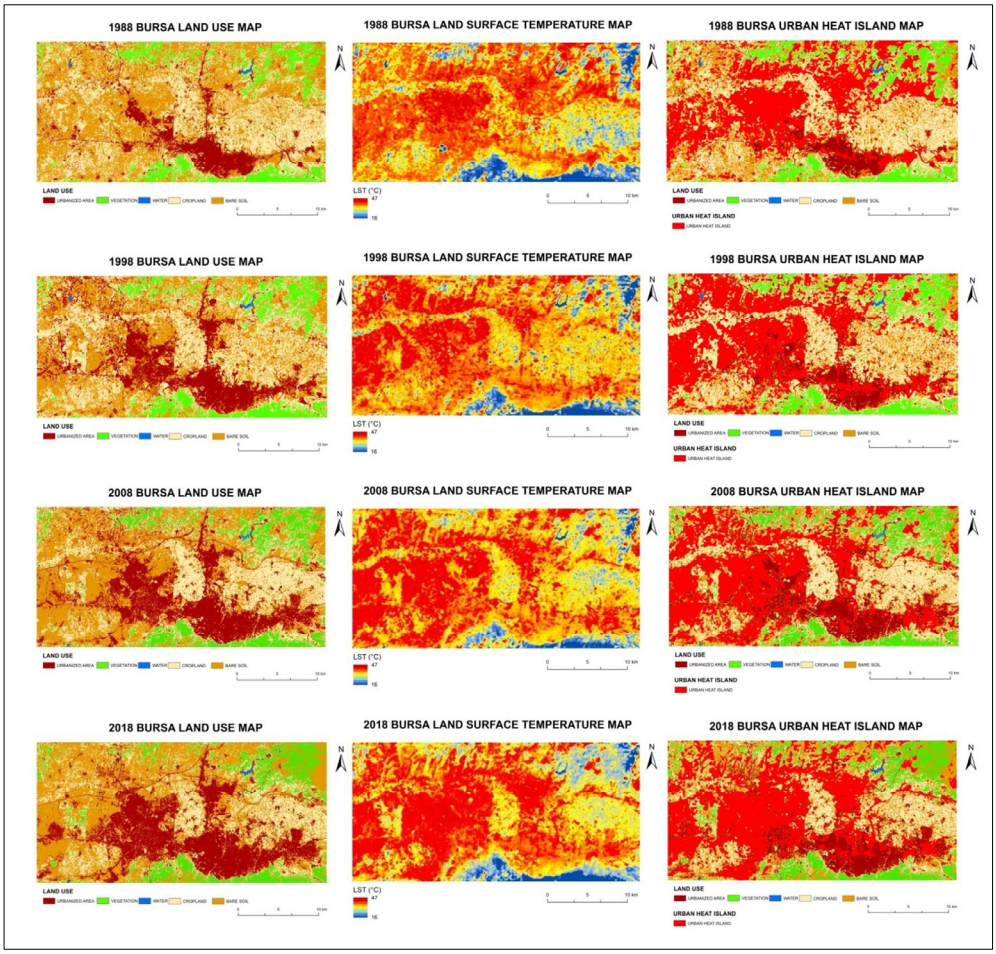

Figure 2.28 Land use, LST and UHI Maps produced for Bursa for the years 1988, 1998, 2008 and 2018.

2.5 Summary

Walkability is increasingly becoming a central theme in urban planning and design, mainly due to the increased demand for sustainable urban development. It is humanity's first mode of transportation. A mode which does not require external energy sources and helps to keep people happy, healthy and active.

In the first section of this chapter, a search and summary on walkability associated literature reveals the many factors influencing the subject. There have been multiple studies conducted not just in the urban planning domain but in medicine and social sciences. This indicates how far-reaching the impacts of walkability are. As an activity, it positively impacts mental and physiological health of individuals. As a form of recreation, it enables social interaction and enhances community sense (Baobeid et al., 2021).

Built environment, urban heat and human health are intricately linked with car-oriented development. Active travel modes, including walkability, are largely impacted by environmental and social factors. For example, the UHI effect in cities comprised of low albedo materials, facilitate the absorption and retention of heat, which increases human exposure to heat associated illnesses and discourages outdoor activity (Piracha & Chaudhary, 2022). Understanding urban heat and its relationship with pedestrian environments is one of the main aims of this thesis. However, the question remains: how can pedestrian-oriented planning include urban heat factors?

As Table 2.6 illustrates, walkability factors are mostly evaluated at the neighbourhood scale. This is because the data gathering methods use surveys and interviews. Built environment features are extremely varied within adjacent neighbourhoods. Moreover, pedestrian behaviour is difficult to predict.

McCormack et al. (2008), Shatu et al. (2019), Lee & Shepley (2020), Villaveces et al. (2012), Jansson (2019), Chiang et al. (2017) and Chen et al. (2015) employed survey questionnaires to investigate associations between walkability parameters

specific to their research and walkability. For example, McCormack et al. (2017) used face-to face interviews and follow up telephone surveys responses to investigate the association between the proximity and mix of neighbourhood destinations and physical activity by analysing physical activity behaviours of adults (in Perth, Western Australia).

Survey questionnaires are an excellent method to gather large amounts of data and interpret statistical trends between multiple variables to deliver precise results. This increases the reliability of the findings and eliminates the researcher's bias. They are also a good tool to assess subjective parameters (Jones et al., 2013). However, the survey method may not apply to every research, especially those primarily concerned with geo-spatial characteristics.

GIS is another tool used in walkability research as both, a data gathering and data analysis tool. Sun et al. (2015) employed GIS software to map daily walking trips, produce a 3D pedestrian network and evaluate accessibility. The ability to visualize complex spatial analyses in a GIS makes the measure more interpretable and easier to communicate (Sun et al., 2015). It also supports efficient computation, enables greater accuracy and allows the user to manage and extract large spatial data sets more systematically (user-friendly) (Graham et al., 2011).

A closer review of studies analyzing pedestrian thermal comfort, reveals that microclimate measurements of Mean radiant temperature, wind speed and wind direction provide the most accurate picture of outdoor thermal sensation (Nasrollahi et al., 2020). Meanwhile, the shade effect provided by vegetation, specifically trees is by far the best heat mitigation strategy (Nasrollahi et al., 2020). However, Samira et al. (2017) found that the influence of urban trees on air temperature and pedestrian thermal comfort depends largely on tree cover, type, geometry, health and prevailing meteorological conditions. For example, Leuzinger et al. (2010) writes that small-leaved trees remain cooler than large-leaved trees.

When mapping urban heat hotspots, it is critical to layer information about vegetation health and/or density. Since vegetation significantly impacts local

temperatures, an assessment of vegetation patterns and distribution would be an important contribution to this study.

In the later section of this chapter, an overview of UHI, physical drivers of UHI and UHI types establishes a baseline understanding of urban heat and how it can be assessed. Each type of UHI has a different spatial range and level of impact. For example, Surface Heat Island (SUHI) impacts human thermal comfort and can be assessed by the land surface layer.

Since in-situ data collection is not a viable option, spatial analysis through remote sensing techniques is the most feasible and cost-effective method. A description of remote sensing techniques to derive geo-referenced data from satellite images is followed by an overview of satellite data products.

The main parameters of urban heat are identified by combining learnings from existing studies on UHI detection. The example of Bursa, Turkey by Yamak et al. (2021) and Nanjing, China by Wang et al. (2020) establish a sound understanding of the expected mapping outcomes of this study. Learnings from both examples are crucial in highlighting good practices in the temporal mapping of land surface characteristics of cities. It is determined that mapping of LST, NDVI and LULC best captures urbanization patterns, vegetation density and distribution, and surface temperatures over time.

The next chapter explores the relation between multi-scalar impacts of urban heat and their relation with thermal comfort associated walkability. It also discusses the relevance of urban design interventions and urban planning policies to enhance walkability at different scales.

CHAPTER 3

CLIMATE AND COMFORT

Contextualizing the relationship between urban heat, thermal comfort, and walkability according to urban design is an integral part of this literature review. This is because a vast body of scientific literature relating to each of these individual topics already exists. However, urban thermal issues with respect to climate change and their subsequent impact on walkability in the city are rarely discussed.

This chapter aims to establish theoretical links between the impact of climate change and anthropogenic interference on cities, urban heat dynamics and thermal comfort associated walkability by reinforcing the importance of scale-appropriate strategies in urban design.

To effectively mitigate the effects of climate change on urban heat, it is important to consider the effect of weather conditions, overall climate, and air quality on human wellbeing. Climate-responsive urban design considers the fundamental elements of micro-climates such as wind, sun, and temperatures to mitigate the effects of extreme weather events in urban areas (Tapias & Schmitt, 2014). Therefore, the creation of thermally comfortable microclimates in urban areas is important.

Much like walkability, thermal comfort is not exclusively a micro-scale issue. Studies on thermal comfort at urban scales stress the importance of linking pedestrians and climate (Taleghani et al., 2015). In addition, there is a lack in understanding the role of urban features to enhance thermal comfort in urban spaces (Eslamirad et al., 2022). There is an overall lack of studies which explore the relationship and cause-effect elements between thermal comfort associated walkability and multi-scalar urban design strategies.

In this regard, this chapter seeks to understand the dynamics of climate and comfort by exploring relevant frameworks in existing literature to assess thermal comfort, how it relates to microclimate conditions, common approaches to mitigate local thermal stress, and how micro-scale thermal conditions relate to meso- and macro-level urban design frameworks. The last section includes a summary of the most relevant climate-responsive, urban design strategies which generate scale by scale associations with walkability. In this way, this chapter contextualizes the issue of how thermal comfort associated walkability can be enhanced through urban design interventions at different scales.

3.1 Approaches to Thermal Comfort

As described in Chapter 2, thermal comfort is a significant and necessary factor of walkability related decisions among pedestrians. This section of the chapter will describe in detail the relation between walkability and thermal comfort.

Human thermal comfort can be defined as the condition of mind which expresses satisfaction with the thermal environment, the absence of thermal discomfort or conditions where 80-90% of people do not express dissatisfaction (Yilmaz & Toy, 2007). The human response to the thermal environment is almost impossible to express as a function of a singular environmental factor (Yilmaz & Toy, 2007). Common thermal comfort variables include air temperature, wind speed, relative humidity, radiant temperature, activity, and clothing (ASHRAE Standard 55, 2004). The human body has a low tolerance for changes in temperature. As a result, humans make a variety of efforts to regulate their response to the temperature they feel.

Approaches to thermal comfort include a wide spectrum of research areas and objectives. Indoor spaces have relatively more static, stable, and controlled microclimate conditions while outdoor spaces exhibit a more complex microclimate (Oke, 2017). However, a major challenge in studying thermal comfort is to consider the variety of complex and equally confounding parameters which affect outdoor

thermal comfort. Human-based or physical approaches and different spatio-temporal scales of the built environment provide a necessary distinction in appropriate thermal comfort strategies (Aghamolaei et al., 2022).

As Hoppe (2002), writes, there are three approaches in the assessment of thermal comfort:

1) Psychological: thermal comfort is assessed based on human perception
2) Thermo-physiological: thermal comfort is assessed based on individual characteristics such as age, gender, clothing, and activity at the time.
3) Human body heat balance: thermal comfort is assessed based on the balance of the body's thermal conditions and environmental conditions.

On the other hand, Aghamolaei et al. (2022) defines approaches to thermal comfort into two main categories:

1) Physical and environmental approaches,
2) Human-based approaches.

The analyses based on physical features mainly focus on built environment characteristics such as landscape features and urban morphology. Different studies investigate the geometrical and morphological characteristics of urban areas at different scales such as streets, neighborhoods, districts, and city scale (Aghamolaei et al., 2022). Studies focusing on human-based approaches highlight that humans have various thermal preferences based on their individual characteristics, preferences, and tolerance thresholds (Aghamolaei et al., 2022).

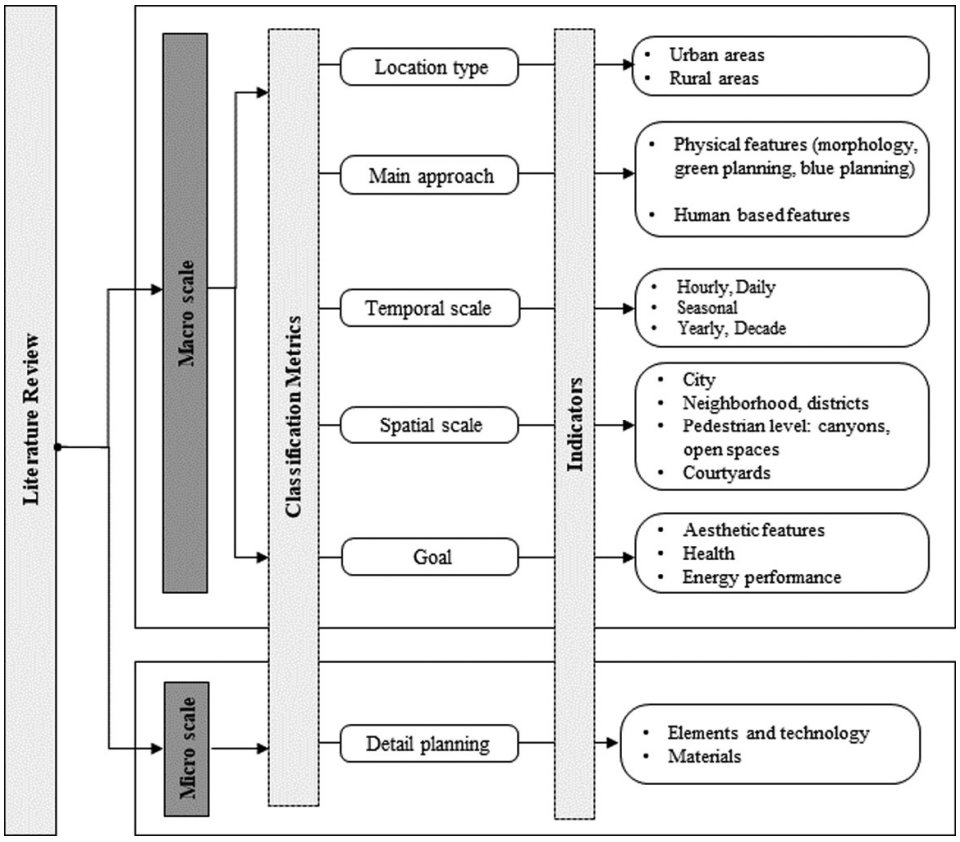

Figure 3.1: Aghamolaei et al., (2022)'s categorisation framework of outdoor thermal comfort studies over two scales, macro and micro

As shown in Figure 3.1, Aghamolaei et al. (2022) summarize the many approaches to outdoor thermal comfort by systematically categorizing related literature over two scales, macro, and micro. Figure 3.1 also highlights the relevance of assessing thermal comfort at multiple scales across different geographical contexts, time periods and environmental features.

However, Aghamolaei et al. (2022) also note that inspite of the valuable contribution of thermal comfort research at various spacious and temporal scales, most studies do not provide a comprehensive picture of temporal variation and spatial distribution of thermal comfort associated factors.

3.2 Contextualizing Microclimate and Thermal Comfort

Strategic urban design can mitigate local thermal stress while enhancing climate resilience in urban areas (Xiao & Yuizono, 2022). As mentioned in the previous chapter, with continuously intensifying urban temperatures, extreme weather events will become increasingly common. Urban populations will be at greater risk due to increasing urban temperatures, including risks to human health, low-quality outdoor environments, and atmospheric pollution (Yu et al., 2022).

Thermally comfortable urban environments can positively influence people's behavior, how they use outdoor spaces, and improve the quality of life in cities. In contrast, low-quality and uncomfortable spaces cause people to rush home (Eslamirad et al., 2022).

With regards to thermal comfort, much progress has been made in identifying and implementing design strategies to enhance occupants' indoor comfort. However, owing to the complexity of outdoor environments, the thermal comfort of outdoor spaces has not been studied adequately (Yu et al., 2022). Therefore, it is important to understand the factors affecting outdoor thermal comfort as it is an important indicator of walkability related decisions among pedestrians in urban areas.

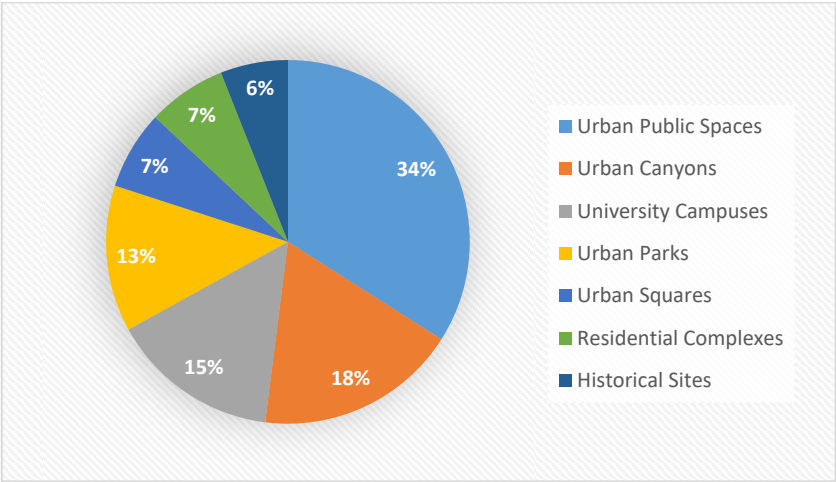

Figure 3.2: Usage percentage of urban space types in thermal comfort studies according to Nasrollahi et al. (2020)

At the city scale, it is necessary to mitigate the effects of rising UHI effects in urban spaces to improve the outdoor thermal comfort of residents (Yu et al., 2022). Figure 3.2 reveals the types of urban spaces used in thermal comfort studies, as reviewed by Nasrollahi et al. (2020). 34% of the reviewed studies are performed in public spaces. University campuses and urban canyons have a high share as well. Similarly, urban parks are also very common, with a percentage share of 13%. Studies about residential complexes, urban squares and historical sites have the smallest share in thermal comfort studies.

According to Lin (2009), the most important climatic factor affecting thermal comfort is the solar radiation and temperature in the microclimate. For example, Gholami et al. (2022) found that pedestrians in open spaces can feel 3 ℃ warmer than on narrow shaded streets. In addition, outdoor microclimate is an important factor influencing the quality of urban spaces (Eslamirad et al., 2022).

Even so, an important question remains: *what is microclimate?* According to Valsson & Bharat (2008), microclimate represents the climate patterns of a relatively small region (or area). Microclimates are influenced by climatic variables such as temperature, wind speed and direction, humidity, different seasons, and the physical characteristics of the region or space. Local meteorological factors also have a strong impact on microclimates, such as sea breezes in coastal cities, urban heat conditions, urban-rural air circulation, and so on (Koerniawan, 2016).

The concept of scale is an important aspect of assessing changes in climate or atmospheric processes within the surface layer. As mentioned in the previous chapter, LST, NDVI and LULC maps represent surface characteristics. Therefore, incorporating microclimate analyses in such analyses first requires an understanding of different climatic scales found in urban areas.

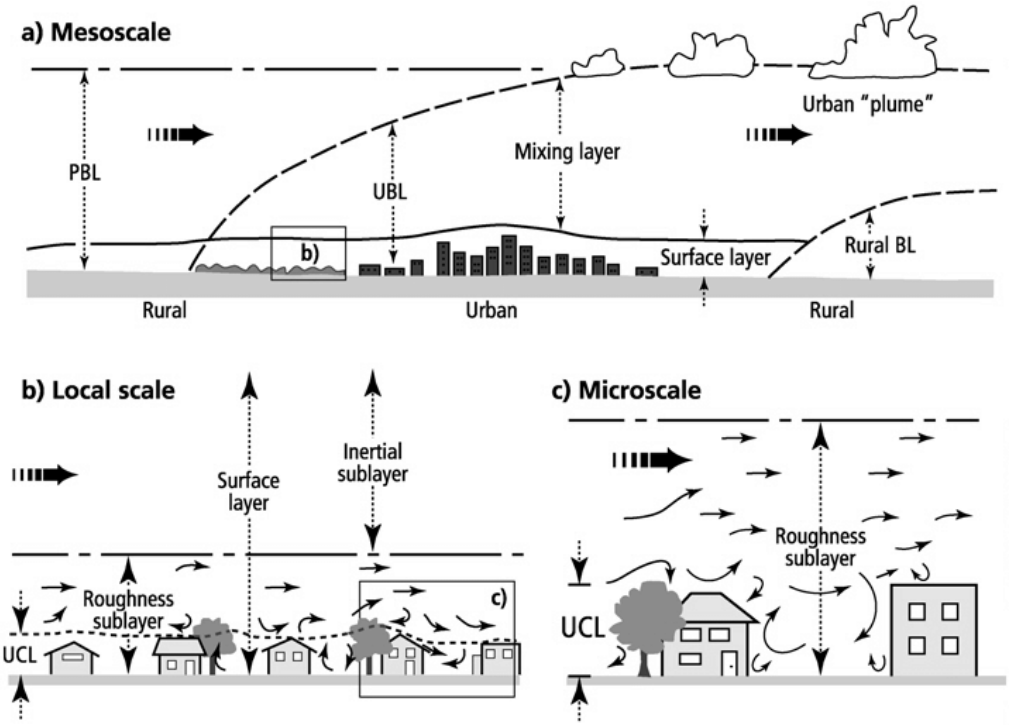

Figure 3.3: a) Mesoscale b) Localscale and c) Microscale. Climatic scales and vertical layers found in urban areas. PBL (Planetary Boundary Layer), UBL (Urban Boundary Layer), UCL (Urban Canopy Layer) (Oke, 2006).

The Inertial Sublayer (ISL) represents the part of the atmosphere which links both the regional and local scale. It reflects the effects that the surface introduces in the atmospheric boundary layer structure. The Roughness Sublayer (RSL) consists of two vertical segments: the upper part which is termed as the RSL (as shown in Figure 3.3), and the bottom part which is denoted as the Urban Canopy Layer (UCL). The RSL can be denoted as a transition or intermediary layer between the UCL, the microclimate scale and the ISL. Common practice indicates that urban climate researchers usually try to avoid this scale (RSL) due to the high number of uncertainties and difficulties in measurements (Núñez Peiró et al., 2019).

The UCL (as shown in Figure 3.3), on the other hand, represents the climatic context which is most influenced by urban life. Anthropogenic emissions are generated and

emitted at this scale. Most importantly, the human experience associated with air quality, thermal comfort, physical activity is also captured at this scale. Moreover, most of the urban design and urban planning strategies are implemented at this scale, such as traffic planning, regulating the use of certain construction materials, increasing vegetation in streets and parks. Therefore, urban design strategies at the micro-scale to improve microclimatic conditions can most significantly impact human life (Núñez Peiró et al., 2019).

In conclusion, designing for the optimization of microclimates can inarguably have positive impacts on walkability by improving thermal comfort conditions. However, with the rise in global warming and increase in summer temperatures, climate change scenarios will significantly impact urban microclimates compared to rural areas. Urban morphology, anthropogenic emissions, vegetation, and soil quality can alter the environmental performance of urban areas at the micro-scale (Tumini & Rubio-Bellido, 2016).

Therefore, urban design strategies to enhance pedestrian thermal comfort should consider the impact of changing climate and rising temperatures on microclimates, and the concurrent exchange between different climatic scales. In this regard, a multi-scalar approach to climate-responsive urban design strategies should be prioritized. As a result, surface layer characteristics are more important, easy to measure and quantify.

3.3 A Multi-scalar Approach to Thermal Comfort and Walkability

An important aim of this chapter is to explore the interdependencies between the built environment and walkability in cities through the lens of urban microclimates and thermal comfort. Buildings, urban spaces, and landscapes together create specific microclimates that differ from the macro-level climate (Yang et al., 2022). Information about macro-level climate is derived from meteorological weather

stations usually located at nearby airports and may differ from the specific microclimate conditions in cities.

It is possible to assess the walkability capacity of urban spaces at different scales or levels through a variety of parameters (Ak, 2018). Macro-level walkability features are concerned with regional, metropolitan, city and town-level properties. To enhance walkability at this scale, and to influence travel behavior in a sustainable manner, it is critical to examine land use patterns, transportation system characteristics and develop 'macro' land-use policies (Ak, 2018).

Referring to the summarized walkability factors in Table 2.6, it is important for urban populations to have accessibility to public transit corridors, retail and community services, green areas, and daily activity destinations. These features may be best strategized and implemented in meso- and micro- level environments.

Meso-level walkability features are concerned with neighborhoods, districts, or suburbs (Ak, 2018). Most studies that perform correlational analyses between walkability and travel behavior focus on meso-scale urban form. Such analyses include variables like housing density, population demographics, land-use mix and so on. They also include variables relating to street infrastructure, such as block size, intersection density and dead-end density (Park et al., 2014). These variables are usually measured with GIS tools based on administrative boundaries. As Park et al. (2014) highlight, the use of administrative boundaries of census blocks or census tracks is the most efficient method to utilize open-access data.

Micro-level walkability features are concerned with street-level physical attributes that are directly perceived by pedestrians (Park et al., 2014). Similarly, Ak (2018) writes that walkable public spaces are those which accommodate diversity, are attractive, safe, comfortable and, with greater connection to their surroundings and local destinations.

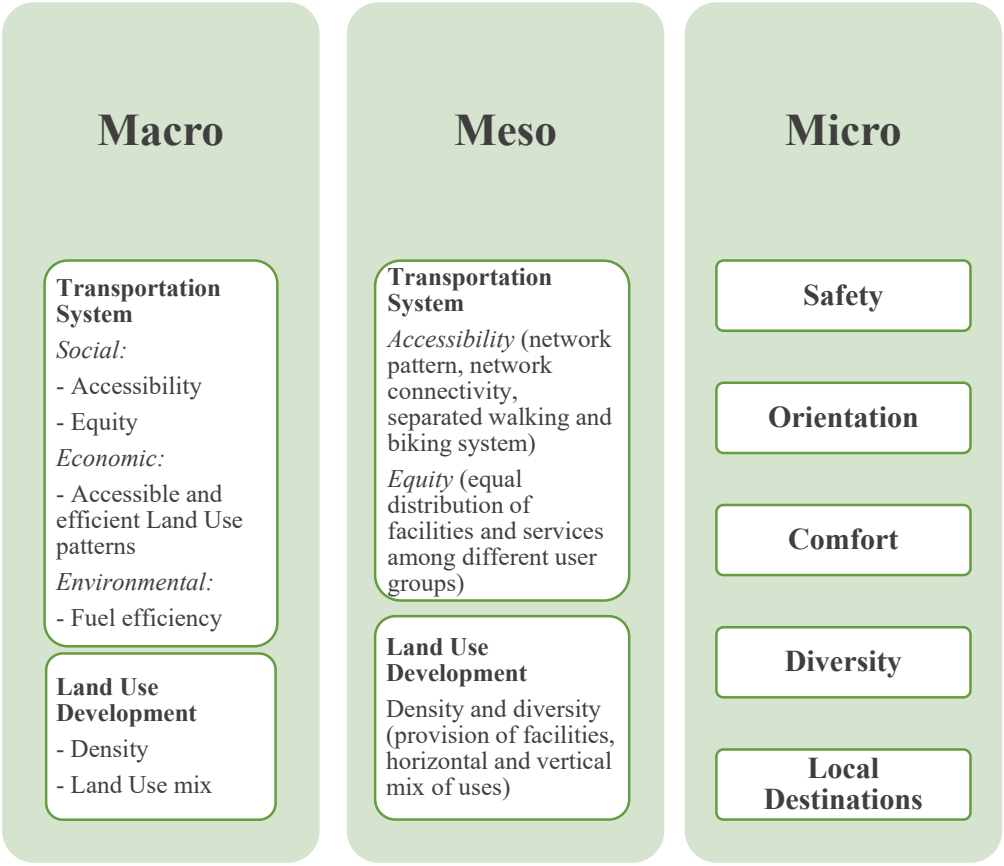

Figure 3.4: Macro-, meso-, and micro-level walkability measures as summarized by Ak (2018)

The issue of scale is often raised in walkability associated literature. According to Ak (2018), walkability of cities should be studied, planned, and designed based on three major scales: macro-scale, meso-scale, and micro-scale (As shown in Figure 3.4). Figure 3.4 shows a systematic categorization of walkability parameters and highlights the importance of walkability and its multi-level impact in urban areas. Such considerations can also be integrated in urban design frameworks with the aim of prioritizing pedestrian-oriented cities.

Learnings from Figure 3.1, Figure 3.3 and Figure 3.4 highlight the significance of assessing thermal comfort of pedestrian environments through a multi-scalar approach.

3.4 Climate-Responsive Urban Design Strategies for Mitigating Urban Heat and Improving Walkability

There are various approaches to ascertain the causes and consequent effects of urban thermal patterns and to present solutions to overcome the negative impacts on cities. There are also certain criteria to assess the impact of heat mitigation strategies including environmental temperatures (air and surface temperatures), energy saving potential and outdoor air quality. However, these criteria must be prioritized based on the diverse conditions and constraints of different geographical contexts and urban regions (Aflaki et al., 2017). It is also important to consider the comfort level of pedestrians since the thermal characteristics of outdoor environments significantly impact pedestrian activities and spaces. Better thermal comfort leads to better quality of outdoor spaces and more people in outdoor environments (Nasrollahi et al., 2020).

This section presents a review of scale dependent urban design strategies derived from existing literature.

3.4.1 Macro-scale Strategies

Green Areas

Tumini & Rubio-Bellido (2016), write that the implementation of passive strategies at urban level will result in better quality of urban microclimates. To provide a comfortable climate, public spaces should include a sizeable amount of street vegetation, high building density and deep streets with a high level of connectivity between them (Mouda et al., 2019).

Klemm et al. (2014) found that in hottest period of the day in Utrecht, Netherlands, parks were approximately 0.8 K cooler than the city center and 0.3 K warmer than the grassland outside the city. These findings can be attributed to the lower surface temperatures, evapotranspiration of vegetation, lack of hard surfaces, and long wave radiation from surfaces in parks and the open grassland outside the city (Klemm et al., 2014).

Radhi et al. (2015) used computational-fluid-dynamics (CFD) analysis to assess the effect of artificial islands on climatic parameters in Bahrain. They found that there is a mean radiant temperature difference of up to 5 °C between vegetated areas and concrete surface.

However, the impact of each of these strategies also depends on the regional climate and geographical context. Alexandri & Jones (2008) found that employing green roofs and green walls could result in a greater difference in urban air temperatures in hotter climates. This may be because hotter and drier climates provide a higher potential for heat reduction.

To facilitate the above-mentioned strategies, urban green spaces should also be accessible, located in accordance with their purpose and must be within walking distance of neighborhoods and corresponding sub-scales (Aydemir et al., 2004). However, the distribution of urban green spaces in neighborhoods, districts and the city are not always equal (Atanur et al., 2022). While urban green areas play a big role in regulating urban temperatures, it is also important for these areas to be equally accessible from their immediate surroundings.

Another important aspect of climate change mitigation through urban green spaces is to provide a well-functioning urban green infrastructure network. It can encourage walkability from residential areas across public open spaces and natural green corridors, to urban activities and recreational spaces even under extreme weather conditions (Caprì et al., 2016). Moreover, a green network designed within and around built areas can also lessen the intensity of urban heat islands.

Land use Mix

Reducing the area of mixed-use land types and increasing green space can significantly reduce temperatures (Chen & Lin, 2021). Many studies highlight that extreme heat is unevenly distributed across urban areas and that land use and cover change are one of the significant contributors to this phenomenon (Chen & Lin, 2021).

For example, an analysis on the formation of heat stress in the city of Nanjing revealed that changes in LULC significantly impact heat stress (Min et al., 2019). The analysis also found that bare soil and impervious surfaces increase LST. In this regard, it is important to assess how different spatial compositions influence LST patterns.

According to Chen & Lin. (2021) artificial land use, particularly mixed use, commercial use, and industrial use positively affects extreme heat. On the other hand, green space and water resources have a negative effect on extreme heat. Residential areas do not significantly impact LST.

However, it must also be noted that walkability is positively associated with land use mix. As King et al. (2015) states, greater destination mix is associated with greater walking frequency. Therefore, macro-level mitigation strategies should consider spatial heterogeneity of the influences of land use on temperature and its impact on walkability.

Urban form

Urban geometry, which involves canyons made up by building heights and street widths can dictate how heat gains dissipate throughout the day. For example, in deep canyons, the sky view factor is limited which results in lower radiation losses than in open spaces. Li et al. (2020) found that more compact urban clusters lead to higher UHI intensities. As a result, urban geometry plays a crucial role in the rate of heat loss in urban areas (Sakar & Çalışkan, 2019).

The building height to street width (H/W) ratio is a major contributing factor of UHI intensity (Oke, 1981). In terms of pedestrian thermal comfort, the shade created by buildings plays an important role in relieving extreme heat conditions. For example, Jamei & Priyadarsini (2017) found that increasing the height of buildings results in a reduction of temperature of up to 4 ℃ in Melbourne, Australia. Rodríguez-Algeciras et al. (2018) investigated the impact of different H/W ratios of courtyards in the warm and humid climate of Cuba. They found that a H/W ratio of 3, as compared to a H/W ratio of 0.5 resulted in a reduction of mean radiant temperature of up to 20 ℃.

Increasing H/W ratios and the consequent shading effect can increase thermal comfort in urban canyons during warm seasons. On the other hand, increasing H/W in urban canyons can also intensify the UHI effect. In this regard, the effect of H/W is two-fold and must be carefully studied.

Increasing H/W ratio to improve thermal comfort seems to be associated with the shading effect created by buildings. While shade from buildings positively impacts pedestrian thermal comfort, it is more harmful for overall climate (at the urban scale).

Different urban geometries and two-dimensional street sections can create various microclimate conditions. It is also important to consider the climate of the region. For example, in very hot climates, denser urban geometries may alleviate thermal comfort due to the increased shading effect. In a different climate, the same urban geometry can cause thermal dissatisfaction in outdoor environments (Nasrollahi et al., 2020).

3.4.2 Meso-scale Strategies

Green Areas

Wong et al. (2009) found that applying greenery over large areas positively impacts microclimate conditions. The use of green infrastructures to reduce the thermal

storage capacity and absorption of excessive solar radiation include street trees, green roofs, and urban parks (Yao et al., 2022).

Urban parks are a key component of blue and green infrastructure in cities. They exert a cooling effect by creating local cool islands where the temperature inside the park is significantly lower than its surroundings. In this way, urban parks can significantly reduce surrounding LSTs (Yao et al., 2022).

Factors which contribute to the cooling effect of parks include features such as the spatial arrangement of parks and tree canopy size (Balany et al., 2020). By simulating the effect of eight different spatial arrangement of parks, Lin & Lin (2016) found that a greater park diversity, an evenly distributed park and a larger park area significantly contribute to the reduction of temperature.

In terms of thermal comfort conditions, it is important to consider the aggregate effect of surface materials covering urban streets such as roads, pavements and building facades (Nasrollahi et al., 2020). An important feature of urban materials is their albedo value which relates to their color. Dark-colored materials such as concrete and asphalt have low albedo while light-colored surfaces have high albedo values (Balany et al., 2020). Replacing conventional materials with cool material reduce surface temperatures by 8.5 ℃ to 10 ℃ for concrete and 6 ℃ to 9 ℃ for asphalt surfaces (Tsoka, 2017).

Similarly, combining grass surfaces in green infrastructure can improve thermal comfort conditions. However, in areas where open spaces are limited, green roofs are often considered a suitable addition to green infrastructure in cities. On the contrary, green roofs give a very low improvement to thermal comfort in cities, especially at the pedestrian level (Balany et al., 2020). The combination of grass, trees and shrubs is more effective in reducing air temperature and improving street level thermal comfort than the application of green roofs (Balany et al., 2020).

Increasing Shade

Mitigating measures oriented towards reducing heat gains in the summer such as providing shading systems can significantly reduce heat storage in urban canyons (Tumini & Rubio-Bellido, 2016). Shade from trees is of great importance in outdoor environments. Urban trees have the potential to offset the UHI effect (Akbari et al., 2001). Complete shading by healthy trees, where no direct sunlight penetrates the tree canopy eliminates over 90% of the solar energy falling on a surface (Enete et al., 2012).

However, the cooling potential of street trees depends on the planting density (spacing between trees), geometry of the street and the level of canopy coverage. In this regard, evergreen trees and trees with broad leaves provide more shade compared to deciduous plants and trees with narrow leaves (Enete et al., 2012). Kong et al. (2017) found that trees with dense canopies and large crowns have a sizeable effect on the improvement of thermal comfort conditions by blocking solar radiation.

Street orientations and urban canyons

Vasilikou & Nikolopoulou (2020) found that high density spaces with greater interconnectivity can result in a different thermal sensation between streets and squares. They also found that sequential movement along spaces with complex urban morphological characteristics can enhance diversity in thermal sensation.

Street orientation alters the microclimate by influencing the exposure of canyon surfaces to solar radiation (Balany et al., 2020). Algeciras et al. (2018) found that asymmetrical streets and streets in the East-West orientation are the most thermally stressed. However, in arid climates, North-South canyons provide lower outdoor thermal comfort (Sanagar Darbani et al., 2021).

3.4.3 Micro-scale Strategies

Street Vegetation - Trees

Green areas can significantly mitigate unfavorable thermal conditions at street level (Tumini & Rubio-Bellido, 2016). Street trees are instrumental for improving thermal comfort and walkability (Siqi & Wang, 2021). Siqi & Wang, (2021) found that street trees impact pedestrian perceptions by causing a reduction of up to 3 seconds per 100 meters in perceived travel time (PTT). The presence of street trees also reduces peak mean radiant temperature by 4.23 ℃.

Kong et al. (2017) analyzed the impact of different tree types on outdoor thermal conditions in Hong Kong. They found that trees with larger crowns are preferable to trees with small crowns. *Ficus macrocarpa, Acacia confusa*, and *Macaranga tanarius* are some good examples of trees with large crowns. Morakinyo et al. (2018) found that tree height, crown diameter, trunk height and leaf-area index are the most important features of trees for improving outdoor thermal comfort.

Street level tree planting strategies must be designed according to street type and local climates. In the hot and dry climate of Pheonix, Arizona, Zhao et al. (2021) found that planting trees with an equivalent distance of two trees in between and creating clusters without overlapping the canopies was the most suitable scenario to enhance outdoor thermal comfort.

Increasing Shade

Blocking solar radiation using shading strategies is another important factor affecting outdoor thermal comfort especially in summer months (Nasrollahi et al., 2020).

Li et al. (2022) investigated the relationship between three types of shading in high-rise building estates with air temperature values. The three types of shading, as visualized in Figure 3.5 are tree shading, building shading and building-tree integrated shading. They concluded that building-tree integrated shading provides the most significant cooling effect, followed by building shading and tree shading. Similarly, Dai et al. (2019) found that increasing building shade area by 1% lowers the LST by 0.79%.

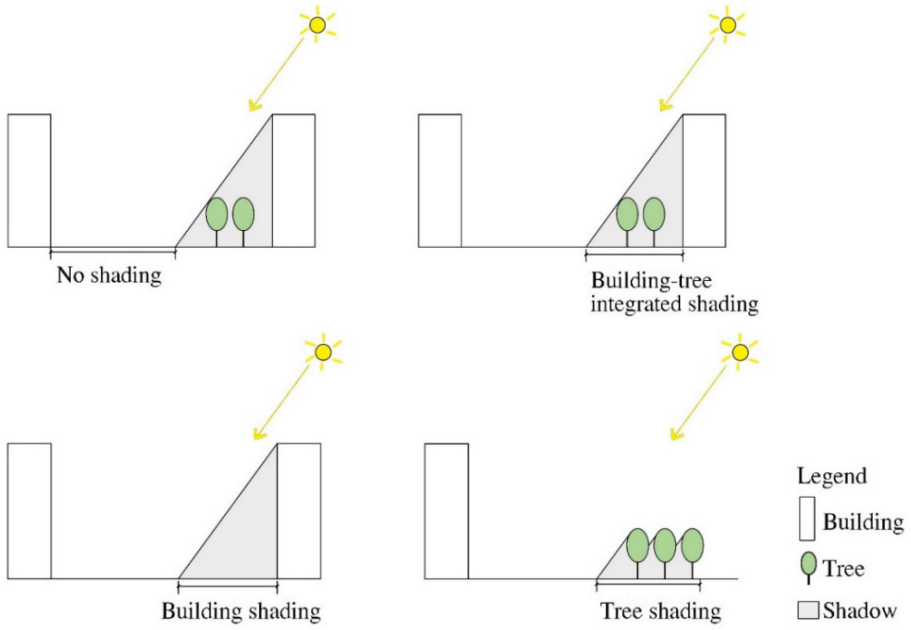

Figure 3.5 Types of shading in high-rise building estates investigated by Li et al. (2022)

As a result, it can be stated that tree arrangement relative to street canyons and buildings is a more effective cooling strategy. However, these considerations are specific to site conditions specific to micro-scale characteristics like street morphology and cannot be applied to city-wide analyses (Park et al., 2021).

Cool Pavements

The albedo of urban surfaces plays an important role in regulating urban temperatures. Generic paving materials can reach peak summer temperatures

between 48 °C and 67 °C. The extra heat is then delivered to the atmosphere above these surfaces (Vardhu & Sharma, 2023). For example, Akbari et al., 2001 found that for every 0.25 increase in albedo, there is a 10 °C decrease in pavement temperature.

Başçıl Erkaya, (2022) notes although grass has a low-albedo value, grass-covered surfaces reduce the surface temperature up to 10 °C compared to other pavement materials. As a result, techniques like the use of coatings or grass pavers can be used to enhance thermal performance of pavements (Vardhu & Sharma, 2023).

3.4.4 Concluding Remarks

Mitigating urban heat requires a comprehensive understanding of macro-, meso-, and micro-level factors. A major challenge in the study of urban heat is that many characteristics and factors vary among cities. For example, the size of the urban agglomeration, urban form, density, thermal characteristics of rural surfaces, construction materials and street geometry (Li et al., 2020).

The appropriate contextualization of urban measurements is an important aspect of urban climate research especially when it overlaps with walkability and thermal comfort. It has been observed that microclimate changes cannot be due to a single factor and that more than one variable affects an area at the same time. For this reason, when conducting future studies, a holistic approach should be adopted instead of considering the parameters affecting the microclimate separately (Başçıl Erkaya, 2022).

Evidence-based design guidelines for thermally comfortable cityscapes are needed which support urban planners, policy makers, and city managers in their decision making. Strategies informed by climate-specific and high-quality data which favor the preservation, maintenance and development of urban green spaces are needed. Urban planners, policy makers, and city managers also need to anticipate on

increasing urban heat due to climate change and provide healthy and thermally comfortable living environments in the future (Klemm et al., 2014)

CHAPTER 4

RESEARCH METHODOLOGY

This chapter provides a detailed outline of the research methodology including the design of the methodology, selection of mapping variables, study areas and the data acquisition process.

Learnings from the previous chapters highlight that walkability is influenced by multiple parameters. The literature review (chapters 2 and 3) also contextualizes the issue of outdoor thermal comfort in cities, its relationship with walkability and microclimate, and how it is impacted by macro-, meso- and micro-level urban design strategies. It categorically addresses the importance of scale-dependent, climate-responsive approaches to urban design and relevant heat mitigation strategies that can alleviate pedestrian thermal comfort in cities.

Examining pedestrian behavior is highly subjective and varied across different social, economic, and environmental factors. The selection of an appropriate method also depends on the scale of the study and availability of data.

Within the context of urban design, walkability research methods can be categorized into four groups:

1) Surveys, questionnaires, and interviews (subjective)
2) Direct audit tools or stock-taking usually performed by trained auditors (subjective)
3) GIS tools (objective)
4) Mixed methods, which combine information from secondary data sources or data obtained through direct measurements or surveys (Telega et al. 2021).

GIS-based analyses can have far-reaching implications and high level of applicability in the domain of soft mobility. As the literature review demonstrates,

when examining pedestrian environments, the most common elements using GIS tools are traffic intensity, route calculations, street layout, network density, population density, land use multifunctionality and pedestrian catchments. However, at the urban level, it is quite challenging to systematically analyze and encourage thermal comfort associated walkability.

The methodology proposed in this thesis represents a first step towards the development of an analytical framework to explore the relationship between walkability and rising urban temperatures. With the aim to investigate the resilience of walkable segments in the city to heat associated climate extremities, the author proposes a methodology to:

- Evaluate thermal properties of walkable urban environments.
- Assess the impact of land use composition and vegetation health on LST.
- Conduct a temporal, multi-scalar analysis through the creation of LST, NDVI and LULC maps.
- Assess the impact of increased vegetation on hourly variations on near-surface air temperatures in four different building blocks with distinct street features.

At the macro-scale, provincial and metropolitan level of Ankara is analyzed to spatialize LST hotspots, distribution of vegetation and land cover types. At meso-scale, the district of Çankaya and neighborhoods within the boundaries of Çayyolu district are analyzed to assess the distribution of LST, vegetation and land types. At the micro-scale, selected building blocks located on the main arteries within the neighborhood of Çayyolu, are analyzed to reveal the impact of urban design features on near surface air temperature.

Each of the above-mentioned urban heat indicators, namely, LST, NDVI and LULC are mapped for selected years between 1990 and 2021 corresponding to dates exhibiting peak summertime temperatures. In this way, the immediate and long-term changes in climate, urban development patterns, composition of vegetation and land

use mix can be compared with corresponding surface temperature patterns to understand the key drivers of rising urban temperatures.

Moreover, the mapping results of each of the above-mentioned scales (provincial, metropolitan, district and neighborhood) are interpreted based on the urban design strategies proposed in Chapter 3. In this way, urban heat indicators and their effect on thermal comfort associated walkability are examined by linking scale-specific urban planning and design strategies and policies with the empirical findings from the mapping results.

4.1 Study Area

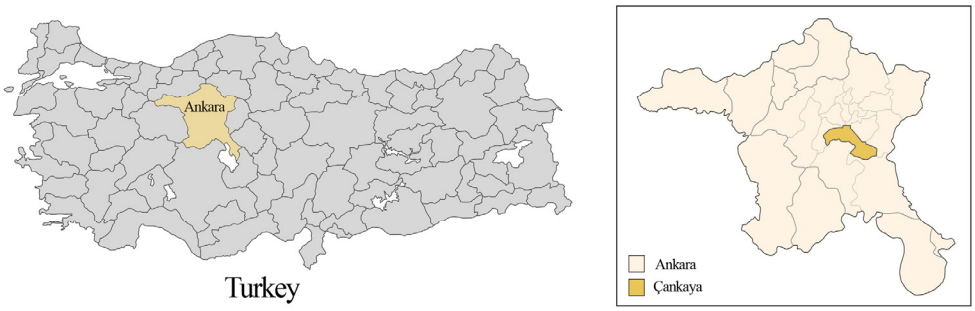

Figure 4.1: Location of Ankara and the Çankaya district in Turkey

Ankara is in the Anatolian region of Turkey and is comprised of 25 districts. It has a continental climate. The annual average temperatures demonstrate similar upward trends parallel to the increase of global temperatures. According to IPCC (n.a), if climate change measures are not prioritized, the annual average temperatures in Turkey will rise by 2.5 – 4°C.

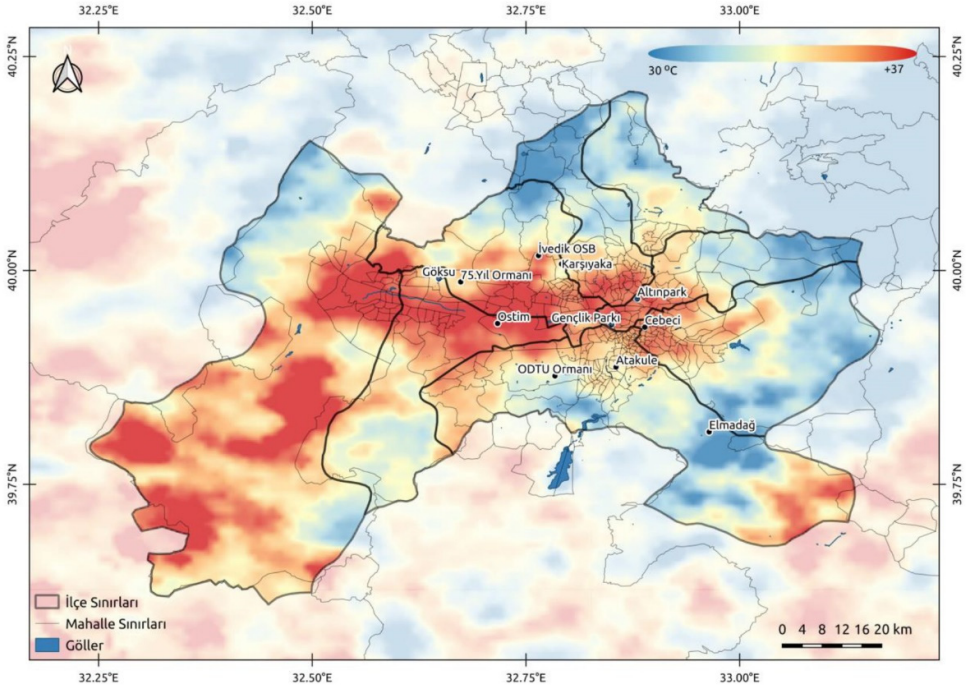

Figure 4.2 Average Surface Temperatures Ankara (Ankara Municipality, 2022)

Projected scenarios indicate that Ankara will be facing climatic hazards in the future with an increase in heat waves and a rise in UHI effects. Similarly, Ankara faces another climatic hazard, with the recent increase in urban flooding events owing to cloudbursts and increased precipitation levels. This is mainly due to the intense urbanization in the previous decade, lack of permeable surfaces, extensive use of concrete and asphalt as urban surfaces and lack of vegetation and tree covers (Ankara Municipality, 2022)

Figure 4.3: Average Summer Daytime Maximum Surface Temperature with Ankara Province Highlighted (NASA SEDAC, 2016)

As depicted in Figure 4.3, Ankara has the largest distribution of highest average summer daytime surface temperatures. In comparison, Istanbul has a sizeable distribution of summer daytime averages, but in the 35 - 40°C range. The alarmingly high averages and the fact that the city continues to expand makes a compelling case to study Ankara.

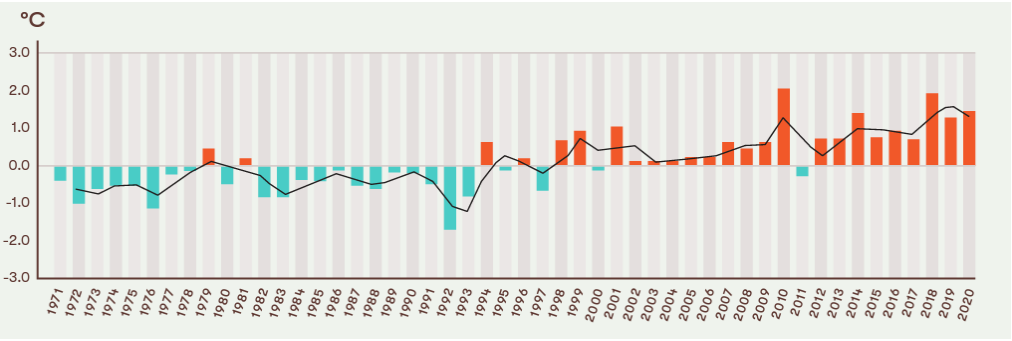

Figure 4.4 Turkey Mean Temperature Anomalies (Çağlayan et al., 2021)

Figure 4.4 highlights the increasing trend of mean temperature anomalies since the 1990s. The author notes that a temporal mapping of daytime surface temperatures is necessary to spatialize heat patterns and identify key contributors of these changes.

In this thesis, the district of Çankaya, in Ankara is analyzed. Çankaya is the largest municipality in Ankara, consisting of 124 neighborhoods with an area of 268 km^2 and a population density of 796 inhabitants per square kilometer. It is the most densely populated district with a residential population of nearly 1 million residents and daytime population of more than 2 million. This is indicative of the daily mobility flows to and from this region (Hayrullahoğlu & Varol, 2022).

Çankaya exhibits a high demand for mobility and daily pedestrian flows. It includes shopping malls, business centers, historical sites, and the main institutional bodies of Turkey. An abundance of transportation alternatives, a high commuter adjusted population and high-level transportation relations with the rest of the city makes this district the densest and the most dynamic (Hayrullahoğlu & Varol, 2022).

Çayyolu, a sub-district of Çankaya, is analyzed to deepen the understanding of neighborhood level characteristics. The selection of this specific area is due to the rapidly increasing development in the area. New construction, mostly in the form of residential complexes and mega-sized retail stores have increased and continue to expand (Akkar Ercan et al., 2021). For this reason, an analysis of district of Çayyolu further elucidates on the relationship between the previously mentioned indicators.

At the meso-scale, main arteries in Çayyolu, signified by availability of public transport and pedestrian frequency will be analyzed. An in-depth analysis of the walkable segments reveals the sensitivity of the pedestrian experience to urban design features (i.e., street level vegetation, tree canopy, green areas, and surface materials). These findings can deepen the understanding of the interaction between LST, urban vegetation and urban surface materials and provide useful insight about the configuration of urban vegetation at the landscape level to improve urban thermal environment.

4.2 Methodology

One of the key goals of this thesis is to develop a methodology to identify factors affecting the resilience of walkable urban areas to heat associated hazards. A multi-scalar temporal mapping of Ankara is produced to identify and monitor changes in land characteristics and to understand their influence on urban heat.

In Turkey, the current meterorological network cannot adequately reflect the "real" climatic conditions, especially the variability in air or land temperature at the regional and local scales.

Meteorological stations in Ankara are not uniformly distributed. In this sense, LST maps can be retreived at high spatial (60 m) resolution and temporal (daily) resolution, allowing for a better understanding of energy balance changes and land surface conditions at detailed spatial scales (El Kenawy et al., 2019). Overall, remotely sensed data can potentially contribute to a more reliable diagnosis of different climatic and environmental variables (e.g, vegetation, land surface emissivity, land surface temperature) (El Kenawy et al., 2019).

Urbanization changes the natural biophysical environment through alterations in LULC patterns. Urban expansion removes vegetation covers and replaces natural areas. This causes changes not only in the hydrological cycle, but also in the energy balance, regarding energy transfer and storage, that occurred naturally before anthropic interference (Kaiser et al., 2022). As a result, there are changes in the thermal characteristics of land surfaces, humidity, air temperature, wind speed and direction.

As Zhang & Sun (2019) write, changes in urbanization patterns result in an increase in the Earth's surface temperature (LST) and consequently leads to the formation of heated cores, thermal or humid cores, or even as heat pockets. The presence of vegetation influences LST by regulating the exchange of latent and sensitive heat, the absorption and selective reflection of solar radiation (Kaiser et al., 2022).

Such correlations between surface temperatures, surface greenness, and land use patterns can be observed by using Land Surface Temperature (LST), Normalized Difference Vegetation Index (NDVI) and Land Use/Land Cover (LULC) values using remote sensing techniques (Kaiser et al., 2022).

A comparison of these maps can shed light on the relation between different land types, land use patterns, vegetation types, vegetation density and surface temperature hotspots. They can also provide a more accurate reading of built-up and green areas and their relative distribution. In this way, this research can uncover the dynamics of urban heat and their relation to microclimatic features and thermal comfort conditions in walkable spaces.

Since the size of the study area covers an expansive geography and requires analysis of data from millions of data points recorded consistently for simultaneous observations of surface emissivity and land cover, satellite remote sensing techniques are the most feasible.

According to weather data, the hottest months recorded for Ankara are July and August. This was the time range chosen to compare changes for the selected years between 1990 to 2021 (as specified in Table 4.1).

To produce the above-mentioned maps, Landsat images from the USGS database were used. The images, along with the vector drawing (shapefile) of the study area is used as raw data inputs in GIS software. With GIS, formulas for each of the indicators will be applied to the relevant bands layered in the satellite images. This will generate geo-referenced information (maps) which will be classified according to specified ranges. For example, in Figure 4.3, the average summer daytime maximum surface temperature is divided into 6 temperature ranges.

However, it must be noted that understanding the relationship between LST, urban vegetation and land use patterns is complex and scale dependent. For a more thorough understanding and to increase the reliability of derived inferences from the produced maps, the same indicators at a higher scale, will be produced at five levels;

1) Ankara province, 2) Ankara city, 3) Çankaya district, 4) Çayyolu sub-district and 5) Selected building blocks on arterial street segments in Çayyolu.

4.3 Data Collection and Processing

For producing LST, NDVI and LULC maps, Landsat images were downloaded from the USGS Earth Explorer online portal (https://earthexplorer.usgs.gov/). Landsat-5, Landsat-7 and Landsat-8 satellite images were obtained for the dates listed in Table 4.1.

Table 4.1 Details of Landsat satellite images

Number	Satellite	Sensor	Date Acquired
1	Landsat 5	TM	27.08.1990
2	Landsat 5	TM	12.07.2000
3	Landsat 7	TM	15.08.2006
4	Landsat 8	OLI & TIRS	24.08.2018
5	Landsat 8	OLI & TIRS	16.08.2021

To define the geographical limits of the areas to be processed, vector data of district, sub-district and neighborhood boundaries were accessed from open-data sources; DIVA-GIS (https://www.diva-gis.org/), The Humanitarian Data Exchange (https://data.humdata.org/) and OpenStreetMap (https://www.openstreetmap.org/).

Google Earth imagery is chosen as a base map to improve orientation and cognitive understanding of the reader. For each mapping scale, special consideration was attributed to the level of detail expressed in each outcome.

To increase the reliability of data, boundaries within each mapping extent were carefully chosen based on the precision of the information.

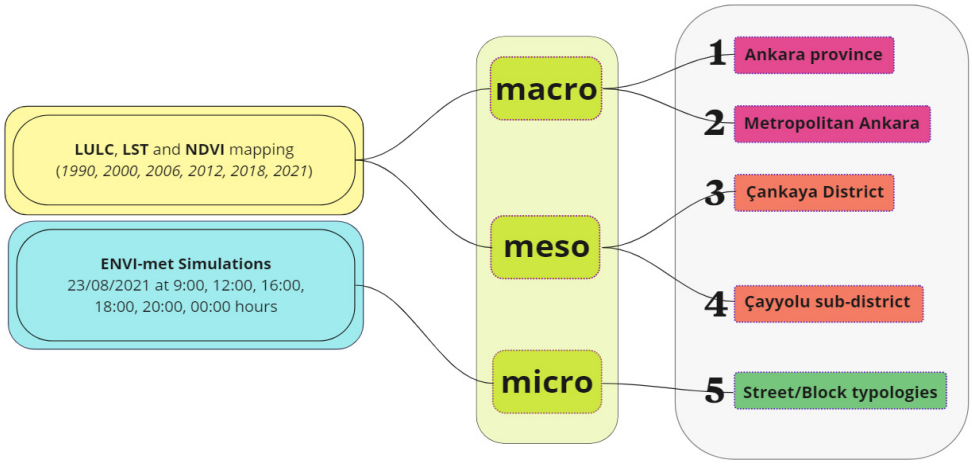

Figure 4.5 Organization of mapping scales

For Ankara Province Maps, the map extents are defined by the administrative boundary of the province and the district boundaries within (as portrayed in Figure 4.6). This provides an understanding of land composition and can point to positive and negative growth of key land types within the provincial boundaries.

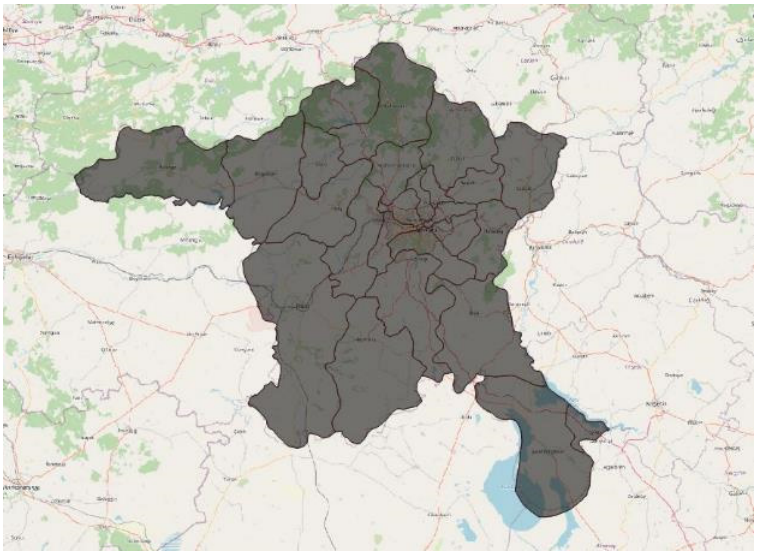

Figure 4.6 Ankara Province Boundaries

With regards to the city of Ankara, since the metropolitan extents continue to grow outwards, they almost exist as virtual boundaries. For this reason, no specific boundary was defined. A rectangle, as shown in Figure 4.7, measuring 60 km by 55 km was drawn to include the extent of urban and surrounding rural areas to be able to make an observable comparison, while also monitoring changes in urban patterns over time.

Figure 4.7 Ankara Metropolitan virtual limits with district boundaries

For a finer reading of the mapped variables, neighborhood boundaries are crucial to enhance comparability of temporal changes and distribution of land-types. For this reason, district and neighborhood boundaries were extracted from Open Street Map for the mapping of Çankaya level, as depicted in Figure 4.8.

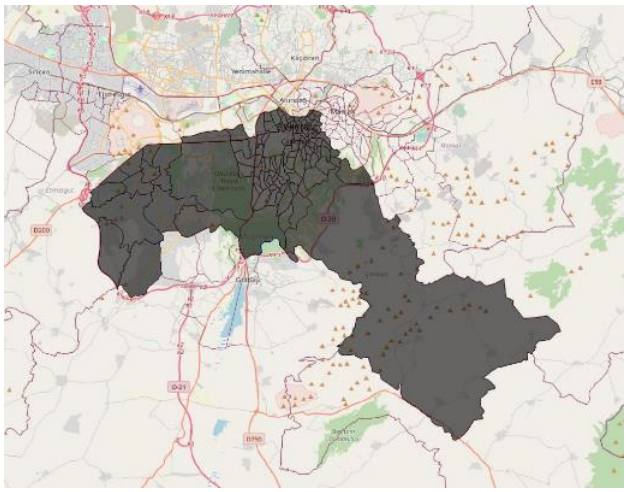

Figure 4.8 Çankaya boundaries with neighbourhood boundaries

At the sub-district level, the neighborhoods that constitute Çayyolu define the extents of this mapping scale (Figure 4.9).

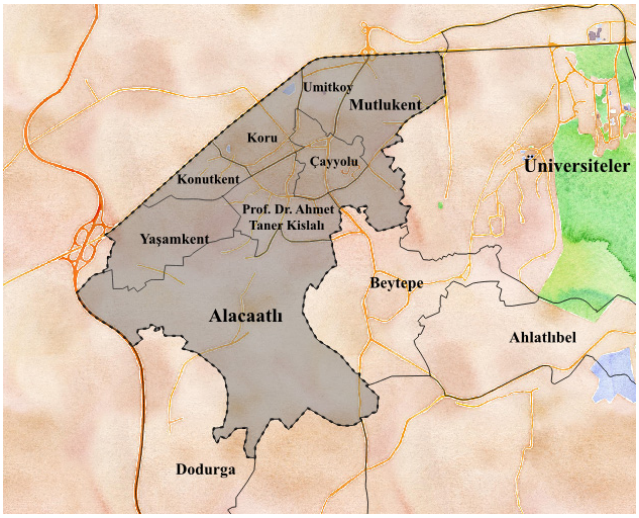

Figure 4.9 Neighborhood of Çayyolu with 8 sub-neighborhoods

Since Landsat images have a standard resolution of 30 m, the resolution of produced maps remained unchanged throughout the mapping scales. However, the above-mentioned delineations of provincial, district, sub-district and neighborhoods boundaries were chosen to enhance the readability and interpretive capacity at each scale.

Table 4.2 Type of maps produced for each selected year and selected scales.

	Ankara Province	**Ankara City**	**Çankaya (district)**	**Çayyolu (sub-district)**
1990	LULC, NDVI, LST	LULC, NDVI, LST	LULC, NDVI, LST	LULC, NDVI, LST
2000	LULC, NDVI, LST	LULC, NDVI, LST	LULC, NDVI, LST	LULC, NDVI, LST
2006	LULC, NDVI, LST	LULC, NDVI, LST	LULC, NDVI, LST	LULC, NDVI, LST
2012	LULC	LULC	LULC	LULC
2018	LULC, NDVI, LST	LULC, NDVI, LST	LULC, NDVI, LST	LULC, NDVI, LST
2021	NDVI, LST	NDVI, LST	NDVI, LST	NDVI, LST

For the street level analysis of main arteries of Çayyolu, Google Earth images and CAD drawings will be used to produce accurate plans of the selected arteries. An analysis of urban design characteristics such as surface materials, pavement continuity, street signage, street vegetation, crosswalks, urban furniture and building entrances will help deepen the understanding of walkable environments and support findings of maps created.

4.4 Production of Land Use Land Cover Maps (LULC)

The Copernicus Land Monitoring Services have been utilized to produce Land Use Land Cover maps. Copernicus is the European Union's Earth observation program, where high resolution imagery is interpreted using national in-situ data, satellite

image processing, GIS integration and generalization. The required maps were obtained from the website (https://land.copernicus.eu/). All data is free and openly accessible. In terms of Land Cover maps, there are two main databases, derived from different data sources, namely: CORINE Land Cover (CLC) and Urban Atlas.

For this study, CLC maps were utilized due to a wider time range of mapped changes. The CORINE Land Cover (CLC) inventory was initiated in 1985 (reference year 1990). Updates have been produced in 2000, 2006, 2012, and 2018. The maps are available in raster and vector format. It consists of an inventory of land cover in 44 classes. CLC uses a Minimum Mapping Unit (MMU) of 25 hectares (ha) for areal phenomena and a minimum width of 100 m for linear phenomena.

For this study raster images for the years 1990, 2000, 2006, 2012, and 2018 were downloaded. The obtained data was processed in QGIS to crop the data within the selected boundaries. Since the data includes the entire European region, the map was clipped for the administrative boundaries of Ankara Province. These maps have an accuracy threshold of 85%. Since accuracy assessment checks have already been performed by the publishers of this data, no additional assessments were performed.

LULC Nomenclature

Anthropogenic interference, such as the rapid expansion of cities results in the loss of natural areas and alterations in the natural biophysical environment. Due to the intensification of urban expansion, the local physical environment and specific regional climates, the city develops its own urban climate (Kaiser et al., 2022).

Table 4.3 CORINE Land Cover Nomenclature

Level 1	Level 2	Level 3
1 Artificial surfaces	11 Urban fabric	111 Continuous urban fabric
		112 Discontinuous urban fabric
	12 Industrial, commercial and transport units	121 Industrial or commercial units
		122 Road and rail networks and associated land
		123 Port areas
		124 Airports
	13 Mine, dump and construction sites	131 Mineral extraction sites
		132 Dump sites
		133 Construction sites
	14 Artificial, non-agricultural vegetated areas	141 Green urban areas
		142 Sport and leisure facilities
2 Agricultural areas	21 Arable land	211 Non-irrigated arable land
		212 Permanently irrigated land
		213 Rice fields
	22 Permanent crops	221 Vineyards
		222 Fruit trees and berry plantations
		223 Olive groves
	23 Pastures	231 Pastures
	24 Heterogeneous agricultural areas	241 Annual crops associated with permanent crops
		242 Complex cultivation patterns
		243 Land principally occupied by agriculture, with significant areas of natural vegetation
		244 Agro-forestry areas
3 Forest and semi natural areas	31 Forests	311 Broad-leaved forest
		312 Coniferous forest
		313 Mixed forest
	32 Scrub and/or herbaceous vegetation associations	321 Natural grasslands
		322 Moors and heathland
		323 Sclerophyllous vegetation
		324 Transitional woodland-shrub
	33 Open spaces with little or no vegetation	331 Beaches, dunes, sands
		332 Bare rocks
		333 Sparsely vegetated areas
		334 Burnt areas
		335 Glaciers and perpetual snow
4 Wetlands	41 Inland wetlands	411 Inland marshes
		412 Peat bogs
	42 Maritime wetlands	421 Salt marshes
		422 Salines
		423 Intertidal flats
5 Water bodies	51 Inland waters	511 Water courses
		512 Water bodies
	52 Marine waters	521 Coastal lagoons
		522 Estuaries
		523 Sea and ocean

Learnings from the literature review indicate that strategies to improve thermal comfort of pedestrians include vegetation, water bodies, shading (from trees and buildings), orientation of urban form and solar-reflective materials. McCormack et al. (2020) writes that proximity and mix of destinations can positively contribute to walking and physical activity.

In this regard, the nomenclature of land cover types (as shown in Table 4.3) is a useful classification to examine the changes in land surface dynamics over time. As shown in Table 4.2, for each of the mapping scales and selected dates, the classified LULC types were quantified and tabulated to:

1) Monitor changes in land cover classes over time
2) Cross-examine the effects of different land cover types on LST and vegetation greenness (NDVI)
3) Determine how different land covers specific to the urban landscape of Ankara impact urban heat at different scales.
4) Determine which types of vegetation covers have a significant cooling effect on LST patterns.

4.5 Calculation of Land Surface Temperature (LST)

There are several methods to extract LST from satellite imagery including:

- Single Channel Algorithm (SCA)
- Mono-Window Algorithm (MWA)
- Split-Window Algorithm (SWA)
- Radiative Transfer Equation (RTE) (Yamak. et al, 2021)

It is important to choose a suitable algorithm based on the different conditions in different study areas. Jiang & Ling (2021) found that the spatial distribution of the four algorithms was basically the same. The study also found that MWA has the greatest precision for LST results in areas with artificial surfaces, vegetation and cultivated land. The SWA has higher accuracy in wetlands while RTE and SCCA have higher accuracy in water bodies. MWA and SWA are more suitable for LST retrieval in summer due to the high water content in those months (Jiang & Ling, 2021). As a result of these findings, this thesis uses MWA for Landsat retrieval.

Figure 4.10 describes the methodology followed to produce LST and NDVI maps using MWA method.

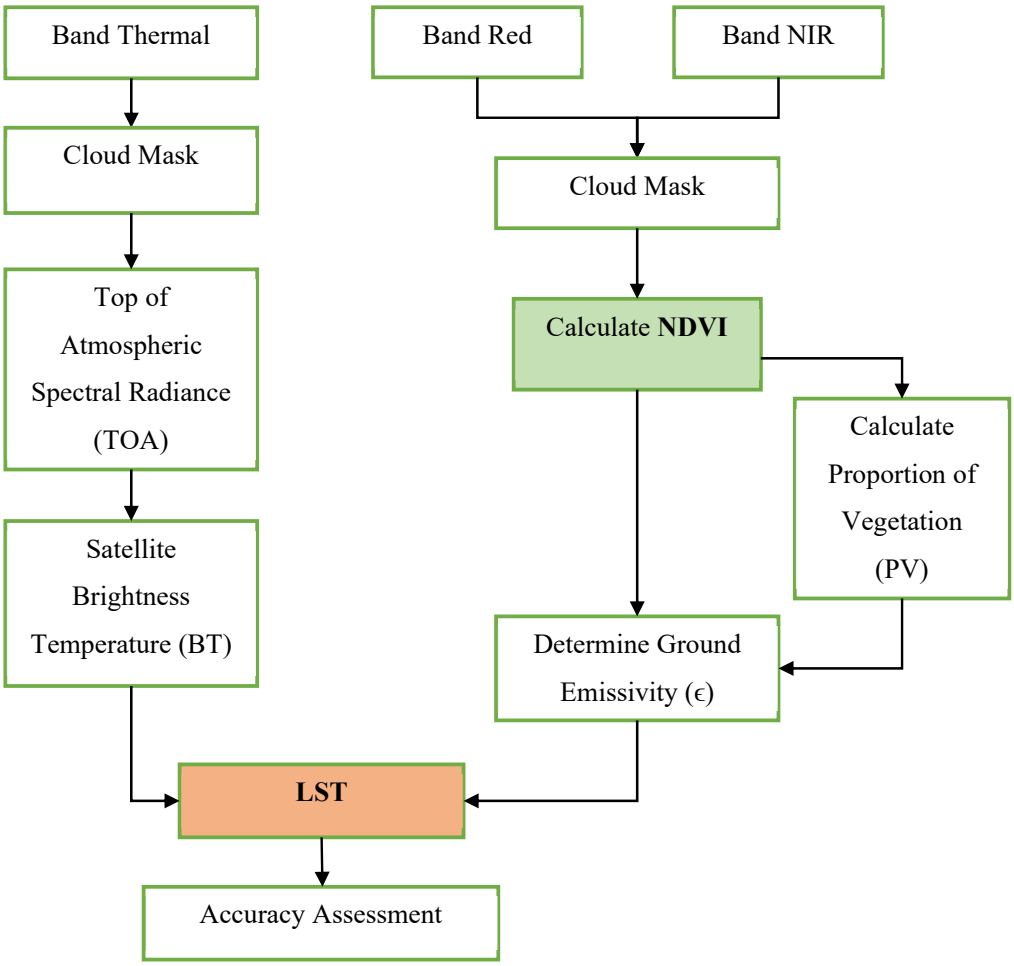

Figure 4.10 Methodology for producing LST and NDVI maps

Cloud Masking

Clouds obscure parts of the Earth's surfaces in satellite imagery. As a result, the presence of clouds and their shadows in the acquired Landsat images affect classification or any type of analyses that use Landsat imagery as data inputs. Clouds are colder and brighter and result in abnormal values. For example, when LST is extracted, pixels covered with clouds will show negative values. This is a misrepresentation of land surface characteristics and alters the minimum and mean

values of extracted LST. For this reason, the relevant bands of Landsat images were pre-processed by removing pixels covered with clouds and their shadows.

To do this, a QGIS plugin, 'Cloud Masking' was employed to identify clouds and their shadows in Landsat images and remove those exact pixels from the data. This ensured accurate calculation and readings of LST and NDVI.

Extraction of NDVI

The NDVI was calculated using NIR (Near-Infrared) and red bands, and the output NDVI image was used to calculate the emissivity. The reason for utilizing NDVI in LST estimation is that the measure of vegetation present is a significant factor and NDVI can be used to induce general vegetation conditions (Weng et al. 2004).

Extraction of LST

To calculate LST, Landsat 8, Landsat 7 and Landsat 5 thermal bands (Table 4.1 Details of Landsat satellite images, were obtained from USGS Earth Explorer. A set of equations were applied through a raster image calculator (QGIS). This study used USGS formulas (U.S. Geological Survey. (n.d.). The processing steps of the LST calculation are as follows.

1) Calculation of Top of Atmospheric (TOA) spectral radiance:

$$TOA\ (L) = M_L * Q_{cal} + A_L$$

Where,
M_L = Band-specific multiplicative rescaling factor from the metadata
Q_{cal} = corresponds to band 10.
A_L = Band-specific additive rescaling factor from the metadata

2) Conversion of radiance to Brightness Temperature (BT):

$$BT = (K_2 / (\ln (K_1 / L) + 1)) - 273.15$$

Where,

K_1 = Band-specific thermal conversion constant from the metadata

K_2 = Band-specific thermal conversion constant from the metadata

L = TOA

The band specific metadata constants can be found in Table 4.4.

Table 4.4 Applied metadata values used for LST estimation (USGS, 2019)

	Landsat 5 (band 6)	**Landsat 7 (band 6)**	**Landsat 8 (band 10)**
Thermal Constant			
$\mathbf{K_1}$	607.76	666.09	774.8853
$\mathbf{K_2}$	1260.56	1282.71	1321.0789
Rescaling Factor			
$\mathbf{M_L}$	0.055375	0.067087	0.0003342
$\mathbf{A_L}$	1.18243	-0.06709	0.1

3) Calculation of Normalized Differential Vegetation Index (NDVI)

$NDVI = NIR– Red / NIR + Red$

Since the thermal bands are numbered differently for different Landsat missions, the formulae listed below were used as a reference.

For Landsat 4-7, calculation of NDVI = (Band 4 – Band 3) / (Band 4 + Band 3). For Landsat 8-9, NDVI = (Band 5 – Band 4) / (Band 5 + Band 4).

4) Calculation of the Proportion of Vegetation (PV)

$Pv = ((NDVI – NDVImin) / (NDVImax – NDVImin))^2$

NDVImin and NDVImax values correspond to the specific images being processed and the minimum and maximum NDVI values obtained.

5) Calculation of Land Surface Emissivity (ε)

$\varepsilon = 0.004 * Pv + 0.986$

where 0.986 corresponds to a correction value of the equation

6) Calculation of Land Surface Temperature (LST)

$Ts = BT / \{1 + [(\lambda BT/\rho) \ln \varepsilon\lambda]\}$

Where, ρ = 14388 × 10−2 μm K and λ values can be found in Table 4.5 below.

Table 4.5 λ values for Landsat bands

Satellite	Band	λ (μm)
Landsat 4, 5 and 7	6	11.45
Landsat 8	10	10.8

After following the above-mentioned calculations, LST maps in the form of raster images are obtained. The images are further refined by attributing specific colors to LST values. In this way all maps refer to one legend bar and allow the reader to compare changes easily. The next stage is concerned with the validation of retrieved LST values which is described in the following section.

Validation of results

Validation of LULC

An accuracy assessment for the LULC maps was not performed by the author since the data was extracted from CORINE Land Cover CLC inventory. The data is already evaluated for accuracy with a reported thematic accuracy of over 85% (EEA, 2021).

Validation of LST

LST values retrieved from satellite images are difficult to validate. LST is a complex variable and is affected by multiple factors that enforce rapid change both spatially and temporally. It is not unusual for LST to vary from more than 1 K less in less than a minute over certain land cover types or more than 10 K over just a few centimetres of distance (Arabi et al., 2021).

In summer, extremely arid climate conditions and increase in net radiation combine together to instensify warming effect at the surface. This is because of the reduction in cloudiness and the decrease in the soil and atmospheric moisture necessary for atmospheric cooling. Land-atmosphere interactions and feedbacks amongst seasons with the atmospheric boundary layer determine sensible heat fluxes and latent heat fluxes and impact exchange between land surface and atmosphere. In typical arid and semi-arid climates, soil drying can suppress evapotranspiration and induce a reduction in relative humidity (RH). These regions are characterized by lack of vegetation. All these configurations especially over bare soil regions, combine together to contribute to a dramatic increase in LST (El Kenawy et al., 2019).

The performance of LST is highly driven by seasonality. El Kenawy et al., (2019) state that LST estimations perform well during autumn and spring, while LST over estimates maximum air temperature with values exceeding 5 C in winter and summer.

As Wang et al. (2019) and Arabi et al., (2021) write, the three common methods for LST validation, include:

1) temperature-based method (directly compares the satellite-retrieved LST with in-situ LST measurements),
2) radiance-based method, and
3) cross validation method (validates the derived LST with another LST product) .

Due to the lack of in-situ measurements, satellite-retrieved LST were cross-validated against MODIS daytime LST data. Although, MODIS produces global daily LST data at 1 km spatial resolution, MODIS LST data can be used in cross-validation with Landsat retrieved LST (Çolak & Sunar, 2022).

To further validate the retreived LST, the results are also compared with another extraction method, which is calculated using Ermida et al., (2020)'s Google Earth Engine (GEE) open source code where LST is estimated using Statistical Mono-Window (SMW) algorithm. Besides Landsat data, this LST production code makes use of two other datasets:

1) Atmospheric data from the re-analyses of the National Center for Environmental Prediction (NCEP) and National Center for Atmospheric Research (NCAR)
2) Surface emissivity from the Advanced Spaceborne Thermal Emission and Reflection Radiometer Global Emissivity Database (ASTER GED) developed by the National Aeronautics and Space Administration's (NASA) Jet Propulsion Laboratory (JPL) (Ermida et al., 2020).

The LST data for cross validation from MODIS and SMW methods were retreived for the same dates as the Landsat LST. The mean LST for each image were computed in QGIS and tabulated parallel to the Landsat derived mean LST. The absolute difference was calculated to reveal the bias and allow the author to compare the values. The mean values are then plotted on a graph to detect the trends in data.

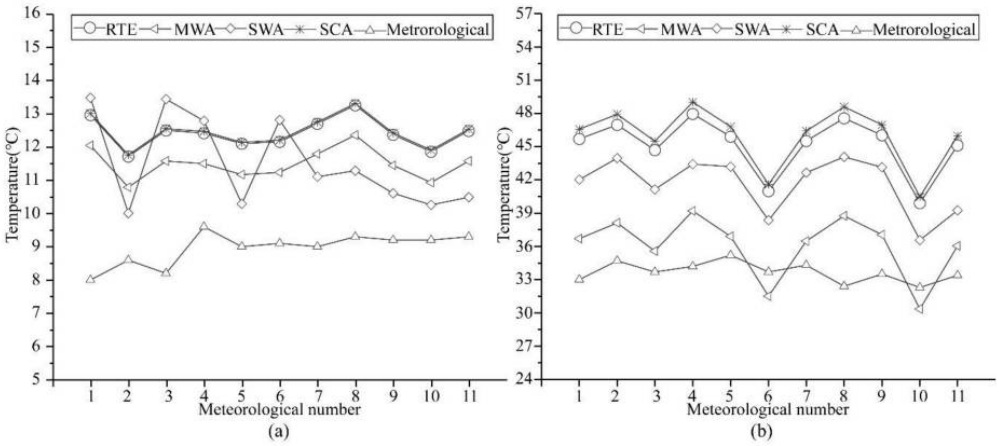

Figure 4.11 Comparison of local meteorological data with the retrieval results of four algorithms. (a) are the LST retrieval results compared with meteorological stations data on 21 January 2020; (b) are the LST retrieval results compared with meteorological stations data on August 16 2020 (Jiang & Ling, 2021).

Jiang & Ling (2021) performed a temperature-based validation by comparing data from meteorological stations with RTE, MWA, SWA and SCA retrieval results. As Figure 4.11 illustrates, while linear data trends are similar, summertime MWA values are closest to in-situ LST. The authors also note that there is almost no variation in the spatial patterns of LST retrieved from the above-mentioned algorithms.

Cross-validation with MODIS LST and SMW LST may produce some anomalies, but this can be expected due to the differences in atmospheric corrections in each product. The more important observation is to examine trends followed by the data.

4.6 Simulation of micro-climatic conditions

Natural phenomena are often very complex, which makes them difficult to study and understand. One way to address complexity is to apply analysis models that allow the understanding and anticipation of these phenomena, and such is the case of using climate models to assess the impact of urban morphological changes on local meteorological conditions. Their projections and results give essential information

for the improvement of management and decision making because they investigate the degree to which climate change derives from natural variability, human intervention, or combinations thereof.

This section of the methodology concerns with the microclimate simulation of four building blocks, typical to the neighborhood of Çayyolu.

Akkar Ercan et al. (2021) write that Kanuni Sultan Süleyman Boulevard is one of the main arteries of Çayyolu based on high traffic volumes, especially in the peak morning and evening hours. Banga Bandhu Street and Alacaatlı Street together operate as the main commercial corridor of Alacaatli due to its proximity to Koru Metro Station and a strong association with retail services and gastronomic activities. Arcadium shopping center is an important commercial landmark and economic center with a mix of building typologies in surrounding areas.

Çayyolu also has a unique topographic structure which consists of hills, valleys, and stream beds. These geomorphological features have a high potential to support the continuity of green areas at macro-scale. However, in Çayyolu, there is no continuity of green areas and neighborhood level green spaces are dispersed with unequal access between different residential sites (Akkar Ercan et al., 2021).

Based on the description of above-mentioned landmarks and key features typical to Çayyolu, four types of building blocks with distinct street features were selected.

The four scenarios include:

- Alacaatlı Street: A main street section, 20 m in width, a car park on one side and 3 story retail buildings on the other with minimal vegetation and permeable surfaces.
- 2584 Street and Doğan Taşdelen Boulevard: A 7 m wide street with a mall building (Arcadium) on one side and a 35m high apartment block on the other.

- 2710 Street: A residential street with private villas on one side and a steep (and mostly barren) hill on the other. Very minimal vegetation except for domestic green spaces.
- Kanuni Sultan Süleyman Boulevard: A high-rise apartment block with parking lot and ground level retail space.

The intention for this analysis is to examine the sensitivity of localized urban environments and observe temporal (hourly) changes in air temperature values at an elevation of 1.5m (average pedestrian height).

4.6.1 Microclimatic computer simulation using ENVI-met

Changes in microclimate conditions are manifested by extreme heat events (Kim & Hong, 2021). With respect to the research questions posed in this thesis, it is necessary to model existing urban blocks and test the performance of buildings, vegetation, and urban features from a microclimate perspective. Interestingly, the relationship between pedestrian movement and unusual microclimates (such as extreme heat) has not been sufficiently studied and is neglected in contemporary urban planning practices (Kim & Hong, 2021). Microclimate can be assigned to small sized structures or areas, up to a few meters. This scale is relevant for human health and is the major contributing factor to walkability associated decisions among pedestrians.

ENVI-met enables an accurate modelling of changes in solar radiation by building structures and surrounding elements, effects of vegetation with respect to photosynthesis rates, potential temperature of leaves and soil moisture based on the assigned location (or local climatic zones). The main output produced by ENVI-met is the flow around and between buildings by simulating heat and water vapor exchanges at the ground surface, urban surface materials and vegetation (Alves et al., 2022).

ENVI-met is a three-dimensional microclimate model for simulating microscale climate conditions in an urban environment. It is notable for its ability to simulate interactions of the surface-vegetation-atmosphere and facilitates the investigation and quantification of the effects of urban planning and design on outdoor microclimate conditions (Alves et al., 2022). Typical output resolution can vary between 0.5 to 10 m in space and 10 seconds increments in time. It is a prognostic model based on the fundamental laws of thermo-dynamics and fluid dynamics (Sodoudi et al., 2012).

4.6.2 Model Input Data

To effectively model the microclimatic conditions of the selected scenarios (mentioned in previous section), typological conditions of each scenario were modelled in ENVI-met. Measurements of street widths, building dimensions, green spaces, and topography were retrieved from Google Earth. Next, the tree locations were placed in the exact locations by overlaying Google Earth images with the built model.

For each scenario, two models were created:

1) A base scenario with an almost exact recreation of existing conditions
2) A design scenario with increased vegetation, pigmented asphalt, increased permeability of ground surface and trees with greater canopy cover.

Elements that constitute the alternative design scenario take reference from the literature review and the empirical findings from LST, NDVI and LULC maps.

1) Dense Tree Canopy: creates shade, increases evapotranspiration.
2) Pigmented Asphalt and Light Gray Sidewalks: Surfaces that reflect solar radiation without reaching harmful levels of glare conditions.
3) Increased vegetation: 4 m and 2 m high hedges, 2 m grass in bare soil areas because grass has lower albedo than bare soil.
4) Soil type: Loamy soil as it has better absorptive capacity than sandy soil.

Once the models for each scenario were prepared, pre-defined conditions are defined for each model before starting the simulation processing:

1) Simulation cycle of 24 hours (0700 to 0700)
2) Date of simulation: 23rd August 2021 (corresponding to the dates of earliest LST map)
3) Maximum (32°C) and minimum (18°C) temperature (retrieved from AccuWeather website)
4) North orientation

After the completion of the simulation calculation, the potential air temperature (at an elevation of 1.5 m) was selected as the mapping variable. The potential air temperature maps with a resolution of 2 m were created using the Leonardo plugin (available in ENVI-met) for the hours 9:00 am. 12:00 pm, 4:00 pm, 6:00 pm, 8:00 pm and 12:00 pm.

The results are displayed in a matrix which facilitates a comparative analysis of the effect of different microclimatic conditions in each scenario. Another benefit of using ENVI-met simulations is the ability to visualize and monitor temporal changes between different hours of the day, especially between day and night. Hourly variations of air temperature values are presented in graphs.

CHAPTER 5

RESULTS

5.1 Land Use Land Cover (LULC) Mapping

5.1.1 Macro-scale LULC: Ankara Province

LULC maps for the years 1990, 2000, 2006, 2012 and 2018 are illustrated in Figure 5.1 and Figure 5.2. The quantified surface area values of each Land Type are listed in Table 5.1.

Between 1990 and 2018, artificial surfaces increased by 82.8%. The largest increase in artificial surfaces occurred between 1990 and 2006 with a percentage increase of 34.81%.

Ankara Çevre Yolu, a 110 km long motorway is part of a large-scale, centrally coordinated national-level transport plan (initiated in late 1990s) designed to increase the capacity of automobility in Turkish cities (Çalişkan, 2011). In 2000, the appearance of a continuous strip of road and railway associated land indicates the completion of a ring road around the city of Ankara and subsequently marks a shift in mobility patterns.

While there is an overall increase in artificial surfaces, a significant increase in industrial/commercial units is also observed in the west, north-west and south-western areas of Metropolitan Ankara.

Agricultural areas decreased by 4.83% between 1990 and 2018. The area covered by agricultural surfaces shows a negative trend throughout, with the largest percentage decrease calculated as 2.67%, occurring between 2000 to 2006. This could be due to

moisture loss in soils over time, a climate change associated impact. For example, within the category of agricultural areas, ‘permanently irrigated lands’ decreased by 16%, ‘complex cultivation patterns’ (defined as mosaic of small, cultivated land parcels with different cultivation types) decreased by 48%, and ‘agricultural lands with natural vegetation’ decreased by 16%.

The overall change in forest and semi-natural areas between 1990 and 2018 is minimal, with a percentage increase of 0.93%. As demonstrated in Table 5.1, the highest recorded surface area was in 2006, after which there was a steady decline from 2006 to 2018.

Wetlands almost doubled between 1990 and 2018, with an approximate percentage increase of 236%. The largest increase in wetland areas was between 2000 and 2006, from a total coverage of 95.34 km² in 2000 to 257.83 km² in 2006. Water bodies demonstrate an overall decline of 2.29% from 1990 to 2018. The highest land coverage is in 1990 with total surface area of 628.42 km². By 2018, this area reduced to 614 km².

Between 1990 and 2018, a segment of the Çubuk stream, in the district of Sincan, changes from ‘water body’ to ‘agricultural land with natural vegetation’. There may be multiple causes which may have led to the change in land type. It may be because of climate-driven dynamics or agricultural activities in the region. Even so, the alteration of active streams alters the landscape of the area in terms of ecological and social sustainability (Kaymaz, 2019).

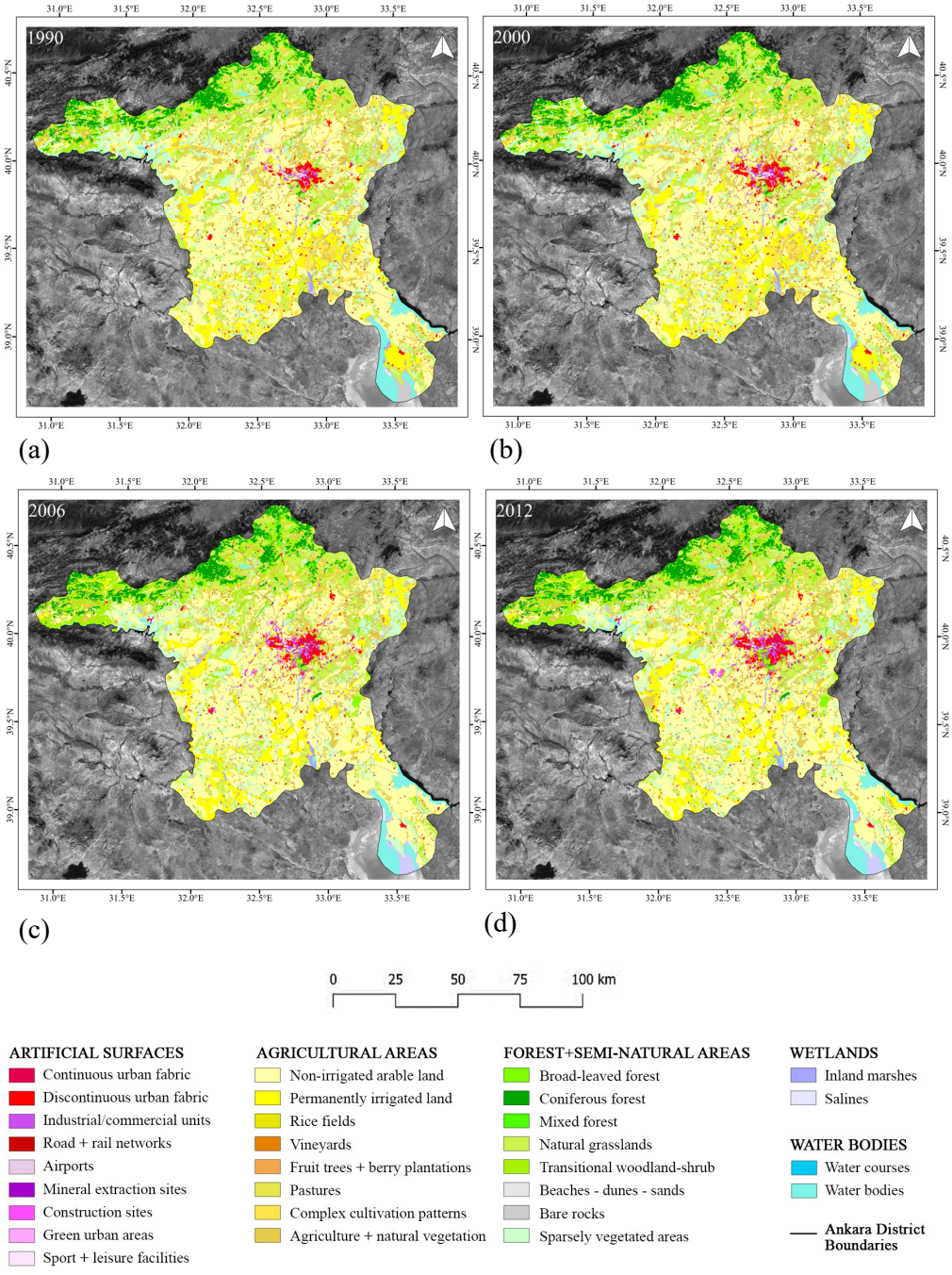

Figure 5.1 Macro-scale LULC: Ankara Province. (a).1990, (b). 2000, (c) 2006, (d) 2012

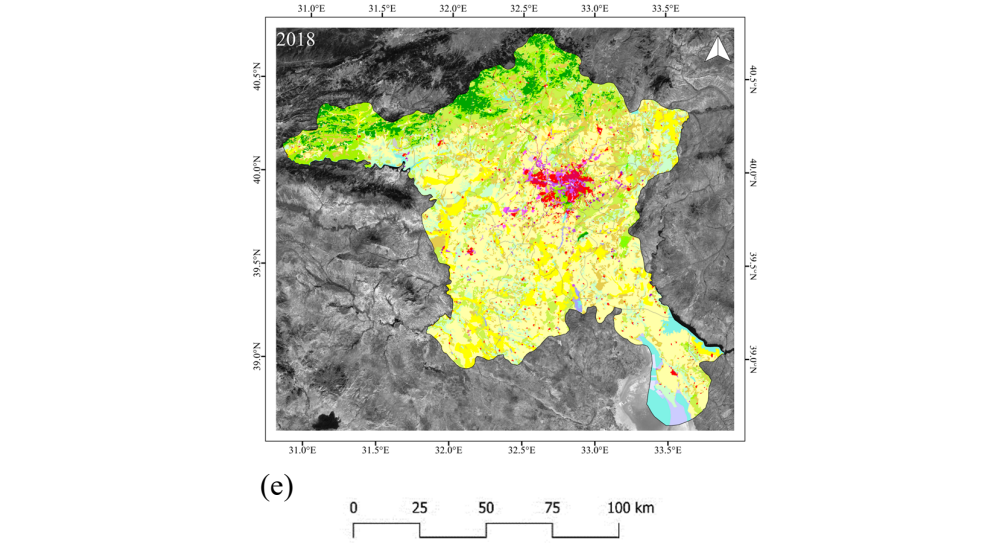

Figure 5.2 Macro-scale LULC: Ankara Province (e) 2018

Table 5.1 Quantified LULC classes

	Total Surface Area (km^2)				
Class Type	*1990*	*2000*	*2006*	*2012*	*2018*
Artificial Surfaces	551.54	743.51	831.89	888.85	1008.24
Agricultural Areas	15010.27	14853.26	14456.68	14398.99	14284.64
Forest and Semi-natural areas	9358.8	9331.68	9477.3	9459.3	9445.8
Wetlands	83.19	95.34	257.83	260.53	279.5
Water bodies	628.42	608.43	608.52	624.55	614.04

Colour coded values for each Class Type (horizontal row)

Highest Value — Lowest Value

5.1.2 Macro-scale LULC: Metropolitan Ankara

LULC maps confined to metropolitan limits of Ankara city are illustrated in Figure 5.4 and Figure 5.5, while the quantified surface area changes in LULC classes are enlisted in Table 5.2.

From 1990 to 2018, artificial surfaces increased by approximately 116%. The most significant increase occurred between 1990 to 2000, with a 46.78% increase in the 10-year span. 2000 onwards, the Metropolitan area of Ankara rapidly densifies in terms of urbanization patterns. While the footprint of continuous and discontinuous urban fabric intensifies significantly over time, 'industrial or commercial units' also increase by 142% (between 1990 and 2018). Industrial and/or commercial units expand towards the northwest of the city, possibly due to the construction of the Ankara-Istanbul highway. Similar patterns are observed in the northeast of the city, along the boulevard linking the airport and the city of Ankara.

Agricultural areas decreased by 19% between 1990 and 2018, declining from 2296.72 km² to 1858.75 km². Forest and semi-natural areas peaked in 2012 with an area of 698.38 km² and increase overall by approximately 10% between 1990 and 2018. In the METU area, natural grasslands changed to transitional woodland over time, which indicates the growth of METU forest.

The areas classified as wetlands depict negligible changes. From 1990 to 2018, the overall change is approximately 4.8%. Water bodies, on the other hand, decreased by 22.25% between 1990 and 2018. The most significant decline occurred between 2000 to 2006 with a percentage decrease of 14.07%.

The land covered by Atatürk Farm Forest is classified as a combination of 'sport and leisure facility' and 'industrial/commercial unit' in the years 1990 and 2000. However, from 2006 onwards, the Atatürk Farm Forest area is comprised of 'permanently irrigated land', 'industrial/commercial unit' and 'construction sites'. The area that is considered a construction site is the site of AnkaPark, a new theme park, which has since been permanently closed (as of February 2020). Later sections

of this chapter discuss the impact of these activities on the corresponding LST and NDVI patterns.

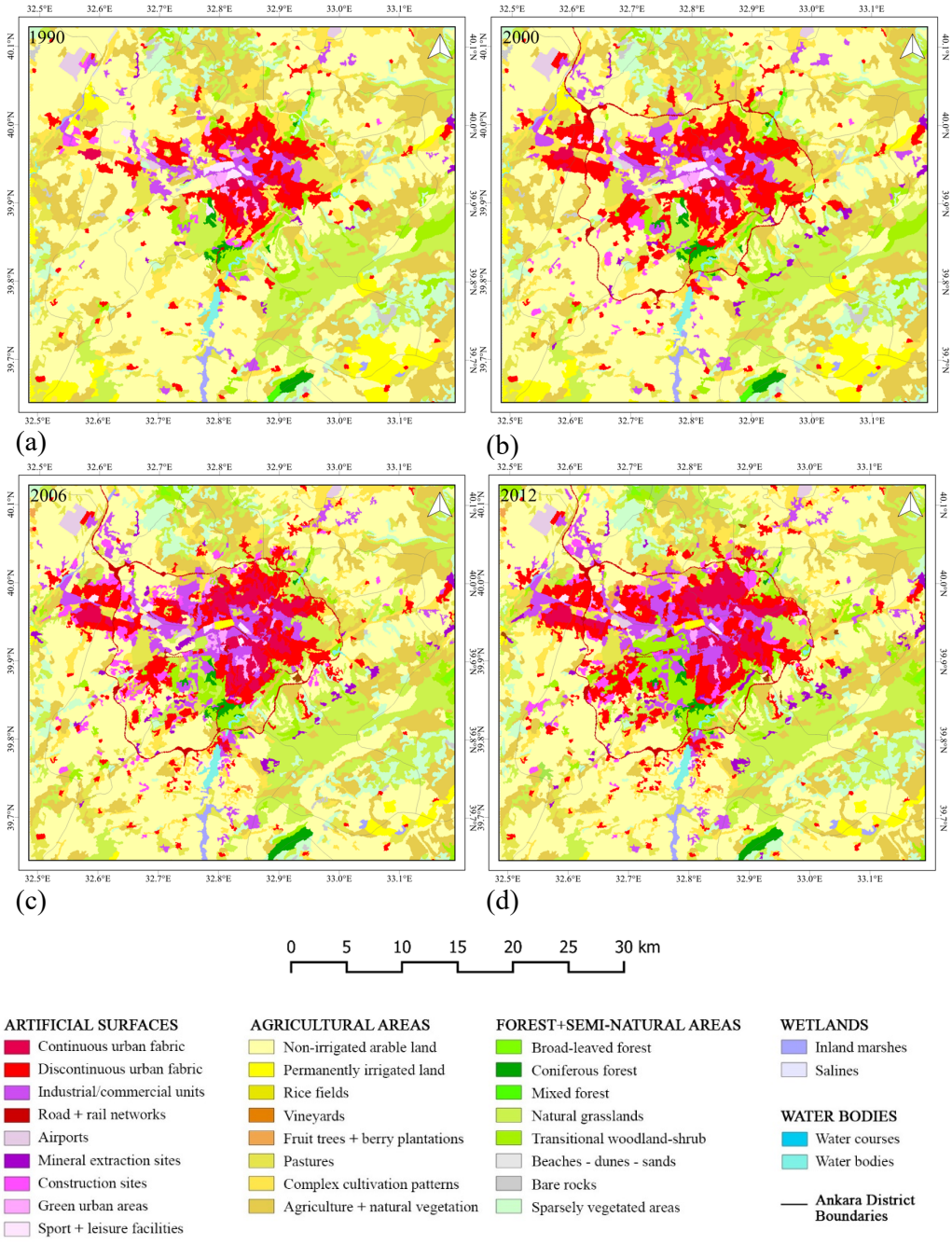

Figure 5.4 Macro-scale LULC: Metropolitan Ankara. (a).1990, (b). 2000, (c) 2006, (d) 2012

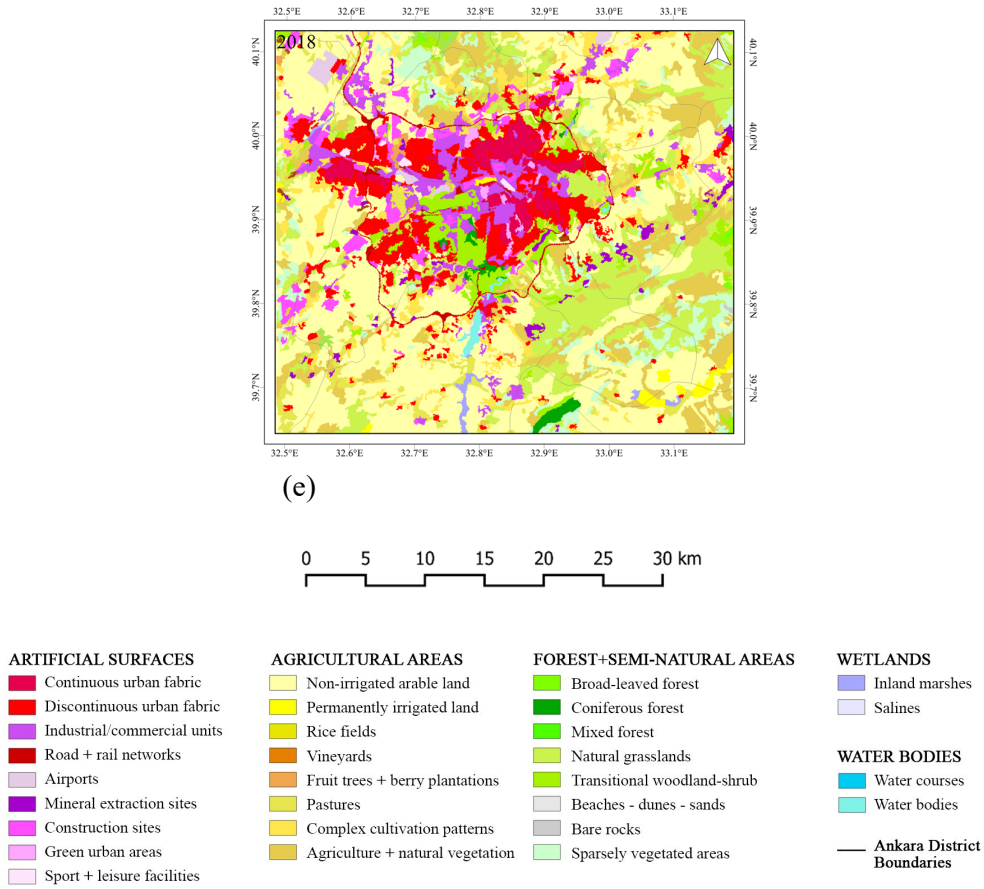

Figure 5.5 Macro-scale LULC, Metropolitan Ankara: (e) 2018

Table 5.2 Quantified LULC values

	Total Surface Area (km^2)				
Class Type	*1990*	*2000*	*2006*	*2012*	*2018*
Artificial Surfaces	325.35	477.56	557.82	599.52	704.81
Agricultural Areas	2296.72	2161.1	2013.58	1953.56	1858.75
Forest and Semi-natural areas	627.52	611.17	679.49	698.38	688.16
Wetlands	12.1	12.1	12.72	12.68	12.68
Water bodies	12.18	11.94	10.26	9.73	9.47

Colour coded values for each Class Type (horizontal row)

5.1.3 Meso-scale LULC: Çankaya District

The results of LULC classification are illustrated in Figure 5.6: and Figure 5.7:, while the surface areas of each class are quantified in Table 5.3. Artificial surfaces increased the most from 1990 to 2000, with an increase of 53.81%. From 2000 to 2006, artificial surfaces increased by almost 18%. an increase from 1990 to 2018, an increase of 107.65% is observed.

With regards to the urbanization trends, the rapid expansion of built areas towards the west of the city has changed the composition of land types in Çankaya district within a short time span. In spite of the rapid expansion in the western part of Çankaya, green urban areas such as parks, gardens, public squares with greenery, or green recreational spaces are not as accessible in Çayyolu as compared to neighborhoods in the central areas of Çankaya.

The detection and in-depth classification of areas undergoing rapid transition, such as construction sites (as seen in Figure 5.6: and Figure 5.7:) can help monitor the

changes in different land surface characteristics which potentially impact thermal comfort conditions in those areas. The later sections of this chapter elaborate on the impact of urban expansion on LST characteristics.

The highest coverage percentage of agricultural areas is observed in 1990 with 242.64 km². In 2018 it reduced by 31.8% to 165.55 km². The change in forest and semi-natural areas remains low with an overall increase of 3.59% from 1990 to 2018.

Wetlands and water bodies remained stagnant with little to no change throughout the analyzed period.

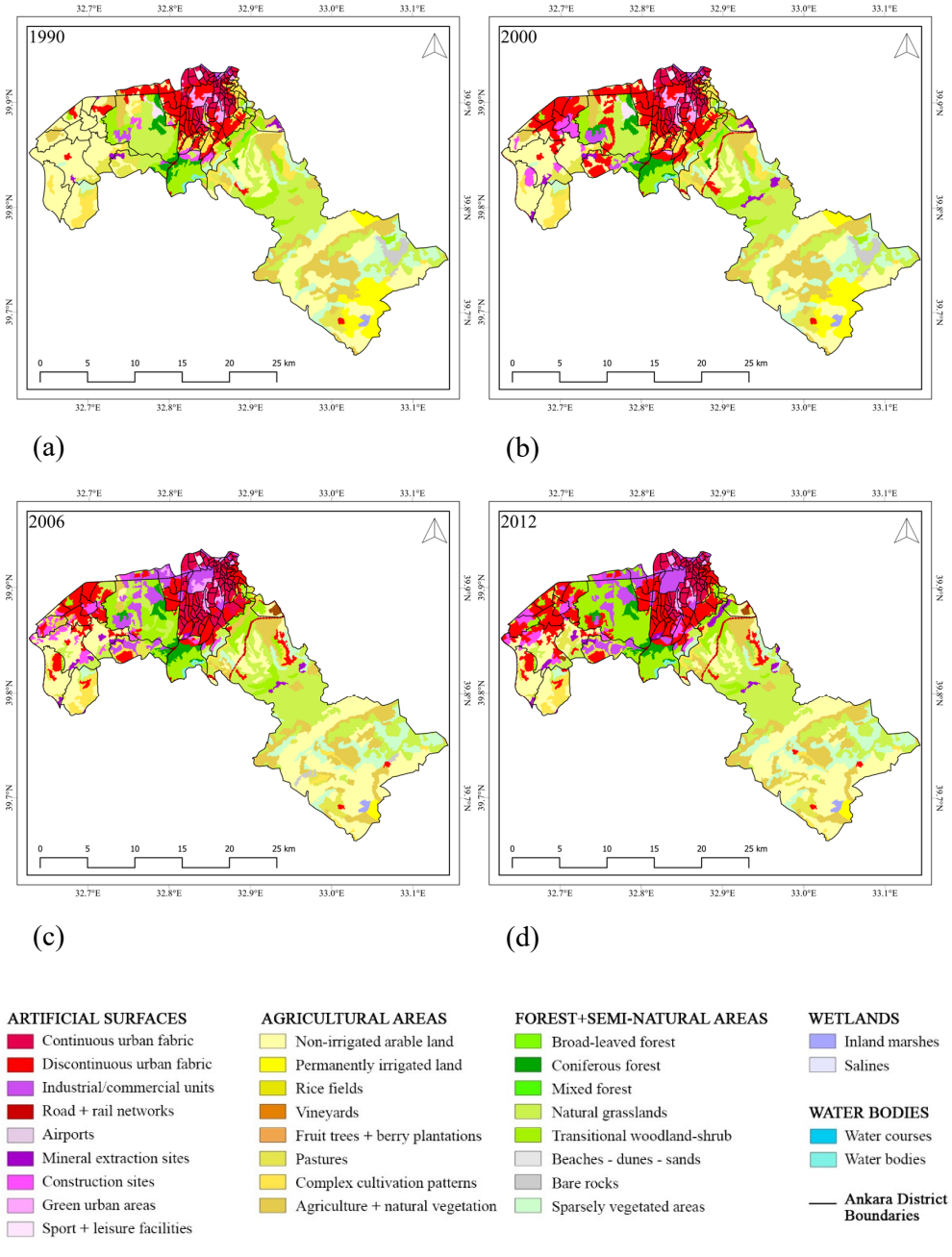

Figure 5.6: Meso-scale LULC, Cankaya District, Ankara: (a) 1990, (b) 2000, (c) 2006, (d) 2012, (e) 2018

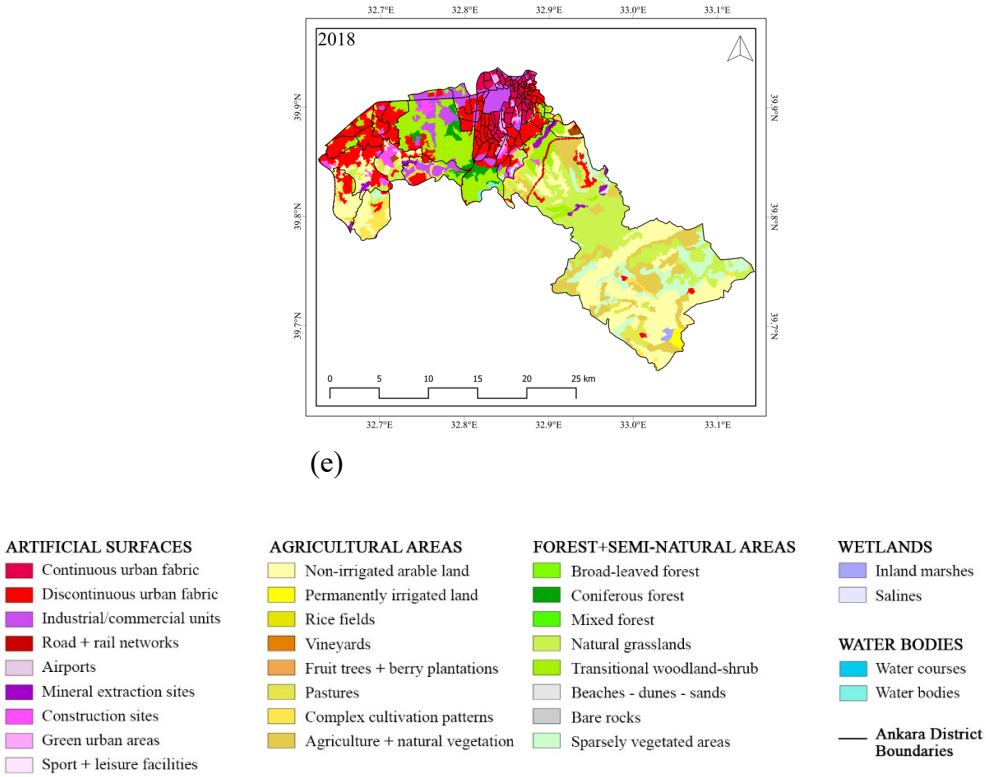

(e)

Figure 5.7: Meso-scale LULC, Cankaya District, Ankara: (e) 2018

Table 5.3: Quantified LULC values

	Total Surface Area (km^2)				
Class Type	*1990*	*2000*	*2006*	*2012*	*2018*
Artificial Surfaces	66.29	101.96	120.41	129.5	137.65
Agricultural Areas	242.64	213.73	184.1	170.83	165.55
Forest and Semi-natural areas	160.13	153.37	164.56	168.75	165.88
Wetlands	1.08	1.08	1.08	1.08	1.08
Water bodies	0.94	0.94	0.93	0.92	0.92

Colour coded values for each Class Type (horizontal row)

Highest Value — Lowest Value

5.1.4 Meso-Scale: Çayyolu Sub-district

The maps displayed in Figure 5.8: to Figure 5.9: illustrate the LULC changes in the subdistrict of Çayyolu. The quantified areas are shown in Table 5.4. From 1990 to 2000, artificial surfaces increased by more than 6 times (574.13%) their original coverage. This was the largest increase across all the successive intervals recorded. Overall, the increase in artificial surfaces maintained positive growth and increased by approximately 1000% in 2018 when compared to the coverage in 1990.

Agricultural areas decreased steadily from 1990 to 2012. From 2012 to 2018, negative growth is observed but at half the rate (21%) of changes observed in preceding time intervals (41-42%). Forest and semi-natural areas remained steady at 1.18 km² from 1990 to 2000 but increased by almost 5 times in 2000. The highest covered area is observed in 2012 (6.85 km²). Wetlands and waterbodies remain undetected in Çayyolu.

The scale of these maps enables the reader to spatialize the changes, specific to neighborhoods within the sub-district of Çayyolu. As a result, the author can make additional comments on the LULC changes to create more useful inferences of the data derived at this scale.

Artificial surfaces and infrastructural links are the main drivers of change in the urban landscape of Çayyolu. For example, the growth of artificial surfaces emerged along Eskişehir boulevard. This may be because Eskişehir boulevard is an important intra-urban infrastructural element which links the new urban fabric with the city center. The construction of Ankara Çevre Yolu (motorway) also defines the extent of urban expansion in this neighborhood. The motorway is also a distinguishing element which separates the rural and urban lands of Metropolitan Ankara.

In addition, the LULC patterns also indicate that while new construction reached the western extents of Yaşamkent and Alacaatlı, urban expansion also continued towards the south, along Kanuni Sultan Süleyman Boulevard. This signifies the creation of a new artery in Çayyolu region.

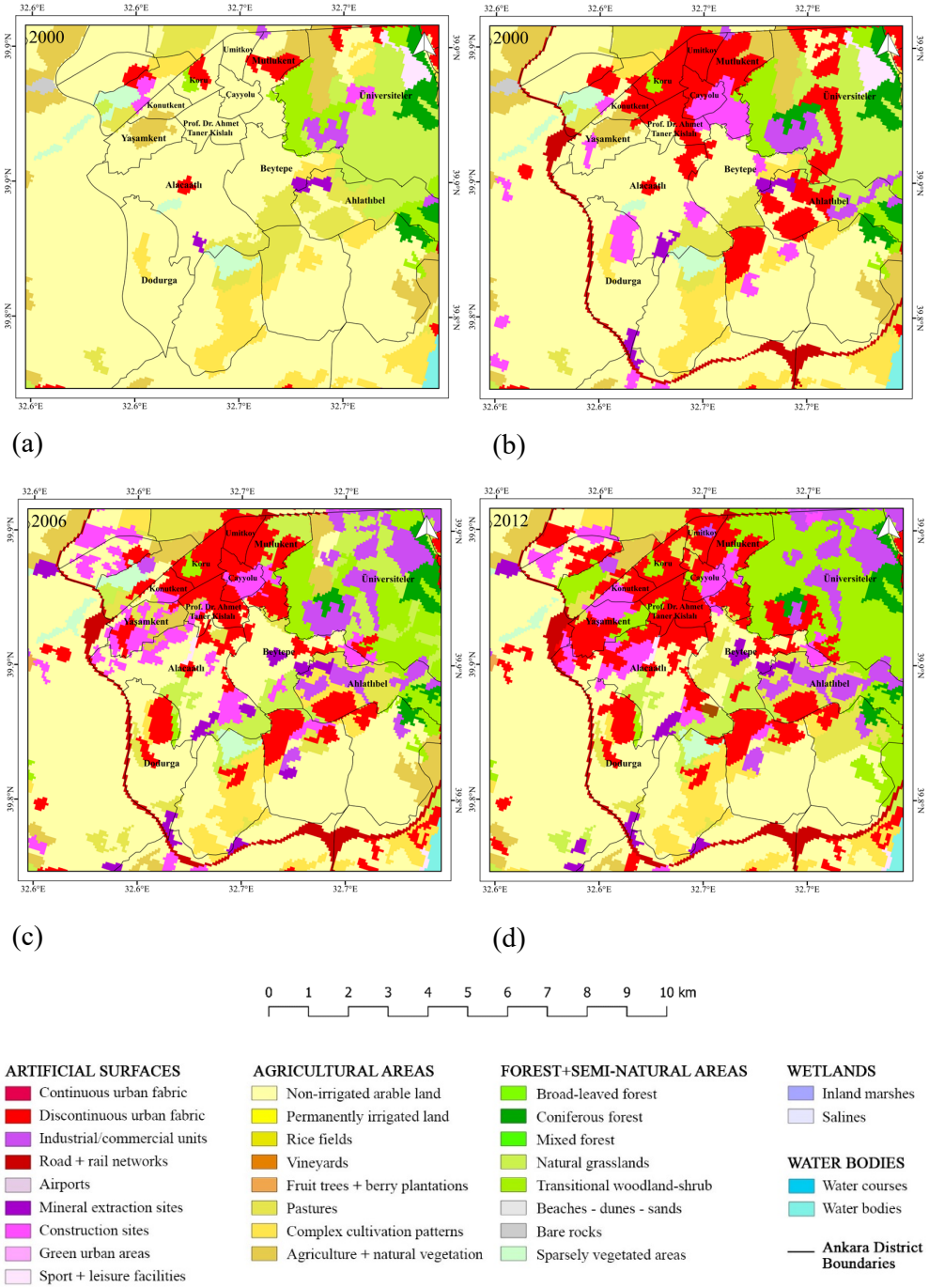

Figure 5.8: Meso-scale LULC, Cayyolu Neighborhood, Ankara : (a) 1990, (b) 2000, (c) 2006, (d) 2012

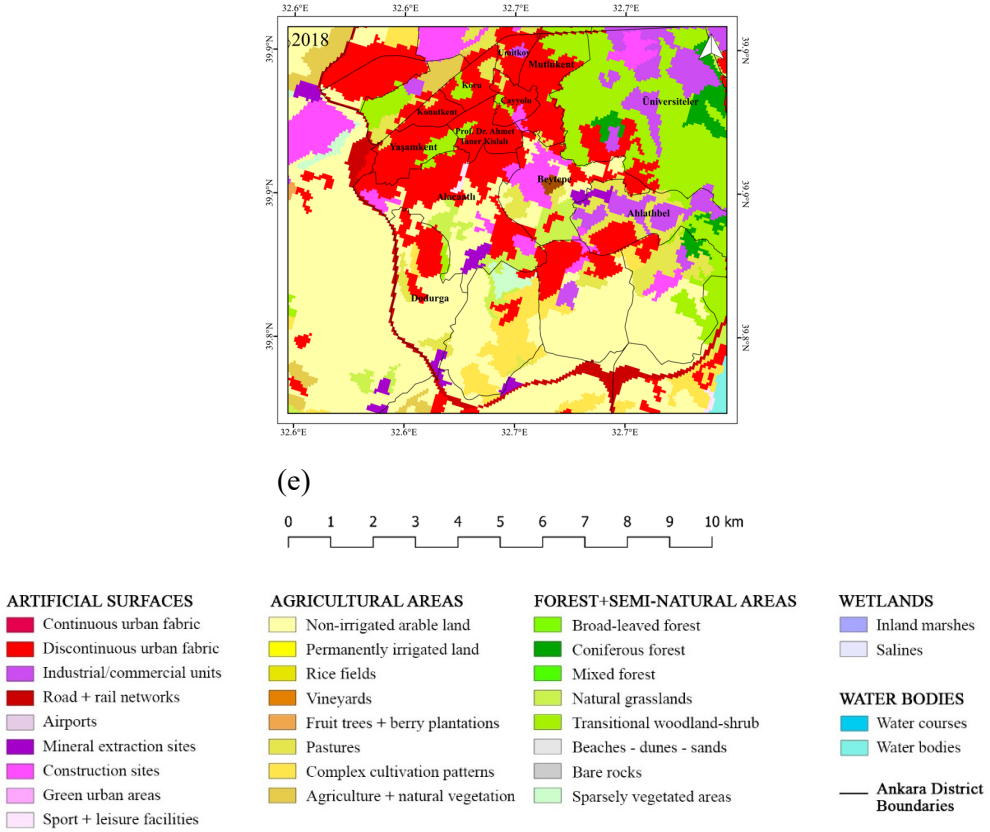

Figure 5.9: Meso-scale LULC, Cayyolu Neighborhood, Ankara : (e) 2018

Table 5.4 Quantified LULC values

		Total Surface Area (km²)				
Class Types		*1990*	*2000*	*2006*	*2012*	*2018*
Artificial Surfaces		2.86	19.28	24.6	28.93	31.4
	Discontinuous urban fabric	2.46	13.47	15.56	20.3	27.84
	Industrial/commercial units	0.13	0.13	n/a	0.25	0.25
	Road and rail networks	n/a	0.19	0.32	0.38	0.38
	Mineral extraction sites	0.24	0.58	0.83	0.63	0.7
	Dump sites	n/a	n/a	n/a	0.28	n/a
	Construction sites	0.03	4.91	7.62	6.84	1.98
	Sport and leisure facilities	n/a	n/a	0.27	0.25	0.25
Agricultural Areas		39.66	23.24	13.66	7.92	6.25
	Non-irrigated arable land	35.35	17.98	10.71	6.58	5
	Pastures	1.35	2.3	1.28	1.32	1.23
	Complex cultivation patterns	0.02	0.02	n/a	n/a	n/a
	Agricultural land and natural vegetation	2.94	2.94	1.67	0.02	0.02
Forest and Semi-natural areas		1.18	1.18	5.44	6.85	6.05
	Natural grasslands	n/a	n/a	4.63	2.64	2.11
	Transitional woodland shrub	0.6	0.6	0.71	4.13	3.86
	Sparsely vegetated areas	0.58	0.58	0.1	0.08	0.08
Wetlands		n/a	n/a	n/a	n/a	n/a
Water bodies		n/a	n/a	n/a	n/a	n/a

5.2 Land Surface Temperature (LST) Mapping

This section of the chapter reveals the results of the LST maps at each scale with tabulated values of mean, minimum and maximum LST. Visual patterns observed in the maps and trends observed in the recorded data are described in each sub-section.

5.2.1 Macro-scale LST: Ankara Province

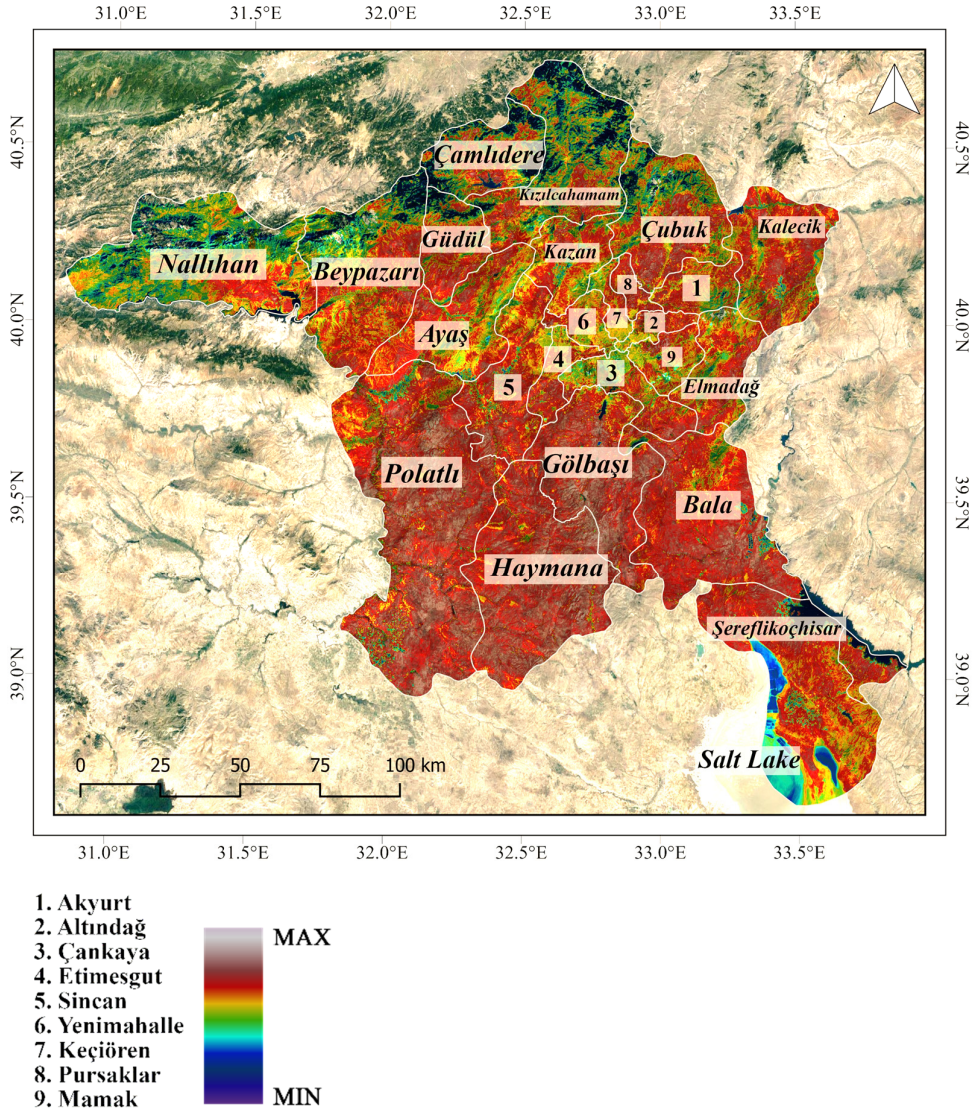

Figure 5.10: Ankara Province 2021 LST map with district boundaries

With respect to the trends in mean LST values (Table 5.5), there is a steady increase from 1990 onwards. The mean LST in 1990 is 28.79 ℃. The highest mean value is recorded in 2018. The lowest minimum LST values are also recorded in 1990. In 2000 and 2006 they remain unchanged at 12.72 ℃ and increase to 16.29 ℃ in 2018.

The largest change in maximum LST values occurs between 1990 and 2000, after which it remains at 47-48 ℃. In 2021, the maximum LST is at 43.8 ℃.

The districts of Çamlıdere, Kızılcahamam, Çubuk, Güdül, Beypazarı and Nallıhan depict lowest LST patterns. This can be attributed to a high distribution of forestland and semi-natural areas including coniferous forests, natural grasslands, mixed forests, and national parks. LST distribution patterns in this region remain relatively cooler compared to the rest of the province until 2018 when higher LST values (>36 ℃) are observed in the region.

High LST zones are more significant in dry landscape (non-irrigated arable land and sparsely vegetated lands) regions spanning from west and southwest to the south. These regions include the district of Polatlı, Haymana, Bala and Gölbaşı. The distribution of high LST patterns in these regions are most prominent in 2018 and 2021 (Figure 5.10 and Figure 5.11).

Water bodies and wetlands including Salt Lake and Kızılırmak River in the south-east and Mogan Lake in southern part of Metropolitan Ankara consistently show low LST values.

The appearance of green corridors, characterized by lowest LST values and land cover types comprised of permanently irrigated lands, agricultural lands, grasslands, and natural vegetation can be observed in the rural districts of Ayaş, Kazan, Polatlı, Sincan, Güdül, Akyurt, Çubuk, and Elmadağ.

For example, in the district of Ayaş (Figure 5.10), a cross-comparison of LST patterns with LULC maps from section 5.1.1 indicates that the green corridor is primarily comprised of natural grasslands, agricultural lands with complex cultivation patterns, transitional woodland shrubs and lands principally occupied by agricultural with significant areas of natural vegetation. It also connects with a green corridor comprised of permanently irrigated agricultural lands which runs through Beypazarı and merges with Sarıyar Dam in the southeast section of Nallıhan district, bordering the provincial boundaries of Ankara.

Similarly, a green corridor, comprised of permanently irrigated agricultural lands, is also observed in the north-west region of Polatlı district. Some cool spots are also consistently observed in the south-west region of Polatlı.

The connection of green corridors with the urban agglomeration of Metropolitan Ankara can be observed in a few locations. For example, a green corridor can be seen emerging from forestlands in the northern region in Çubuk and continues through Pursaklar and Keçiören. Over time, with the increase in industrial (or commercial) units, new construction zones, and built-up areas along this corridor, the concentration of low LST areas begins to shrink.

In the metropolitan area of Ankara, where the highest concentration of artificial surfaces can be observed, LST patterns have continued to intensify from 1990 onwards. Rural and built-up lands experience surface warming over time. This can be attributed to global warming and climate change associated impacts.

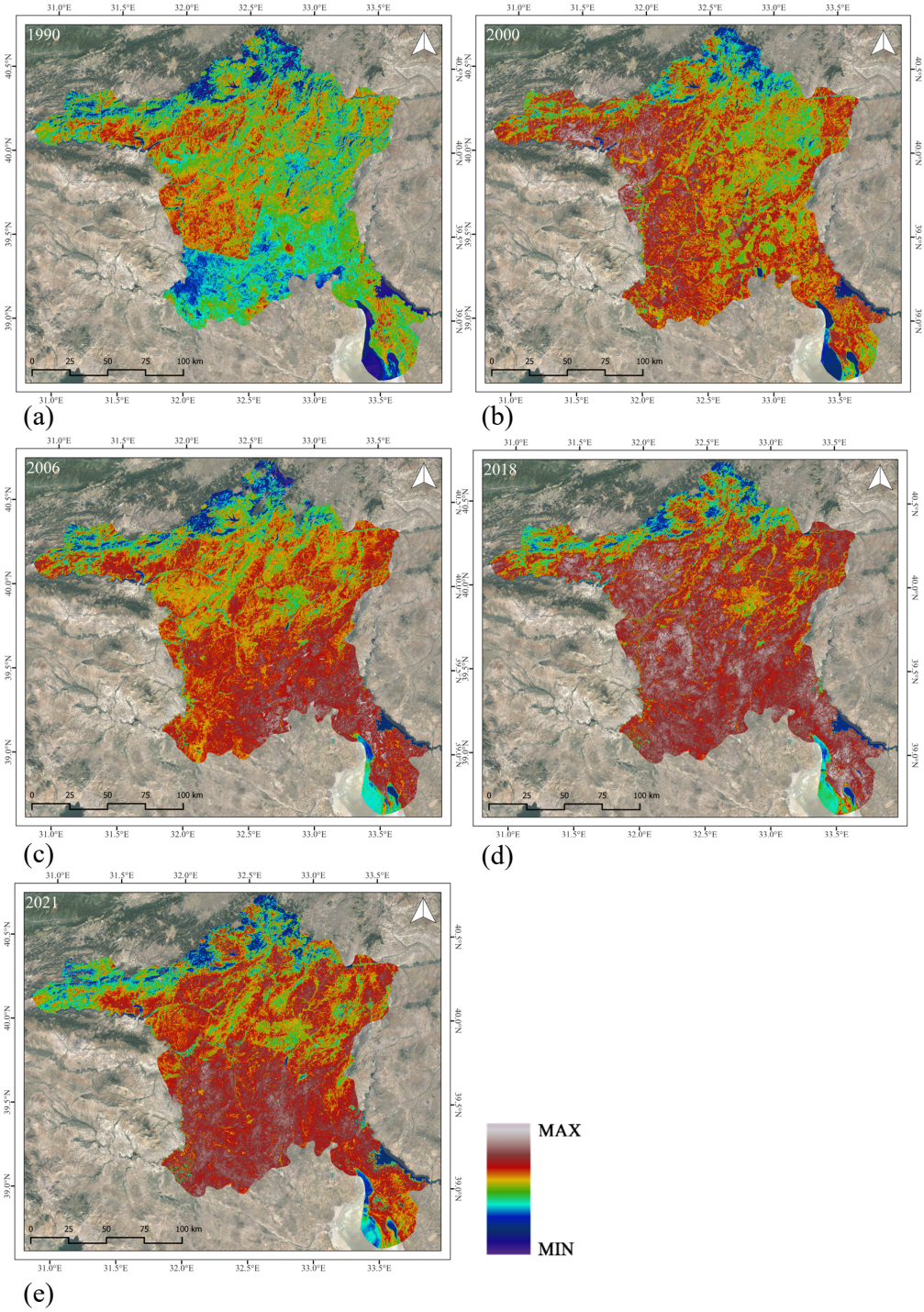

Figure 5.11: Macro-scale LST: Ankara Province. (a).1990, (b). 2000, (c) 2006, (d) 2018, (e) 2021

Table 5.5 LST values for Ankara Province

Date	Year	LST (min) ℃	LST (max) ℃	Mean ℃	Standard deviation ± ℃
27.08.1990	1990	8.87	40.24	28.79	±4.20
12.07.2000	2000	12.72	48.43	32.92	±4.43
15.08.2006	2006	12.72	48.44	33.09	±4.48
24.08.2018	2018	16.29	47.02	35.58	±4.58
16.08.2021	2021	13.14	43.80	33.71	±4.60

5.2.2 Macro-scale LST: Metropolitan Ankara

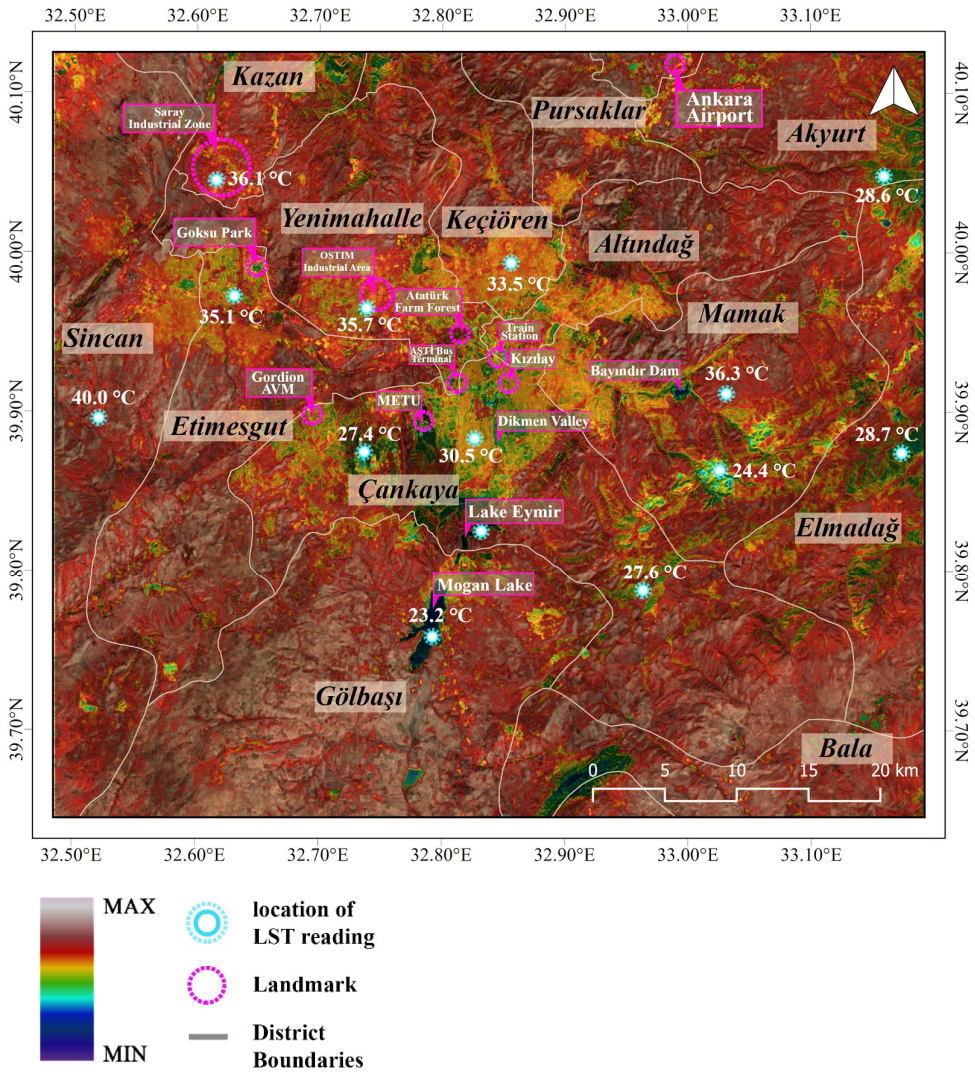

Figure 5.12: Metropolitan Ankara: 2021 LST map with district boundaries

LST patterns specific to the built environment in Metropolitan Ankara and its peripheral areas are more discernible at this scale. Since 1990, there is an overall increase in LST values (Table 5.6). Between 1990 and 2000, minimum LST increased by approximately 0.5 ℃ (from 15.97 ℃ to 16.46 ℃). Between 2000 and

2006, maximum LST increased by 6 ℃ and mean LST by 4 ℃. Between 2006 and 2018, mean LST increased by 2.12 ℃, and minimum LST increased by 2.4 ℃.

The highest mean LST is recorded in 2018. When visually assessing LST patterns depicted in Figure 5.13, it can be observed that the 1990 LST map shows the most amount of 'cool spots' in the built environment. From 1990 onwards 'cool spots' begin to either disappear or become sparser with time. Compared to other districts, Çankaya has a higher concentration of 'cool spots', especially in 2006, 2018 and 2021. For example, residential areas in Keçiören have barely any visible cool spots. This may be attributed to the Land Use composition and lack of green areas. As a result, inequitable access to green areas and cool spots in different neighborhoods of Ankara may affect thermal comfort conditions between those neighborhoods.

Despite the overall warming of surface temperatures over the years, a green corridor (passing through Bayındır Dam) in the district of Mamak consistently shows lower LSTs than its surrounding lands.

Industrial areas in Ankara, namely, OSTİM and Saray, show high LST values (Figure 5.12). In some cases, significant hotspots appear over large-scale industrial buildings with a surface temperature difference ranging from 5 ℃ to 10 ℃ between the building roof surface and the immediate surroundings (adjacent road surface or car park).

The LST patterns in Atatürk Farm Forest have dramatically changed. In 1990, Atatürk Farm Forest appears to be a sizeable cool spot in the center of the city but with time, it demonstrates high LSTs comparable to the LSTs of bare soil rural lands. Despite these findings, there is still potential for this land to be an important green area because of its central location in the city. By increasing accessibility and enhancing walkability, it can become a necessary recreational space for pedestrians. In terms of LST patterns, it can improve thermal comfort conditions in surrounding areas by positively influencing the microclimate of surrounding neighborhoods.

The LST patterns of residential neighborhoods in the vicinity of Göksu Park show a high variation in LST values between residential blocks and the motorway which passes through it. Ankara Çevre yolu, the city motorway with four lanes on each side is almost devoid of any vegetation but has the capacity to accommodate active travel modes like walking and cycling, especially when it passes through residential neighborhoods. Traffic calming measures, green paths and dedicated lanes can be created to facilitate safe crossing of pedestrians and cyclists through the motorway and to encourage multi-modal transport modes.

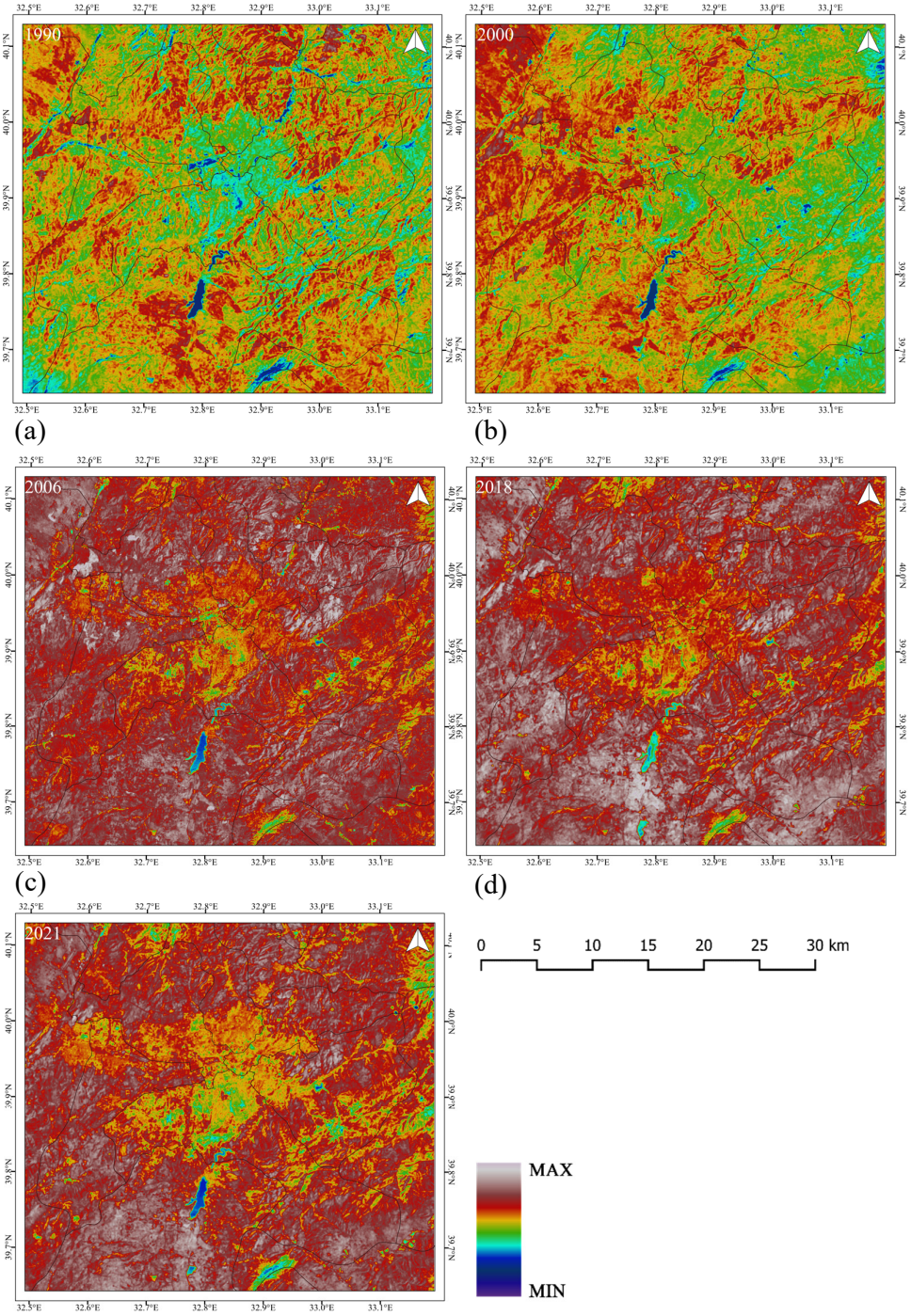

(a) (b) (c) (d) (e)

Figure 5.13: Macro-scale LST, Metropolitan Ankara: (a) 1990, (b) 2000, (c) 2006, (d) 2018, (e) 2021

Table 5.6: LST values for Metropolitan Ankara

Date	Year	LST (min) ℃	LST (max) ℃	Mean ℃	Standard deviation ± ℃
27.08.1990	1990	15.97	41.58	29.20	±2.79
06.08.2000	2000	16.46	39.47	29.50	±2.52
23.08.2006	2006	19.18	45.50	33.51	±2.79
24.08.2018	2018	21.58	45.09	35.63	±2.87
16.08.2021	2021	20.28	44.43	34.37	±3.06

5.2.3 Meso-scale LST: Çankaya District

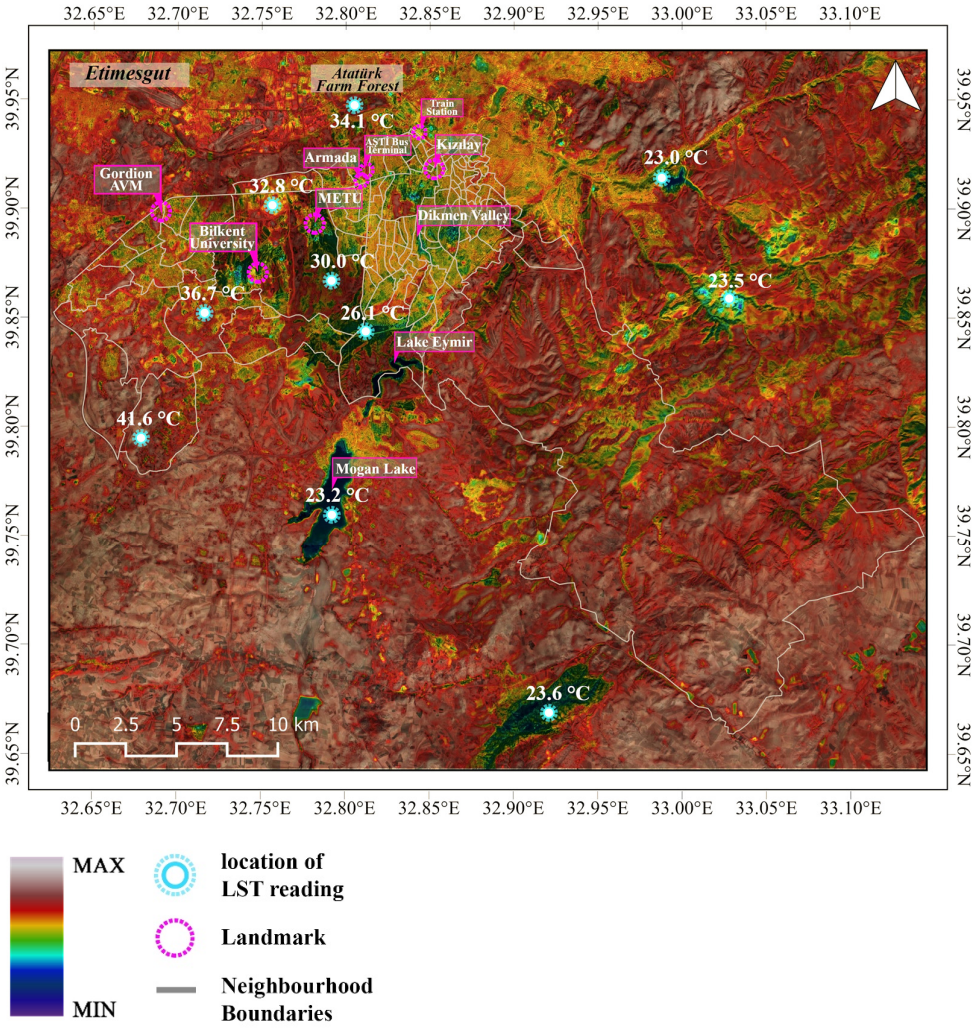

Figure 5.14: Çankaya District: 2021 LST map with neighborhood boundaries

As Table 5.7 depicts, maximum LST exceeded 40 °C, 2006 onwards within the district of Çankaya. In 1990, mean, minimum and maximum LSTs were at their lowest compared to succeeding years. Between 1990 and 2000, maximum LST increased by 0.4 °C and mean LST increased by nearly 0.5 °C. Highest LST is recorded in 2018 at 43.3 °C.

Minimum LST increased steadily from 1990 onwards. In 2000 and 2006 it remained between17 °C to 20 °C while in 2018 and 2021 it increased to 21-22 °C. Mean LST also shows a steady incline 1990 onwards and peaks in 2018 (34.70 °C) after which it declines to 33.20 °C.

In the southeastern part of Çankaya, a few “cool spots” can be observed in the 1990 map but they appear to shrink from 2000 onwards and disappear completely in 2021. Generally, cooler regions in the built areas appear near or around active urban parks, such as Dikmen Valley or forested land.

Lake Eymir consistently shows the lowest LST in all maps shown in Figure 5.15. The surface temperature of Lake Eymir is approximately 14 °C lower than the surface temperature of surrounding ground materials. This is because water reflects solar radiation and water heats and cools down slower than land surfaces. Moreover, riparian vegetation along Lake Eymir also behaves as a buffer between water and land surfaces by influencing and regulating heat gains. In this sense, water bodies such as lakes, ponds, rivers positively influence human-wellbeing by enhancing thermal comfort conditions (Dufour, 2019).

The METU campus consistently depicts low LST values compared to its urban surroundings. This is mostly due to the presence of METU forestland which consists of coniferous and mixed forests. In areas where trees are densely packed, LST remains in the 24-25 °C range. However, in areas with sparsely located trees and bare soil, especially towards the southern region of the campus, the corresponding LST increases. This is why variations in LST can be seen within the METU campus region.

It is also worth noting that the built-up area on campus grounds demonstrates unique microclimate conditions when comparing the LST characteristics of built-up areas in the rest of the city. This may be a result of the cooling capacity of dense vegetation in surrounding campus forestland, linear planning of university buildings with a variety of open spaces, and a very low ratio of built-up to green area.

Similarly, areas in the vicinity of active urban parks like Dikmen Valley Park, experience low LSTs. Dikmen Valley is also an important green corridor with a high cooling capacity. The cooling effect of Dikmen Valley can be perceived at both macro- and meso-scales.

Other parks like Öveçler Valley, Seğmenler Park, Portakal Çiçeği park and Botanik Park also have a significant cooling effect in LST patterns. It is worth mentioning that while these parks contribute significantly to the regulation of LST in their immediate neighborhoods, their proximity to one another also creates a synergy which impacts the regulation of LST patterns on a larger scale.

In this sense, the district of Çankaya has a higher capacity to regulate LST patterns, especially in neighborhoods near or adjacent to the above-mentioned parks. However, the neighborhood of Çayyolu, does not have any parks or green areas that can potentially regulate neighborhood level LST patterns. Hence, while Çankaya has a comparatively higher potential to regulate LSTs, there are still some inequities regarding the size and location of green areas within the district itself.

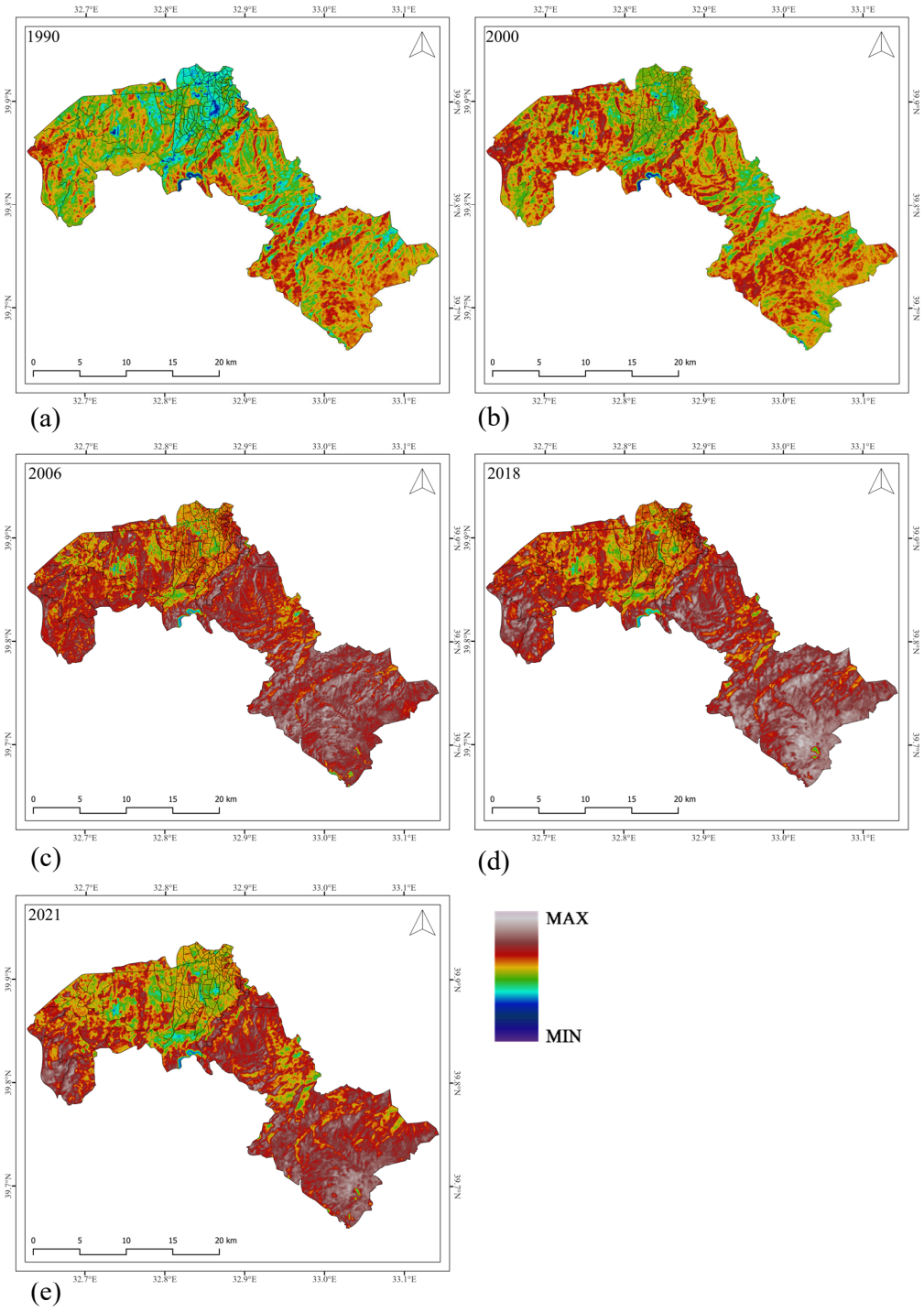

Figure 5.15: Meso-scale LST, Cankaya District, Ankara: (a) 1990, (b) 2000, (c) 2006, (d) 2018, (e) 2021

Table 5.7: LST values for Çankaya District

Date	Year	LST (min) ℃	LST (max) ℃	Mean ℃	Standard Deviation
27.08.1990	1990	16.91	37.92	28.76	±2.80
06.08.2000	2000	17.37	38.31	29.21	±2.21
23.08.2006	2006	19.63	41.76	33.00	±3.32
24.08.2018	2018	22.29	43.26	34.70	±3.16
16.08.2021	2021	21.45	41.78	33.20	±3.23

5.2.4 Meso-scale LST: Çayyolu Neighborhood

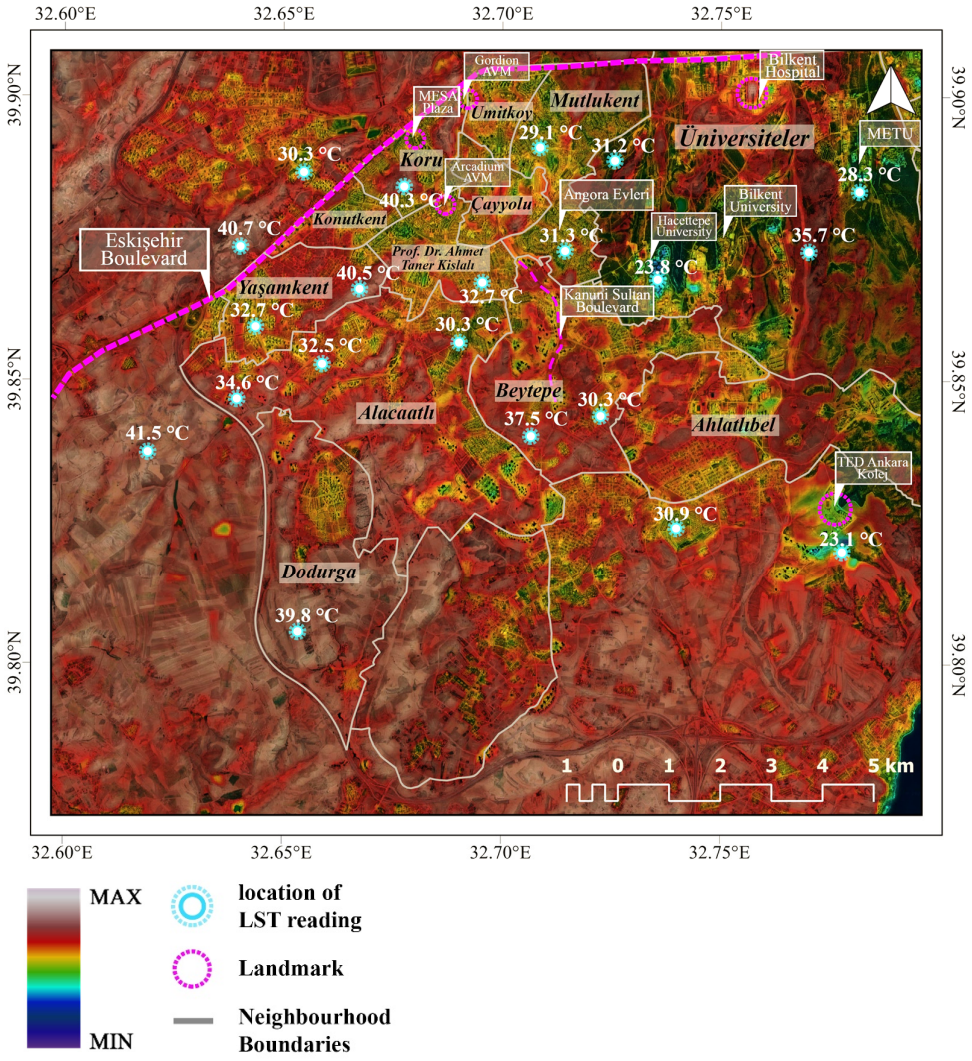

Figure 5.16: Çayyolu Neighborhood: 2021 LST map with district boundaries

Eight sub-neighborhoods constitute the neighborhood of Çayyolu. As shown in Figure 5.17:, Çayyolu includes Alacaatlı, Yaşamkent, Konutkent, Koru, Mutlukent, Çayyolu, Ümitköy and Prof. Dr. Ahmet Taner Kışlalı Neighborhood.

Like LST trends for Metropolitan Ankara, the obtained LST values at this scale, show an overall increase 1990 onwards. The highest LST is observed in 2018 (41.85 °C). From 1990 onwards, mean LST increased gradually and peaked in 2018 at 33.63 °C and dropped to 32.11 °C in 2021. Lowest minimum LST is observed in 1990 and highest in 2018 (Figure 5.17 and Table 5.8).

In terms of LST patterns observed in the maps, areas in Çayyolu consistently show high LST in bare soil areas. 2006 onwards, high LSTs are also observed in the southwestern areas as well. In 1990, 'cool spots' are observed in Alacaatlı, Prof. Dr. Ahmet Taner Kışlalı, Mutlukent and Çayyolu neighbourhoods. However, in 2018 and 2021 maps, they appear to be almost diminished. The western portion of the maps, which is comprised primarily of bare soil (non-irrigated arable land) areas depict very high LSTs.

In terms of equitable access to green space, some disparities in the distribution of 'cool spots' are worth noting. For example, LST patterns over some residential sites in Alacaatlı appear as isolated islands. These sites are linked through roads but are surrounded by bare soil lands with little to no vegetation. This creates a very high difference in LST between the site and its surrounding land (up to 10 °C).

On the contrary, residential sites in Prof. Dr. Ahmet Taner Kışlalı neighbourhood, near Arcadium shopping center show little variation in LST patterns. Perhaps this can be attributed to the compact planning of sites in relation to the arrangement of building blocks and close proximity between different sites, and increased vegetation including densely packed trees and grass surfaces. The only notable variations in LST patterns can be observed in car park areas and commercial buildings where LST increases by up to 3°C.

As Chapter 3 explains, shaded areas enhance thermal comfort and positively contribute to walkability associations among pedestrians. In Yaşamkent, the area with high-rise residential towers and '*siteler'* (a mixed-use high-rise gated complex) show lower LST than areas with low- to medium-density residential buildings with minimal vegetation. This could be due to the shadows created by high-rise buildings

that last throughout the day and obstruct solar radiation on the ground and street surfaces.

However, shade from trees has a greater cooling effect than shade from buildings (Rehman et al., 2021). In this regard, some residential areas exemplify the effect of dense vegetation on LST patterns. For example, Angora Evleri, a gated residential community shows low LST values (between 28-31 °C in 2021) compared to its immediate surroundings (as shown in Figure 5.16). This could be because the domestic green spaces in the community, such as private gardens and green frontages are well-maintained, with shrubs, manicured grass and small quantities of paved surfaces (Dizdaroglu, 2019). Residents in the area are also largely involved in urban farming in their backyards (Dizdaroglu, 2019).

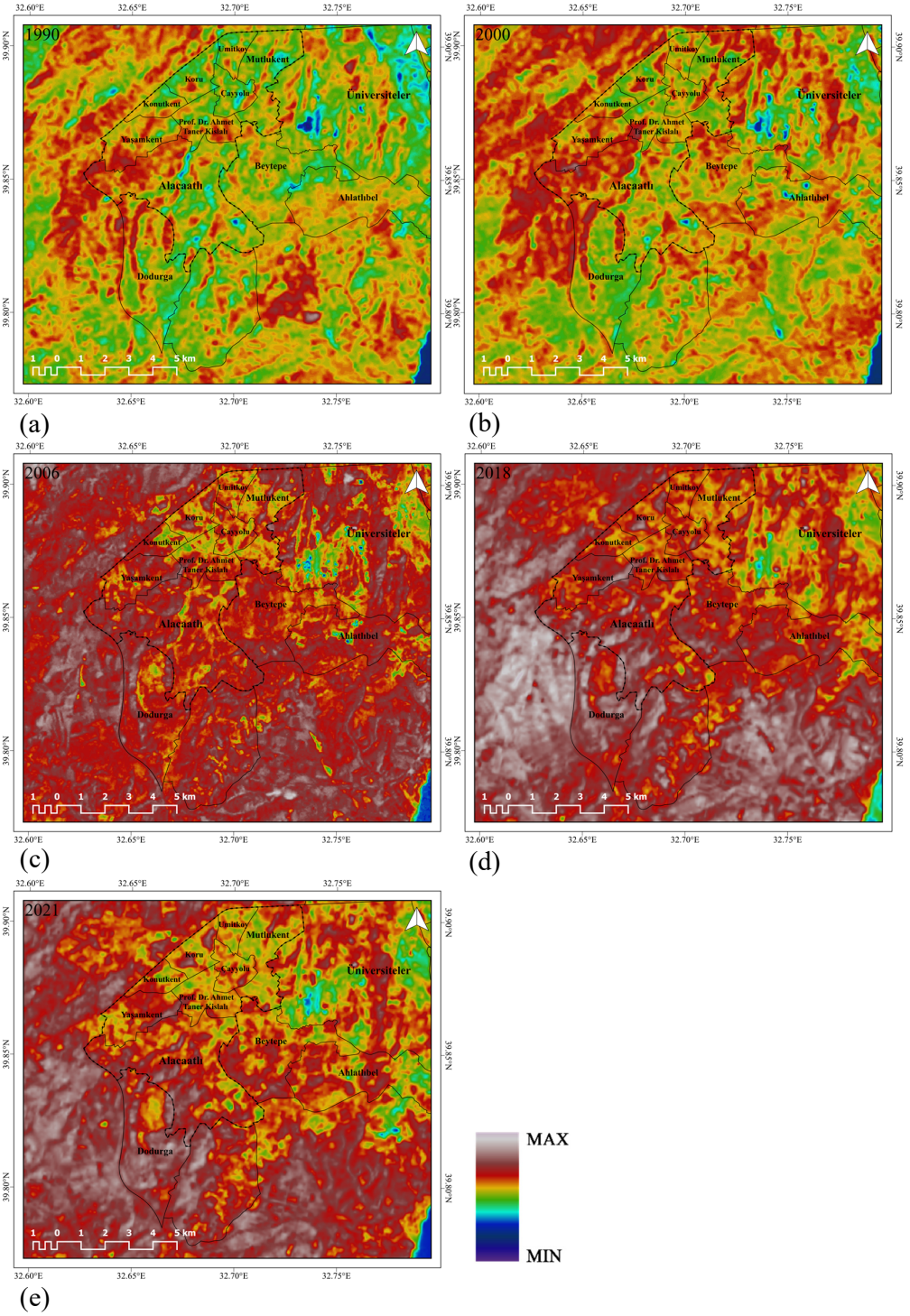

Figure 5.17: Meso-scale LST, Cayyolu Neighborhood, Ankara: (a) 1990, (b) 2000, (c) 2006, (d) 2018, (e) 2021

Table 5.8: LST values for Çayyolu Neighborhood

Date	Year	LST (min) ℃	LST (max) ℃	Mean ℃	Standard Deviation
27.08.1990	1990	21.40	35.97	29.09	±2.22
06.08.2000	2000	22.28	38.31	30.14	±2.09
15.08.2006	2006	25.30	39.86	31.54	±2.27
24.08.2018	2018	27.93	41.85	33.63	±2.36
16.08.2021	2021	25.46	40.40	32.11	±2.45

5.2.5 Accuracy Assessment

Table 5.9 shows the mean LST values retrieved from the MWA algorithm, SMW algorithm in GEE and MODIS (MOD11A1) Land product. For each date, it lists the absolute error between MWA – SWA values and MWA – MODIS values. Figure 5.18: shows the linear trends of mean LST values derived from each of the above described methods.

MODIS and SMW derived mean LST values for 2006 are approximately 11 ℃ higher than MWA derived values. The differences between MWA and SMW derived mean LST values for 1990, 2000, 2006, 2018 and 2021 are 6.5 ℃, 8.43 ℃, 11.28 ℃, 7.55 ℃, and 7.76 ℃ respectively. The differences between MWA and MODIS derived mean LST values for 2000, 2006, 2018 and 2021 are 9.30 ℃, 11.04 ℃, 5.25 ℃ and, 4.29 ℃ respectively.

Table 5.9: Absolute difference between MWA, SMW and MODIS derived LST

Date	MWA LST Mean ℃	SMW LST Mean ℃	Absolute Error ± ℃
27.08.1990	29.20	35.70	-6.5
06.08.2000	29.50	37.93	-8.43
15.08.2006	33.51	44.79	-11.28
24.08.2018	35.63	43.18	-7.55
16.08.2021	34.37	42.13	-7.76
Date	**MWA LST Mean ℃**	**MODIS LST Mean ℃**	**Absolute Error ± ℃**
06.08.2000	29.50	38.80	-9.30
15.08.2006	33.51	44.55	-11.04
24.08.2018	35.63	40.88	-5.25
16.08.2021	34.37	38.66	-4.29

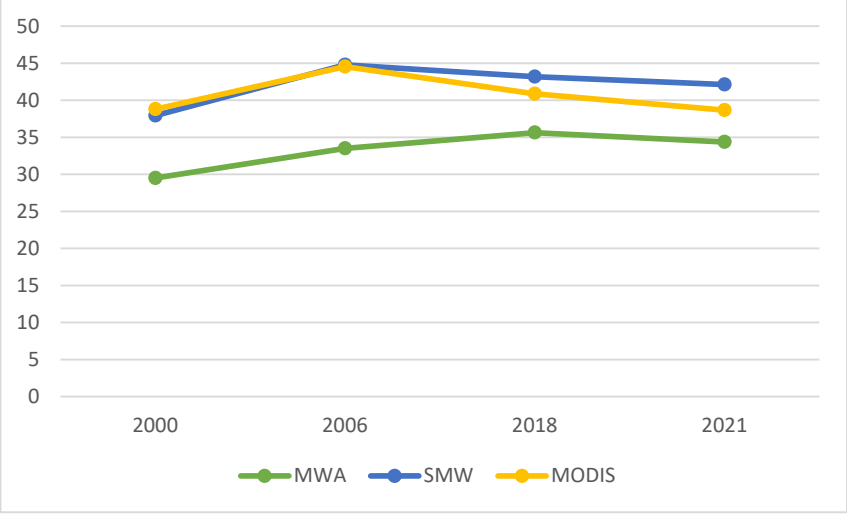

Figure 5.18: Comparison of LST retrieval results of three methods

5.3 Normalized Difference Vegetation Index Mapping

This section of the chapter discusses the results of NDVI maps and the corresponding descriptive statistics.

5.3.1 Macro-scale NDVI: Ankara Province

The NDVI maps of Ankara province are shown in Figure 5.19: and their descriptive statistics are summarized in Table 5.10. The NDVI values ranged from -0.74 to 0.75 in 1990, -0.69 to 0.97 in 2000, -0.67 to 0.75 in 2006, -0.51 to 0.66 in 2018 and -0.40 to 0.66 in 2021. In all five maps, areas with high NDVI values are observed in the north and northeastern parts of the province. Forestland and natural areas depict high NDVI values.

There is an overall higher concentration of low NDVI values in the southwestern, south, and southeastern region of the province.

In the western areas of Polatlı district, a network of permanently irrigated lands appears as a green corridor in NDVI maps. It also correlates with LST patterns and shows very low LSTs (compared to surrounding areas). This means that the moisture content in the soil and the vegetative cover of these agricultural lands contributes to the ecological value of rural lands. In the 2021 map, the green areas appear more fragmented and lose their original quality as a consolidated green area.

Overall, areas principally associated with active streams (cultivated land around and adjacent to streams), permanently irrigated lands, natural grasslands, and areas with natural vegetation show high NDVI values in all maps, especially in 1990. They create a network of green corridors which are crucial for the regulation of urban LSTs and overall physiology of the region. However, they appear to be more fragmented and less intense in 2021. These changes reflect the harmful effects of urbanization and changing climate conditions on the ecological value of the region.

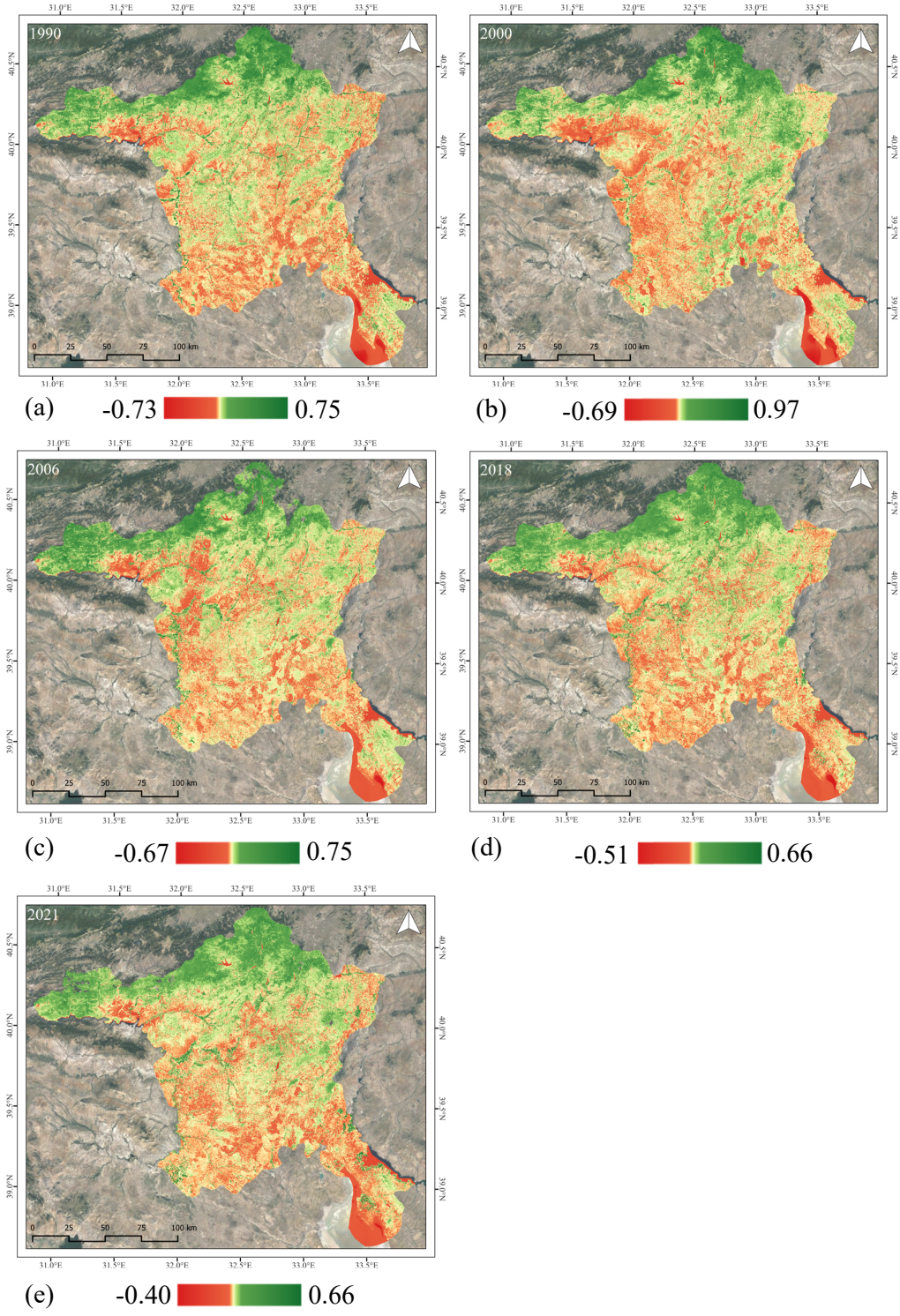

Figure 5.19: Macro-scale NDVI, Ankara Province: (a) 1990, (b) 2000, (c) 2006, (d) 2018, (e) 2021

Table 5.10: NDVI values for Ankara Province

Date	Year	NDVI min	NDVI max	Mean	Standard Deviation
27.08.1990	1990	-0.73	0.75	0.07	±0.12
06.08.2000	2000	-0.69	0.97	0.13	±0.15
15.08.2006	2006	-0.67	0.75	0.05	±0.11
24.08.2018	2018	-0.51	0.66	0.15	±0.08
16.08.2021	2021	-0.40	0.66	0.15	±0.08

5.3.2 Macro-scale NDVI: Metropolitan Ankara

The NDVI maps for Metropolitan Ankara are shown in Figure 5.20 and the descriptive statistics are summarized in

Table 5.11 5.11. The NDVI values ranged from -0.54 to 0.75 in 1990, -0.49 to 0.73 in 2000, -0.40 to 0.64 in 2006, -0.30 to 0.65 in 2018 and -0.38 to 0.65 in 2021. The highest maximum NDVI value was in 1990, while the lowest minimum NDVI was in 2006.

From 1990 to 2021, maximum NDVI values decline gradually with an overall difference of 0.1 while mean NDVI values show an increase of 0.8. Ataturk Farm Forest and METU forestland show high NDVI values which indicates the presence of healthy vegetation. However, they appear to weaken 2018 onwards. Similarly, green corridors are observed in the northwestern and northeastern regions of the map, but they start to weaken in 2018 and become more fragmented in 2021.

The degradation of Atatürk Form Forest makes a compelling case for the urgency to protect an important and valuable natural landmark of Ankara. Comparing the changes in NDVI patterns between 1990 and 2021 indicates that Atatürk Form Forest is under serious threat of urbanization. Due to its prime location, cooling capacity,

and connectivity with urban green corridors, it is an integral part of the green infrastructure of the city.

In the district of Keçiören, changes in NDVI patterns highlight the rate of urban expansion in the area. The distribution of lowest NDVI values continue to expand from 1990 onwards. This indicates that there has been a rapid urban expansion in the area which also correlates with LULC maps. The LULC maps in Section 5.1.2 show an expansion of artificial surfaces including continuous urban fabric, industrial and commercial unit land types in Keçiören.

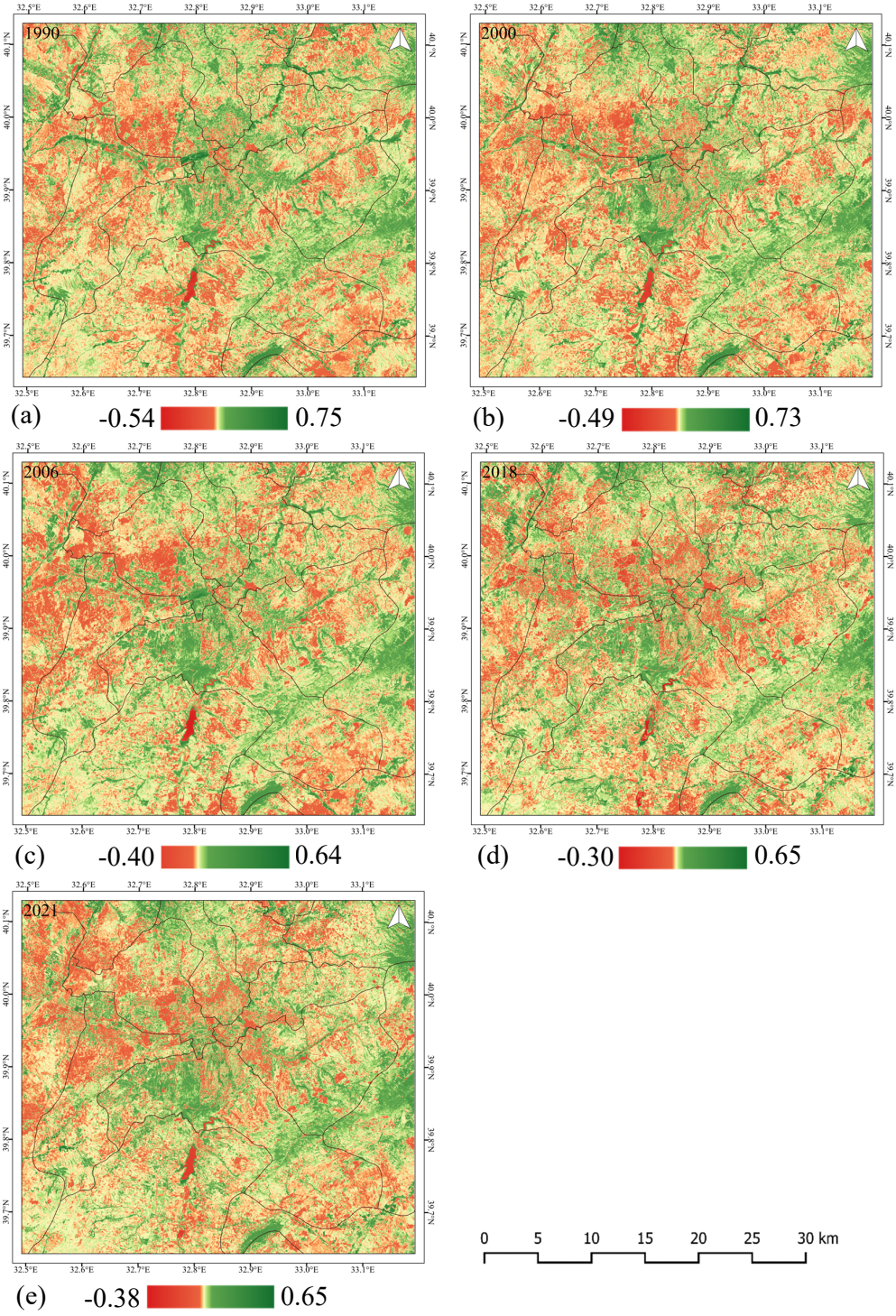

Figure 5.20: Macro-scale NDVI, Metropolitan Ankara: (a) 1990, (b) 2000, (c) 2006, (d) 2018, (e) 2021

Table 5.11: NDVI values for Metropolitan Ankara

Date	Year	NDVI min	NDVI max	Mean	Standard Deviation
27.08.1990	1990	-0.54	0.75	0.06	±0.08
06.08.2000	2000	-0.49	0.73	0.07	±0.08
15.08.2006	2006	-0.40	0.64	0.03	±0.06
24.08.2018	2018	-0.30	0.65	0.14	±0.06
16.08.2021	2021	-0.38	0.65	0.14	±0.06

5.3.3 Meso-scale NDVI: Çankaya District

NDVI maps for Çankaya district are shown in Figure 5.21: and the corresponding descriptive statistics are summarized in Table 5.12. NDVI values ranged from -0.49 to 0.71 in 1990, -0.39 to 0.72 in 2000, -0.28 to 0.60 in 2006, -0.19 to 0.63 in 2018, and -0.14 to 0.60 in 2021. Highest NDVI values are observed in valley parks (i.e., Dikmen Valley), METU and Bilkent forests, and ravines.

METU forest consistently shows high NDVI values. However, transitional woodland areas within METU lands show median NDVI values and these areas have high LSTs as well.

Neighborhoods between Mevlana Boulevard and Dikmen valley, which can be cited as West Dikmen show high NDVI patterns in 1990. The area of West Dikmen is classified as ‘discontinuous urban fabric’ in the LULC maps from 1990 through 2021.

From 2000 onwards, due to the unplanned expansion of this area the lowest NDVI values are observed in West Dikmen. As Özdemirli (2014) writes, problems relating to the urban redevelopment plans of West Dikmen occurred due to the dual structure

of the previous redevelopment plans of 1988. The mismatch in construction rights (some were granted at plot level, while some at building block level) resulted in high density and low-quality construction. This is also reflected in the NDVI values due to the lack of planned green spaces, well distributed parks, and well-maintained residential gardens.

The Imrahor creek, which meets Lake Eymir in the south consistently shows high NDVI values between 1990 and 2021 and appears to be an important green infrastructure element for the city.

According to the maps in Figure 5.21:, NDVI patterns indicate that vegetation quality in the Çayyolu region has significantly declined since 1990. This is because of the fragmentation of green corridors which are observed in 1990 map but continue to disintegrate over time, especially between 2018 and 2021. However, the rapid expansion of Çayyolu also shows an increase in NDVI values due to the increase in domestic green spaces and community greens, especially in Koru and Umitkoy.

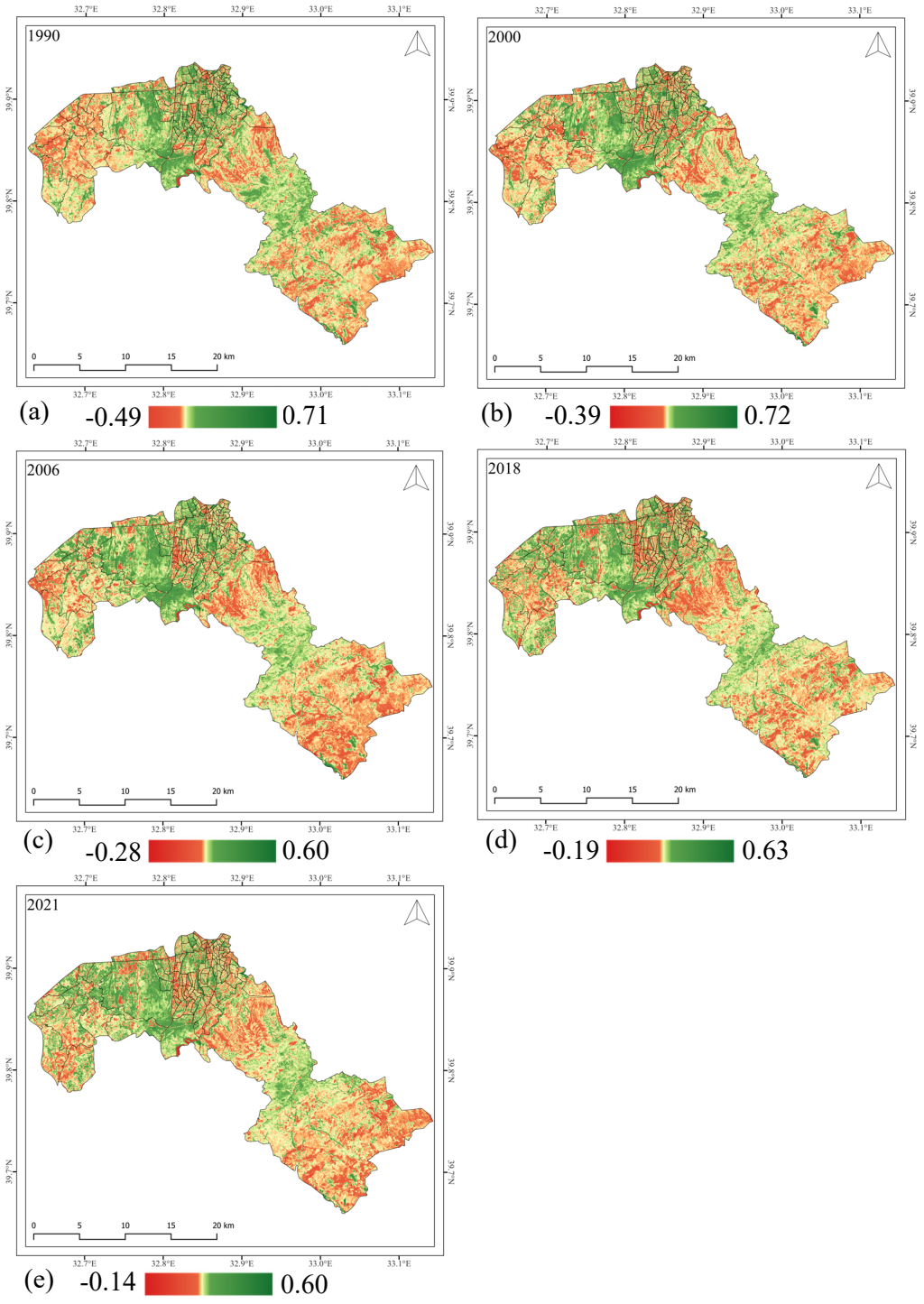

Figure 5.21: Meso-scale NDVI, Çankaya District: (a) 1990, (b) 2000, (c) 2006, (d) 2018, (e) 2021

Table 5.12: NDVI values for Çankaya District

Date	Year	NDVI (min) ℃	NDVI (max) ℃	Mean ℃	Standard Deviation
27.08.1990	1990	-0.49	0.71	0.06	±0.07
06.08.2000	2000	-0.39	0.72	0.08	±0.08
15.08.2006	2006	-0.28	0.60	0.04	±0.06
24.08.2018	2018	-0.19	0.63	0.14	±0.06
16.08.2021	2021	-0.14	0.60	0.14	±0.06

5.3.4 Meso-scale NDVI: Çayyolu Neighborhood

NDVI maps for the neighborhood of Çayyolu are shown in Figure 5.22: and the descriptive statistics corresponding to these maps are summarized in Table 5.13. The NDVI values ranged from -0.11 to 0.61 in 1990, -0.11 to 0.65 in 2000, -0.11 to 0.52 in 2006, -0.11 to 0.55 in 2018 and -0.09 to 0.51 in 2021. From 1990 to 2021, mean NDVI values increased in Çayyolu. Maximum NDVI values reduced from 0.61 in 1990 to 0.51 in 2021.

In terms of NDVI patterns, several green corridors (corresponding to high NDVI values) are observed in the 1990 maps. Campus sites of Bilkent and METU consistently show the highest NDVI values owing to the presence of transitional woodland, coniferous and mixed forest land types. The green areas in the northwest corner of the maps, which consist of the residential neighborhood of Bağlıca appear more and more fragmented over time. Similar patterns are observed in the Alacaatlı and Yaşamkent.

In the 1990 map, a green corridor passing through Umitkoy, Prof. Dr. Ahmet Taner Kışlalı and Alacaatlı can be observed. However, in the 2021 map, it is almost invisible and some portions of it show the lowest NDVI values. The surrounding areas, however, have become greener (as compared to NDVI patterns in 1990) which

can be attributed to the development of residential green areas and neighborhood along with the urban expansion of residential and commercial areas in Çayyolu over time.

In the southeast portion of the 1990 map a green corridor can be observed which appears to shrink over time. A cross comparison with the LULC map indicates that the high NDVI values can be ascribed to high levels of soil moisture and healthy vegetation. However, it appears that with the expansion of artificial surfaces, most of the natural lands were lost to new construction and resulted in the fragmentation of this green corridor.

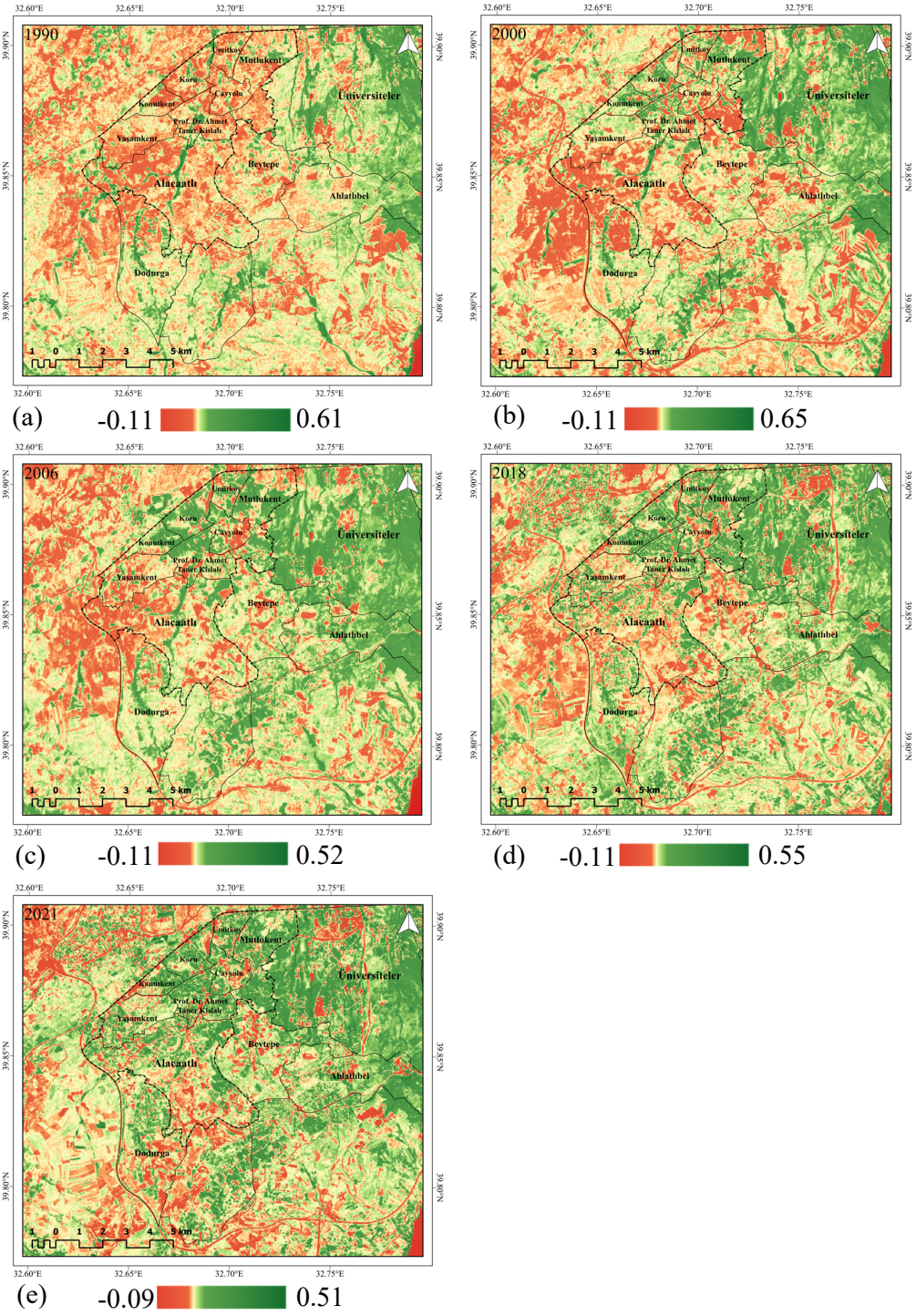

Figure 5.22: Meso-scale NDVI, Çayyolu Neighborhood: (a) 1990, (b) 2000, (c) 2006, (d) 2018, (e) 2021

Table 5.13 NDVI values for Çayyolu Neighbourhood

Date	Year	NDVI (min)	NDVI (max)	Mean	Standard Deviation
27.08.1990	1990	-0.11	0.61	0.03	±0.05
06.08.2000	2000	-0.11	0.65	0.06	±0.07
15.08.2006	2006	-0.11	0.52	0.04	±0.06
24.08.2018	2018	-0.11	0.55	0.15	±0.06
16.08.2021	2021	-0.09	0.51	0.16	±0.06

5.4 Microclimate Simulations

This section of the chapter presents the microclimate simulation results calculated using ENVI-met. Four typical urban blocks were selected, as described in the methodology chapter, and modelled in ENVI-met (Figure 5.24:). For each block, the results of the real-world scenario and an alternative 'green' scenario are compared by visualizing the air temperature (1.5 m elevation) maps at selected times of the day. Significant features of each block and their results are presented in a matrix along with short descriptions of the statistical data and observed patterns in the maps. Figure 5.23: describes the locations of selected blocks.

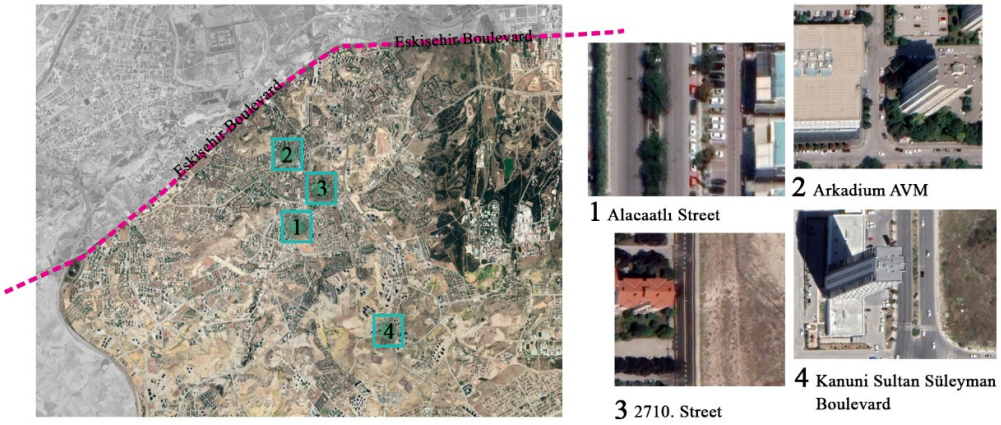

Figure 5.23: Diagram depicting locations of selected blocks

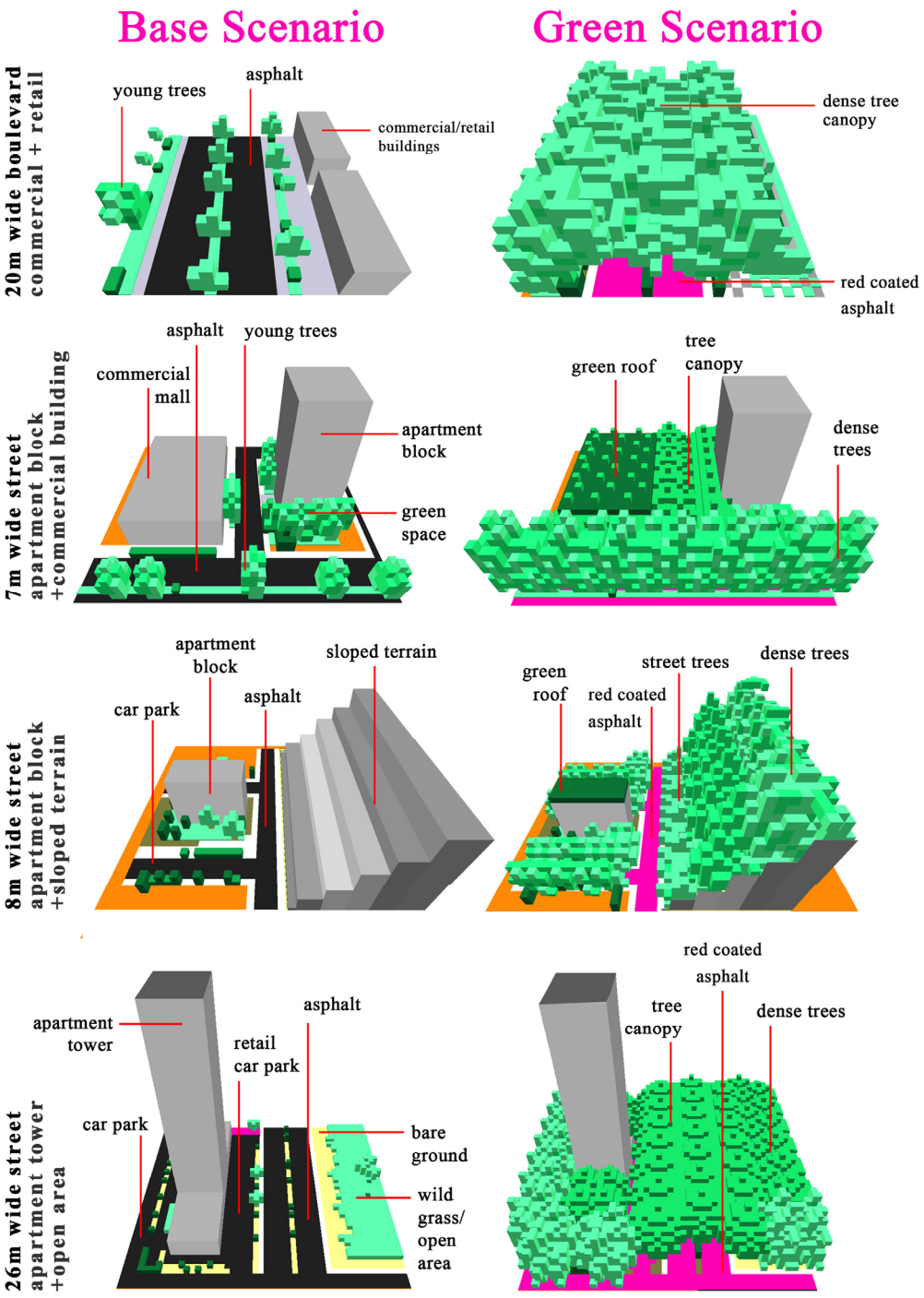

Figure 5.24: Digitized models for both scenarios created using ENVI-met software

5.4.1 20m wide boulevard: Alacaatlı Caddesi

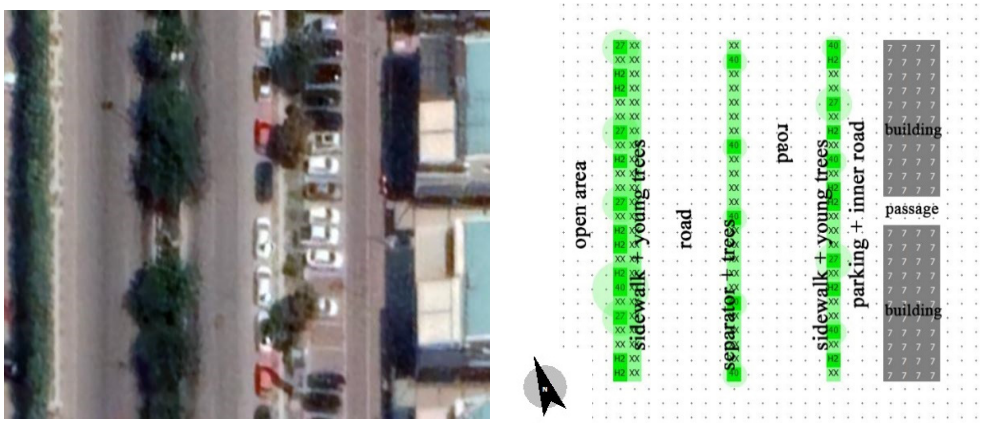

Figure 5.25: Google Earth Screen shot and base model produced in ENVI-met

Base Scenario:

During daytime hours, the coolest areas appear around buildings. After 9:00 pm, temperatures continue to rise and peak at 04:00 pm (32.1 ℃). 4:00 pm onwards, temperatures begin to decline and are at their lowest at 5:00 pm (20.3 ℃)

With regards to temperature gradients, nighttime temperatures indicate that the hottest areas are in asphalt covered surfaces. Comparing the appearance of hottest temperature patterns between day and night, the nighttime maximum temperatures have a larger coverage, primarily on asphalt areas. This indicates that hotspots are more pronounced at nighttime.

Green Scenario:

Hottest areas in daytime hours are less concentrated on roads and more around the eastern exterior of buildings. Roads that are now lined with dense tree cover and high Leaf Area Density (LAD), consistently show lowest air temperature values in daytime hours. High temperatures on asphalt surfaces are only seen at 9:00 am. At 8:00 pm and 12:00 am (midnight), highest temperature areas are observed on asphalt surface but are less spread out when compared to base scenario maps.

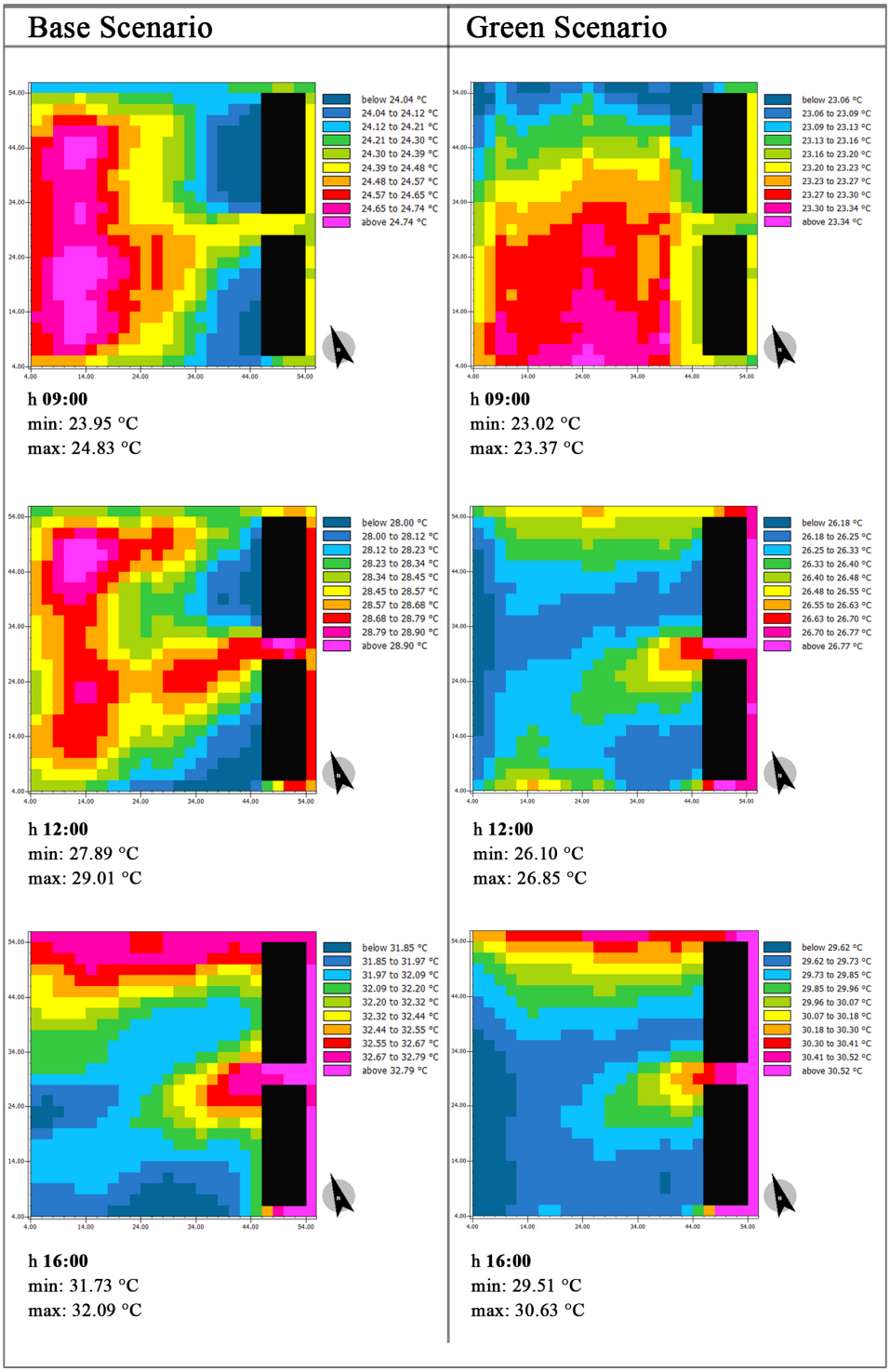

Figure 5.26: Air Temperature in Base and Green Scenario, x-y view at z = 1.4 m at 09:00, 12:00 and 16:00 hours on 23rd August 2021

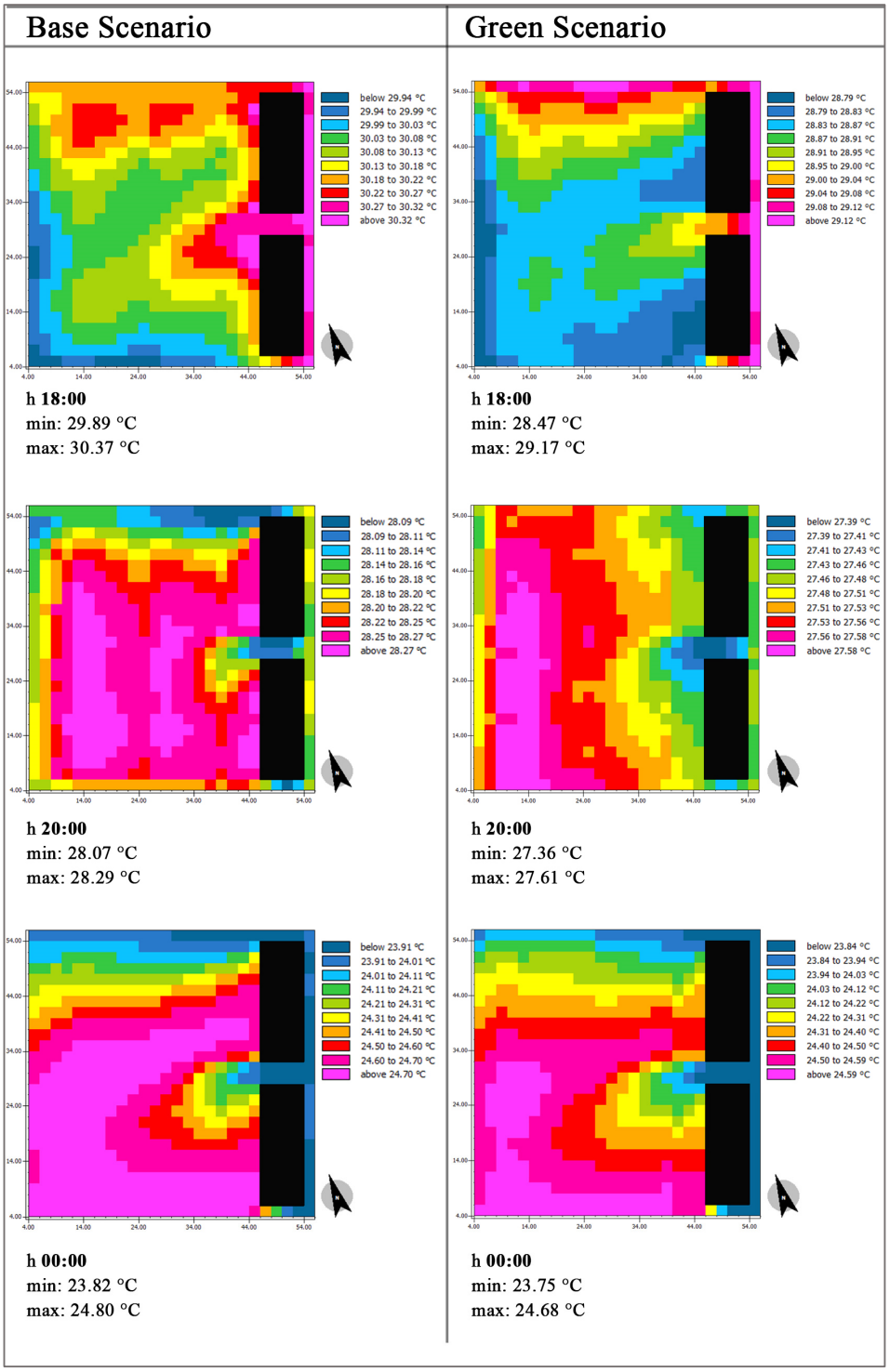

Figure 5.27: Air Temperature in Base and Green Scenario, x-y view at z = 1.4 m at 18:00, 20:00 23rd August 2021 and 00:00 hours on 24th August 2021

To better understand and compare air temperature oscillation of the two models, an hourly average air temperature profile was plotted using temperatures output from the software. Results are shown in Figure 5.28:. There is a marked difference between the two models in daytime hours. For example, at 14:00 hours the air temperature in the green scenario is 2.7 ℃ lower than the air temperature in the base model. It appears that vegetation largely affects the regulation of daytime temperatures. Lower temperatures in the green model continue until 22:00 after which the two models depict almost similar air temperature values with minimal differences.

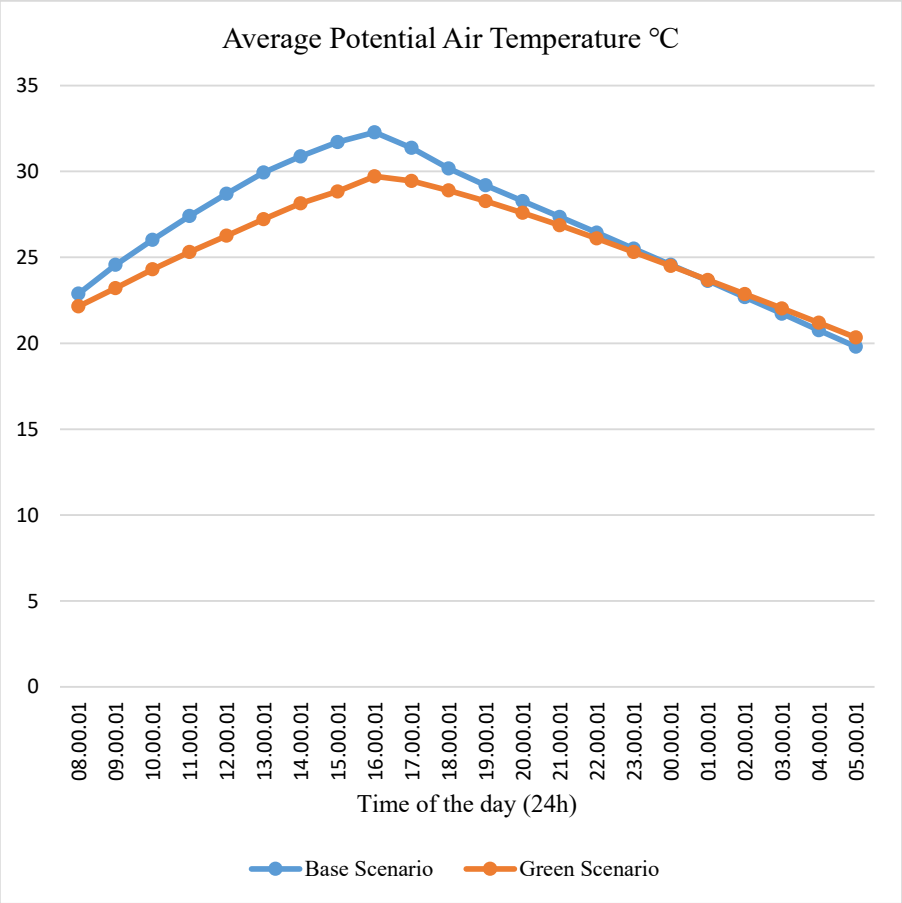

Figure 5.28: Hourly Air Temperature (℃) Values for 23rd and 24th August 2021 at z=1.4m of Base and Green Scenario

5.4.2 7m wide street: Arkadium AVM

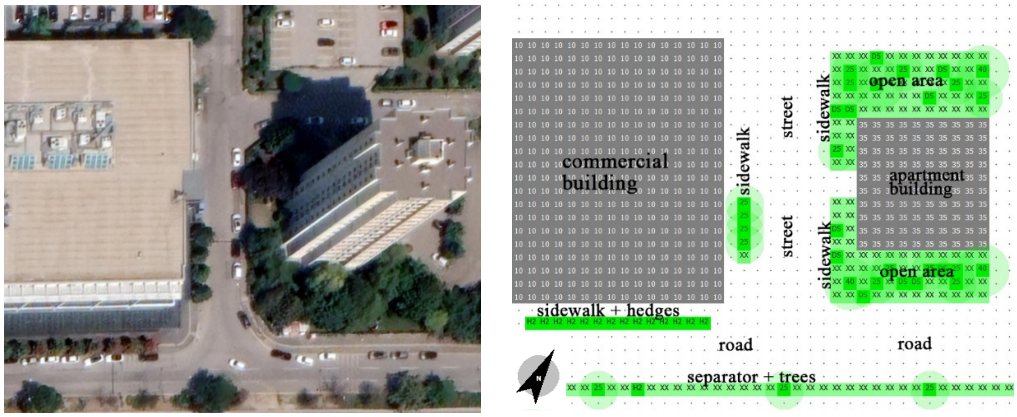

Figure 5.29: Google Earth Screen shot and base model produced in ENVI-met

Base Scenario

The hottest spots appear on asphalt surfaces. A concentration of cool spots consistently appears on the vegetated green space in the apartment building block. At 6:00 pm hotspots appear on the road in the southmost part of the map. Air temperature peaks at 4:00 pm (30.8 ℃) and is lowest at 5:00 am (19.7 ℃). At 12:00 pm the highest variation in minimum (26.5 ℃) and maximum (28.9 ℃) values is observed with a difference of 2.4 ℃.

Green Scenario

Differences in minimum air temperature values between base and green scenario occur in the range of 0.01 ℃ to 0.9 ℃. Statistical air temperature readings from the green scenario are always lower than the base scenario. Cool spots are consistently observed in the green space around the apartment block. Lowest variations in the minimum (27.1 ℃) and maximum (27.6 ℃) values are observed at 8:00 pm which explains why maximum readings are observed over asphalt surfaces.

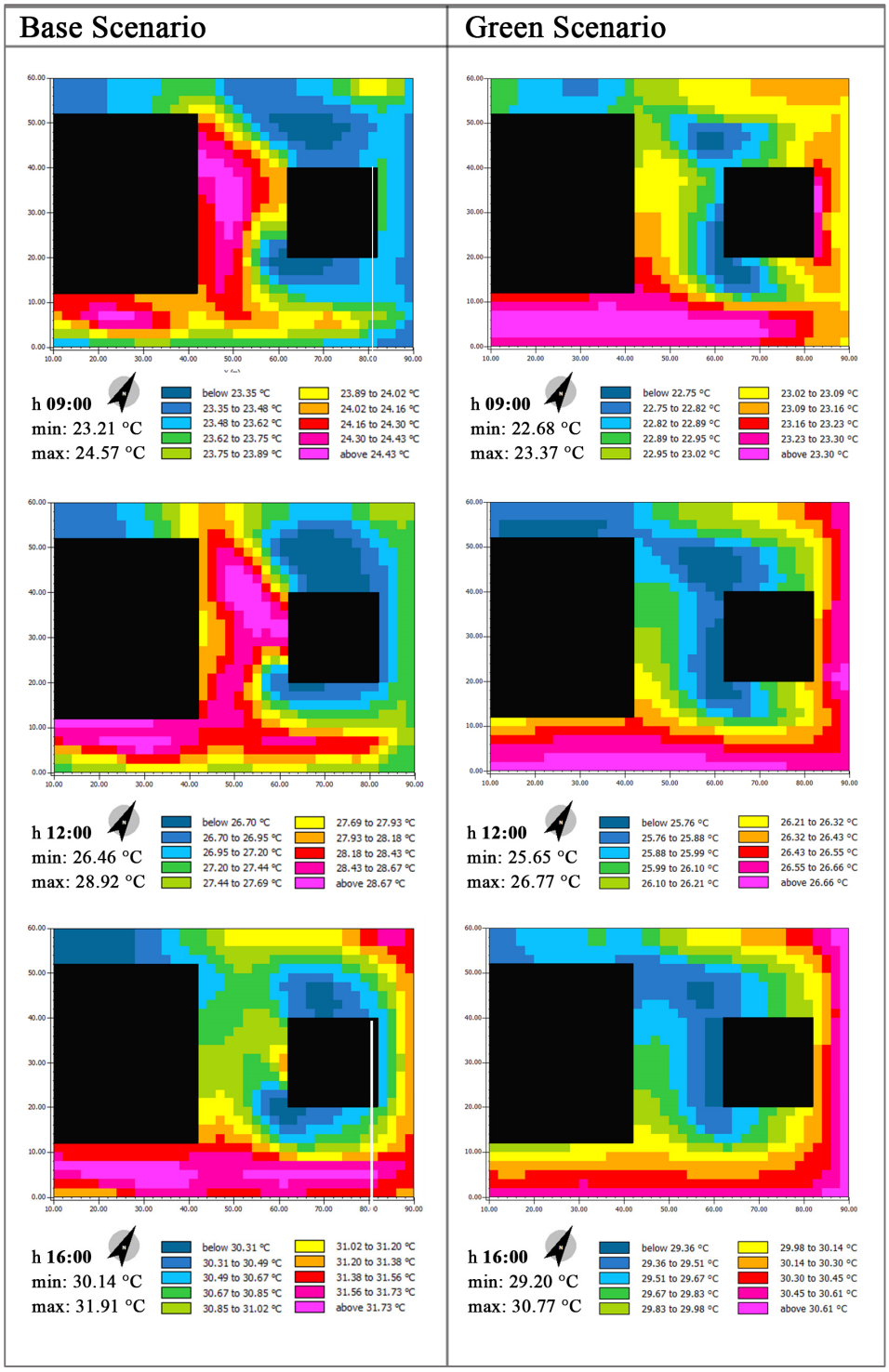

Figure 5.30: Air Temperature in Base and Green Scenario, x-y view at z = 1.4 m at 09:00, 12:00 and 16:00 hours on 23rd August 2021

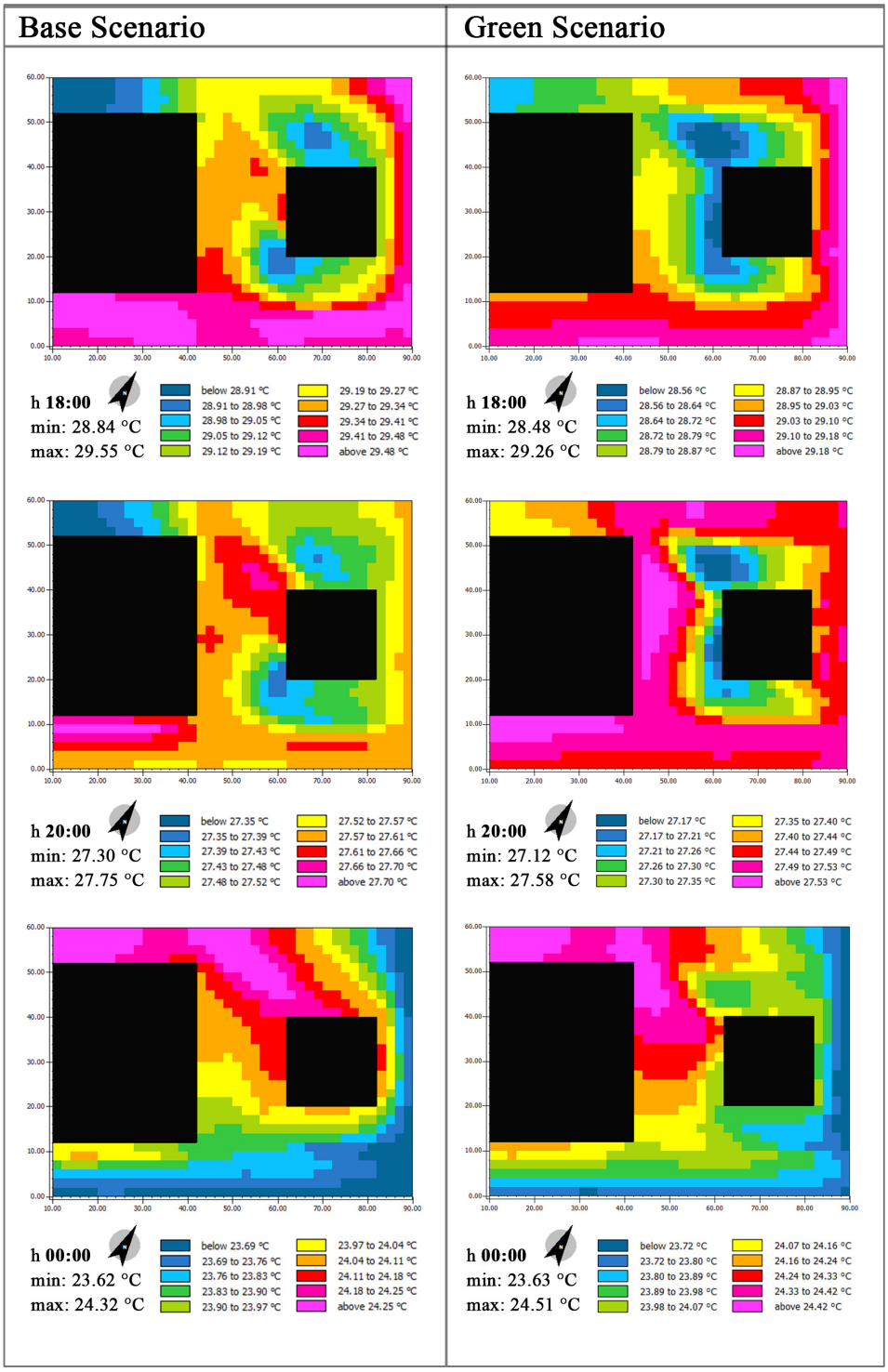

Figure 5.31: Air Temperature in Base and Green Scenario, x-y view at z = 1.4 m at 18:00, 20:00 23rd August 2021 and 00:00 hours on 24th August 2021

Differences in plotted values of average air temperatures in both scenarios indicate that daytime temperatures are more affected by increased vegetation. As shown in Figure 5.32:, from 11:00 am to 3:00 pm air temperatures in the green scenario are approximately 1.0 ℃ lower than the base scenario. At nighttime, between 7:00 pm and 12:00 am temperature differences are negligible. Similarly, at 9:00 am temperature differences are minimal. However, 9:00 am onwards, significant differences are observed between 10:00 and 5:00 pm.

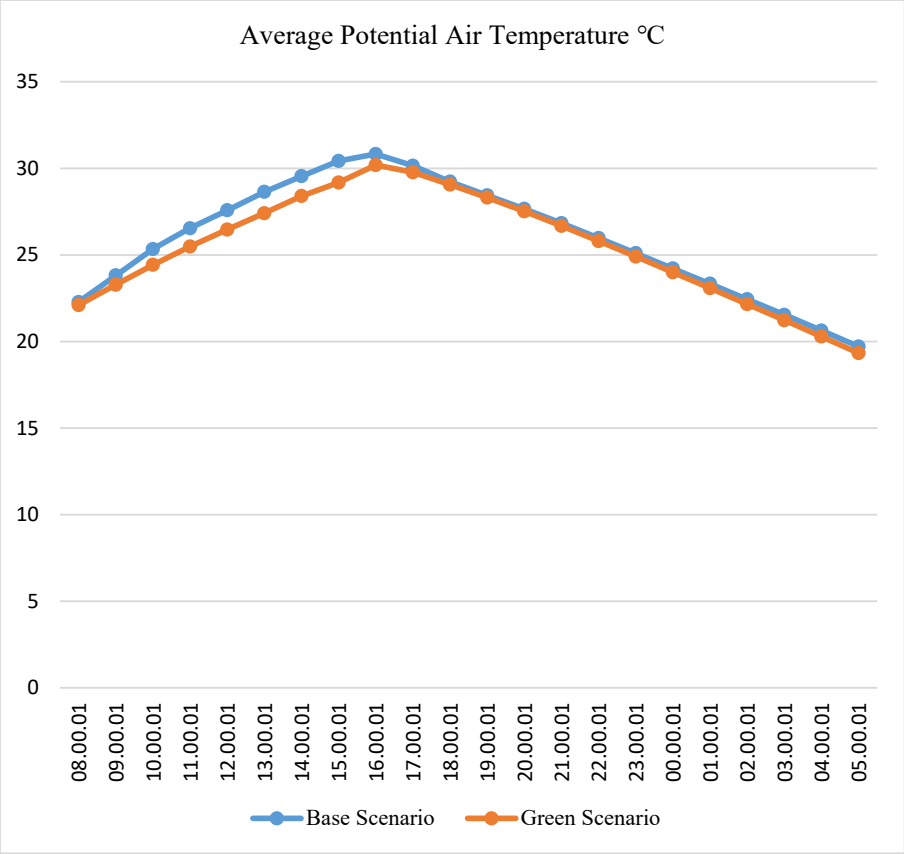

Figure 5.32: Hourly Air Temperature (℃) Values for 23rd and 24th August 2021 at z=1.4m of Base and Green Scenario

5.4.3 8m wide street: 2710. Sokak

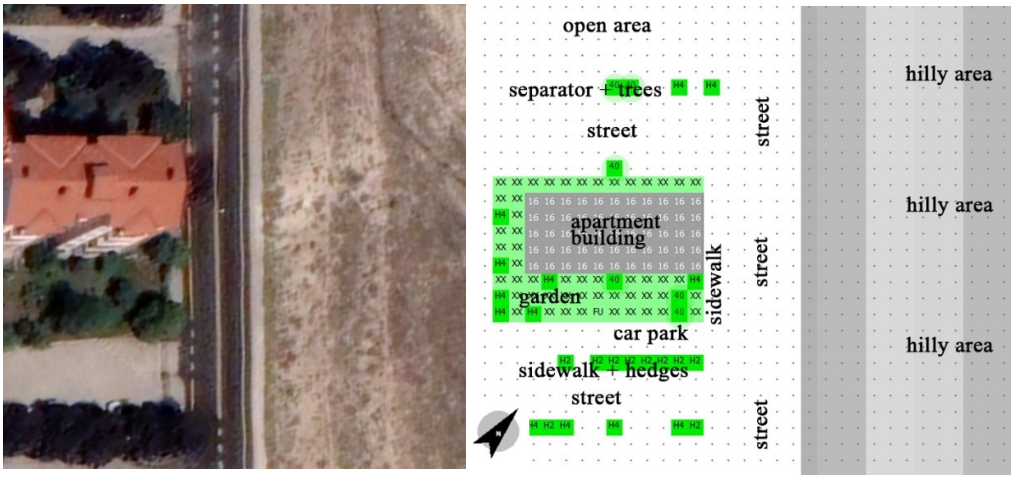

Figure 5.33: Google Earth Screen shot and base model produced in ENVI-met

Base Scenario

The coolest areas are observed on the sloped terrain throughout the day. At 8:00 pm onwards a change is observed where the sloped terrain shows high variations in air temperature. Hotspots are largely concentrated on asphalt roads up until 8:00 pm after which a change is observed. At 12:00 am the highest temperatures are observed on the sloped terrain.

Green Scenario

Statistical readings of air temperature values in the green scenario are consistently lower than readings from base scenario. However, 8:00 pm readings show a minimal and almost negligible difference. The largest coverage of hotspots on asphalted surfaces is observed at 12:00 pm while the smallest hotspots are observed at 8:00 pm. Overall, the most exceptional changes in air temperature patterns between base and green scenario are observed at 9:00 am and 8:00 pm. At 9:00 am, cool spots are significantly reduced and barely appear on the map. At 8:00 pm hotspots are very minimal and appear in the car park area and near the street on the west section of the map.

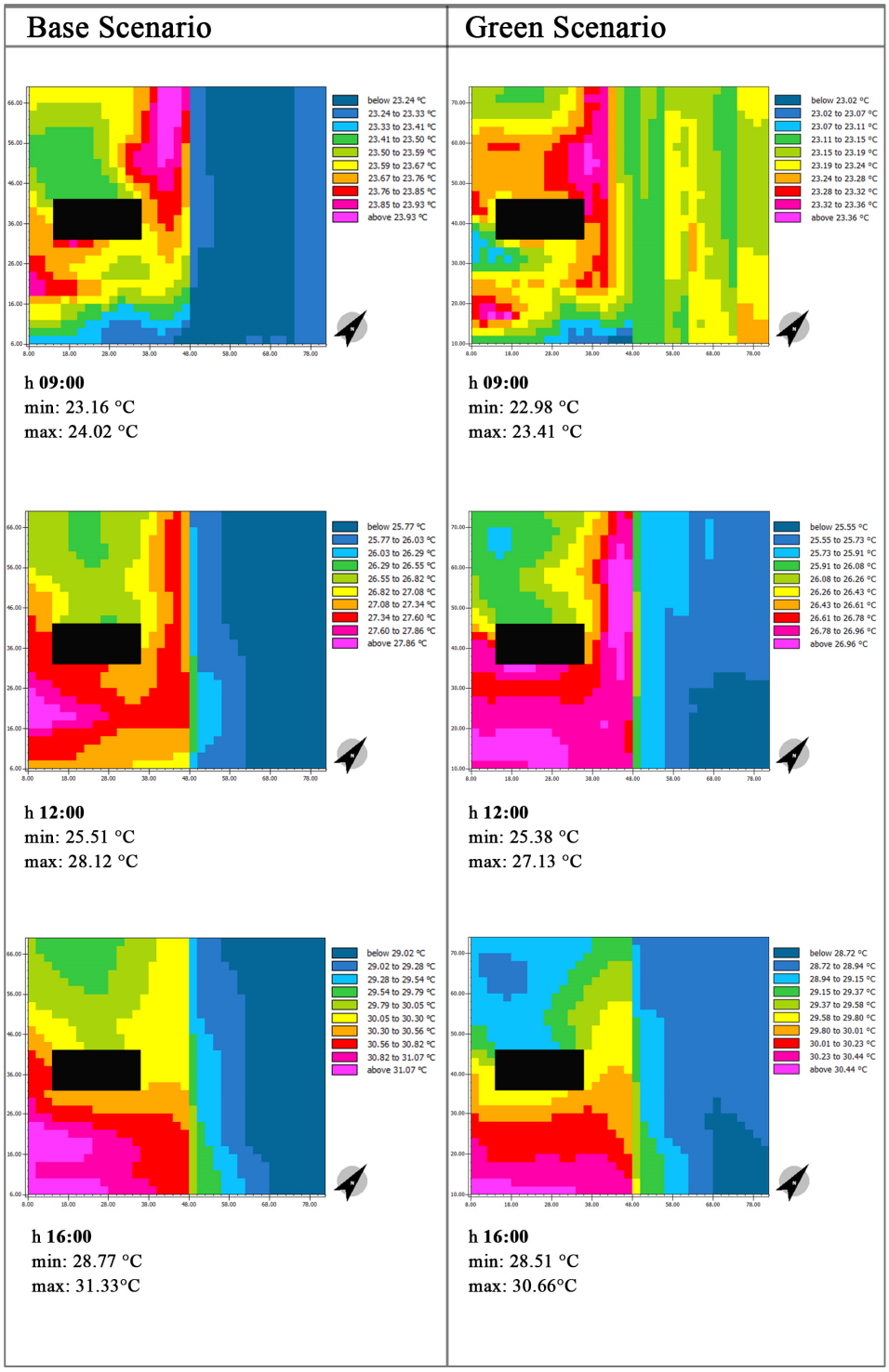

Figure 5.34: Air Temperature in Base and Green Scenario, x-y view at z = 1.4 m at 09:00, 12:00 and 16:00 hours on 23rd August 2021

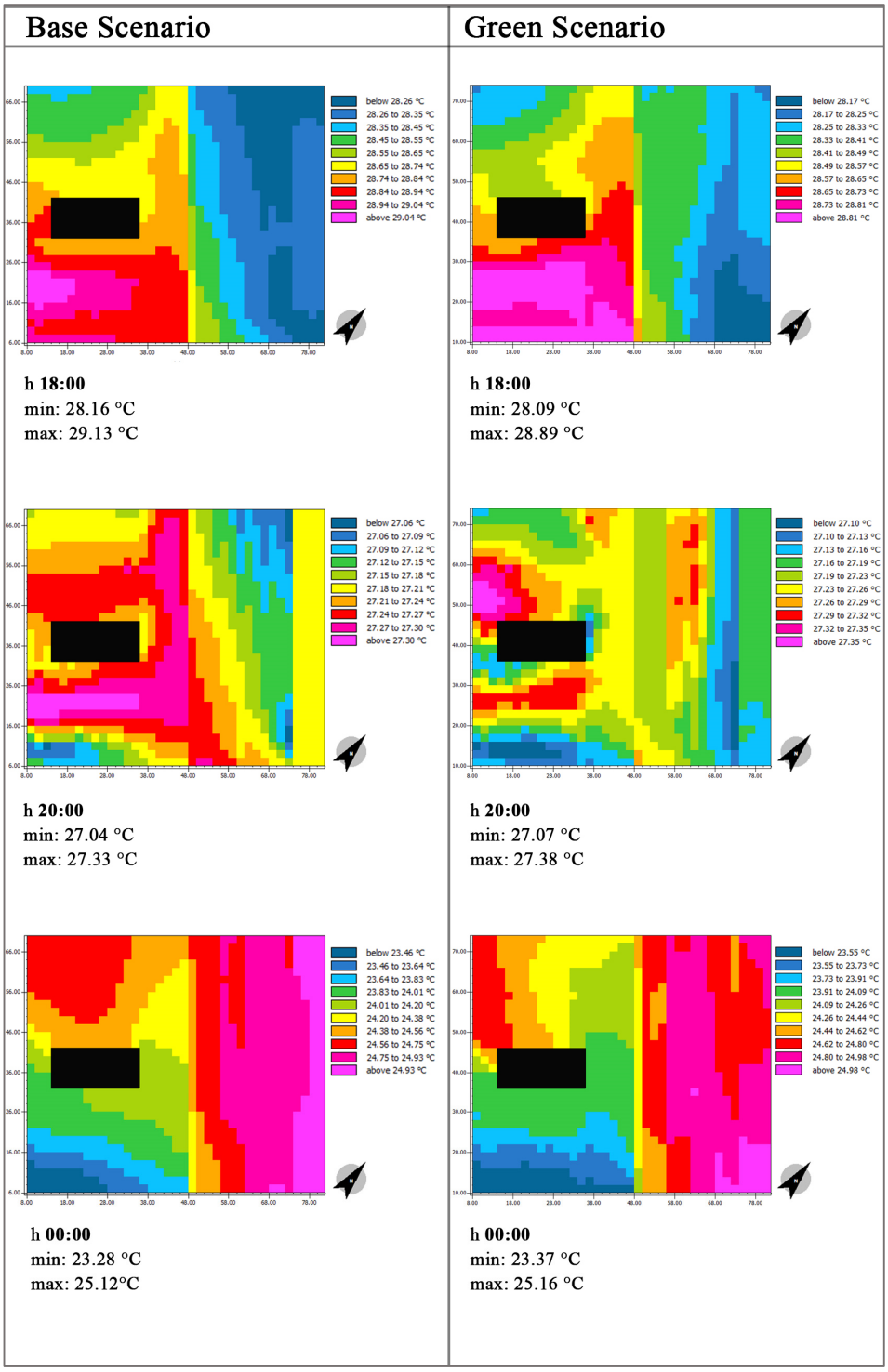

Figure 5.35: Air Temperature in Base and Green Scenario, x-y view at z = 1.4 m at 18:00, 20:00 23rd August 2021 and 00:00 hours on 24th August 2021

Minimal differences are observed between the two scenarios (Figure 5.36:). However, the green scenario still shows lower daytime temperatures. Between 8:00 am and 3:00 pm, green scenario values are upto 0.7 ℃ lower than the base scenario. Virtually no difference is observed in nighttime temperatures.

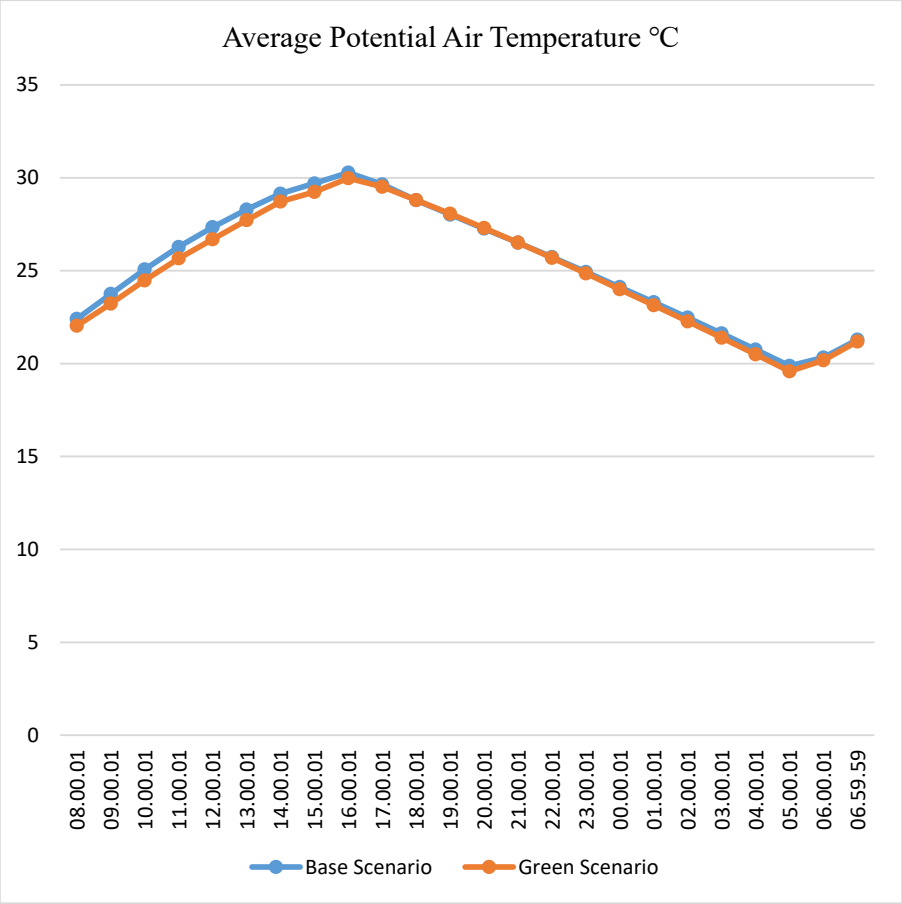

Figure 5.36: Hourly Air Temperature (°C) Values for 23rd and 24th August 2021 at z=1.4m of Base and Green Scenario

5.4.4 26m wide boulevard: Residential Tower Block

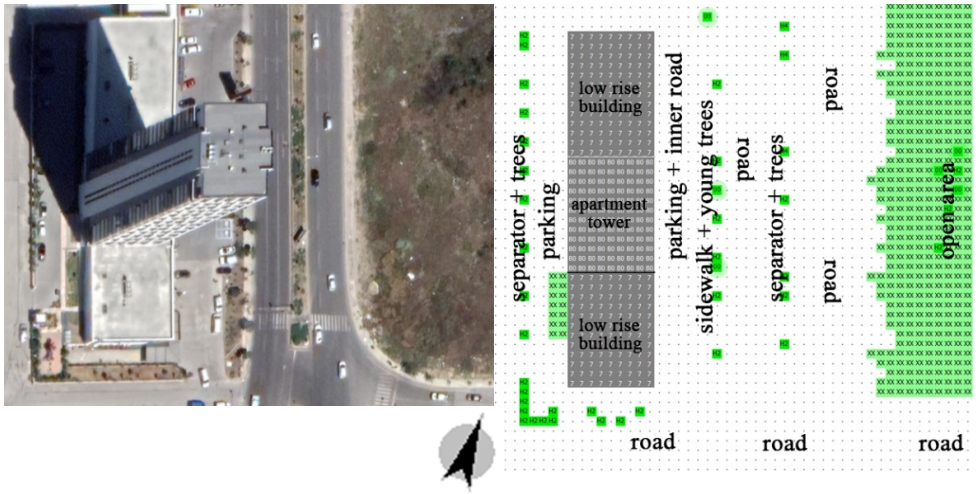

Figure 5.37: Google Earth Screen shot and base model produced in ENVI-met

Base Scenario

At 9:00 am and 12:00 pm, high air temperature values appear mostly on asphalt and bare soil surfaces. At 9:00 am the hottest areas are near the building edge, in the car park area. At 4:00 pm and 6:00 pm similar patterns can be observed, with the highest temperature covering the open area (opposite to the tower block) and asphalt road in the southern portion of the map. At 8:00 pm, the highest temperatures are observed over asphalt surfaces. At 12:00 am the grassy open area shows the lowest temperature.

Green Scenario

The addition of high LAD trees and coated asphalt significantly improve daytime temperatures, and this is reflected in the maps as well. Large cool spots are observed in the 9:00 am, 12:00 pm, 4:00 pm, 6:00 pm and 8:00 pm temperature maps. At 9:00 am and 12:00 pm hotspots appear on mostly asphalt surfaces, but they are significantly smaller compared to base scenario maps.

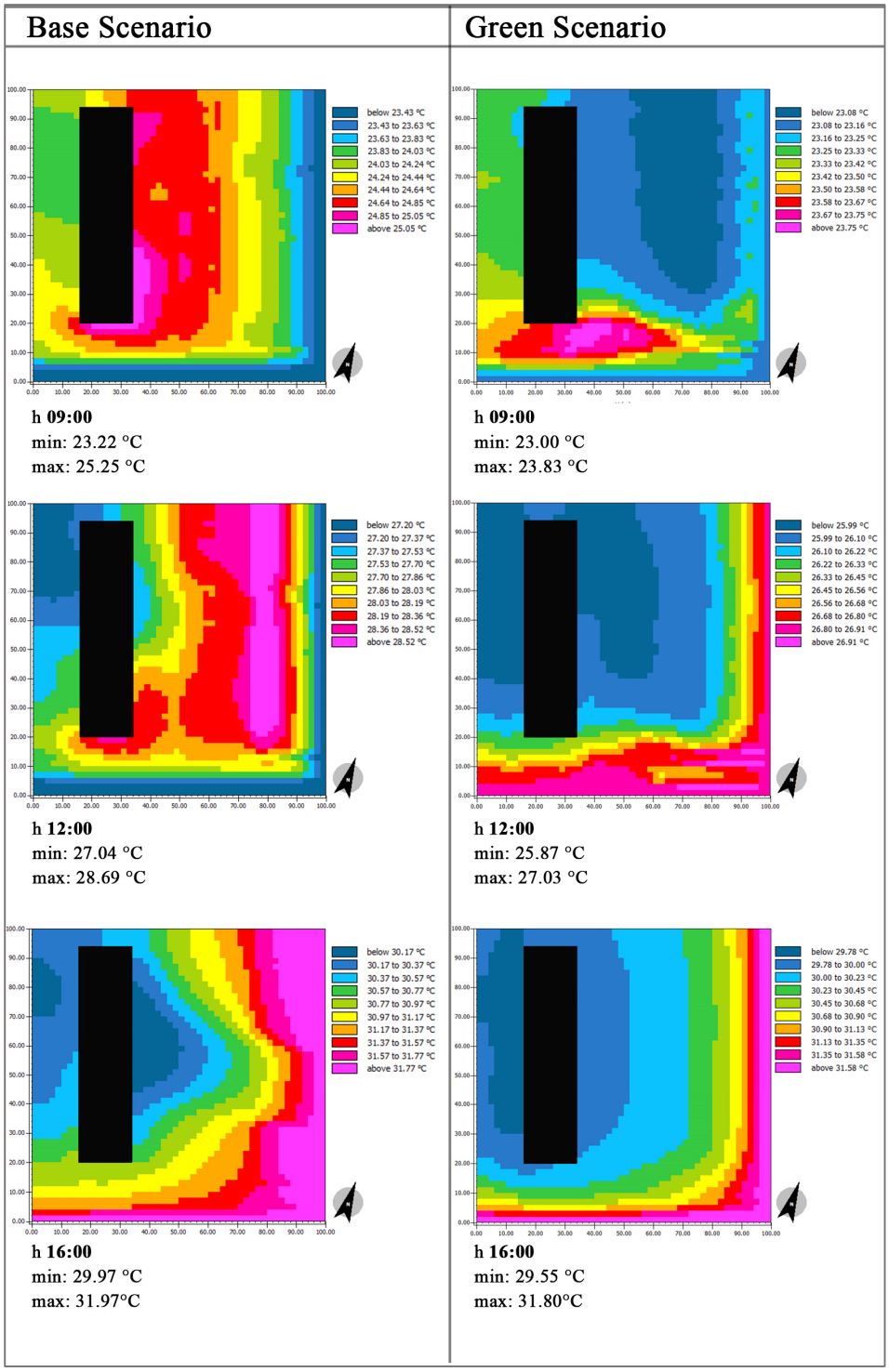

Figure 5.38: Air Temperature in Base and Green Scenario, x-y view at z = 1.4 m at 09:00, 12:00 and 16:00 hours on 23rd August 2021

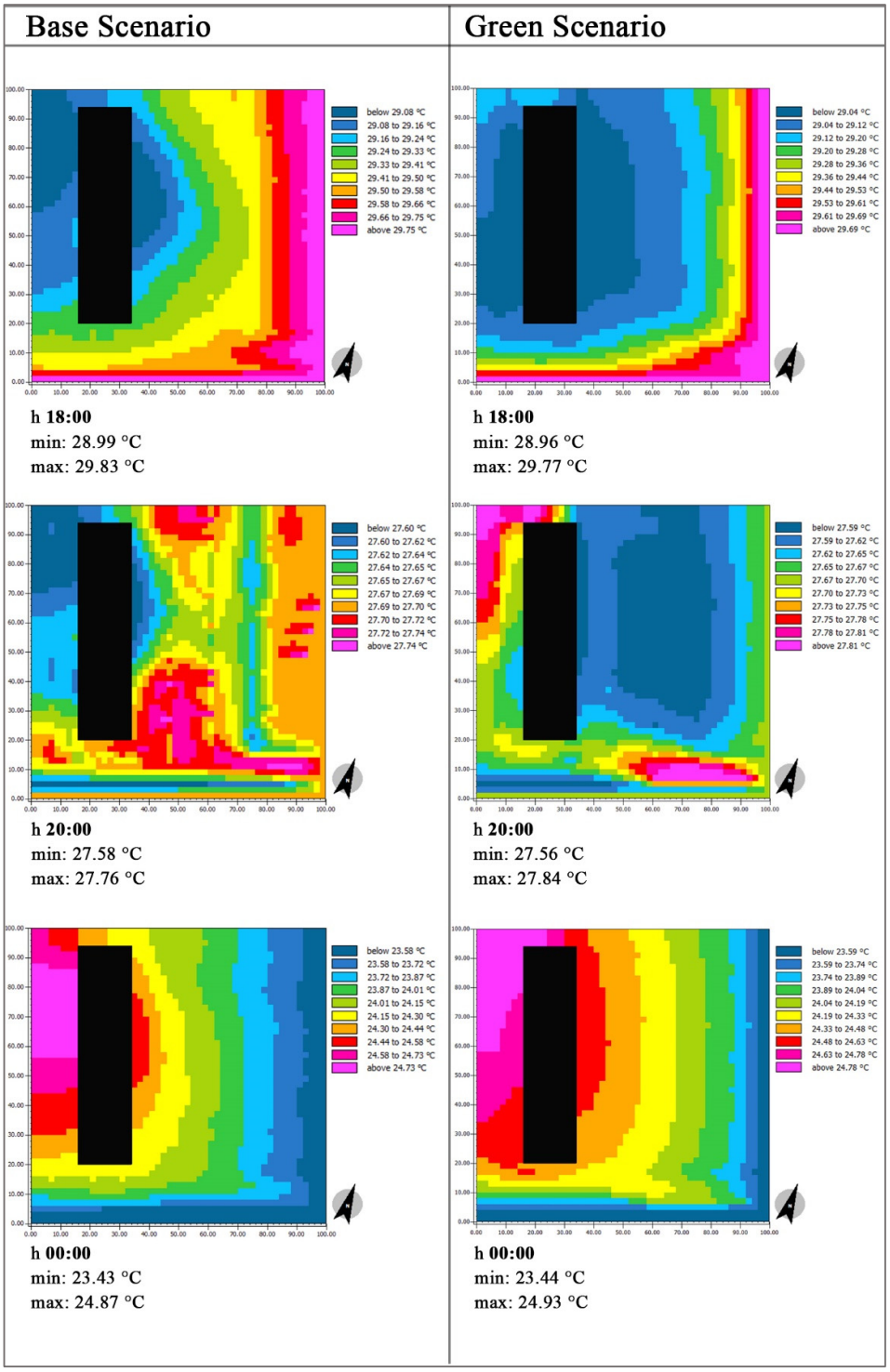

Figure 5.39: Air Temperature in Base and Green Scenario, x-y view at z = 1.4 m at 18:00, 20:00 23rd August 2021 and 00:00 hours on 24th August 2021

As shown in Figure 5.40:, a comparison of plotted air temperature values indicate that daytime temperatures are significantly reduced in the green scenario. The largest difference occurs at 10:00 am when green scenario values are 2.2 ℃ lower than the base scenario. Night time values are almost unchanged with little to no variations between the two scenarios. Peak temperatures (at 4:00 pm) are almost exactly matched.

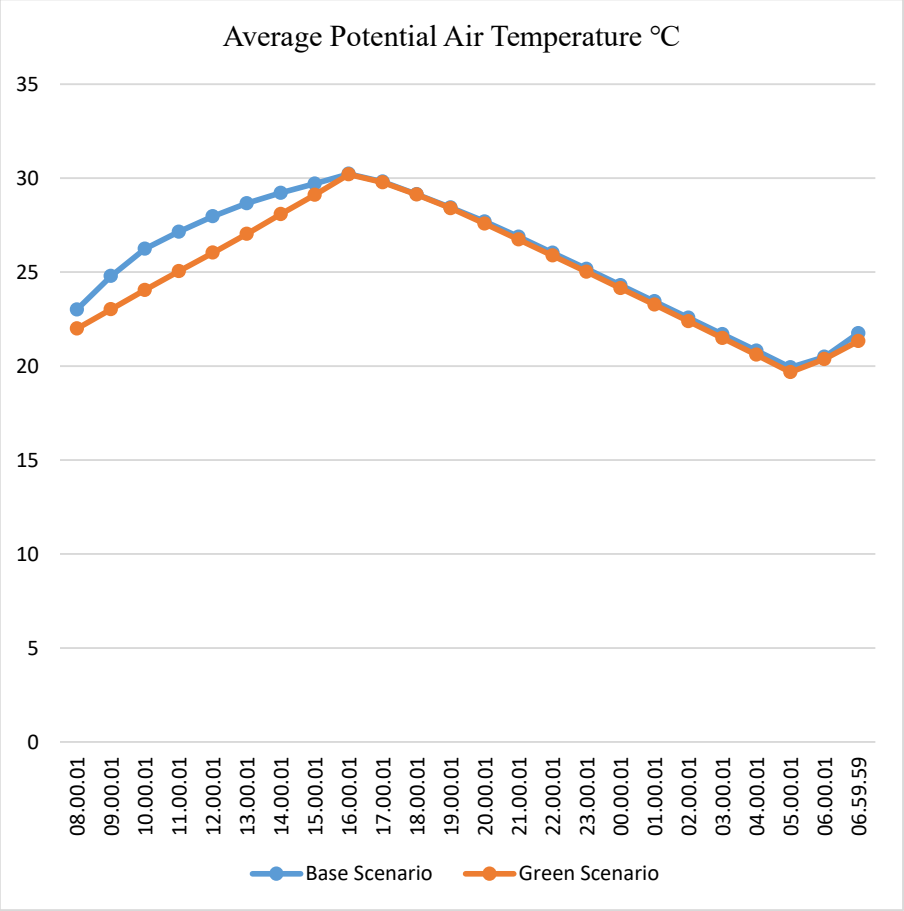

Figure 5.40: Hourly Air Temperature (℃) Values for 23rd and 24th August 2021 at z=1.4m of Base and Green Scenario

CHAPTER 6

INTERPRETING THE RESEARCH OUTCOMES

In this thesis, a series of assessment techniques, at provincial, metropolitan, district, neighbourhood and street scale have unravelled the complexity of urban heat patterns. Proposing urban design strategies to effectively mitigate urban heat is a scale-dependent and multi-dimensional issue which impacts the daily life of humans in a profound way.

Due to the paucity of high-resolution meteorological data of air temperature values, it is not possible to accurately map localized air temperature. In this sense, remote sensing techniques provide time-synchronized temperature data at multiple scales. Another major benefit is that remote sensing data is publicly available and access to the data is not restricted by regional or local authorities.

Remotely sensed LST mapping has been widely used to assess surface-temperature based UHI (Zhang et al., 2014). Many studies have found that LST and air temperature are correlated, and the relationship is affected by land cover types and other factors. As a result, remotely sensed data is often used as a proxy for air temperature in urban heat island studies.

From the outset, this research aimed to integrate an understanding of urban heat by exploring the relationship between urbanization, vegetation, and thermal characteristics of urban surfaces with respect to thermal comfort associated walkability in the city.

In this regard, a synchronized mapping of LULC, NDVI and LST through remote sensing techniques proved beneficial in the assessment and spatial analysis of urban heat patterns. A detailed classification of different land cover types also provides valuable insight into the role played by different spatial configurations and land use

mix. Important lessons learnt from these maps are summarized in the following paragraphs.

The European Environment Agency (2019) states that climate change may lead to the degradation of agricultural areas. Between 1990 and 2018, agricultural areas in the Metropolitan area of Ankara reduced by 19%. While this is mainly due to the outward expansion of urban areas within the province, it could also be due to a decline in soil quality, especially in rural lands not in immediate vicinities of cities and towns.

Bare soil coupled with moisture loss can significantly impact LST and leads to soil degradation which is further accelerated by heat waves. Continuing moisture loss can increase water demand for irrigation in agriculture and lead to smaller crop yields and even desertification (EEA, 2019). Moreover, due to moisture loss, valuable topsoil can be affected by the soil sealing effect which can impact the quality and health of vegetation.

Between 1990 and 2021, mean LST increased by 5 ℃ in the metropolitan area of Ankara. However, changes in LST indicate that rural surfaces have also warmed considerably. In addition to urban areas, rural lands are getting hotter as well. Typically in dry or desert regions, LST maps demonstrate very high LST in peripheral areas. While Ankara is not classified as a desert region, the presence of agrarian rural landscapes and bare soil could be why higher LST is observed in the outskirts as compared to urban areas.

Observing the expansion of urban fabric in Metropolitan Ankara, urban areas including residential communities are now emerging further and further from the city center. Especially noting the expansion in Çayyolu, many residential sites appear as islands surrounded by bare soil and sparsely vegetated areas. In this regard, protecting the quality of bare soil areas can mitigate the excessive heat gains in summertime which may adversely affect the residents of sub-urban communities in Çayyolu. Moreover, it is also equally important to protect green corridors in sub-urban areas and rural lands so that residents may have access to these spaces for

recreational purposes or to engage in productive activities like urban farming and communal gardening.

Between 1990 and 2021, mean NDVI increased from 0.03 to 0.16. Meanwhile, maximum NDVI changed from 0.65 to 0.51. A range of 0.2 to 0.5 is attributed to sparse vegetation such as shrubs and grasslands (Brown, 2018). While temporal NDVI values in the case of Çayyolu may indicate that vegetation greenness has improved, the change is almost negligible. A reduction of maximum NDVI and increase in mean NDVI also indicates that NDVI distribution is more homogenized. This certainly does not mean that vegetation density has increased. Despite a visible increase in 'greenness', the appearance of ecological corridors has deteriorated and become more fragmented, and this is also reflected in LST patterns.

Areas with high NDVI values correlated with low LST values. Sparse or unhealthy vegetation does not effectively mitigate heat. For example, areas classified as transitional woodland in METU campus area, despite having considerable number of trees do not have a significant cooling effect as compared to areas classified as coniferous and mixed forests. It is therefore crucial to consider vegetation density and health when designing for temperature regulation. In this sense, green areas such as spaces with high LAD trees, densely vegetated green areas and urban parks play a crucial role in regulating urban heat.

METU forest is a good example of an ecological buffer between the city and campus area. In this way METU campus exhibits its own microclimate conditions which protect the built areas on campus from extreme heat conditions. Expansion of urban areas in Ankara would benefit greatly from macro- and meso-level urban design interventions to create resilient microclimates and reduce heat-associated vulnerabilities. Moreover, vegetation and shading strategies can be integrated into new developments to improve microclimate conditions, enhance connectivity between green infrastructure elements in the city and to improve micro-scale walkability conditions.

Similarly, the intra-urban and inter-city road network including highways and boulevards are also extremely vulnerable to extreme heat stress due to the extensive use of asphalt, other artificial surfaces, and their proximity to bare soil lands. In addition, they are not supportive of active travel modes, especially when passing through residential areas (e.g., Etimesgut). To improve these conditions, strategies like cool pavements, pigmented asphalt, green buffers, and shade trees with large canopies can be integrated in areas with residential and commercial land use types. In areas where the motorway passes through bare soil and agricultural lands, design interventions should include green buffer zones between road surfaces and agricultural lands.

The thermal properties of barren land, construction sites, high-density residential areas and industrial sites contribute to the warming of urban areas. On the contrary, valley parks, water bodies (lakes, rivers, and streams), and forestland behave as 'heat sinks' and significantly contribute to lowering urban LST.

Construction sites demonstrate high LST patterns because when land is prepared for construction, the site is cleared of vegetation and topsoil is concreted. The separation of land types such as construction sites and built environment fabric under the category of Artificial Surfaces is a useful distinction which highlights the environmental impact of urban spaces in transition.

While green roofs do not significantly contribute to pedestrian thermal comfort, they play a considerable role in regulating air temperature in urban canyons (Perini & Magliocco, 2014). Upon inspection of hotspots appearing over buildings in Çankaya, it was found that commercial and healthcare buildings show significant hotspots with temperature differences of up to 10 °C between the building and the surrounding ground surface. These buildings include Cepa and KentPark shopping centers, Ankara City Hospital and Bilkent center.

The areal site of Atatürk Farm Forest, an important historical conservation site and natural landmark has significantly reduced over time which is also reflected in the increase in LSTs. It has been under the threat of urbanization and development for

years, mostly owing to the 1990 Development plan (Akkar Ercan et al., 2021). Over the years, the quality of soil and vegetation has deteriorated. However, it is an important part of the green infrastructure of the city and can significantly improve walkability by enhancing connectivity between neighborhoods and providing a recreational space for pedestrians.

When comparing the distribution of LST patterns in Metropolitan Ankara, the district of Çankaya has more 'cool' spots than any other district. This is because of the presence and cooling capacity of well-maintained ecological parks like Dikmen Valley, Botanik Park Seğmenler Park, and Portakal Çiçeği park. Meanwhile neighborhoods in the north of Ankara such as Altındağ, Keçiören and Yenimahalle depict dense urban patterns with minimal green urban spaces.

As underlined in the literature review, urban parks are a necessary element of green infrastructure. Green infrastructure not only regulates urban and local temperatures, but it also alleviates thermal comfort conditions. Access to green areas also contributes to increased walkability. However, in areas where open green spaces are not possible, such as in dense urban areas, tree canopies, cool pavements, grass surfaces and active frontages in residential areas can significantly alleviate thermal comfort conditions.

Trees play a great role in improving thermal comfort for pedestrians as opposed to grass surfaces. This is because in addition to the cooling effect created by evapotranspiration processes, trees also provide shade by blocking solar radiation. For example, sports fields in Ankara consistently show LST hotspots, despite having well-maintained and continuous grass surfaces. This may be because open sports fields do not have any shading devices and receive solar radiation throughout the day.

The literature review also highlights the importance of increasing shade at macro-, meso- and micro-level to regulate urban temperatures, improve urban microclimates and alleviate thermal comfort conditions.

The importance of shade as an effective heat mitigation strategy is observed in areas with high-rise buildings. Boulevards adjacent to tall buildings show reduced LSTs as compared to areas with low-rise buildings due to the differences in shaded areas. Similarly, areas with dense vegetation also show low LSTs. Moreover, a comparison of the building blocks modelled in ENVI-met shows that building-tree integrated shading is the most effective cooling strategy for thermal comfort conditions. In this regard, blocking solar radiation and increasing shaded spaces in walkable environments significantly improves thermal comfort for pedestrians.

In the case of microclimate simulations of typical pedestrian blocks, it should be mentioned that modelling near surface air temperature, at 1.5m elevation is a viable metric to measure the sensation of thermal comfort experienced by pedestrians. Therefore, the results of the microclimate simulations are a valuable contribution to this research. They not only visualize micro-scale temperature patterns at a higher resolution (2m) but also show hourly variations in air temperature. ENVI-met simulations also enable an analysis of nighttime features which was one of the crucial unanswered questions: “How do asphalt and building surfaces behave at night?” and “Are UHIs more apparent at night?”.

In addition, the main findings from LULC, LST and NDVI maps, ENVI-met simulations uncovered valuable findings about micro-scale walkability considerations. As shown in Figures 5.26 to 5.40, air temperature results of the alternate ‘green’ scenarios with high LAD trees, dense canopies and pigmented asphalt validate the assumption that lack of vegetation and extensive asphalt surfaces lead to an increase in near surface air temperatures. The comparison of average daytime air temperature values between base and green scenario show a variation of 1-3 ℃. At nighttime, hottest temperatures appear over asphalt surfaces. While increasing vegetation does not significantly impact nighttime air temperature, it does reduce the appaearance and size of nighttime hotspots.

CHAPTER 7

CONCLUSION

In recent years climate-associated risks have dominated the global narrative surrounding sustainability. It has influenced a number of fields, including social sciences, urban planning, architecture, geo-informatics and environmental science. Often, research within these domains overlap, creating new synergies. The design of this research often leaned into other technological domains, especially earth sciences. These overlaps have certainly been encouraging enough to merit further investigation and to inspire more collaborative exploration.

This research proposes a viable methodology using publicly available data and reinforces the importance of multi-scalar urban climatological maps for designing thermally resilient spaces and to inform future planning decisions.

In this thesis, the literature review explores the significance of different factors including thermal comfort as an indicator of pedestrian behaviour and frequency. It provides insight into various walkability parameters and describes the methodology, main findings and variables through which previous studies have evaluated walkability. It also contextualizes the significance of studying urban heat in relation to walkability and explains how thermal comfort relates to urban microclimates, urban heat dynamics and climate change. It also provides an overview of climatic effects on walkability, remote sensing techniques and the role of Landsat-derived estimations of LST, LULC and NDVI in monitoring physiological changes of urban environments.

The study of thermal characteristics of various urban surface materials and landscape components is a valuable tool for uban planners and designers. It can faciliate the

climatic rehabilitation in urban areas and improve the outdoor thermal environment (Yang et al., 2015).

The research methodology proposed in this thesis proved beneficial in many aspects. First and foremost, it provides a systematic and indepth analysis of land-use charcteristics including land surface temperatures, vegetation density and land use composition.

Climate change is accelerated by many factors. Anthropogenic climate change is largely influenced by changing land dynamics owing to the replacement of natural areas with new urban developments. As a result, the increase of built environment patterns significantly impact microclimates in urban areas.

In this regard, NDVI maps are very helpful in monitoring and understanding land surface characteristics in relation to vegetation density, environmental changes and changing climate conditions such as deforestation, drought and desertification. LST maps helped to identify highly spatialized 'hot spots' and 'cool spots' in the urban fabric. Comparing NDVI, LULC and LST maps proved instrumental in understanding land surface and urban heat dynamics.

In Ankara, hot spots appeared over commercial buildings, sports fields, the central bus station (AŞTİ) and the city hospital (Ankara Bilkent Şehir Hastanesi). Specific land types which consistently show high LST patterns are bare soil areas, non-irrigated agricultural lands, sparsely vegetated areas and natural grasslands.

Areas that show the lowest LST values are ground surfaces that receive shade from tall buildings, METU forest land with coniferous and mixed forest types, urban parks, waterbodies (lakes, creeks, dams, rivers and streams) and permanently irrigated agricultural lands. Cool spots also appeared in residential and community green spaces, pocket parks and areas with riparian vegetation (vegetation bordering waterbodies).

Therefore, green infrastructure and shading strategies can build urban resilience and reduce the negative impact of extreme heat (Ozment et al., 2019). In this regard, it is

increasingly important to integrate these considerations in multi-scalar urban design strategies. The macro-, meso- and micro-level climate-responsive urban design strategies which were summarized in Chapter 3 played an integral role in the interpretation of the spatio-temporal LULC, NDVI and LST maps. These strategies also helped in identifying key design elements of thermally resilient walkable spaces. This further facilitated the design of the alternate green scenarios which were calculated in ENVI-met.

Moreover, the research methodology proposed in this thesis is scalable and can provide localized high-resolution LST patterns for an accurate and systematic assessment of temperature hotspots in the city. It enables the identification of local heat islands that emerge within the city can be examined with respect to the land types, land use dynamics and vegetation density.

The rural landscapes of Ankara appear to be heading towards desertification and drought related problems. In the medium-term and long-term planning initiatives, multi-scalar assessments are needed and mitigate the environmental effects of harmful development patterns. Furthermore, derelict urban sites and large-scale construction activities are extremely harmful for urban temperatures and cause excessive heat gain. Native plant and tree species should be preserved. Heat sinks in the form of urban parks, valley parks, forestland, active streams are the most valuable features of cities. They not only regulate temperatures but also encourage active mobility.

With regards to equitable access to green spaces, not all residential communities have access to green areas like urban parks or community green spaces. This not only discourages walkability but also contributes to the rise in urban LSTs. Therefore, special attention should be paid to the distribution of green spaces in the city. In this regard, the planning, maintenance and preservation of green corridors in Ankara is especially important.

In conclusion, walkability is not only the focus of transport planning but also a significant yet unattended part of urban planning and design. This thesis attributes to

this aspect by demonstrating and validating the role of urban design on walking. Improved thermal comfort conditions and their effect on walking behavior of individuals can be obtained by design of the urban environment.

7.1 Challenges of the research

Within the existing literature, approaches to thermal comfort assessments largely focus on microscale parameters. The novelty of this study is that it includes a multi-scalar temporal assessment of urban heat which then informs the analysis of microclimate conditions. With respect to human thermal comfort, it is important to mention that humans perceive the environment differently (Santos Nouri et al., 2022). Psycho-sociological factors significantly contribute to individuals' thermal perceptions of their environment (Santos Nouri et al., 2022). While this study reveals the variability of surface and/or near surface temperature patterns in multiple scales, it would also benefit greatly from a spatialized assessment of tolerable thermal comfort thresholds in pedestrianized public spaces. However, this type of research goes beyond the current scope of the study.

The surface temperature mapping with Landsat images only reveals daytime LST. Many studies have highlighted that UHI is most apparent at nighttime, because heat is released slower in urban areas, as compared to rural areas which means that urban areas are warmer at night (Lee et al., 2013). This is because of the storage and re-radiation of solar radiation in urban areas due to construction materials, (asphalt roads, buildings, etc) and decreased sky view factors (Fokaides et al., 2016). However, nighttime LST is difficult to estimate and entirely impossible with Landsat images.

Other notable limitations in this study are related to the methodology and data accessibility. Cloud covers hinder the availability of Landsat images. Only images with minimal cloud cover of up to 10% are usable. Otherwise, clouds can block major portions of the mapping area. Moreover, on May 31, 2003, the scan-line

corrector (SLC) of Landsat 7 ETM+ failed permanently, resulting in systematic data gaps on retrieved imagery. This severely impacted the spatial continuity of acquired data (Yin et al., 2017, Wang et al., 2021). It is precisely due to this malfunction that reliable images were not found for the month July or August 2012. This impacted the cross-comparability of temporal Landsat retrieved data with temporal LULC maps.

In this study, publicly available CORINE LULC data was utilized. However, CORINE maps are geographically limited since the product is only available for the European region (including Turkey). With advances in technology and machine learning algorithms, LULC maps can now be easily derived with a variety of classification techniques including supervised, unsupervised, and object-based classification (Alshari & Gawali, 2021). Future studies can benefit from these methods to derive LULC classification if the required data is inaccessible for the desired geographical context.

Another limitation of this research is the difficulty in validating LST accuracy. As described in the Methodology chapter, reference LST estimates are required to evaluate the accuracy of satellite based LST. According to Guillevic et al. (2018), directly comparing satellite-derived LST against in-situ LST is the only 'true' validation approach. However, in-situ measurements are costly and time-consuming. At present there are less than 20 in-situ LST validation stations worldwide that provide reliable data. Due to the paucity of in-situ LST data, reliable validation of the Landsat-derived LST remains a challenge.

Interpreting LST and NDVI maps requires a keen eye and specialized knowledge. Multiple statistical methods are used for the analysis of LST-NDVI relationships. However, correlation analyses or the use of statistical methods to analyze the relationships were beyond the parameters of this research. Perhaps future researchers should review existing and upcoming scientific literature to be cognizant of interpretation and representation methods.

With regards to microclimate analysis, ENVI-met simulation is costly in terms of time and effort. Each simulation calculation takes approximately 12 to 24 hours for a small parcel measuring 50m x 50m x 40m. For an urban block, it may take up to three days. Since it is a relatively new tool, availability of information about troubleshooting and resolving technical issues is also limited.

7.2 Recommendations for future work

For future experiments, one solution could be to produce nighttime mapping of LST, creating a more accurate representation of UHI patterns in Ankara. The proposed temporal mapping method can also include seasonal distribution of LST and NDVI to improve the method of change detection. For example, it would be useful to compare spring, summer, autumn and wintertime LST patterns within the same year. It also raises the opportunity to compare seasonal patterns of urban heat over time.

It should also be mentioned that urban heat assessments of cities with arid, semi-arid or desert climates would be an invaluable addition to scientific literature. This would initiate a deeper understanding of relationships between rural-urban temperature differences.

While the outcomes of this thesis are specific to the case of Ankara, it serves as an example of a continuously densifying city where both rural and urban lands are facing the threat of extreme heat brought on by climate change. In this regard, a systematic risk assessment, with respect to vulnerability, susceptibility and sensitivity of people, vegetation, and buildings exposed to heat stress can help quantify the true impact of extreme heat as a hazard.

In the case of micro level assessment, other variables like Physiological Equivalent Temperature (PET) can also be calculated in ENVI-met simulations. The PET considers the influence of the multiple variables (i.e., air humidity, air temperature, and wind velocity as well as short- and long-wave radiation) on humans and is a useful indicator of the thermal environment. PET results, as an indicator of thermal

stress, can be easily interpreted by users, such as urban planners without prior knowledge of modern human biometeorological terminology because of its widely known unit (in degrees Celsius).

Moreover, additional variations in microclimatic features such as the use of artificial water features, changes in soil moisture, soil type or seasonal variations in temperatures can further enhance the comparative analysis of typical pedestrian blocks in the city.

Visualizing the complexity of pedestrian thermal comfort and urban heat dynamics creates challenges for the urban designer. Despite the availability of data and a variety of geospatial analysis tools, specialized skills are needed for quantifying heat associated vulnerabilities and risk assessments.

From the perspective of active travelers, it would be beneficial to have access to spatialized temperature data to better influence walkability associated behaviours and encourage active travel. In the same way, live temperature data can be integrated in future pedestrian associated tools where a comfortable walking route is suggested based on the identification of hot and cool spots between route origin and desired destinations.

In conclusion, it is imperative to actively strive for accurate layering of climatological conditions within urban design frameworks, and gain insight as to the thermal performance of urban environments by leveraging the technological advances in earth observation and geospatial analysis tools. Future research would greatly benefit from publicly accessible, standardized and high-resolution climate maps of Turkey’s main urban centres.

REFERENCES

Aflaki, A., Mirnezhad, M., Ghaffarianhoseini, A., Ghaffarianhoseini, A., Omrany, H., Wang, Z.-H., & Akbari, H. (2017). Urban Heat Island Mitigation Strategies: A state-of-the-art review on Kuala Lumpur, Singapore and Hong Kong. *Cities*, *62*, 131–145. https://doi.org/10.1016/j.cities.2016.09.003.

Aghamolaei, R., Azizi, M. M., Aminzadeh, B., & O'Donnell, J. (2022). A comprehensive review of outdoor thermal comfort in urban areas: Effective parameters and approaches. *Energy & Environment*. https://doi.org/10.1177/0958305x221116176.

Akbari, H., Pomerantz, M., & Taha, H. (2001). Cool surfaces and shade trees to reduce energy use and improve air quality in urban areas. *Solar Energy*, *70*(3), 295–310. https://doi.org/10.1016/s0038-092x(00)00089-x.

Akbari, H., Pomerantz, M., & Taha, H. (2001). Cool surfaces and shade trees to reduce energy use and improve air quality in urban areas. *Solar Energy*, *70*(3), 295–310. https://doi.org/10.1016/s0038-092x(00)00089-x.

Akkar Ercan, Z. M., Erişen, Y., & Tiryaki, İ. D., (2021). *Sustainable green urbanism: envisioning new agents for planning and designing sustainable green spaces in Ankara.* Ankara: İdealkent.

Akman, S. (2016). *Conserving and managing modern campus heritage:"alley" as the spine of METU campus, Ankara.* [Masters Thesis, Middle East Technical University].

Alkhatib, M. Q., Cabrera, S. D., & Gill, T. E. (2012). Automated detection of dust clouds and sources in NOAA-AVHRR satellite imagery. *2012 IEEE Southwest Symposium on Image Analysis and Interpretation*. https://doi.org/10.1109/ssiai.2012.6202462

Alshari, E. A., & Gawali, B. W. (2021). Development of classification system for LULC using remote sensing and GIS. *Global Transitions Proceedings*, *2*(1), 8–17. https://doi.org/10.1016/j.gltp.2021.01.002.

Alves, F. M., Gonçalves, A., & del Caz-Enjuto, M. R. (2022). The use of envi-met for the assessment of nature-based solutions' potential benefits in industrial parks—a case study of Argales Industrial Park (Valladolid, Spain). *Infrastructures*, *7*(6), 85. https://doi.org/10.3390/infrastructures7060085.

Arabi Aliabad, F., Zare, M., & Ghafarian Malamiri, H. (2021). Comparison of the accuracy of daytime land surface temperature retrieval methods using LANDSAT 8 images in arid regions. *Infrared Physics & Technology*, *115*, 103692. https://doi.org/10.1016/j.infrared.2021.103692

Arbeck. (2015, December 14). *File:the difference between Digital Surface Model (DSM) and Digital Terrain Models (DTM) when talking about digital elevation models (DEM).SVG*. Wikimedia Commons. Retrieved January 19, 2023.https://commons.wikimedia.org/wiki/File:The_difference_between_Digital_Surface_Model_%28DSM%29_and_Digital_Terrain_Models_%28DTM%29_when_talking_about_Digital_Elevation_models_%28DEM%29.svg.

Arif, V., & Yola, L. (2020). The primacy of microclimate and thermal comfort in a walkability study in the tropics: A Review. *Journal of Strategic and Global Studies*, *3*(1). https://doi.org/10.7454/jsgs.v3i1.1025.

Atanur, G., Ersoy Mirici, M., Ersoz, N. D., & Han, K. (2022). A preliminary assessment on the accessibility of urban green spaces: The case of bursa, Yıldırım. *GSI Journals Serie A: Advancements in Tourism Recreation and Sports Sciences.* https://doi.org/10.53353/atrss.1038032.

Balany, F., Ng, A. W., Muttil, N., Muthukumaran, S., & Wong, M. S. (2020). Green Infrastructure as an urban heat island mitigation strategy - A Review. https://doi.org/10.20944/preprints202009.0018.v1.

Baobeid, A., Koç, M., & Al-Ghamdi, S. G. (2021). Walkability and its relationships with health, sustainability, and livability: Elements of physical environment

and evaluation frameworks. *Frontiers in Built Environment*, *7*. https://doi.org/10.3389/fbuil.2021.721218.

Belge, Z. S. (2020). *Mobility and the role of pedestrians in making public space: Mersin Coastal Park* [Doctoral Thesis, Middle East Technical University].

Bigazzi, A., Gill, G., & Winters, M. (2021). Contrasting perspectives on the comfort and safety of pedestrians interacting with other road users. *Transportation Research Record: Journal of the Transportation Research Board*, *2675*(3), 33–43. https://doi.org/10.1177/0361198121992272.

Böcker, L., Dijst, M., & Prillwitz, J. (2013). Impact of Everyday Weather on Individual Daily Travel Behaviours in Perspective: A Literature Review. *Transport Reviews*, 33(March 2015), 71–91.

Boehmer, T. K., Hoehner, C. M., Wyrwich, K. W., Ramirez, L. K. B., & Brownson, R. C. (2006). Correspondence Between Perceived and Observed Measures of Neighborhood Environmental Supports for Physical Activity. *Journal of Physical Activity and Health*, 3(1), 22–36. https://doi.org/10.1123/JPAH.3.1.22.

Branea, A., Danciu, M., Gaman, M. & Badescu, S. (2016). *Challanges regarding the study of urban heat islands: Ruleset for researchers.* Risk Reduction for Resilient Cities, Bucharest, Hungary.

Brown, B. B., Werner, C. M., Amburgey, J. W., & Szalay, C. (2007). Walkable route perceptions and physical features. *Environment and Behavior*, *39*(1), 34–61. https://doi.org/10.1177/0013916506295569.

Brown, J. (2018). *NDVI, the Foundation for Remote Sensing Phenology*. USGS.gov | Science for a changing world. https://www.usgs.gov/special-topics/remote-sensing-phenology/science/ndvi-foundation-remote-sensing-phenology#overview.

Çağlayan, Ç., Güner, M. E., Yavuz, M., Gacal, F., Beykan, N., & İlhan, A. (2021). *Turkey heat waves and public health briefing*. Health and Environmental

Alliance EU. https://ghhin.org/resources/heatwaves-and-public-health-in-turkiye/.

Caliskan, O. (2011). Motionscape: The image of space in Motion (An attempt at conceptualization in the case of Ankara). *Journal of Architectural and Planning Research*. 28.

Caprì, S., Ignaccolo, M., Inturri, G., & Le Pira, M. (2016). Green Walking Networks for Climate Change Adaptation. *Transportation Research Part D: Transport and Environment*, *45*, 84–95. https://doi.org/10.1016/j.trd.2015.08.005.

Casali, Y., Aydin, N. Y., & Comes, T. (2022). Machine learning for spatial analyses in urban areas: A scoping review. *Sustainable Cities and Society*, *85*, 104050. https://doi.org/10.1016/j.scs.2022.104050.

Center for International Earth Science Information Network - CIESIN - Columbia University (2016). *Global Urban Heat Island (UHI) Data Set, 2013.* [Data set]. Palisades, New York: NASA Socioeconomic Data and Applications Center (SEDAC). https://doi.org/10.7927/H4H70CRF.

Chen, L., Wen, Y., Zhang, L., & Xiang, W.-N. (2015). Studies of thermal comfort and space use in an urban park square in cool and cold seasons in Shanghai. *Building and Environment*, *94*, 644–653. https://doi.org/10.1016/j.buildenv.2015.10.020.

Chen, T.-L., & Lin, Z.-H. (2021). Impact of land use types on the spatial heterogeneity of extreme heat environments in a metropolitan area. *Sustainable Cities and Society,* 72, 103005. https://doi.org/10.1016/j.scs.2021.103005.

Chiang, Y.-C., Sullivan, W., & Larsen, L. (2017). Measuring neighborhood walkable environments: A comparison of three approaches. *International Journal of Environmental Research and Public Health*, *14*(6), 593. https://doi.org/10.3390/ijerph14060593.

Chong, S., Mazumdar, S., Jalaludin, B., & Hatfield, J. (2022). Associations between walkability and pedestrian related injuries is modified by sociodemographic characteristics. *Injury*, *53*(12), 3978–3986. https://doi.org/10.1016/j.injury.2022.09.014.

Çiçek, İ., & Doğan, U. (2005). Ankara'da şehir ISI Adasinin incelenmesi detection of urban heat island in Ankara, Turkey. *Co*. https://doi.org/10.1501/cogbil_0000000049.

Çiçek, İhsan & Doğan, Uğur. (2006). Detection of urban heat island in Ankara, Turkey. *Nuovo Cimento- Societa Italiana di Fisica Sezione C*. 29. 399-409. 10.1393/ncc/i2005-10028-2.

Coffel, E. D., de Sherbinin, A., Horton, R. M., Lane, K., Kienberger, S., & Wilhelmi, O. (2018). The science of adaptation to extreme heat. *Resilience*, 89–103. https://doi.org/10.1016/b978-0-12-811891-7.00007-4.

Çolak, E., & Sunar, F. (2022). Investigating the usefulness of satellite-retrieved land surface temperature (LST) in pre- and post-fire spatial analysis. *Earth Science Informatics*. https://doi.org/10.1007/s12145-022-00883-8.

Definition:Principles And Recommendations. Report, COST Action CA16208 CONVERGES, 20 pp. (https://converges.eu/resources/riparian-zone-riparian-vegetation-definition-principles-and-recommendations/).

Dihkan, M., Karsli, F., Guneroglu, N., & Guneroglu, A. (2018). Evaluation of urban heat island effect in Turkey. *Arabian Journal of Geosciences*, *11*(8). https://doi.org/10.1007/s12517-018-3533-3.

Dizdaroglu, D. (2019) 'Measuring residential sustainability performance: an indexing approach', Int. J. Sustainable Development, Vol. 22, Nos. 1/2, pp.1–23.

Dufour S., Rodríguez-González P.M. (2019). *Riparian Zone/Riparian Vegetation.*

Edmondson, J. L., Stott, I., Davies, Z. G., Gaston, K. J., & Leake, J. R. (2016). Soil surface temperatures reveal moderation of the urban heat island effect by trees and shrubs. *Scientific Reports*, *6*(1). https://doi.org/10.1038/srep33708.

El Kenawy, A. M., Hereher, M. E., & Robaa, S. M. (2019). An assessment of the accuracy of Modis land surface temperature over Egypt using ground-based measurements. *Remote Sensing*, *11*(20), 2369. https://doi.org/10.3390/rs11202369.

Enete, I., Alabi, O. & Chukwudelunzu, V.C. (2012). Tree canopy cover variation effects on urban heat island in Enugu city Nigeria. *Developing Country Studies, 2*, 12-18.

Erkaya, B. D. (2022). *Investigation Of The Impacts Of Building And Urban Parameters On Urban Heat Island Formation In Ankara* [Master's Thesis, Middle East Technical University].

Ermida, S. L., Soares, P., Mantas, V., Göttsche, F.-M., & Trigo, I. F. (2020). Google Earth engine open-source code for land surface temperature estimation from the landsat series. *Remote Sensing*, *12*(9), 1471. https://doi.org/10.3390/rs12091471.

Eslamirad, N., Sepúlveda, A., De Luca, F., & Sakari Lylykangas, K. (2022). Evaluating outdoor thermal comfort using a mixed-method to improve the environmental quality of a university campus. *Energies*, *15*(4), 1577. https://doi.org/10.3390/en15041577.

European Environment Agency (EEA). (2021) *CORINE Land Cover Product User Manual (Version 1.0)*, European Union, Copernicus Land Monitoring Service. https://land.copernicus.eu/user-corner/technical-library/clc-product-user-manual.

Forsyth, A. (2015). What is a walkable place? The walkability debate in urban design. *URBAN DESIGN International*, *20*(4), 274–292. https://doi.org/10.1057/udi.2015.22.

Frank, L. D., & Engelke, P. O. (2001). The built environment and human activity patterns: Exploring the impacts of urban form on Public Health. *Journal of Planning Literature*, *16*(2), 202–218. https://doi.org/10.1177/08854120122093339.

Fyhri, A., Hof, T., Simonova, Z., & Jong, M. (2011). The influence of perceived safety and security on walking. Cost. http://resolver.tudelft.nl/uuid:a1a0efe9-88a0-4d4d-bbfe-bdc817e9a4c5.

Gholami, M., Torreggiani, D., Tassinari, P., & Barbaresi, A. (2022). Developing a 3D city digital twin: Enhancing walkability through a green pedestrian network (GPN) in the city of Imola, Italy. *Land*, *11*(11), 1917. https://doi.org/10.3390/land11111917.

Graham, S. R., Carlton, C., Gaede, D., & Jamison, B. (2011). *student column*: The benefits of using geographic information systems as a community assessment tool. *Public Health Reports*, *126*(2), 298–303. https://doi.org/10.1177/003335491112600224.

Greenberg, E., Natapov, A., & Fisher-Gewirtzman, D. (2019). A physical effort-based model for pedestrian movement in topographic urban environments. *Journal of Urban Design*, *25*(1), 86–107. https://doi.org/10.1080/13574809.2019.1632178.

Grover, A., & Singh, R. (2015). Analysis of Urban Heat Island (UHI) in relation to Normalized Difference Vegetation Index (NDVI): A comparative study of delhi and Mumbai. *Environments*, *2*(4), 125–138. https://doi.org/10.3390/environments2020125.

Guigoz, Y., Giuliani, G., Nonguierma, A., Lehmann, A., Mlisa, A., & Ray, N. (2017). Spatial data infrastructures in Africa: A gap analysis. J*ournal of Environmental Informatics*, 30(1).

Guillevic, P., Göttsche, F., Nickeson, J., Hulley, G., Ghent, D., Yu, Y., Trigo, I., Hook, S., Sobrino, J.A., Remedios, J., Román, M. & Camacho, F. (2018). Land Surface Temperature Product Validation Best Practice Protocol. Version 1.1. In P. Guillevic, F. Göttsche, J. Nickeson & M. Román (Eds.),

Good Practices for Satellite-Derived Land Product Validation (p. 58): Land Product Validation Subgroup (WGCV/CEOS), doi:10.5067/doc/ceoswgcv/lpv/lst.001.

Hayrullahoğlu, G., & Varol, Ç. (2022). Understanding mobility dynamics using urban functions during the COVID-19 pandemic: Comparison of pre-and post-new normal eras. *Asia-Pacific Journal of Regional Science*, *6*(3), 1087–1109. https://doi.org/10.1007/s41685-022-00247-6.

He, Y., Rentschler, J., Avner, P., Gao, J., Yue, X., Radke, J. (2022). Mobility and Resilience : A Global Assessment of Flood Impacts on Road Transportation Networks. Policy Research Working Papers; World Bank, Washington, DC. *World Bank.* https://openknowledge.worldbank.org/handle/10986/37452 License: CC BY 3.0 IGO.

Hinkle, J. C. (2014). Emotional fear of crime vs. perceived safety and risk: Implications for measuring "fear" and testing the Broken Windows Thesis. *American Journal of Criminal Justice*, *40*(1), 147–168. https://doi.org/10.1007/s12103-014-9243-9.

Höppe, P. (1999). The physiological equivalent temperature - A Universal index for the biometeorological assessment of The thermal environment. *International Journal of Biometeorology*, *43*(2), 71–75. https://doi.org/10.1007/s004840050118.

Huong, H. T., & Pathirana, A. (2013). Urbanization and climate change impacts on future urban flooding in can Tho City, Vietnam. *Hydrology and Earth System Sciences*, *17*(1), 379–394. https://doi.org/10.5194/hess-17-379-2013.

Jamei, E.; Priyadarsini, R. Urban development and pedestrian thermal comfort in Melbourne. *Solar Energy* 2017, *144*, 681–698.

Jansson, C. (2019). *Factors important to street users' perceived safety on a main street* [Doctoral Dissertation, KTH]. Retrieved from http://urn.kb.se/resolve?urn=urn:nbn:se:kth:diva-260049.

Jia, S., & Wang, Y. (2021). Effect of heat mitigation strategies on thermal environment, thermal comfort, and walkability: A case study in Hong Kong. *Building and Environment*, *201*, 107988. https://doi.org/10.1016/j.buildenv.2021.107988.

Jiang, Y., & Lin, W. (2021). A comparative analysis of retrieval algorithms of land surface temperature from landsat-8 data: A case study of shanghai, China. *International Journal of Environmental Research and Public Health*, *18*(11), 5659. https://doi.org/10.3390/ijerph18115659.

Jones, T. L., Baxter, M. A. J., & Khanduja, V. (2013). A quick guide to survey research. *The Annals of The Royal College of Surgeons of England*, *95*(1), 5–7. https://doi.org/10.1308/003588413x13511609956372.

Kaiser, E. A., Rolim, S. B., Grondona, A. E., Hackmann, C. L., de Marsillac Linn, R., Käfer, P. S., da Rocha, N. S., & Diaz, L. R. (2022). Spatiotemporal influences of LULC changes on land surface temperature in rapid urbanization area by using Landsat-TM and Tirs Images. *Atmosphere*, *13*(3), 460. https://doi.org/10.3390/atmos13030460.

Katzschner, L. & Thorsson, S. (2009). *Microclimatic Investigations as Tool for Urban Design.* The Seventh International Conference on Urban Climate, Yokohama, Japan. http://www.ide.titech.ac.jp/~icuc7/extended_abstracts/pdf/397076-1-090514162300-002.pdf.

Kaymaz, I., (2019). *The Lost Streams of Ankara: A Case Study of Bentderesi.* 4th World Multidisciplinary Civil Engineering-Architecture-Urban Planning Symposium (WMCAUS), Prague, Czech Republic.

Kim, H., & Hong, S. (2021). Differences in the influence of microclimate on pedestrian volume according to land-use. *Land*, *10*(1), 37. https://doi.org/10.3390/land10010037.

Kim, S. W., & Brown, R. D. (2021). Urban heat island (UHI) variations within a city boundary: A systematic literature review. *Renewable and Sustainable Energy Reviews*, *148*, 111256. https://doi.org/10.1016/j.rser.2021.111256.

King, T. L., Bentley, R. J., Thornton, L. E., & Kavanagh, A. M. (2015). Does the presence and mix of destinations influence walking and physical activity? *International Journal of Behavioral Nutrition and Physical Activity*, *12*(1). https://doi.org/10.1186/s12966-015-0279-0.

Kızılca, A. B. (2022*). Evaluation of the impact of public space design on the land surface temperature by using geographical information systems: the example of Taksim Square Urban Design Competition* [Master's Thesis, Middle East Technical University].

Klemm, W., Heusinkveld, B. G., Lenzholzer, S., Jacobs, M. H., & Van Hove, B. (2015). Psychological and physical impact of urban green spaces on outdoor thermal comfort during summertime in the Netherlands. *Building and Environment*, *83*, 120–128. https://doi.org/10.1016/j.buildenv.2014.05.013.

Koerniawan, M. D. (2016). *Effect of Urban Structure on Thermal Comfort and Walking Comfort in Jakarta* [Doctoral Dissertation, The University of Kitakyushu].

Kong, L., Ka-Lun, K., Yuan, C., Chen, Y., Xu, Y., Ren, C., Ng, E. (2017) Regulation of outdoor thermal comfort by trees in Hong Kong. *Sustainable Cities and Society*. 31, 12–25. https://doi.org/10.1016/j.scs.2017.01.018.

Konrad, C.P. (2003). *Effects of Urban Development on Floods* (Fact Sheet 076-03). U.S. Geological Survey. https://pubs.usgs.gov/fs/fs07603/pdf/fs07603.pdf.

Kuhn Videira , M. L. C. da S. (2017). *Campus As A City - City As A Campus A morphological approach to university precincts in urban context* [Doctoral Thesis, Universidade De Lisboainstituto Superior Técnico]. https://www.academia.edu/34830699/CAMPUS_AS_A_CITY_CITY_AS_A_CAMPUS_A_morphological_approach_to_university_precincts_in_urban_context.

Labdaoui, K., Mazouz, S., Moeinaddini, M., Cools, M., & Teller, J. (2021). The street walkability and Thermal Comfort index (SWTCI): A new assessment tool combining street design measurements and Thermal Comfort. *Science of*

The Total Environment, *795*, 148663. https://doi.org/10.1016/j.scitotenv.2021.148663.

Lee, D., Pietrzyk, P., Donkers, S., Liem, V., van Oostveen, J., Montazeri, S., Boeters, R., Colin, J., Kastendeuch, P., Nerry, F., Massimo, M., Gorte, B. & Verbree, E. (2013). Modelling and observation of heat losses from buildings: The impact of geometric detail on 3D heat flux modelling. In *Proceedings 33rd AERSel Symposium" Towards Horizon 2020: Earth Observation and Social Perspectives", Matera, Italy, 3-6 June 2013-Geomatics Synthesis Project*.

Lee, J., & Shepley, M. M. C. (2020). College campuses and student walkability: Assessing the impact of smartphone use on student perception and evaluation of Urban Campus Routes. *Sustainability*, *12*(23), 9986. https://doi.org/10.3390/su12239986.

Lee, S., & Talen, E. (2014). Measuring walkability: A note on auditing methods. *Journal of Urban Design*, *19*(3), 368–388. https://doi.org/10.1080/13574809.2014.890040.

Leuzinger, S., Vogt, R., & Körner, C. (2010). Tree surface temperature in an urban environment. *Agricultural and Forest Meteorology*, *150*(1), 56–62. https://doi.org/10.1016/j.agrformet.2009.08.006.

Li, W., Zhou, Z., Zhang, S., & Feng, J. (2022). Study on relationship between shading and outdoor air temperature based on the comparison of two high-rise residential estates with Field Measurements. *Buildings*, *12*(11), 1813. https://doi.org/10.3390/buildings12111813.

Li, Y., Schubert, S., Kropp, J. P., & Rybski, D. (2020). On the influence of density and morphology on the urban heat island intensity. *Nature Communications*, *11*(1). https://doi.org/10.1038/s41467-020-16461-9.

Lin, B.-S., & Lin, C.-T. (2016). Preliminary study of the influence of the spatial arrangement of urban parks on local temperature reduction. *Urban Forestry & Urban Greening*, *20*, 348–357. https://doi.org/10.1016/j.ufug.2016.10.003.

Lin, T.-P. (2009). Thermal perception, adaptation, and attendance in a public square in hot and humid regions. *Building and Environment*, *44*(10), 2017–2026. https://doi.org/10.1016/j.buildenv.2009.02.004.

Liu, C. & Titheridge, H. (2016). *The Influence of Built Environment and Perceived Walkability on Walking Behaviour in Taiwan.* World Conference on Transport Research - WCTR 2016, Shanghai, China.

Louafi, S. & Saliha, A. (2017). Evaluation of Effect of Tree Canopy on Thermal and Environment. *SBLAB 2017 – International Conference on Advances on Sustainable Cities and Buildings Development*. Porto, Portugal.

Lynch, K., Banerjee, T., & Southworth, M. (1990). *City sense and city design: Writings and projects of Kevin Lynch*. MIT Press.

McCartney, S., Mehta, A., Shandas, V., Gallo, K., Paris, G., Nix, S., Quintero, T., Tomlinson, A., & Xian, G. (2020). *Satellite Remote Sensing for Urban Heat Islands.* NASA Applied Remote Sensing Training Program (ARSET). https://appliedsciences.nasa.gov/join-mission/training/english/arset-satellite-remote-sensing-urban-heat-islands.

McCormack, G. R., Giles-Corti, B., & Bulsara, M. (2008). The relationship between destination proximity, Destination Mix and physical activity behaviors. *Preventive Medicine*, *46*(1), 33–40. https://doi.org/10.1016/j.ypmed.2007.01.013.

Meeder, M., Aebi, T., & Weidmann, U. (2017). The influence of slope on walking activity and the pedestrian modal share. *Transportation Research Procedia*, *27*, 141–147. https://doi.org/10.1016/j.trpro.2017.12.095.

Michalak, R. (2014). *Sustainable management increases forests' carbon sequestration function in the UNECE region*. UNECE. Retrieved January 20, 2023, from https://unece.org/media/press/883.

Min, M., Lin, C., Duan, X., Jin, Z., & Zhang, L. (2019). Spatial distribution and driving force analysis of urban heat island effect based on raster data: A case study of the nanjing metropolitan area, China. *Sustainable Cities and Society,* 50, 101637. https://doi.org/10.1016/j.scs.2019.101637.

Morakinyo, T. E., Lau, K. K.-L., Ren, C., & Ng, E. (2018). Performance of Hong Kong's common trees species for outdoor temperature regulation, thermal comfort and energy saving. *Building and Environment*, *137*, 157–170. https://doi.org/10.1016/j.buildenv.2018.04.012.

Mouada, N., Zemmouri, N., & Meziani, R. (2019). Urban morphology, outdoor thermal comfort, and walkability in hot, dry cities: *International Review for Spatial Planning and Sustainable Development*, *7*(1), 117–133. https://doi.org/10.14246/irspsda.7.1_117.

Muhlrad, N. (2007). *A short history of pedestrian safety policies in Western Europe*. Researchgate. Retrieved January 19, 2023. https://www.researchgate.net/publication/228815417_A_SHORT_HISTORY_OF_PEDESTRIAN_SAFETY_POLICIES_IN_WESTERN_EUROPE.

Munawar, H. S., Hammad, A. W., & Waller, S. T. (2022). Remote Sensing Methods for flood prediction: A Review. *Sensors*, *22*(3), 960. https://doi.org/10.3390/s22030960.

Nasrollahi, N., Ghosouri, A., Khodakarami, J., & Taleghani, M. (2020). Heat-mitigation strategies to improve pedestrian thermal comfort in Urban Environments: A Review. *Sustainability*, *12*(23), 10000. https://doi.org/10.3390/su122310000.

Nayar, V., & Najafi, F.T. (2012). *Travel Behavior of Students Reaching Their Origin and Destination at the University of Florida*. 2012 ASEE Southeast Section Conference, Starkville, USA.

Nouri, A. S., Charalampopoulos, I., & Matzarakis, A. (2022). The application of the physiologically equivalent temperature to determine impacts of locally defined extreme heat events within vulnerable dwellings during the 2020

Summer in Ankara. *Sustainable Cities and Society*, *81*, 103833. https://doi.org/10.1016/j.scs.2022.103833.

Núñez Peiró, M., Sánchez-Guevara Sánchez, C., & Neila González, F. J. (2019). Source area definition for local climate zones studies. A systematic review. *Building and Environment*, *148*, 258–285. https://doi.org/10.1016/j.buildenv.2018.10.050.

O'Hare, D. (2006). *Urban Walkability in the Subtropical City: Some Intemperate Considerations from SEQ*. In Kennedy, R (Ed.) Subtropical Cities 2006 Conference Proceedings: Achieving Ecologically Sustainable Urbanism in a Subtropical Built Environment. Queensland University of Technology, Australia. http://www.subtropicalcities2006.qut.edu.au/Papers.html, pp. 131-136.

Oke, T. R. (2005). Towards better scientific communication in urban climate. *Theoretical and Applied Climatology*, *84*(1-3), 179–190. https://doi.org/10.1007/s00704-005-0153-0.

Oke, T. R., Mills, G., Christen, A., & Voogt, J. A. (2017). *Urban climates*. Cambridge University Press.

Oke, T.R. (1981). Canyon geometry and the nocturnal urban heat island: Comparison of scale model and field observations. *Journal of Climatology , 1*, 237-254.

Özdemirli, Y. K. (2014). Alternative strategies for urban redevelopment: A case study in a squatter housing neighborhood of Ankara. *Cities*, 38, 37–46. https://doi.org/10.1016/J.CITIES.2013.12.008.

Ozment,S., Ellison,G., Jongman,B. (2022). *Nature-Based Solutions for Disaster Risk Management : Booklet (English)* (Report No. 134847). World Bank Group. http://documents.worldbank.org/curated/en/253401551126252092/Booklet.

Parapari, D. M., Reicher, C., & Gruehn, D. (2015). *Adaptation to climate change and thermal comfort investigating adaptation and Mitigation Strategies for*

Kerman, Iran, based on Iranian traditional urbanism and the German experiences in the Ruhr (thesis).

Park, K., & Lee, M.-H. (2019). The development and application of the urban flood risk assessment model for reflecting upon urban planning elements. *Water*, *11*(5), 920. https://doi.org/10.3390/w11050920.

Park, S., Deakin, E., & Lee, J. S. (2014). Perception-based walkability index to test impact of Microlevel walkability on sustainable mode choice decisions. *Transportation Research Record: Journal of the Transportation Research Board*, *2464*(1), 126–134. https://doi.org/10.3141/2464-16.

Park, Y., Guldmann, J.-M., & Liu, D. (2021). Impacts of tree and building shades on the urban heat island: Combining Remote Sensing, 3D Digital City and spatial regression approaches. *Computers, Environment and Urban Systems*, *88*, 101655. https://doi.org/10.1016/j.compenvurbsys.2021.101655.

Perini, K., & Magliocco, A. (2014). Effects of vegetation, urban density, building height, and atmospheric conditions on local temperatures and thermal comfort. *Urban Forestry & Urban Greening*, *13*(3), 495–506. https://doi.org/10.1016/j.ufug.2014.03.003.

Pettorelli, N., Schulte to Buehne, H., Shapiro, A., & Glover-Kapfer, P. (2018). *Conservation Technology Series Issue 4: SATELLITE REMOTE SENSING FOR CONSERVATION.* WWF United Kingdom. 10.13140/RG.2.2.25962.41926.

Piracha, A., & Chaudhary, M. T. (2022). Urban Air Pollution, urban heat island and human health: A review of the literature. *Sustainability*, *14*(15), 9234. https://doi.org/10.3390/su14159234.

Radhi, H., Sharples, S., & Assem, E. (2015). Impact of urban heat islands on the thermal comfort and cooling energy demand of artificial islands—a case study of Amwaj Islands in Bahrain. *Sustainable Cities and Society*, *19*, 310–318. https://doi.org/10.1016/j.scs.2015.07.017.

Rahman, M. A., Dervishi, V., Moser-Reischl, A., Ludwig, F., Pretzsch, H., Rötzer, T., & Pauleit, S. (2021). Comparative analysis of shade and underlying surfaces on cooling effect. *Urban Forestry & Urban Greening*, *63*, 127223. https://doi.org/10.1016/j.ufug.2021.127223.

Rashidi, S. (2019). *Analyzing safety toward a walkable campus: a case-study of Middle East Technical University* [Master's Thesis, Middle East Technical University].

Rehman, A., Qin, J., Shafi, S., Khan, M. S., Ullah, S., Ahmad, K., Rehman, N. U., & Faheem, M. (2022). Modelling of land use/cover and LST variations by using GIS and Remote Sensing: A case study of the Northern Pakhtunkhwa mountainous region, Pakistan. *Sensors*, *22*(13), 4965. https://doi.org/10.3390/s22134965.

Rodríguez-Algeciras, J., Tablada, A., & Matzarakis, A. (2017). Effect of asymmetrical street canyons on pedestrian thermal comfort in warm-humid climate of Cuba. *Theoretical and Applied Climatology*, *133*(3-4), 663–679. https://doi.org/10.1007/s00704-017-2204-8.

Rodríguez-Algeciras, J., Tablada, A., Chaos-Yeras, M., De la Paz, G., & Matzarakis, A. (2018). Influence of aspect ratio and orientation on large courtyard thermal conditions in the historical centre of Camagüey-cuba. *Renewable Energy*, *125*, 840–856. https://doi.org/10.1016/j.renene.2018.01.082.

Sahar, S., Ines, I. & Ulrich, C. (2012). Using the ENVI-MET program to simulate the micro climate in new Town. *HASHTGERD*. 10.13140/2.1.1739.2005.

Sakar, B., & Çalışkan, O. (2019). Design for Mitigating Urban Heat Island: Proposal of a Parametric Model. *ICONARP International Journal of Architecture and Planning*, 7, 158–181. https://doi.org/10.15320/ICONARP.2019.84.

Sanagar Darbani, E., Monsefi Parapari, D., Boland, J., & Sharifi, E. (2021). Impacts of urban form and urban heat island on the Outdoor Thermal Comfort: A pilot study on Mashhad. *International Journal of Biometeorology*, *65*(7), 1101–1117. https://doi.org/10.1007/s00484-021-02091-3.

Shatu, F., Yigitcanlar, T., & Bunker, J. (2019). Objective vs. subjective measures of street environments in pedestrian route choice behaviour: Discrepancy and correlates of non-concordance. *Transportation Research Part A: Policy and Practice*, *126*, 1–23. https://doi.org/10.1016/j.tra.2019.05.011.

Shi, H., & Chen, J. (2018). Characteristics of climate change and its relationship with land use/cover change in Yunnan Province, China. *International Journal of Climatology*, *38*(5), 2520–2537. https://doi.org/10.1002/joc.5404.

Sun, G., Haining, R., Lin, H., Oreskovic, N. M., & He, J. (2015). Comparing the perception with the reality of walking in a hilly environment: An accessibility method applied to a university campus in Hong Kong. *Geospatial Health*, *10*(1). https://doi.org/10.4081/gh.2015.340.

Sun, G., Oreskovic, N. M., & Lin, H. (2014). How do changes to the built environment influence walking behaviors? A longitudinal study within a university campus in Hong Kong. *International Journal of Health Geographics*, *13*(1). https://doi.org/10.1186/1476-072x-13-28.

Swiers, R., Pritchard, C., & Gee, I. (2017). A cross-sectional survey of attitudes, behaviours, barriers and motivators to cycling in university students. *Journal of Transport & Health*, *6*, 379–385. https://doi.org/10.1016/j.jth.2017.07.005.

Taleghani, M., Kleerekoper, L., Tenpierik, M., & van den Dobbelsteen, A. (2015). Outdoor thermal comfort within five different urban forms in the Netherlands. *Building and Environment*, *83*, 65–78. https://doi.org/10.1016/j.buildenv.2014.03.014.

Tanaka, T., Tanaka, K., Suyama, K., Honda, S., Senjyu, H., & Kozu, R. (2015). A comparison of objective physical activity, muscle strength, and depression among community-dwelling older women living in sloped versus non-sloped environments. *The Journal of Nutrition, Health & Aging*, *20*(5), 520–524. https://doi.org/10.1007/s12603-015-0602-0.

Tapias, E., & Schmitt, G. (2014). Climate-sensitive urban growth: Outdoor thermal comfort as an indicator for the design of Urban Spaces. *The Sustainable City IX*. https://doi.org/10.2495/sc140521.

Telega, A., Telega, I., & Bieda, A. (2021). Measuring walkability with GIS—methods overview and new approach proposal. *Sustainability*, *13*(4), 1883. https://doi.org/10.3390/su13041883.

Tomlinson, C. J., Chapman, L., Thornes, J. E., & Baker, C. (2011). Remote Sensing Land Surface Temperature for Meteorology and climatology: A Review. *Meteorological Applications*, *18*(3), 296–306. https://doi.org/10.1002/met.287.

Toy, S., Yilmaz, S., & Yilmaz, H. (2007). Determination of bioclimatic comfort in three different land uses in the city of Erzurum, Turkey. *Building and Environment*, *42*(3), 1315–1318. https://doi.org/10.1016/j.buildenv.2005.10.031.

Tsoka, S. (2017). Investigating the relationship between urban spaces morphology and local microclimate: A study for thessaloniki. *Procedia Environmental Sciences*, *38*, 674–681. https://doi.org/10.1016/j.proenv.2017.03.148.

Tumini, I., & Rubio-Bellido, C. (2016). Measuring climate change impact on urban microclimate: A case study of concepción. *Procedia Engineering*, *161*, 2290–2296. https://doi.org/10.1016/j.proeng.2016.08.830.

U.S. Environmental Protection Agency. (2008). *Reducing urban heat islands: Compendium of strategies.* Draft. https://www.epa.gov/heat-islands/heat-island-compendium.

U.S. Geological Survey. (n.d.). *Landsat Normalized Difference Vegetation Index*. https://www.usgs.gov/landsat-missions/landsat-normalized-difference-vegetation-index.

Using the USGS landsat level-1 data product. Using the USGS Landsat Level-1 Data Product | U.S. Geological Survey. (n.d.). Retrieved January 2, 2023, from

https://www.usgs.gov/landsat-missions/using-usgs-landsat-level-1-data-product.

Valsson, S. & Bharat, A. (2008). Natural and Man-made Parameter induced Spatial Variation in Microclimate. *Environment Architecture,* 28-34. https://www.researchgate.net/publication/299410961_Natural_and_man-made_parameter_induced_spatial_variations_in_microclimate.

Vardhu, V. A., & Sharma, D. A. (2023). Classification, mitigations and methods to detect UHI: A Review. *International Journal of Scientific Research in Engineering and Management*, *07*(02). https://doi.org/10.55041/ijsrem17711.

Vasilikou, C., & Nikolopoulou, M. (2019). Outdoor thermal comfort for pedestrians in movement: Thermal walks in complex urban morphology. *International Journal of Biometeorology*, *64*(2), 277–291. https://doi.org/10.1007/s00484-019-01782-2.

Villaveces, A., Nieto, L. A., Ortega, D., Ríos, J. F., Medina, J. J., Gutiérrez, M. I., & Rodríguez, D. (2012). Pedestrians' perceptions of walkability and safety in relation to the built environment in Cali, Colombia, 2009–10. *Injury Prevention*, *18*(5), 291–297. https://doi.org/10.1136/injuryprev-2011-040223.

Wang, M., Zhang, Z., Hu, T., & Liu, X. (2018). A practical single-channel algorithm for Land Surface Temperature Retrieval: Application to landsat series data. *Journal of Geophysical Research: Atmospheres*. https://doi.org/10.1029/2018jd029330.

Wang, Q., Wang, L., Wei, C., Jin, Y., Li, Z., Tong, X., & Atkinson, P. M. (2021). Filling gaps in landsat ETM+ SLC-off images with sentinel-2 MSI images. *International Journal of Applied Earth Observation and Geoinformation*, *101*, 102365. https://doi.org/10.1016/j.jag.2021.102365.

Wang, R., Hou, H., Murayama, Y., & Derdouri, A. (2020). Spatiotemporal analysis of land use/cover patterns and their relationship with land surface temperature

in Nanjing, China. *Remote Sensing*, *12*(3), 440. https://doi.org/10.3390/rs12030440.

Wong, N. H., Tan, A. Y. K., Tan, P. Y., & Wong, N. C. (2009). Energy simulation of vertical greenery systems. *Energy and buildings*, *41*(12), 1401-1408.

Xian, G., & Crane, M. (2005). Assessments of urban growth in the Tampa Bay watershed using Remote Sensing Data. *Remote Sensing of Environment*, *97*(2), 203–215. https://doi.org/10.1016/j.rse.2005.04.017.

Xiao, J., & Yuizono, T. (2022). Climate-adaptive landscape design: Microclimate and thermal comfort regulation of station square in the Hokuriku region, Japan. *Building and Environment*, *212*, 108813. https://doi.org/10.1016/j.buildenv.2022.108813.

Yamak, B., Yağci, Z., Bilgilioğlu, B. B., & Çömert, R. (2021). Investigation of the effect of urbanization on land surface temperature example of Bursa. *International Journal of Engineering and Geosciences*. https://doi.org/10.26833/ijeg.658377.

Yang, X., & Zhao, L. (2015). Diurnal thermal behavior of pavements, vegetation, and water pond in a hot-humid city. *Buildings*, *6*(1), 2. https://doi.org/10.3390/buildings6010002.

Yang, Y., Wang, D., & Dogan, T. (2022). How the urban microclimate and outdoor thermal comfort can affect intra-city mobility patterns: Evidence from New York City. *2022 Annual Modeling and Simulation Conference (ANNSIM)*. https://doi.org/10.23919/annsim55834.2022.9859328.

Yao, X., Yu, K., Zeng, X., Lin, Y., Ye, B., Shen, X., & Liu, J. (2022). How can urban parks be planned to mitigate urban heat island effect in "Furnace cities" ? an accumulation perspective. *Journal of Cleaner Production*, *330*, 129852. https://doi.org/10.1016/j.jclepro.2021.129852.

Yilmaz, E. (2013). *Ankara Şehrinde Isı Adası Oluşumu* [Doctoral Thesis, Ankara University].

Yin, G., Mariethoz, G., & McCabe, M. (2016). Gap-filling of landsat 7 imagery using the direct sampling method. *Remote Sensing*, *9*(1), 12. https://doi.org/10.3390/rs9010012.

Yu, H., Fukuda, H., Zhou, M., & Ma, X. (2022). Improvement strategies for microclimate and thermal comfort for urban squares: A case of a cold climate area in China. *Buildings*, *12*(7), 944. https://doi.org/10.3390/buildings12070944.

Yüksel, Ü., & Yilmaz, O., (2008). A Study on Determining and Evaluating Summertime Urban Heat Islands in Ankara at Regional and Local Scale Utilizing Remote Sensing and Meteorological Data. *Journal of The Faculty of Engineering and Architecture of Gazi University*, Vol.23, No.4, 937-952. https://avesis.gazi.edu.tr/yayin/ab8a4d25-b659-4b5c-b9d5-06849ba7d459/a-study-on-determining-and-evaluating-summertime-urban-heat-islands-in-ankara-at-regional-and-local-scale-utilizing-remote-sensing-and-meteorological-data.

Zhang, P., Bounoua, L., Imhoff, P., Wolfe, R. E. & Thome, K. (2014). Comparison of MODIS Land Surface Temperature and Air Temperature over the Continental USA Meteorological Stations. Canadian Journal of Remote Sensing, 40(2), 110-122, DOI: 10.1080/07038992.2014.935934.

Zhang, Y., & Sun, L. (2019). Spatial-temporal impacts of urban land use land cover on land surface temperature: Case studies of two Canadian urban areas. *International Journal of Applied Earth Observation and Geoinformation*, *75*, 171–181. https://doi.org/10.1016/j.jag.2018.10.005.

Zhao, Q., Sailor, D. J., & Wentz, E. A. (2018). Impact of tree locations and arrangements on outdoor microclimates and human thermal comfort in an urban residential environment. *Urban Forestry & Urban Greening*, *32*, 81–91. https://doi.org/10.1016/j.ufug.2018.03.022.

Zook, J. B., Lu, Y., Glanz, K., & Zimring, C. (2011). Design and Pedestrianism in a smart growth development. *Environment and Behavior*, *44*(2), 216–234. https://doi.org/10.1177/0013916511402060.